Active Probing Feedback based Self Configurable Intelligent Distributed Antenna System

For Relative and Intuitive Coverage and Capacity Predictions for Proactive Spectrum Sensing and Management

Kumar, Ambuj

DOI (link to publication from Publisher):
10.5278/vbn.phd.engsci.00148

Publication date:
2016

Document Version
Publisher's PDF, also known as Version of record

ACTIVE PROBING FEEDBACK BASED SELF CONFIGURABLE INTELLIGENT DISTRIBUTED ANTENNA SYSTEM

FOR RELATIVE AND INTUITIVE COVERAGE AND CAPACITY PREDICTIONS FOR PROACTIVE SPECTRUM SENSING AND MANAGEMENT

BY
AMBUJ KUMAR

DISSERTATION SUBMITTED 2016

AALBORG UNIVERSITY
DENMARK

ACTIVE PROBING FEEDBACK BASED SELF CONFIGURABLE INTELLIGENT DISTRIBUTED ANTENNA SYSTEM

For Relative and Intuitive Coverage and Capacity Predictions for Proactive Spectrum Sensing and Management

Ambuj Kumar

AALBORG UNIVERSITY
DENMARK

Dissertation submitted

.

Dissertation submitted: September 25, 2016

PhD supervisor: Prof. Albena Mihovska,
Aalborg University, Denmark

PhD Co-supervisor: Prof. Dr. Ramjee Prasad,
Aalborg University, Denmark

PhD committee: Associate Professor Rasmus Løvenstein Olsen (chair.)
Aalborg University, Denmark

Professor Thipparaju Rama Rao
SRM University, India

Director Sudhir Dixit
Skydoot Inc., USA

PhD Series: Faculty of Engineering and Science, Aalborg University

ISSN (online): 2246-1248
ISBN (online): 978-87-7112-730-0

Published by:
Aalborg University Press
Skjernvej 4A, 2nd floor
DK – 9220 Aalborg Ø
Phone: +45 99407140
aauf@forlag.aau.dk
forlag.aau.dk

Printed in Denmark by Rosendahls, 2016

CV

Ambuj Kumar received Bachelor of Engineering in Electronics & Communications from Birla Institute of Technology (BIT), Ranchi, India in the year 2000. As a part of the Bachelor programme, he carried through Internship Training in 1999 at the Institut für Hochfrequenztechnik, Technical University, (RWTH), Aachen (Germany). After graduation, Ambuj Kumar worked at Lucent Technologies Hindustan Private Limited, a vendor company, during the period 200-2004. His major responsibilities were the Mobile Radio Network Design, Macro and Microcell planning, and Optimization for the GSM and the CDMA-based Mobile Communication Networks. There, he was involved in pan-India planning and optimizing the MCNs of various service providers for both the green field and the incumbent deployments. During the period 2004 to 2007, he worked with Hutchison Mobile Services Limited (now Vodafone), a servie provider company, where he was involved in planning, deployment, and optimization of the Hutch's rapidly expanding GSM and Edge networks across India. Afterwards, he joined Alcatel- Lucent, New Delhi in 2007 and continued until 2009. Here, he worked in Network Presales Department and contributed in network rollouts for various pan-India servie providers. He worked for three months in the year 2009 as Research Associate at the Centre for TeleInFrastruktur (CTIF), Department of Electronic Systems, Aalborg University, and his research area was on 'Identification of Optimization parameters for Routing in Cognitive Radio'. Ambuj Kumar was awarded research scholarship under European Commission -Erasmus Mundus "Mobility for Life" programme for doing PhD and joined CTIF, Department of Electronic Systems, Aalborg University, Aalborg, (Denmark), in the year 2010. Ambuj Kumar has also worked as a Collaborative Researcher at the Vihaan Networks Limited (VNL), India. The work of PhD research was conceptualized at VNL; there he developed test-bed facilities for experimental studies on 'Advanced Alternative Networks'. Currently, he is working as Research Assistant in the eWall Project, funded by the European Commission, at the Faculty of Science and Engineering (Department of Electronic Systems) since 2015. His research interests are radio wave propagation, cognitive radio, visible light communications, and distribute antenna systems, etc. He has several research publications in these areas.

DANSK RESUME

Ambuj Kumar fik Diplomingeniør i Elektronik & kommunikationsmidler fra Birla Institute of Technology (BIT), Ranchi, Indien i år 2000. Som en del af bacheloruddannelsen, han gennemførte Praktik Træning i 1999 på Institut für Hochfrequenztechnik Tekniske Universitet (RWTH), Aachen (Tyskland). Efter endt uddannelse, Ambuj Kumar arbejdede på Lucent Technologies Hindustan Private Limited, en sælger selskab i perioden 200-2004. Hans store ansvarsområder var Mobile Radio Network Design, Makro og Microcell planlægning og optimering for GSM og CDMA-baserede mobilkommunikationsnet. Der blev han involveret i pan-Indien planlægning og optimering af kanalnetværk af forskellige udbydere for både det grønne felt, og de etablerede installationer. I perioden 2004 til 2007 arbejdede han med Hutchison Mobile Services Limited (nu Vodafone), en servie udbyder selskab, hvor han var involveret i planlægning, implementering og optimering af Hutch hastigt ekspanderende GSM og EDGE-netværk på tværs af Indien. Bagefter han sluttede Alcatel Lucent, New Delhi i 2007 og fortsatte indtil 2009. Her arbejdede han i Network Presales Institut og bidrog i netværk rollouts for forskellige pan-Indien servie udbydere. Han arbejdede i tre måneder i år 2009 som Research Associate ved Center for Teleinfrastruktur (CTIF), Institut for Elektroniske Systemer, Aalborg Universitet, og hans forskningsområde var på 'Identifikation af optimering parametre for Routing i Cognitive Radio'. Ambuj Kumar blev tildelt forskning stipendium under Europa-Kommissionens -Erasmus Mundus "Mobility for Life" program til at gøre ph.d. og sluttede CTIF, Institut for Elektroniske Systemer, Aalborg Universitet, Aalborg, (Danmark), i år 2010. Ambuj Kumar har også arbejdet som et samarbejdende forsker ved Vihaan Networks Limited (VNL), Indien. Arbejdet med ph.d.-forskning blev konceptualiseret på VNL; der udviklede han test-sengs faciliteter eksperimentelle undersøgelser af 'Avancerede Alternative Networks'. I øjeblikket arbejder han som Research Assistant i eWall Project, finansieret af Europa-Kommissionen på Det Naturvidenskabelige Fakultet og Engineering (Institut for Elektroniske Systemer) siden 2015. Hans forskningsinteresser er radiobølger formering, kognitiv radio, synlige lys kommunikation, og distribuere antennesystemer mv Han har flere forskningspublikationer på disse områder.

ABSTRACT

The network planning, deployment, and, architecture dictate how a Mobile Wireless Communication Network (MWCN) is going to perform through its lifetime. While a deployment, based on poor planning, may result in excessive expenses on compensating pitfalls, an incompetent architecture may lead to a total revamping of the network to a different technology. Whereas such experimental optimizations are mostly performed on a live network, the subscribers' interests are often kept aside. Expecting the 100 percent fulfillment of coverage and capacity demands of all subscribers in the entire service area is not completely feasible for any technology and deployment strategy; however, there is always a scope to mitigate them. The latest swift developments in both technology (such as Long Term Evolution-Advanced or LTE-A and 5th Generation of communications or 5G) and architecture (such as the Cloud-Radio Access Network or C-RAN and Self Organising Network or SON) are clear indicators that the user (subscriber) oriented upgrades are prime in focus. Nonetheless, besides all the new developments, there are always certain cases that the present technology and infrastructures are not able to cope up with. The subscribers' accumulation at random places, the multi-technology environment, the Radio Access Network sharing, resource utilization, etc. are still the eternal challenges that MWCNs are facing even after big leaps in both technologies, architecture and strategy. This is because the basic physics behind how electromagnetic waves flux out from the antennas and its propagation properties remain the same and, the technological and infrastructural advancements are just about utilizing these properties and mitigating the challenges. As an example, a service provider may need to add a capacity sites where it finds a periodical subscriber accumulation. However, for cities with huge versatilities in composition and subscriber base, such iterative approach to solving problems are less effective and often lead to draining of heavy investments on installation, maintenance, and operations. The dissertation defines in a novel way fundamental problems that may arise in an operational network and proposes solution based on an innovative architecture that could accommodate the aforementioned issues more conveniently than other present approaches.

Coverage and capacity are the decisive parameters of a network performance. The impact of the subscriber, moving, grouping and moving in groups of the above phenomena are defined in a novel way as Place Time Coverage (PTCo) and Place time Capacity (PTC) respectively, and we would refer them collectively as Place Time Coverage & Capacity (PTC^2). The dissertation proves through the concept of the PTC^2 that the network performance can severely be degraded by the excessive and unrealistic site demands, the network management inefficiency, and the consequence of the accumulation of subscribers substantially and randomly across the area under investigation (defined here as the Area of Interest or AoI). Both the position and, the time of the position acquired by a subscriber, raises the demand

for service at the very location (termed here as PTC wobble), thereby posing an ongoing capacity demand and poor resource utilisation in the present MWCN. This random accumulation, being more intense and rapid in the highly populated metropolitan cities, tend to affect both the signal propagation and the capacity demand at the point of accumulation more severely.

This PhD research addresses the PTC^2 challenge through a viable solution that is based on injecting intelligence and services in parallel layers through a Distributed Antenna Systems (DAS) network. This approach would enable the remote sites to acquire intelligence and a resource pool at the same time, thereby managing the network dynamics promptly and aptly to absorb the PTC^2 wobble. An Active Probing Management System (APMS) is proposed as a supporting architecture, to assist the intelligent system to keep a check on the variations at each and every site by either deploying the additional antenna or by utilising the service antenna. The probing process is an independent layer and does not use paging channels of service technology, thereby, saving extra traffic channels. Further, it is discussed how this architecture can be compatible with multi-technology and densenet environments. The architecture that is proposed here is termed as Self Configurable Distributed Antenna System (SCIDAS).

An analysis is performed to show how essential the intelligence is to manage the PTC^2 challenge. To this end, a novel supporting algorithm is proposed, defined as *Amoebic Place Time Coverage and Place Time Capacity Response or Amoebic PTC^2 Response (APR)*, which renders "amoeba-like" responses to approaching PTC^2 contributors (user accumulation).

DANSK SUMMARY

Netværket planlægning, implementering, og, arkitektur diktere, hvordan en Mobile Wireless Communication Network (MWCN) kommer til at udføre gennem sin levetid. Mens en implementering, baseret på dårlig planlægning, kan resultere i for store udgifter på at kompensere faldgruber, kan en inkompetent arkitektur føre til en total omlægning af netværket til en anden teknologi. Saadanne eksperimentelle optimeringer er for det meste udført på en levende netværk, bliver abonnenternes interesser ofte holdes til side. Forventer 100 procent opfyldelse af dækning og kapacitet krav fra alle abonnenter i hele serviceområdet er ikke helt muligt for enhver teknologi og implementering strategi; dog er der altid en mulighed for at afbøde dem. De seneste hurtige udvikling i både teknologi (såsom Long Term Evolution-Advanced eller LTE-A og 5. generation af kommunikation eller 5G) og arkitektur (såsom Cloud-Radio Access Network eller C-RAN og Self Organising netværk eller søn) er klare indikatorer at brugerens (abonnent) orienteret opgraderinger er prime i fokus. Ikke desto mindre, foruden alle de nye udviklinger, er der altid visse tilfælde, at den nuværende teknologi og infrastruktur ikke er i stand til at klare op med. Abonnenterne 'ophobning på tilfældige steder, multi-teknologi miljø, Radio Access Network deling, ressourceudnyttelse, etc. er stadig de evige udfordringer, MWCNs står selv efter store spring i begge teknologier, arkitektur og strategi. Dette skyldes, at de grundlæggende fysikken bag hvordan elektromagnetiske bølger flux ud fra antenner og dets formering egenskaber forbliver de samme, og de teknologiske og infrastrukturelle fremskridt er bare om at udnytte disse egenskaber og afbøde udfordringer. Som et eksempel kan en tjenesteudbyder nødt til at tilføje et kapacitet steder, hvor den finder en periodisk abonnent ophobning. Men for byer med enorme versatilities i sammensætning og abonnent base, såsom iterativ tilgang til at løse problemer er mindre effektive og fører ofte til dræning af store investeringer på installation, vedligeholdelse og drift. Afhandlingen definerer på en ny måde fundamentale problemer, der kan opstå i et operationelt netværk og foreslår løsning baseret på en nyskabende arkitektur, der kunne rumme de førnævnte spørgsmål mere bekvemt end andre nuværende tilgange.

Dækning og kapacitet er de afgørende parametre for et netværk ydeevne. Virkningen af abonnenten, flytning, gruppering og bevæger sig i grupper af de ovennævnte fænomener er defineret på en ny måde, som Place Time Dækning (PTCo) og Place tid Kapacitet (PTC) henholdsvis og vi ville henvise dem kollektivt som Place Time Dækning & Kapacitet (PTC2). Afhandlingen viser gennem begrebet PTC2 at netværkets ydeevne alvorligt kan nedbrydes af de alt for store og urealistiske websted krav, ineffektivitet netværkets ledelse og konsekvensen af ophobning af abonnenter væsentligt og tilfældigt over det område, der undersøges (her defineret som interesseområdet eller AOI). Både position og, tidspunktet for den erhvervet af en abonnent position, hæver efterspørgslen efter service på meget

placering (betegnes her som PTC wobble), og udgør dermed en løbende kapacitet efterspørgsel og dårlig ressourceudnyttelse i den nuværende MWCN. Denne tilfældige akkumulering, er mere intens og hurtig i de tæt befolkede storbyer, har tendens til at påvirke både signal udbredelsen og efterspørgslen kapacitet ved punktet for ophobning hårdere.

Denne ph.d.-forskning omhandler PTC2 udfordring gennem en holdbar løsning, der er baseret på indsprøjtning intelligens og tjenester i parallelle lag gennem en Distributed Antenna Systems (DAS) netværk. Denne fremgangsmåde vil gøre det muligt for fjerntliggende steder at erhverve intelligens og en ressource pulje på samme tid, og derved styre nettet dynamik hurtigt og rammende at absorbere PTC2 wobble. Et Active Sondering Management System (APMS) foreslås som en understøttende arkitektur, for at hjælpe det intelligente system til at holde styr på variationerne på hvert eneste websted ved enten at indsætte den ekstra antenne eller ved at udnytte tjenesten antenne. Den sonderende proces er en uafhængig lag og ikke benytter pagingkanaler service teknologi, derved, sparer ekstra trafikkanaler. Endvidere er det diskuteret, hvordan denne arkitektur kan være forenelig med multi-teknologi og densenet miljøer. Arkitekturen der foreslås her, der betegnes som Self Konfigurerbar Distributed Antenna System (SCIDAS).

En analyse er udført for at vise, hvor vigtigt intelligens er at styre PTC2 udfordring. Til dette formål foreslås en roman understøtter algoritme, defineret som Amoebic Place Time Dækning og Place Time Kapacitet respons eller Amoebic PTC2 Response (ÅOP), som gør "amøbe-lignende" reaktioner på nærmer PTC2 bidragydere (bruger akkumulation).

ACKNOWLEDGEMENTS

First and foremost, I am deeply indebted to the Almighty God, who blessed me with the patience and courage in such a way, that my hard work came to finality.

I wish to thank my parents, Geeta and Ashok Chandra, for their love and encouragement, without whom I would never have, what I achieved so far. Their constant support kept my belief, in myself, high, allowing me to realize my own potential.

The work was sponsored by European Commission under their "Erasmus Mundus Mobility of Life" project starting from September 1, 2010.

To begin with, I with all sincerity state that I am highly indebted to my supervisors Dr. Albena Mihovska and Prof. Ramjee Prasad, who have constantly been guiding, encouraging, and showing me path how to do quality research work. It was my great fortune that I had a chance to work under revered Prof. Prasad, a highly acclaimed one of the top world leaders in the field of Information & Communications Technology (ICT).

I am highly thankful to Dr. Neeli R. Prasad, Associate Professor, Department of Electronic Systems, Aalborg University, and Director, CTIF (USA) for her giving constant encouragement and technical guidance out of her busy schedule. I am also equally thankful, for discussing latest trends in the mobile industry, to Dr. Anand R. Prasad, NEC, Japan and Chairman of 3GPP of Mobile Communications Security Standardization Group, whenever I happened to meet him.

I will fail in my endeavour if I do not express my deepest sense of gratitude to Mrs. Jyoti Prasad, my aunt, for showering her affection and blessings. I sincerely thank Mr. Rajeev Prasad, and Dr. Mayuri Prasad for their cooperation and help whenever I needed.

I am thankful to Mr. M.P.S. Alawa, Mr. Bhagirath, and Mr. Vishal Singh, Senior Officers of the Wireless Monitoring Organization, Ministry of Communications & IT, Government of India, for providing support and making available the radio mobile monitoring V/UHF facilities. They also guided and helped me to undertake series of spectrum sensing measurements. With the facilities made available by by them, I had carried out a series of spectrum sensing measurements in different frequency bands that were required as a part of my thesis work. I have special thanks to Dr. P.S.M. Tripathi, another senior officer in the Wireless Planning & Coordination (WPC) Wing, Ministry of Communications & IT, Government of India, who had been awarded PhD degree from the Aalborg University. Dr. Tripathi, during his stay in Aalborg, shared accommodation with me, and he had

constantly been encouraging and providing technical support to me from time to time, which went a long way in the accomplishment of the tedious task of the Ph.D. work.

I will ever be grateful to Mr. Rajiv Mehrotra, the founder, Chief Executive Officer and Chairman of Vihaan Networks Ltd. (VNL) for his constant encouragement and technical support in my endeavour. Mr. Mehrotra helped me to understand the various ways in a Distributed Antenna System (DAS) that can be utilized to spread resources across any mobile network.

I thank my colleague Purnima Lala Mehta for contributing in a paper and for her valuable comments on this thesis.

I thank my friends Anil, Gautam, Kailash, Manoj, Meenakshi, Malvika, Nardya Sudhanshu, Rahul, Vijay, and Vineet for their constant support and encouragement, making my life more beautiful.

Finally, I am obliged and grateful to every one who have ever wished good for me!

TABLE OF CONTENTS

LIST OF FIGURES

LIST OF TABLES

LIST OF ACRONYMS

Acronyms	Abbreviations
AIU	Antenna Interface Unit
AoI	Area of Interest
APMS	Active Probing Management System
APR	Amoebic PTC^2 Response
ARPU	Average Revenu Per User
ASE	Average Spectral Efficiency
BER	Bit Error Rate
BTS	Base Transreceiver Station
CA	Co-Located Antenna
CAGR	Compound Annual Growth Rate
C-DAS	Conventional DAS
CG	Carrier Group
CME	Channel Matrix Estimator
CoW	Cell/Coverage on Wheels
C-RAN	Cloud RAN
CR	Cognitive Radio
DA	Distributed Antenna
DALC	Dominant Antenna Least Correlation
DAS	Distributed Antenna System
DL	Downlink
DSM	Dynamic Spectrum Management
DU	Dense Urban
ERG	Energy Reduction Gain
FCC	Federal Communications Commission
FON	Fiber Optic Network
FU	Follower Unit
GB	Guard Band
GSA	Greedy Selection Algorithm
ICG	Interfering Carrier Group

IMT	International Mobile Telecommunications
ITU	International Telecommunications Union
iPTC	Instantaneous Place Time Capacity
ISa	Intelligent Sub-Architecture
ISA	Incremental Selection Algorithm
JTG	Joint Task Group
LED	Light Emitting Diode
LoS	Line of Sight
LTE	Long Term Evolution
LTI	Linear Time Invariant
MCP	Maneuverable and Controllable Platform
MoU	Master Optical Unit
MRT	Maximum Ratio Transmitter
MWCN	Mobile Wireless Communication Network
NFAP	National Frequency Allocation Plan
NIU	Network Intelligent Unit
NMS	Network Management System
NN	Neuron Network
NPD	Network Parametric Duos
NSP	Network Service Provider
OFBN	Optical Fiber Backhaul Network
OIU	Optical Interface Unit
PDF	Probability Density Functions
PLM	Path Loss Model
PoPP	Proactive Place-Time Predictor
PPP	Poisson Point Process
PTC	Place Time Capacity
PTCo	Place Time Coverage
PTC^2	Jointly PTC and PTCO
PTC^2 EE	PTC2 Environment Estimation
PTE	Place Time Effect
PTI	Place Time Incidence
PTR	Place-Time Repercussion
PTP	Place Time Perplexity

RA	Reconfigurable antenna
RAN	Radio Access Network
RoU	Remote Optical Unit
RRH	Remote Radio Head
RRM	Radio Resource Management
RU	Remote Units
SCISDAS	Self Configurable Intelligent Distributed Antenna System
SINR	Signal to Interference plus Noise Ratio
SMU	Smart Master Unit
SON	Self Organizing Network
SPM	Silent Probing Method
SRU	Smart Remote Unit
SU	Semi Urban
SUE	Spectrum Utilization Efficiency
TDO	T-R Distance Optimiser
TFF	Thin Film Filters
UBH	User Bit Handler
UL	Uplink
V/UHF	V/UHF Mobile Monitoring System
VL	Visible Light
VLC	Visible Light Communications
VLTRX	Visible Light Transceiver
WDM	Wavelength Division Multiplexing
WHISLME	Whisper and Listen Method
WRC	World Radio Conference
WS	White Space
ZFBF	Zero-Forcing Beamforming

CHAPTER 1. INTRODUCTION

It is the eccentricity of the Mobile Wireless Communication Network (MWCN) environment that has compelled me to look beyond the technological arena, on which the network systems are built; and, eventually, this motivated me to do this current research, which analyzes why such approach and architectures are not able to solve the issues of capacity and service provision. Being a Telecom Engineer in India for about eight years, I witnessed the mobile communication revolution (in India) at its maximum pace that has let the technology to gallop from 2G to 4G via 2.5G, 2.9G, and 3G in a very short duration of time. 2.5G and 2.9G were the short-lived intermediate pseudo generations comprising GPRS and EDGE technologies associated to GSM 900 and GSM 1800. In figure 1-1, we can see that a lot of developments have happened in the mobile wireless communication technology; however, the approach towards the Radio Access Network (RAN) is more or less the same (see, figure 1-1). Therefore, although every communication generation is profoundly associated with the technical advancements, not much attention was paid on how the technology disseminates in the network. For every technology, the RAN deployment process remains the same and follows the same phases namely (a) Green Field deployment, (b) Coverage[1] Deployment (c) Capacity[2] Deployment and (d) Network Optimization. From the Green Field phase, which is the very initial stage of the network planning and where (target area) the particular service provider's service is inevitably absent, to a mature network, the deployment undergoes several stages through a process as shown in figure 1-2 [1] [2]. We call the target area as the Area of Interest (AoI), which is deeply investigated while planning the network sites[3]. Figure 1-2 shows the deployment process of an MWCN. Irrespective of the technology that an RAN sites are dealing with, the orbit of the deployment cycle has two perigees, signal, and subscribers. The objective of an MWCN service provider is always to provide right service to the right people. Hence, an RAN network often develops according to the distribution of the subscribers in the AoI. However, as both signal and subscribers are dynamic in nature, therefore, this approach is not sufficient to cater for some specific issues. Recent approaches such as C-RAN [3] [4] and the self-organising network (SON) [5] have been proposed, however, they may not be the solutions the service providers are looking for.

---

[1] The area is said to be covered (by a radiating antenna) if the waves transmitted by the antenna are received with significant strength (detectable by receivers) within that area.

[2] The value that represents the simultaneous calls that can be sustained by a wireless transmitting and receiving device (known as Transceiver or TRX).

[3] The location where the Base Station equipment along with its infrastructure is installed to provide network coverage in the surrounding area.

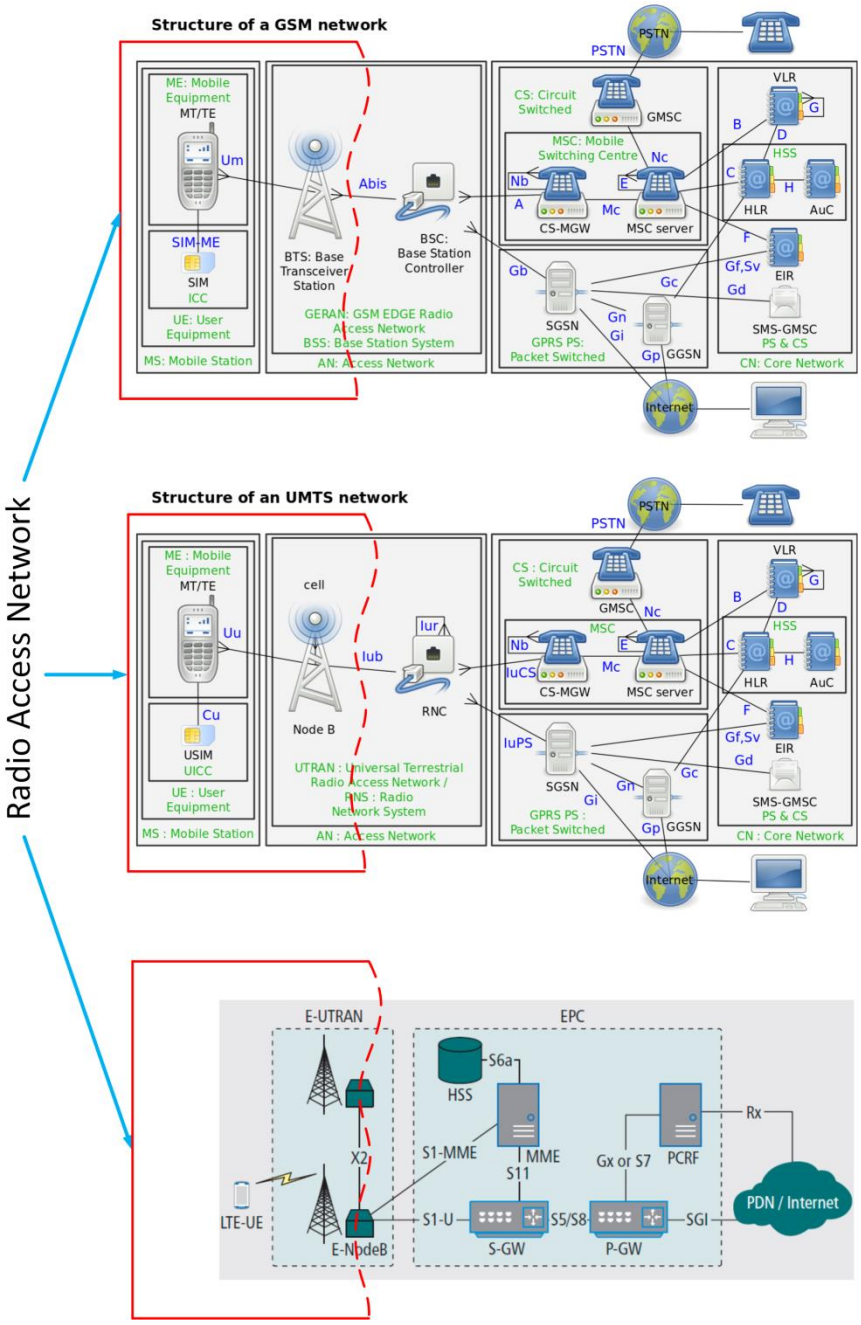

Figure 1- 1: Commonality of RAN Infrastructure deployment between GSM [6], UMTS [7]and LTE Advanced or 4G [8] [9]

1.1. BACKGROUND, MOTIVATION, AND JUSTIFICATION

Figure 1-2 shows a standard procedure of the incremental stages and swaps in the process of deploying or upgrading an MWCN in any AoI. Here, the iteration 'i' represents the steps or phases (in time) that are taken to update the MWCN in a particular AoI. For every phase, the term deployment simply means site rollouts (estimating the needed sites and releasing the required budget), their planning, and, placements at suitable geographical locations for the fulfillment of the partial or complete network demands. The entire process undergoes a rigorous procedure, of which, a simplified version is shown in figure 1-2. The frequency of 'i' depends on how rapidly the new demands (or challenges) are appearing in the network. However, due to practical limitations, the value of 'i' cannot be indefinitely high and, therefore, the network cannot respond to immediate and short-lived challenges. Hence, despite the effort put on the network planing, the objectives of providing seamless coverage and ample capacity at every location are not met. This lag is often compensated by the guarantee of service which revolves around 95-98% of the total duration, thereby filling the gap. However, the following are the visible concerns:

1) Public gatherings often trigger the network eccentricity, and are temporary and random in nature. This may be more problematic as there is no permanent solution for such a temporary and random problem;
2) A huge infrastructure redundancy with every phase-out resulting heavy capital reinvestment for new infrastructure and phasing out old ones;
3) A huge difficulty in spectrum resource management in multi-flavoured AoI comprising densenets, hotspots, rural, etc.;
4) A significant time lapse while newer technology completely sweeps the older one, and hence, the dilemma of coexistence of multiple technologies in the same area;
5) Multiple infrastructural layers can be seen in a single city for various technologies as a service provider may have to start from scratch for a new and every upcoming technology.
6) Because the capacity is limited to the coverage range of a BS, the capacity distribution becomes a challenge.
7) The deviation of the actual performance of the deployed network from what it has been planned for. It is very often and obvious situation of not finding a suitable place to deploy a site at the proposed location. This deviation from proposed to actual deployment, *defined here as* ***Planning Incongruence***, often results in a drop in efficiency. Further, large or unacceptable deviation might result in the involvement of another such site.

8) The poor antenna distribution in the traditional approach often makes it difficult for RF planners to define carrier groups for the network, resulting a low-frequency reuse pattern and more repetition of sites for capacity.

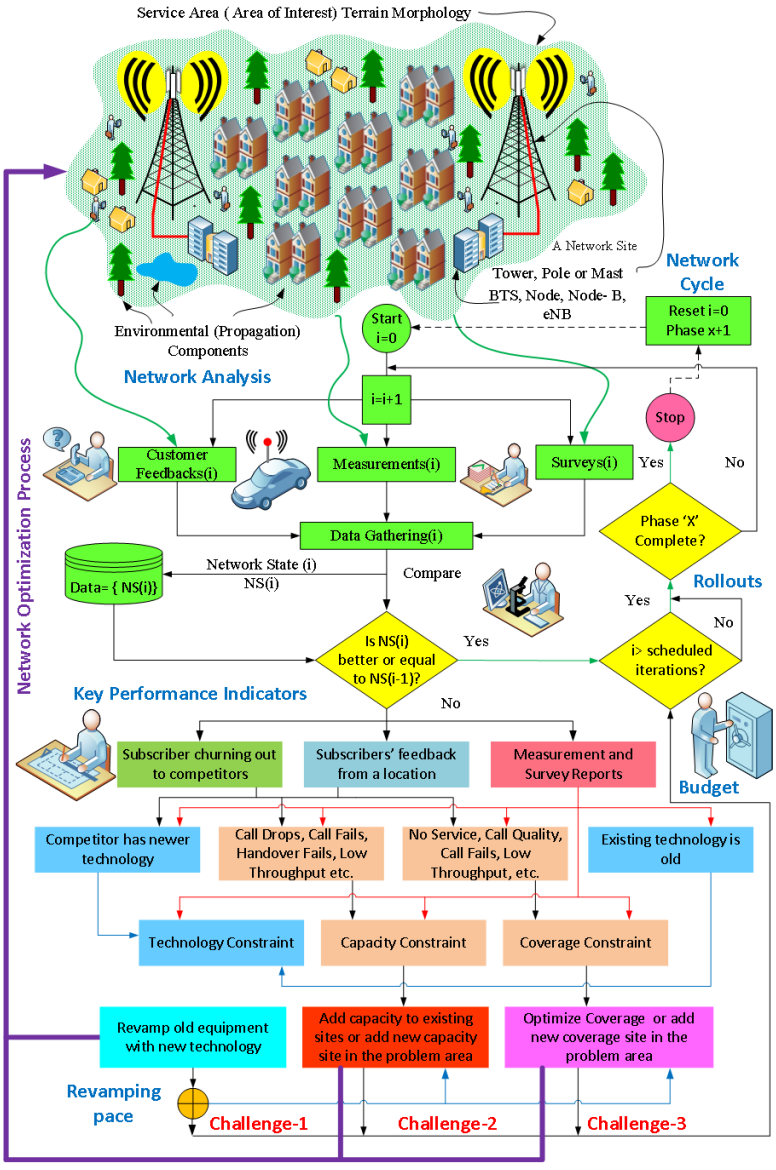

Figure 1- 2: Network Deployment Cycle

1.2. THE RESEARCH PROPOSITION

All the challenges that are discussed above cannot be addressed by a single endeavour. The present thesis identifies the challenges and proposes solutions to the still persistent problem of efficient mobile network deployment.

1.2.1. PROBLEM DEFINITIONS

This PhD research proposes solutions to the following network deployment problems:

(i) The random subscriber accumulation can significantly degrade the network performance by raising capacity demands and deteriorating the SINR in the impacted area. To this end, we have analyzed the currently enabled solutions to deal with the problem and have pointed out why these are inefficient in dealing with the problem.
(ii) The second objective is to measure the phenomena to identify the severity of the impact (i) in various circumstances.
(iii) The third research problem proposes a quantifying model for (i) that allows evaluating (ii) on the coverage and capacity of a network site. An innovative architecture has been proposed that allows to deal with the identified network deployment challenges and that caters for dynamic situations, such as a rapid subscriber accumulation.

1.2.2. RESEARCH SCENARIO

The background for the performed research is the Indian scenario. India, with its more than one billion population and specific traditions and lifestyle, is particularly subject to rapid subscriber accumulation.

1.3. THESIS OUTLINE AND CONTRIBUTIONS

This thesis is organized in 7 Chapters. This chapter also covers the measurement procedures and setups that were followed while performing in-field measurements in various scenarios. Chapter 7 concludes the thesis and also gives plan for future work. The following novel scientific contributions have been made and presented in the various Chapters.

- Chapter 2: Investigates the spectrum utilization and variation in signal strength in heavy gathering situations, based on the in-field measurements performed at various locations and at different times. As contributions, (a) it is found that accumulations iteratively change the spectrum utilization in time and position domains and over-accumulations blocks users from

using resources, and (b) a mathematical formulation is developed to relate a number of people per unit area and received signal strength.

- Chapter 3: A network subscriber, roaming around in an area, creates a demand for service at all places he/she visits. This forces a service provider to cater for all those locations. Thus, as contributions, (a) this chapter identifies users in a novel way as place-time entities and formulates the "demand of service", in terms of both capacity and coverage, as functions of place (position) and time, (b) this chapter investigates the challenges of the present static network deployment paradigm to cater for users that are dynamic in place and time, and (c) this chapter analyzes through mathematical formulations, how the probability distribution function based on which the network dimensioning is carried out, also varies in the place and time domain.
- Chapter 4: An innovative architecture, defined as Self Configurable Distributed Antenna System (SCIDAS), is proposed, and evaluated; to accommodate the Place and Time-based user dynamics, especially in the case when multiple subscribers move in groups.
- Chapter 5: We propose six novel supporting algorithms that collectively operate on the SCIDAS network to mitigate the variations created in the network environment. Two are used for sensing the disturbances (accumulations) and other four are to manage them.
- Chapter 6: A basic model of SCIDAS is developed and investigated empirically to understand the working of SCIDAS.

The following is the outline of this thesis:

Chapter 2. Analysis of Radio Spectrum Management Crisis & Occupancy Measurements

The prime purpose of all investigations, study, and measurements that were conducted and mentioned in this chapter was to identify the suitable location demonstrating the significance of the environmental dynamics. This scenario was used as the reference scenario for the scientific contributions of this thesis. ITU Recommendations were the baseline for conducting the research, and identifying the feasibility of using the system for IMT applications. This chapter, holds a significant importance in understanding closely the impact of the environmental changes on a network system. A holistic picture has been presented about the occupancy/vacancy measurements of the radio spectrum, i.e. the 800, 900 and 1800 MHz bands identified for commercial applications, which have been made in various cities/locations of India. Further, the impact of rapid people accumulation on the received signal power level was studied in the frequency bands mentioned above. It may be mentioned that ITU's Joint Task Group, set up in 2012 has submitted its recommendations identifying several frequency bands including 470-698 MHz for IMT application. In this regard, a decision was taken at the World

Radio Conference (WRC) 2015, scheduled during November 2-27, 2015. Keeping the WRC decision in mind, we performed measurements of the occupancy in the whole band of 470-698 MHz in India, to make a fair assessment that how IMT applications can be introduced in this frequency band. As of now there are no commercial mobile operations in the 1400 MHz band, however, this band is identified by JTG as a potential candidate band for IMT applications. A measurement campaign at a place of rapid accumulation, in India, was carried out to assess the impact of people's gathering in an open area on the received signal power levels in the 1400 MHz band.

Chapter 3. Place time Coverage & Capacity (PTC^2)

For any MWCN, the capacity and coverage requirements of the subscribers are a challenge. This problem aggravates when the coverage and capacity needs are to be catered for a large number of subscribers, particularly, when they accumulate randomly in relatively smaller areas and under extraordinary situations like a carnival, sports events, marathon events, etc. On these occasions, the subscribers move in a group, thereby creating huge capacity demand throughout the locus of the traversed path. From time to time, we come across news about network failing to serve in a crowded environment [10] [11]. In [12], the slowing of the speed of an LTE network in a crowded environment is discussed. The future generation networks (i.e. 5 G) will break the huge capacity demands into smaller high capacity pico-cells, and next to the demand for connectivity 'anytime, anyplace', there would be a need to address a question that the subscriber is 'at what time and at which place'. In order to answer these questions, two new research concepts have been defined, namely the 'Place Time Coverage' and, the 'Place Time Capacity or, collectively PTC^2, to evaluate the impact on the network behaviour. The results of this evaluation have been published in [13] and [14]. In Chapter 3, we show that *random network behaviours seek random responses from the network*, and when the random element is the subscriber accumulation, most of the present MWCN fail to cater them, and therefore, to cater them.

We, further evaluate the consequences of the entwining of the place and time phenomena on simple looking events. From a Network Service Provider's (NSP's) point of view, the PTC^2 is a perpetual challenge. The magnitude of this phenomenon is the motion of high capacity-hungry subscribers either individually or in groups due to any arbitrary triggers. This eventually becomes a problem when the phenomena goes beyond the absorbable limit.

Chapter 4. Self Configurable Intelligent Distributed Antenna System: Architecture.

To address the network dynamics, the obvious solution would be to optimize and expand the network by adding more and more coverage or capacity sites as

described in figure 1-2. Although this leads to considerable expansion of the RAN network, the total offered Erlangs at the CORE Network (see, figure 1-1) are almost the same; which means that the total capacity demand of the network is almost invariable and, therefore, there are no gain in revenues. Therefore, this may not be a feasible solution. Further, the situation also leads to overplanning thereby affecting the network health (poor SINR, etc.). Other disadvantages of overplanning are briefly discussed in the previous section.

The subscriber accumulation is one of the major culprits of raising this random demand. This chapter proposes a solution to the PTC^2 problem in five steps:

(i) An architecture that can accommodate the needed attributes to react as per demand.
(ii) A system to sense the dynamics independent of the technology in use.
(iii) Intelligence to take up a decision based on the sensed information.
(iv) A set of processes this intelligence will employ to react to the situation.
(v) More flexibility in a multi-technology environment.

To incorporate these steps in a single system, in this chapter, we propose an innovative, intelligent and prompt architecture that follows the normative framework of a Distributed Antenna System (DAS), a well-established technique of distributing the resources over a certain area, and utilizing its capabilities in distributing attributes of the network to tackle such issues. As DAS allows resources to stay at some defined location from where it is distributed across the network through suitable "cabled" or wireless networks, we propose both intelligent and service module to reside at the core, that we call as "SCIN," from where they are distributed by under laid DAS based architecture. As to manage the resources and tackle PTC^2 related issues, the network must be iteratively dynamic at every corner of its reach, emphasizing the need of approachability of its intelligent till the last destination (terminal) of the network. Therefore, the system needs to operate in such a way that the resource and intelligence may propagate parallelly in layers, for which, DAS is an excellent platform. The DAS based architecture is proposed in this chapter is termed here as the *Self Configurable Intelligent Distributed Antenna System* (SCIDAS). The findings reported in this Chapter have been partially published in [15]. Further, here a supporting algorithm has been proposed.

To achieve promptness in response, it is required that both intelligence and service must disseminate in parallel. In Chapter 4, we have discussed how this can be achieved by using an efficient technology known as Wavelength Division Multiplexing (WDM). This technology creates wavelength diversity and therefore allows multiple wavelengths to flow through a common Fiber Optic Network (FON). We have utilized this diversity as an opportunity to send intelligent signals to the remote units, that we have termed as **buds** (to differentiate from buds of

present technology base stations), parallel along with services, thereby, reducing latency in response time.

We have also introduced Smart Modules at both SCIN and bud ends. At SCIN, we have Smart Master Unit (SMU), and at bud end, we have Smart Remote Unit (SRU). These units work in coordination with an intelligent unit that we have defined as Network Intelligence Unit (NIU) through the base DAS network architecture.

Another capability of the proposed architecture is the adoption of multiple access technologies. To this end, we have evaluated the feasibility of accommodating newer access technologies. The advent of Light Emitting Diodes (LEDs) led to the realization of Visible Light Communications (VLC), which in turn relieves the burden on licensed/unlicensed radio spectrum for providing communications. In this way, VLC shall emerge as an alternative to communication technology using RF spectrum and proposes a concept for integrating VLC to enable intelligent communication infrastructure. The purpose of incorporating and discussing this feature is because one of the ways of wiseful utilization of the spectrum is to distribute users among various parallel technologies. Shifting of some dedicated statics from RF to VLC may relieve some extra Erlangs of the RF spectrum. The VLC module proposed in this chapter is a suitable avenue for Li-Fi based communications.

Chapter 4 describes the attributes of the SCIDAS architecture in terms of its Expandability (DAS based architecture), Manageability (control on each bud distinctively), Deployability (street furniture, light poles, etc., can be used for difficult areas), Flexibility (co-existence in multiple technologies, can be deployed readily where FON is available), and Adaptability (plug and play feature) with Intelligent and Futuristic attributes (can accommodate future technologies; the access radios of future technologies can work without revamping SCIDAS architecture).

Chapter 5. Active Probing and Self Configurability in SCIDAS

After proposing the architecture, we realized that just the architecture will not be sufficient unless we know how it can be used for the purpose it is proposed, i.e., mitigating PTC^2 problem. To address this task, this chapter explains two things:

a) How SCIDAS senses the accumulations.
b) How these accumulations are catered.

To answer (a), we have elaborated a technique that we used in SCIDAS and defined in Chapter 4 as *Active Probing Technique*. Conventionally, this technique is used to identify the faults in the computer networks and in space research (to remove

environmental errors from the received signals of a distant star), however, a similar approach is used in SCIDAS architecture to obtain a holistic estimation of the area under observation. Active Probing is the salient feature of SCIDAS architecture that involves independent monitoring of the network environment. The real-time measurement reduces a lot of complexity in "prediction" of environmental dynamism. By the virtue of DAS architecture incorporating WDM [16] [17], active probing may involve the service antennas or dedicated separate antennas may be deployed at each site for the monitoring of the subscriber mobility and accumulation in paralle to the service layer. Making it independent of the technology in use, active probing reduces a lot of paging work related to updates. The active probing is the sub-architecture of the intelligent system in SCIDAS that we have defined as Active Probing Management Systems (APMS). The active probing process is performed by two kinds of mechanism that we define as *Whisper and Listen Method* (WHISLME) and *Silent Probing Method* (SPM).

For (b), novel supporting algorithms have been proposed to assist APMS to follow the accumulations and provide additional resources only to the region of accumulation. We have proposed a *Amoebic PTC^2 Response* (APR) mechanism to react according to the PTC^2 occurrences. The APR includes several procedures that are defined separately as individual algorithms. Once such sub-algorithm has been defined as *Channel Matrix Estimator* (CME) and it plays a major role in estimating the PTC^2 wobbles in coordination with other algorithms such as *Transmitter – Receiver Distance Optimizer* (TDO), *PTC^2 Environment Estimatior* (PTC^2 EE), and *Proactive Place-Time Predictor* (PoPP).

Chapter 6. Empirical analysis

In this chapter, empirical analysis was performed across various locations in India to investigate the working of SCIDAS in situations were subscriber accumulations are significant. We chose three locations in India for our experiments namely, the city of Pune, Okhla (Delhi), and, Connaught Place (Delhi). For realistic investigations, we considered the true challenges of the service providers that they face in these locations. We took permissions from the active service providers to use their equipment and network resources for our investigations and, the choice and the period of investigations were chosen by them. In Pune, we hypothesized the SCIDAS deployment that could serve the severe accumulations during the procession of Lord Ganesha's immersion in holy water (river or lake), which happens every year during the month of September. Our CME algorithm predicted the positions where the accumulations are regular and likely to occur, with a considerable efficiency. One recommendation to be made to the service provider based on the findings in this Chapter is to install additional sites at the identified locations that could temporarily serve the hefty accumulations. In this Chapter, while discussing the case of Pune, we investigated how this problem of temporary accumulations can be dealt with SCIDAS. A similar experiment was conducted in

Okhla Delhi where we created an APMS-like system by using industrial spectrum analyzers and service provider's base stations to perform simultaneous and coordinated spectrum sensing at four different locations. This provided a holistic idea of the problematic carriers in the regions, which is one of the purposes of the actual APMS system.

In Connaught Place (CP), initially, the idea was to use vendor's FON and DAS equipment to deploy a working model of SCIDAS. However, as mentioned earlier, this process was halted. However, we used an industrial planning tool to simulate the SCIDAS network in the CP area, and algorithms were developed as programs to generate iteratively results that were iteratively fed in the tool to show dynamics with accumulations. Although, unlike the other two cases, this experiment was not performed in-field, however, we used the latest digital map of the city of Delhi to match with the current morphology of the area. The dynamics, however, was incorporated feeding additional losses in the environment due to accumulations, as identified in Chapter 3.

Pune and Okhla analysis was based on GSM technology. The reason why we chose GSM technology as compared to 3 G and/or 4 G is that:

- The GSM in India was launched way back in 1994. The GSM technology is fully matured by now not only in India but worldwide. The GSM subscriber base in India has crossed more than one billion. For our research work, we needed to have the mobile services that experience massive accumulation of the subscribers in a geographical area or service area. The licenses, for operating the 3 G and 4 G services, to the service providers were issued in India only a few years back. The 4G services were launched only last year (2015) in a few service areas. Because of these reasons, at the time of measurements, we selected GSM services for this research work. Moreover, the GSM service providers offered themselves to conduct measurements in their live network.

- Further, for pan-India coverage, each service provider is compelled to install more than 100,000 sites all over the country for GSM 900/1800 network. This led to the lack of interest for providing 3G and 4G technologies on a massive scale; therefore, there is a significant delay in launching these services. This is also a motivation for us to seek an alternative approach (continuous architecture than a discrete).

- PTC holds the same impact in every technology in service till date. With data/packet technologies (4G and beyond) there is a severe drop in throughput rate with increase in users at a location. As the capacity within an area is related to the number of sites, the only solution to cater PTC

issue is the addition of more sites. This creates heterogeneous networks in LTE environment which is not an efficient solution if the accumulations are random and un-scaled. The functionalities have been discussed in chapter 4 that can mitigate this challenge to a certain level.

1.4. MEASUREMENTS DETAILS

As discussed earlier, a detailed measurement campaign was organized to identify the experiment location for the research work; this included the deployment and investigations through drive tests. We have used the measurement results as a reference scenario to provide the research direction of this thesis. The snapshot of Radio Frequency spectrum sensing and occupancy/vacancy measurements were carried out as follows:

During the Period from April- August 2012 and July-December 2013

A V/UHF Mobile Monitoring System (V/UMMS) was provided by the **Ministry of Communications & Information Technology, Government of India** and with these facilities, an extensive series of spectrum sensing measurements were undertaken in different cities/locations of India, in the frequency bands of 800 MHz (2G CDMA), 900 MHz (2G GSM) and 1800 MHz (2G GSM) both in their DownLink (DL) and Up Link (UL) bands. The cities, where the measurements were carried out were: Ahmadabad, Bhopal, Delhi, Goa, and Mumbai. However, due to the paucity of space, the measurements their analysis conducted at Ahmadabad, Bhopal, and Goa have not been reported in this Thesis.

To investigate the spectrum management capabilities of the proposed SCIDAS architecture, it was inevitable to have a complete knowledge of the radio spectrum environment at all those locations, where the remote units were to be placed. This was achieved by carrying out band occupancy measurements at all such locations, and under various conditions to reveal the coverage footprint and network health status in the whole network area. During this period, separately, the vacancy/occupancy measurements in a commercially available band (GSM 900 down-link, i.e. 935-960 MHz) at suitable selected locations in the capital city of India (Delhi). Based on the study in the frequency band 935-960 MHz, the results were published in [13] and [18].

During the Month of February 2014

The impact of a gathering of authorized mobile subscribers, serviced by the mobile operators in assigned frequency bands of 800, 900 and 1800 MHz, during a season of a carnival, was assessed. Besides, this, the effect of the accumulation of people during a carnival season at a location in Goa, at 1400 MHz, on received signal power level has been studied. The 1400 MHz frequency was chosen, as there are no

mobile operations, hence there is no interference from any near base stations. These measurements were carried out during February 2014.

The details of the measurements and their analysis are included in Chapter 2 of this thesis. The measuring system setup and procedure of the measurements are described below.

It may be mentioned that ITU-Radiocommunications (R)'s Study Group-1, recognizing more complex and challenging tasks for monitoring of radio signals, has been periodically studying the various aspects of measurements and their procedures. The details are contained in the Reports ITU-R SM.1880 [18], ITU-R SM.1809 [19]and also in the 2011 Edition of the ITU Handbook on Spectrum Monitoring [20]. Taking into account these Reports and Handbook, a far more detailed discussion on different approaches to spectrum occupancy measurements, the relevant issues, and possible solutions are available in the Report ITU-R SM.2256 [21].

In order to understand the spectrum occupancy behaviour of different frequency bands (800, 900 and 1800 MHz), which are presently in use for commercial mobile services (IMT) and are recommended by ITU as potential candidate bands (viz 470-698 MHz), for IMT applications, spectrum measurement campaign has been carried out at various locations viz Ahmadabad, Bhopal, Delhi, Goa and Mumbai in India during the period 2012-2014. A series of measurements had also been conducted at Goa at 1400 MHz.

1.5. RADIO FREQUENCY SPECTRUM MEASUREMENTS-SYSTEMS AND PROCEDURES

A brief on the theoretical formulations relating frequency channel occupancy, the measuring setup, and the procedures related to the spectrum measurements for this research is given below.

1.5.1. THEORETICAL FORMULATIONS

A given service area may be illuminated by a spectrum resource that may contain all the carriers of a certain frequency band and available for the entire period of operation. The locations of measurements need to be selected such that the expected signal strength for the emissions of interest is above the threshold level. The relations between these two parameters define an area within which the measurement performed is of relevance to any station operating above a certain effective radiated power level. The frequency channel occupancy (FCO) of one channel is calculated as follows [21]:

$$FCO = {}^{T_0}/_{T_t} \quad \textbf{(1.1)}$$

Where, T_0= Time when the level measured in this channel is above the threshold and T_t = Total duration of monitoring. Assuming a constant revisit time, the FCO can also be calculated as:

$$FCO = {}^{N_0}/_{N_c} \quad \textbf{(1.2)}$$

in which, N_0 = Number of measurement samples with levels above the threshold and N_c= Total number of measurement samples taken from the channel concerned. The measurements present the different aspects of measuring and evaluating spectrum resource occupancy also addressing frequency channel occupancy.

The measurement analysis can be presented optimally by answering specific measurement oriented questions namely, (i) number of channels, (ii) bandwidth, (iii) type of user (s), (iv) threshold level used, (v) occupancy in the busy hour, (vi) and the duration of monitoring.

1.5.2. DETAILS OF MEASURING SETUP

In our work in [18], we have elaborately discussed the measuring setup. The descriptions mentioned in [18] are compact, precise, and well organized. Therefore, instead of re-writing the entire content, we have mentioned the relevant descriptions here, in due quotations, again, for the sake of continuity, clarity, and ready reference.

It may be mentioned that for the purpose of the radio signal measurements, a V/UHF Mobile Monitoring System (V/UMMS) was deployed that satisfies the requirements and is as per the Recommendation ITU-R SM.1723-2 (09/2011)[22]. This MMS is designed to monitor radio signals in two sub-bands i.e. 20-700 MHz (part of VHF band i.e. 30-300 MHz) and 700-3000 MHz (UHF band). "*It may be appreciated that V/UMMS efficiently performs measurement tasks as compared to the fixed monitoring set up. Mobile monitoring system effectively performs in the entire scenario including that of low transmitter power levels, high antenna directivity and specific propagation characteristics. With a view detecting weak signals under low signal-to-noise ratio condition, it would be required to improve the sensitivity of the monitoring system.* " [18].

To detect weak signals, the technologies proposed are broadly (i) increase of the antenna gain (ex. directional antenna, reconfigurable antenna), (ii) decrease the transmission loss (ex. outdoor installation of equipment for minimizing RF cable loss), and (iii) reduction of the receiver noise figure. "*The MMS used for the*

measurements consists of antenna systems, receivers, field-strength meters, frequency measuring equipment, bandwidth measurement, channel occupancy measurement, spectrum analyser, vector signal analyser, decoders, signal generators and recording equipment, etc. Usually, the sensing measurement tasks are normally performed for understanding occupancy/vacancy status of different radio signals in the frequency band (s) of interest. The main spectrum sensing tasks performed with a V/UMMS are for (a) type of emission for compliance with frequency assignment conditions, (b) occupancy measurement, (c) interference measurement, (d) radio coverage measurements, and (e) technical and scientific studies, etc." [18]. The V/UMMS comprising of antenna and measuring facilities is capable of doing the following ITU measurements:

- Modulation: Measurement of the modulation depth, frequency deviation or phase deviation.
- Bandwidth: Selected bandwidth measurement.
- Frequency and level: Frequency and level measurements.
- Noise measurement: Power spectral density and noise-to-signal measurement.

A typical V/UMMS used for measurements carried out at various cities/locations in India is presented at **Appendix-1**. The details about the antenna system, receiving system, procedures of measurements used for carrying out measurements are also highlighted in this Appendix.

1.6. PUBLICATIONS

Part of the the findings, reported in this thesis, have been published as follows.

Journal Publications

1) **Kumar, Ambuj**; Mihovska, Albena D.; and Prasad, Ramjee, 'Spectrum Sensing in relation to Distributed Antenna System for Coverage Predictions', Wireless Personal Communications, Vol. 76, No. 3, doi:10.1007/s11277-014-1724-0, March 2014, p. 549-568.
2) **Kumar, Ambuj**; Mihovska, Albena D.; Kyriazakos, Sofoklis; and Prasad, Ramjee, 'Visible Light Communications (VLC) for Ambient Assisted Living', Wireless Personal Communications, Vol. 78, No. 3, s11277-014-1901-1, July 2014, p. 1699-1717.

Conference Publications

3) Tripathi, P. S. M.; **Kumar, Ambuj** ; Chandra, A; and Sridhara, K., 'Dynamic Spectrum Access and Cognitive Radio' Presented at the 2nd International Conference on Wireless Communications, Vehicular

Technology, Information Theory, Aerospace & Electronic System Technology (Wireless VITAE 2011), pp. 1-5, February 28 to March 3, 2011.

4) **Kumar, Ambu**j; Mehta, P. L.; and Prasad, R., 'Place Time Capacity Place Time Capacity- A Novel Concept for Defining Challenges in 5G Networks and Beyond in India', Presented at the '2014 IEEE Global Conference on Wireless Computing and Networking (GCWCN)', December 2014.
5) **Kumar, Ambuj**; Mihovska, Albena D.; and Prasad, Ramjee, 'Dynamic Pathloss Model for Future Mobile Communication Networks', Presented at the 18th International Symposium on Wireless Personal Multimedia Communications (WPMC) of the Global Wireless Summit-2015, December 13-16, 2015.
6) **Kumar, Ambuj**; Mihovska, Albena D.; and Prasad, Ramjee, 'Self-Configurable Distributed Antenna System for Dynamic Spectrum Management in multi-layered Dense-Nets', Presented at the Fifth International Conference on Wireless Communications, Vehicular Technology, Information Theory, Aerospace & Electronic System Technology (Wireless VITAE 2015)of the Global Wireless Summit-2015, December 13-16, 2015.

Book Chapter

7) Sridhara, K.; Tripathi, P. S. M.; **Kumar, Ambuj**; Chandra, A; and Prasad, Ramjee, 'Multi-users Participation in Bidding Process in a Congested Cellular Network' in book "Globalization of Mobile and Wireless Communications: Today and in 2020'. Signal and Communication Technology Series, Springer, 1st Edition, 2011, XXI, ISBN: 978-94-007-0106-9.

1.7. CHAPTER MAPPING

	Paper 1	Paper 2	Paper 3	Paper 4	Paper 5	Paper 6	Paper 7
Chapter 1							
Chapter 2			√	√			
Chapter 3	√			√	√		
Chapter 4		√		√		√	√
Chapter 5	√		√	√	√	√	
Chapter 6	√					√	√
Chapter 7							

REFERENCES

[1] "GSM Air Interface & Network Planning." [Online]. Available: http://docplayer.net/698900-Gsm-air-interface-network-planning.html. [Accessed: 29-Mar-2016].

[2] International Telecommunication Union (ITU), "Telecom Network Planning for evolving Network Architectures." ITU, Geneva, 28-Feb-2007.

[3] Y. D. Beyene, R. Jantti, and K. Ruttik, "Cloud-RAN Architecture for Indoor DAS," *IEEE Access*, vol. 2, pp. 1205–1212, 2014.

[4] J. Huang, R. Duan, C. Cui, and I. Chih-Lin, "Overview of cloud RAN," in *General Assembly and Scientific Symposium (URSI GASS), 2014 XXXIth URSI*, 2014, pp. 1–4.

[5] "Nokia SON for Mobile Backhaul Executive Summary | Nokia Networks," *Nokia Solutions and Networks*. [Online]. Available: http://networks.nokia.com/file/38006/nokia-son-for-mobile-backhaul-executive-summary. [Accessed: 03-Apr-2016].

[6] "GSM," *Wikipedia, the free encyclopedia*. 03-Apr-2016.

[7] "UMTS (telecommunication)," *Wikipedia, the free encyclopedia*. 09-Apr-2016.

[8] S. Luo, M. Dong, K. Ota, J. Wu, and J. Li, "A Security Assessment Mechanism for Software-Defined Networking-Based Mobile Networks," *Sensors*, vol. 15, no. 12, pp. 31843–31858, Dec. 2015.

[9] "System Architecture Evolution," *Wikipedia, the free encyclopedia*. 01-Apr-2016.

[10] N. U. 04 17 13 9:11 AM, "Why Your Phone Doesn't Work During Disasters--And How To Fix It," *Fast Company*, 17-Apr-2013. [Online]. Available: http://www.fastcompany.com/3008458/tech-forecast/why-your-phone-doesnt-work-during-disasters-and-how-fix-it. [Accessed: 11-Apr-2016].

[11] "Addressing mobile network congestion in emerging markets: commercial strategies." [Online]. Available: http://www.analysysmason.com/About-Us/News/Newsletter/3G-network-congestion-Jul2014/. [Accessed: 11-Apr-2016].

[12] "Network congestion brings down speeds of new 'super-fast' 4G mobile phone services that were supposed to be five times quicker," *Mail Online*, 05-Nov-2014. [Online]. Available: http://www.dailymail.co.uk/news/article-2821197/Network-congestion-brings-speeds-new-super-fast-4G-mobile-phone-services-supposed-five-times-quicker.html. [Accessed: 11-Apr-2016].

[13] A. Kumar, A. Mihovska, and R. Prasad, "Dynamic Pathloss Model for Future Mobile Communication Networks," in *Global Wireless Summit, 2015*, Hyderabad, India, 2015, Presented.

[14] A. Kumar, P. L. Mehta, and R. Prasad, "Place Time Capacity- A novel concept for defining challenges in 5G networks and beyond in India," in *2014 IEEE Global Conference on Wireless Computing and Networking (GCWCN)*, 2014, pp. 278–282.

[15] A. Kumar, A. Mihovska, and R. Prasad, “Self Configurable Intelligent Distributed Antenna System for Resource Management in Multilayered Dense-nets,” in *Global Wireless Summit, 2015*, Hyderabad, India, 2015, Presented.

[16] K. Gupta, T. Mukhopadhyay, and A. Goyanka, “Design and simulation of a chirped Fiber Bragg Grating based demultiplexer for ultra dense Wavelength Division Multiplexing based Passive Optical Networks,” in *2013 IEEE International Conference on Advanced Networks and Telecommunications Systems (ANTS)*, 2013, pp. 1–5.

[17] M. Larrode and A. M. J. Koonen, “All-Fiber Full-Duplex Multimode Wavelength-Division-Multiplexing Network for Radio-Over-Multimode-Fiber Distribution of Broadband Wireless Services,” *IEEE Trans. Microw. Theory Tech.*, vol. 56, no. 1, pp. 248–255, Jan. 2008.

[18] A. Kumar, A. Mihovska, and R. Prasad, “Spectrum Sensing in Relation to Distributed Antenna System for Coverage Predictions,” *Wirel. Pers. Commun.*, vol. 76, no. 3, pp. 549–568, Mar. 2014

[19] ITU R SM.1880, “Spectrum Occupancy Measurements.” ITU, Feb-2011.

[20] ITU-R, “Standard Data Exchange Format For Frequency Band Registrations And Measurements At Monitoring Stations.” ITU, Sep-2008.

[21] ITU, “Itu Handbook on Spectrum Monitoring.” ITU, 2011.

[22] ITU-R, “Spectrum occupancy measurements and evaluation,” *ITU*. [Online]. Available: https://www.itu.int/pub/R-REP-SM.2256. [Accessed: 12-Apr-2016].

[23] ITU-R, “Mobile Spectrum Monitoring Unit, Recommendation.” ITU, Sep-2011.

CHAPTER 2. ANALYSIS OF RADIO SPECTRUM MANAGEMENT CRISIS, AND OCCUPANCY MEASUREMENTS

There are a number of open research challenges related to the random accumulation of subscribers in a Mobile Wireless Communication Network (MWCN). As a first step to addressing these challenges, extensive measurements were performed on a number of suitable locations in India. The purpose of the extensive field measurements was to assess the spectrum occupancy in several frequency bands, which are currently assigned to the commercial mobile networks. The objective of the performed measurements was to identify and assess the existing unutilized portions of the spectrum and how these can be incorporated to increase the capacity of the Areas of Interest (AoI). Based on the recommendations and studies initiated by the International Telecommunications Union (ITU), and performed measurements, a detailed analysis of the current spectrum situation in India for different frequency bands and at various cities/locations, was carried out. An initial model was designed to scan the spectrum to identify its usage and scarcity. The measurement studies allowed assessing the availibilty of un-utilized spectrum (e.g. the white spectrum). The 'white spectrum', can be extrapolated so that some spectrum could be released from a service provider's allocated spectrum size. The amount of 'white spectrum' (WS) varies for the different spectrum bands based on the geographical location and the time of day. This variation may be in the range of less than 5 to more than 50 MHz of the spectrum bandwidth of about 100 MHz. The spectrum occupancy measurements were planned in the frequency bands (800 MHz, 900 MHz, 1800 MHz), which are currently used for commercial mobile applications (IMT) and also in those frequency bands (470-698 MHz and 1400 MHz) that are earmarked for future IMT applications. In Chapter 4, we have introduced an innovative architecture that is defined as the ***Self Configurable Intelligent Distributed Antenna System*** (SCIDAS) that is intended to manage the heavy and itinerant user accumulations. The behaviour of these user accumulations is thoroughly studied in Chapter 3 of this thesis. Apart from proposing the architecture, we needed some experiment results to verify the working of the proposed architecture. We developed a basic model that was required to experimentally verified, for which, some suitable locating was needed for deploying this basic model. The measurements, metioned in this chapter, were intended to help in identifying an area for deployment of the SCIDAS test bed. Further, also, in order to investigate the impact of the rapid subscriber (i.e., users) accumulation in an open area on the received signal power level, detailed measurements at 1400 MHz were carried out. In this open area, people gathered starting in a group of 10 to 1000.

This Chapter is organized as follows. Section-1 briefly describes the growth of mobile subscribers, future projections of wireless devices and thereby the need for additional radio frequency spectrum for such applications. Section 2.2 describes the occupancy measurements in the frequency band 470-698 MHz earmarked for future IMT applications. **Section 2.3** deliberates on the detailed spectrum measurements activities that have been carried out in 800, 900, and 1800 MHz frequency bands in the Indian metro cities of Delhi and Mumbai. This section also summarizes the spectrum occupancy measurements conducted, in these frequency bands, by other researchers in a few countries. **Section 2.4** studies the impact of the dynamic movement of people on the propagation of radio signal at 1400 MHz in Goa (India). The probable research questions are highlighted in **Section 2.5**. **Section 2.6** presents the conclusions and references are given at the end of this chapter.

2.1. INTRODUCTION

In the last few years, there has been an astonishing growth of wireless technology and an increasing number of smart wireless devices resulting in a significant global mobile traffic growth. It is expected that worldwide the mobile devices and connections would reach a figure of over 10 billion by 2018 [1], of which 8 billion would be hand-held or personal mobile-ready devices. Devices such as smartphones, tablets, and many others have made mobile information access essential tools for our day-to-day needs. In the coming years, the radio frequency spectrum, required for the wireless-based systems, will be a significant foundation for the global economic growth and technological challenges. The number of devices being connected to mobile networks worldwide will be around ten times by 2020. As per an estimate, the numbers of subscribers in 2013 were more than 3.4 billion, and by 2020, it is expected that 56% of world population will have their own mobile [1]. The Compound Annual Growth Rate (CAGR) is shown in figure 2-1-1 [2].

The scarcity of radio spectrum alongside its efficient utilization is a major challenge and for tackling this, there could be a number of solutions, viz either (i) identify the additional spectrum bands under the 'Mobile Services' for IMT including Broadband applications or (ii) examining the status of its usage of the unused portion of spectrum already earmarked by ITU and assigned by the Administrations for other services/applications on time/geographical sharing basis or (iii) deploying some spectrum efficient techniques/methodologies including advanced intelligent antenna systems etc or (iv) a combination of all above four solutions in different permutations etc.

This chapter addresses the issues and challenges with regard to (a) the spectrum co-existence and how to enable additional spectrum, and (b) how to utilize the vacant portion of the existing spectrum dynamically. In both cases, (a) and (b), the detailed measurement studies in a different set of frequency bands assigned for IMT

applications, were undertaken. The measurement campaign leads to understand the vacancy and occupancy of a frequency band at a given time and in a geographical area. It is known that the unused portion of the spectrum can be exploited by the deployment of cognitive radios [3, 4]. A Dynamic Spectrum Management (DSM) for the implementation of cognitive radio based network was proposed in [5]. DSM allows the new user to access spectrum which has already been allocated to another user. The definition of cognitive radio (CR) is given in [6]. The cognitive radio technology is a way forward in meeting the challenges of the spectrum scarcity and also provides spectral efficient solutions. CR is an intelligent wireless system that is aware of its surrounding environment and uses the methodology to sense the availability of the free spectrum at a given time and location. CR adapts the statistical variations in the incoming radio signals of assigned spectrum and has the ability to change in certain operating parameters (e.g. transmit-power, carrier frequency, and modulation strategy, etc.) in real-time. In [5], the process of spectrum sensing is described. The relation of spectrum sensing to this PhD research is further explained in Chapter 5 where we propose spectrum sensing algorithms.

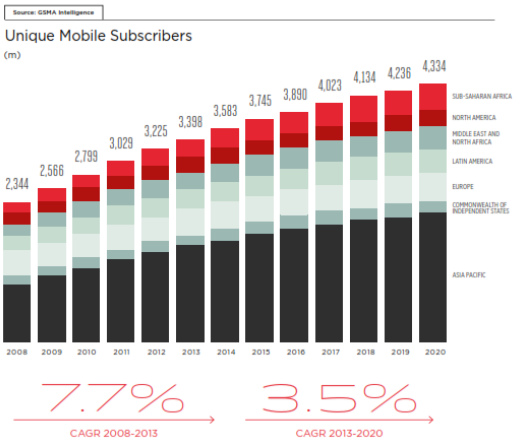

Figure 2-1-1: Mobile Subscriber Growth across Continents [2]

Appendix 2.1 details further the spectrum management proceedure in India for commercial mobile applications [7, 8], the broad principles of the radio spectrum management, the role of ITU in the earmarking of spectrum for various radio services specifically for IMT applications [9], the radio spectrum bands and the roadmap for identification of various frequency bands for IMT applications [10].

2.2. SPECTRUM OCCUPANCY MEASUREMENT IN 470-698 MHZ

It may be noted that as per the Table of Frequency Allocations of Radio Regulations (RR) Articles, each frequency band is shared among different services. In the event of earmarking of a radio service/application in that frequency band, detailed sharing and the co-existence studies are required to be undertaken. The broad principles behind such studies are described in **Appendix 2.2** [11, 12]. This Appendix also highlights co-existence and sharing studies between the existing broadcasting service and proposed IMT applications in the 470-698 MHz frequency band [13, 14, 15, 16]. Further, with a view to understanding the vacancy and occupancy in the frequency band 470-698 MHz, and the behaviour of the radio signals of any existing service (s) in this frequency band, an extensive measurement campaign was undertaken in the dense business areas in the heart of the City of Delhi, India. This place is popularly known as Connaught Place (CP), which is one of the largest financial, commercial and business centers of Delhi and houses the headquarters of several Indian firms surrounded by large establishments of central government offices. This site was intentionally selected as it encompasses a high level of wireless activity. Another location 'Dwarka', a very large area of residential colonies, which is about 25 Km from 'CP' was also selected for measurements of radio signals. These locations are further described in section 2.3.3. This study was aimed to broadly determine the following:

(i) The level of utilization of this frequency band;
(ii) The purpose for which this band is mostly used (i.e. mobile, fixed, broadcasting, etc.);
(iii) The duration and time of the band utilization;
(iv) The number and latitude-longitude of the transmitting locations; and
(v) The background noise level.

From the above-mentioned vacancy and occupancy studies, the band can be potentially identified for the introduction of any new services/applications including IMT. As shown in Table 2-3 [in **Appendix 2.2**], the frequency band 470-698 MHz is shared amongst 'BC', 'Fixed (FX)' and 'Mobile (MO)' services. During the measurements, the spectrum analyzer was tuned to receive radio signals in the frequency band 470-698 MHz. The measuring setup, the procedure of measurements and other details are described in **Appendix-1**. A frequency v/s received power level (in dBµV) spectrum data was recorded. The measured average and peak power levels for both the 'CP' and 'Dwarka' locations are shown in figures 2-2-1 and 2-2-3, respectively.

Analysis of the Frequency Band 470-698 MHz- It may be observed from figures 2-2-1 and 2-2-2, that, for both, CP and Dwarka locations the whole band of 470-698 MHz is fully occupied with power levels of a maximum of 25 dB µV with an average power level of about 10 dBµV. These transmissions appear to be of low-

powered terrestrial links. Because the maximum power throughout is significant, therefore, for low powered multiple Internet of Things (IoT) devices, there would be higher chances of interference/collision. There is an exception of the presence of a very strong signal in the range 508.1 to 518.19 MHz. The maximum power level in the CP area was close to 130 dBµV and the average level of the order of 110 dBµV, In the Dwarka are, the power levels were found to be reduced by about 70% as compared to the CP area. The maximum and average levels are almost comparable, which demonstrates full – time presence of a high powered transmitter, closer to the CP area. This is of a Television (TV) station, as in India 470-698 MHz is also allocated to broadcasting services. It amounts to the fact that the frequency band is almost fully occupied with low powered terrestrial links and a high-powered TV link, and therefore, there appears to be less or no vacancy in this spectrum band.

In the case of future planning for establishing IMT networks in this band, two scenarios appear: either shifting of the existing services/operations to another suitable frequency band (s); or shrinking the existing ones and making room for the introduction of IMT applications. In the first option, for shifting of the existing operations, there might be a huge cost involved in the relocation processes and this would also be time-consuming. However, in the second scenario, detailed co-existence studies are required for the calculation of the 'GB' and the 'geographical separation' between two services/applications. It may be further added that the co-existence of the existing services may require the advance system to cope up with unprecedented interference/collision for IMT devices. A detailed study would be required for enabling sharing of TV and the proposed IMT operations.

Occupancy statistics in CP in 470-698 MHz: *Out of the frequency range 470-698 MHz, the range of signal level values between 510- 518MHz were fairly occupied with occupancy above 30% (maximum 44.6%). Other frequencies were occupied less than 15% (minimum 2.6 %).*

A theoretical formulation of spectrum channel occupancy is given in chapter 1 of this thesis and is described in equations 1.1 and 1.2.

Occupancy statistics in Dwarka in 470-698 MHz: *Dwarka is very dense in all frequency ranges; frequencies in 510-518MHz being most occupied with values above 33% (maximum 47.8%). Other frequencies were also fairly occupied above 26% (minimum 8.7%).*

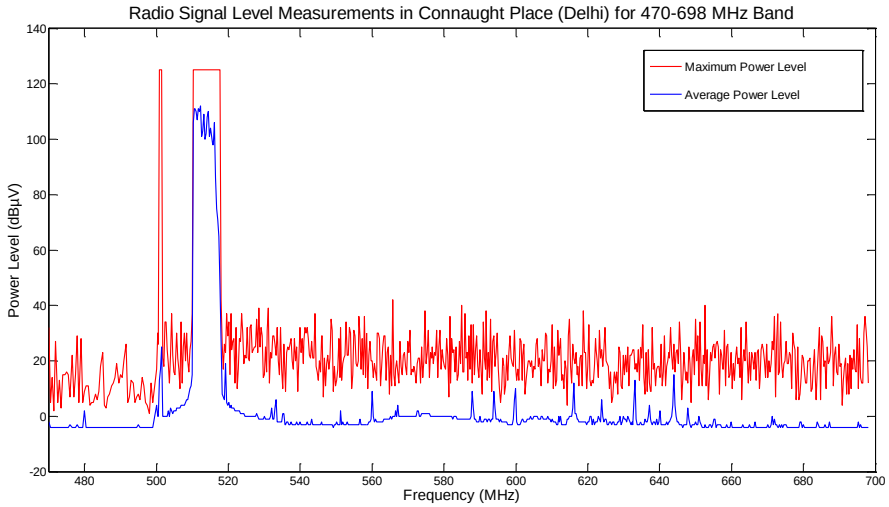

Figure 2-2-1: Radio Signal Level Measurements in C.P. (Delhi) for 470-698 MHz Band

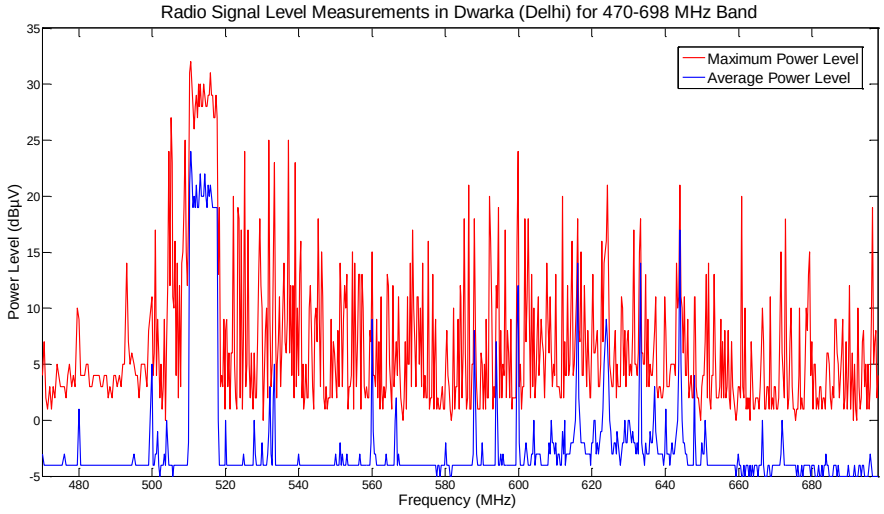

Figure 2-2-2: Radio Signal Level Measurements in Dwarka (Delhi) for 470-698 MHz Band

2.3. RADIO SPECTRUM MEASUREMENTS IN THE FREQUENCY BANDS OF 800, 900, AND 1800 MHZ AT DIFFERENT INDIAN CITIES/LOCATIONS

The frequency bands namely 800 (2G CDMA), 900 (2G GSM), and 1800 (2G GSM) have been used for providing worldwide commercial mobile applications since the late 1980's. Afterwards, the whole world has witnessed tremendous growth of subscribers, thereby putting a lot of stress on the spectrum requirements for IMT applications. Subscribers of mobile telecom services in India have witnessed unprecedented growth during the last decade with an average monthly of 1 to 1.5% particularly since 2004. The demand for spectrum has been increasing over the past several decades due to the increase in subscribers and traffic. One of the missions of the spectrum management is the efficient utilization of spectrum as the growth of telecom is to be sustained and enhanced in terms of teledensity. For that matter, there is now a need for a periodical assessment of the current utilization of the assigned spectrum.

The capacity enhancement techniques, which are available and may be used in the network, need to be examined before enabling the efficient and effective use of spectrum. The demands for spectrum and simultaneous dynamic random movement of the subscribers puts a huge demand on data and voice, and have opened another dimension of complex technological challenges in terms of capacity and coverage needs. The frequency bands for commercial mobile applications have been assigned for the whole of the service area on a 24-hours basis, and theoretically, these should be fully utilized. A revealing analysis of the Federal Communications Commission (FCC) [17] has shown that significant portion of the time, the assigned spectrum for various wireless applications is not in use and stays vacant, which has prompted to study in detail about the occupancy of the spectrum bands. The reported results of FCC demonstrate sporadic and geographical variations in the utilization of spectrum ranging from 15% to 85%. Our research studies in different frequency bands do reveal similar results, which are presented in the following sub-sections. The 'white spaces' thus created 'temporally' and 'geographically' can be put to use for providing public utility services. There are several studies reported in literature about the spectrum occupancy for different regions and in various frequency bands [18-23]. Such experimental results reveal that the spectrum is not fully utilized, and the usages vary with time, location etc. 'Time' means, it is peak hour or less busy hour of utilization, while 'location' means whether the utilization is in an extremely dense or lowly dense areas; or semi-urban areas; or rural areas etc. In the following paragraph, we review the published work in relation to spectrum occupancy.

[18] explored the possibilities of deploying the cognitive radio technology, through spectrum measurement campaigns in the city of San Luis Potosi (Mexico). and showed the underutilisation the 30-910 MHz frequency band. [18] further reported

that in the VHF band, there was a very low activity zone and the majority of the time the power level spectrum was below −70 dBm. [19] presented the spectrum occupancy measurements for the 2.3-2.4 GHz band in Turku (Finland) and Chicago (USA). This band, as per European standards is earmarked for IMT applications. However, in India, 40 MHz out of this band have been assigned for Broadband Wireless Access (BWA) including IMT applications. The spectrum occupancy measurements in Finland and Chicago demonstrated that the usage was rather low and in a certain portion of the band, no signals had been noticed. [20] reported the occupancy measurements for Barcelona (Spain), and Poznan (Poland) in the 400 MHz frequency band. The results revealed that there was a significant amount of the unused spectrum, and the average occupancy was 27% and 22 % in Poznan and in Barcelona respectively. The spectrum utilization data in the 900 MHz, (GSM-based cellular system) was collected in South Africa and was reported in [21]. The measurements were carried out on two locations at Site I (University of Pretoria) and Site II (Johannesburg). The results revealed that at Site I, the utilization of the band was 92%, whereas at Site II, it was about 60%. It was found that there was appreciably less activity at 04:00 hrs compared to 16:00 hrs. The analysis, of the spectrum occupancy in the frequency bands from 56 MHz to 6 GHz, was reported in [22]. The results of occupancy statistics in Bogota, the capital city of Colombia, demonstrated that utilization was very even in this metropolitan city. The TV bands namely 54-88 MHz, 174-216 MHz, and 512-806 were occupied about 12% time. However, GSM 900 was found to be active for about 80%. The paper reported that the frequency band was almost totally un-utilized throughout the period of observations. In [23], the authors reported 48 hours of spectrum occupancy measurements at seven locations in Europe. The measurements were undertaken in the frequency 110-3000 MHz but primarily focusing on the GSM 900 and GSM 1800 bands. The GSM bands are normally quite busy and understanding the traffic pattern including utilization would be revealing. This paper also discussed the occupancy situation in the ISM band. The locations of the measurement campaign were Aachen, Maastricht, Hannover, Leuven, Krefeld, Skopje, and Constance. The GSM bands were found less active during the night hours while the ISM band in outdoors was reported vacant for most of the time in the oudoor scenario. In Skopje, the occupancy of less than 20% in the 20 MHz bandwidth of the ISM band was found. In a nutshell, the results of the spectrum occupancy campaign carried out by these researchers reveal that in the commercial frequency bands, broadly the GSM bands, are occupied slightly more than 80 % of the time during the activity, while other frequency bands are occupied even less 20% time.

2.3.1. CLASSIFICATION OF SERVICE AREA ON THE BASIS OF MOBILE TRAFFIC HANDLING CAPACITY

The mobility of subscribers in a given service area create an accumulation, precisely during the daytime at one place and a vacuum at another place. However,

the total number remains the same. Though this situation may be different in the case of any high peak event (could for a shorter duration) namely carnival, sports event, man-made/natural disaster, where subscribers from another service area (s) do participate. Such an occurrence would lead to an imbalance distribution of the subscribers. The traffic pattern is not uniform in a city or service area, therefore, the coverage area needs to be classified into various types of regions on the basis of traffic. For the calculation of the maximum traffic density handling capability and subscriber base for a given spectrum, the area may be divided into sub-areas on the basis of traffic density i.e. Erlang/ Sq. Km. The service area may be classified broadly say into five regions i.e. Dense Urban (DU), Urban (U), Semi-Urban (SU), Rural (R) and Un-Inhabited Area (UIA). The details of these classifications are enumerated in **Appendix 2.3.**

With this classification of the locations of the wireless networks, it was decided to undertake spectrum occupancy measurements at various locations in India including New Delhi (Capital of India and an extremely dense area) and Bombay (business capital of India and extremely thickly populated). The other cities of India selected for measurements were Ahmadabad, Bhopal, and Goa. These cities can be classified as dense urban/urban/semi-urban areas for the purpose of measurements.

Various regions in India have different flavours like climate, terrain, population density and man-made structures. Another objective of the measurement was to obtain information about the utilized spectrum in the target regions that will be helpful in the signal analysis while optimizing the network. The target location(s) in a city/service area are scanned for many days for the entire spectrum bandwidth (both Uplink and Down Link) in the frequency bands of 800, 900, and 1800 MHz. Based on the measurements, sufficient information was extracted to pinpoint the area where an SCIDAS test bed can be deployed for the proof of concept and also to effectively utilize the vacant portion of operation of a ‘secondary device (may be cognitive radio)’ at any given time of the concerned frequency band in the area of operation. These vacant spaces, in various existing IMT bands, popularly known as ‘white space (WS)’ can be used for introducing newer wireless applications.

2.3.2. SPECTRUM MEASUREMENT CAMPAIGN

The status of allocations of different frequency bands in 800 MHz, 900 MHz and 1800 MHz assigned on a pan-India basis for the commercial mobile applications is given in Table -2.1 of **Appendix 2.1**.

In order to find out how the assigned spectrum for commercial mobile applications is utilized, the spectrum usage pattern was studied over a 24-hour period. This assessment was necessary from the point of view of the future deployment of wireless devices. A series of measurements were undertaken separately at a specific location in all the five cities mentioned above. For the purpose of measurements,

the V/UHF Mobile Monitoring System (V/UMMS) capable of monitoring of radio signal from 30-300 MHz, details of which are described in **Appendix-1**, was utilized. The measurements were taken in both the downlink (DL) and uplink (UL) of the commercial mobile systems operating in the 800 (2G CDMA), 900 (2G GSM), and 1800 (2G GSM) MHz frequency bands. Both the DL and UL frequency bands were scanned for the entire period of day/night long measurements. The radio signal measurements for all the frequency bands were recorded for both the average power level and the maximum power level during the entire period of observations.

To evaluate, the spectrum utilization and possible deviations, the measurements were done as follows:

(i) A single campaign consisted of five sets of measurements conducted subsequently at 2 pm, 5 pm, 8 pm, 11 pm and 2 am on the same day. This was done to avoid the impact in measurements due to changes in weather and other morphological variations;
(ii) For each city, an exclusively commercial and an exclusively residential area were selected for the measurements for placing the measuring Mobile Vehicle (V/UMMS) at a given location. This was done to clearly understand the pattern of spectrum utilization in both commercial and residential areas;
(iii) The times of measurements were chosen in such a way that these included most of the phases of the subscriber behaviour. 2pm was chosen as it is expected that subscribers are traversing the commercial vicinity. Around 5 pm, subscribers are using transport vehicles to leave the commercial place to their other destination. This activity majorly takes place from 5 to 8 pm, and hence, the 8 pm measurement was performed. Around 11 pm, it is expected that most of the subscribers have reached their destinations, and around 2 am, most of the subscribers' activities are on rest, leading to reduced spectrum utilization;
(iv) For every set of measurements, the maximum and average values were measured starting from 30 MHz to 3000 MHz in step size of 1 MHz. Out of this entire bandwidth (2970 MHz), a small portion from 800-1800 MHz was studied in detail; and,
(v) The observations drawn from these measurements have been utilized for further research work reported in this thesis.

2.3.3. DESCRIPTION OF CITIES/LOCATION AND DETAILS ABOUT MEASUREMENTS AND THE ANALYSIS

In this section, we present the measurements only for the cities of Delhi and Mumbai.

Details about cities [Source: www.google.com] in terms of population density (as of 2011 census), coordinates, and terrain conditions are given below. The measurements were carried out using the V/UHF Mobile Monitoring System (V/UMMS), which is capable of monitoring the radio signal from 30-300 MHz.

A. City of Delhi (including the National Capital Region-NCR)

The National Capital Region in India is the designation for the conurbation or metropolitan area which encompasses the entire National Capital Territory of Delhi, which includes New Delhi, as well as urban areas surrounding it in neighbouring states.

- Population/Area: 47,000,000/1,483 sq. km
- Co-ordinates: $28^o66'67" N, 77^o21'67" E$
- Terrain: Flat, Bounded by the Indo-Gangetic alluvial plains in the North and East, by the Thar Desert in the West and by Aravalli. Hill ranges in the South.
- Climate: Humid subtropical climate (Köppen Cwa) comprising a medium vegetation. Weather varies with the different climatic conditions that are faced by this city.
- Status and Man-made Structures: A very high dense population and a humid subtropical. High Dense Urban Very High to low rise Structures comprising of multiple scenarios.

Measurements in Connaught Place Area

Connaught Place (see, figure 2-3-1) is one of the largest financial, commercial and business centers in New Delhi, India. It is often abbreviated as CP (2838'0" N, 7713' 0" E) and houses the headquarters of several Indian/Multi-National firms surrounded by large establishments of central government offices. For undertaking measurements, Mobile Monitoring System (MMS) was parked in the center of CP i.e. near Plaza Cinema Hall.

Figure 2-3-1: Connaught Place (Delhi, India)

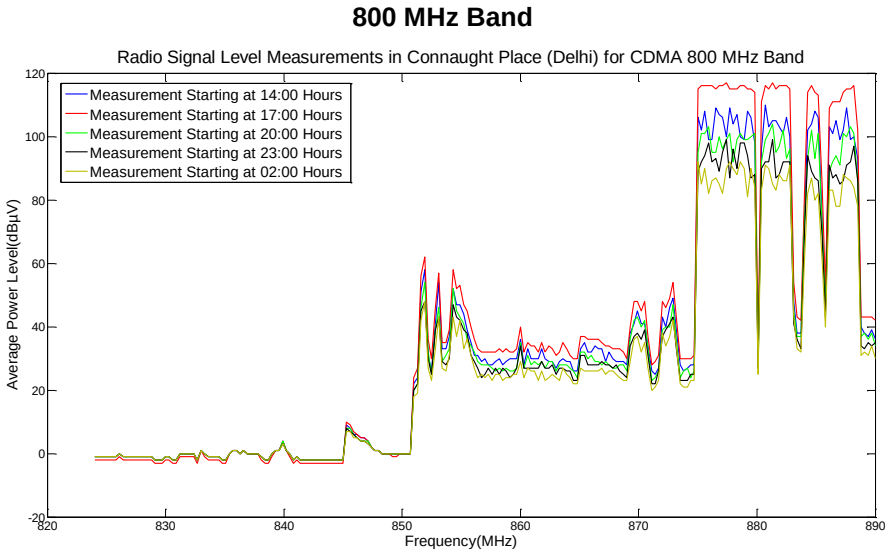

Figure 2-3-2: Average Power Level Measurements in CP (Delhi) for CDMA 800MHz Band

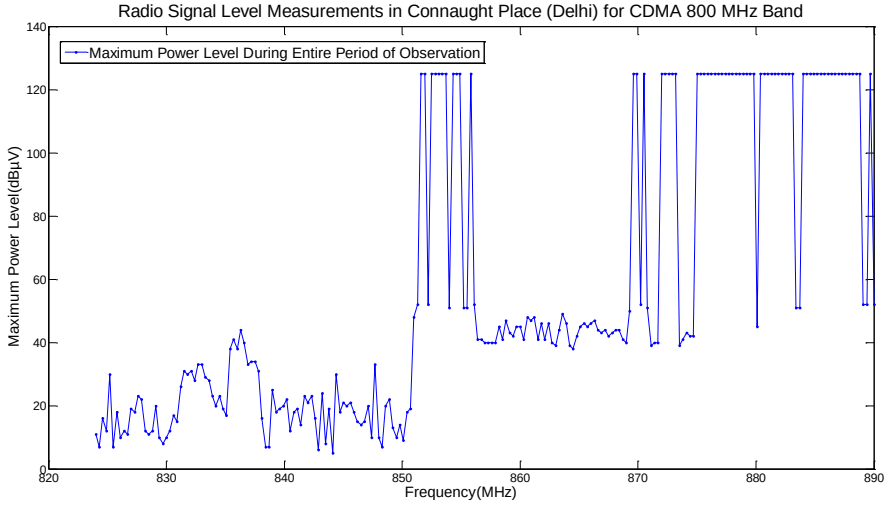

Figure 2-3-3: Maximum Power Level Measurements in CP (Delhi) for CDMA 800MHz Band

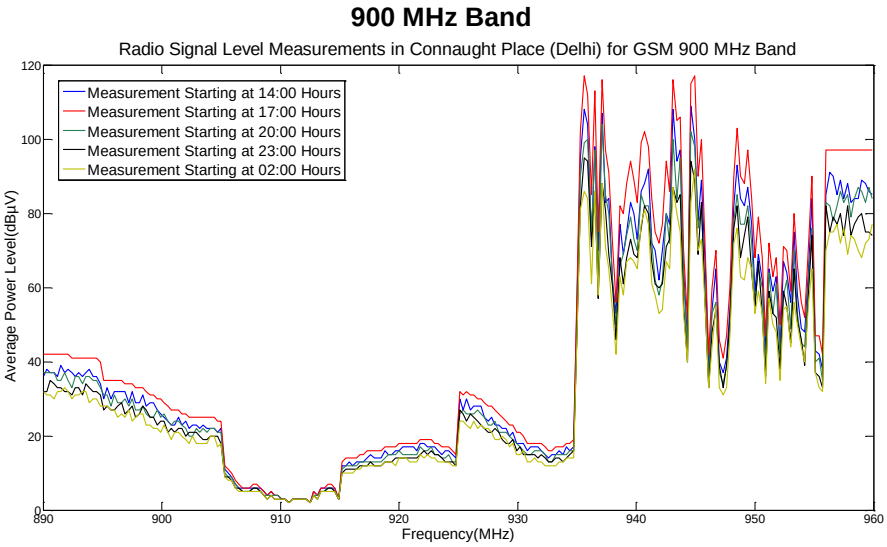

Figure 2-3-4: Average Power Level Measurements in CP (Delhi) for GSM 900MHz Band

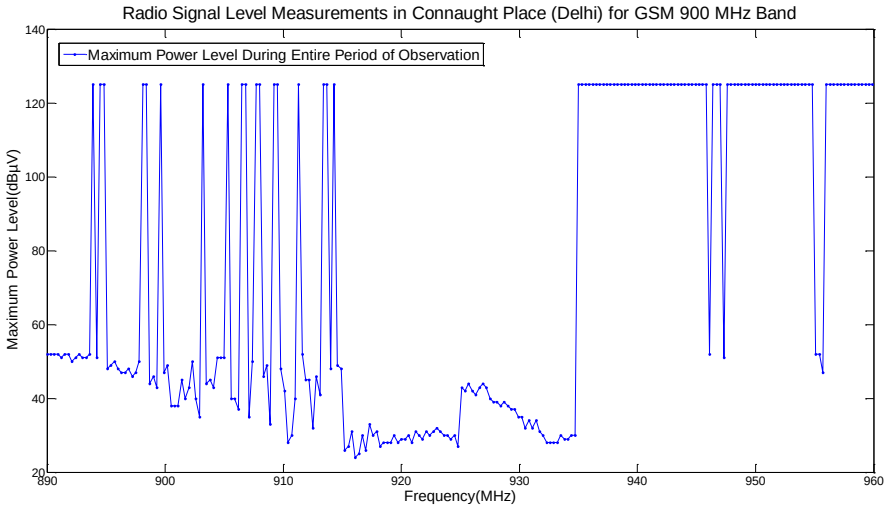

Figure 2-3-5: Maximum Power Level Measurements in CP (Delhi) for GSM 900MHz Band

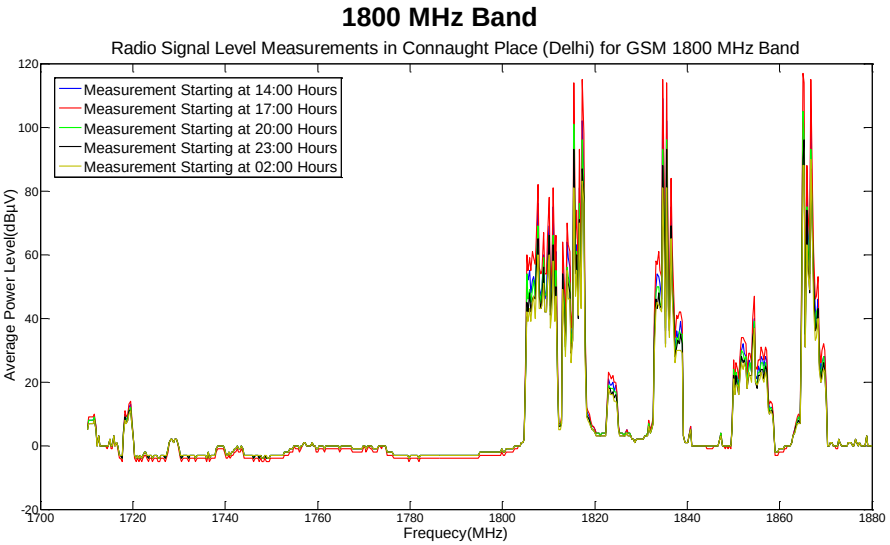

Figure 2-3-6: Average Power Level Measurements in CP (Delhi) for GSM 1800MHz Band

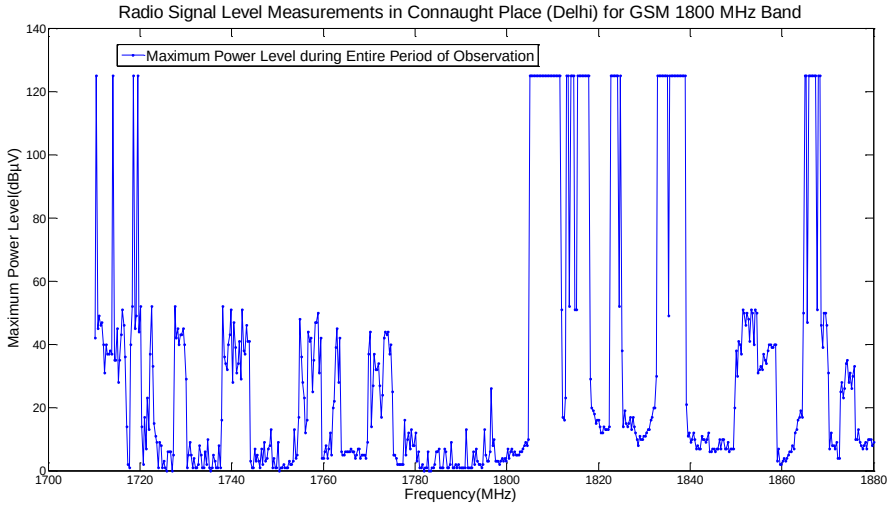

Figure 2-3-7: Maximum Power Level Measurements in CP (Delhi) for GSM 1800MHz Band

Analysis of Spectrum Figures 2-3-2 to 2-3-7

The analysis of these figures for the selected frequency bands (800, 900 and 1800 MHz) of CP, reveals that the average utilization of signals is strongly correlated with the subscriber behaviour (predominantly mobility). It can be seen that the growth and fall of the average signal power are followed by services of all the bands as a common trend. It can be seen from figures 2-3-2, 2-3-4, and, 2-3-6 that 2 pm has lower average utilization than 5 pm. This is due to the fact that 5 pm is the start of closing times of workplaces in CP and people (the potential subscribers) start using these services for negotiating and fulfilling their personal commitments. Also, people do use applications based on these services, while transiting in their vehicles for their respective destinations. This generates a huge magnitude of temporal traffic between 5-8 pm, which has been shown in 8 pm measurements. By 11 pm, most of the day-shift activities are closed and is very much reflected in 11 pm curves. Further, around 2 am, only night-shift workplaces are active, and service utilization is lowest in the entire day. Figures 2-3-3, 2-3-5, and 2-3-7 show that despite various trends in average occupancies, the maximum signal level is significant in all carriers.

Plots of Dwarka Location

Dwarka (figure 2-3-8) is an affluent neighborhood; located about 11 Km from Indira Gandhi International Airport and about 25 Km from CP. Dwarka is a huge residential area with 23 sectors and counting with each sector consisting 50-100 ten to fifteen storied residential buildings with the commercial market at the center of each sector. It is an up-market and one of the most sought-after residential areas/sub-cities and is Asia's largest housing colony.

Figure 2-3-8: Dwarka, $28^o59'21^{"}\ N, 77^o04'60^{"}\ E$

For carrying out detailed measurements, the V/UMMS was placed near sector-10 of Dwarka, which is the most active sector among all of them.

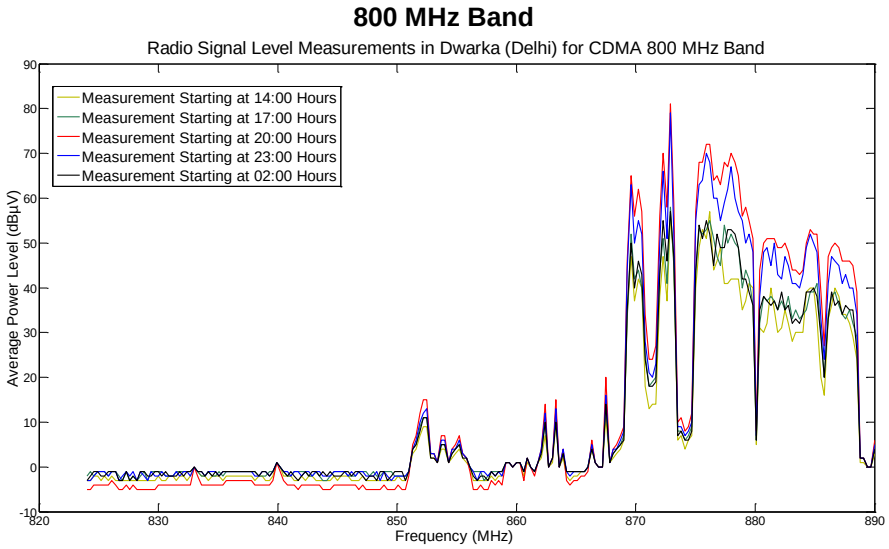

Figure 2-3-9: Average Power Level Measurements in Dwarka (Delhi) for CDMA 800MHz Band

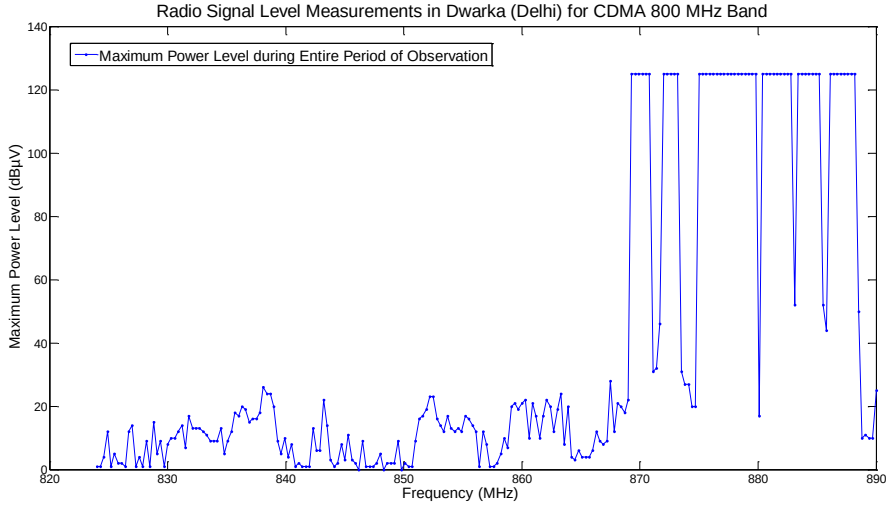

Figure 2-3-10: Maximum Power Level Measurements in Dwarka (Delhi) for CDMA 800MHz Band

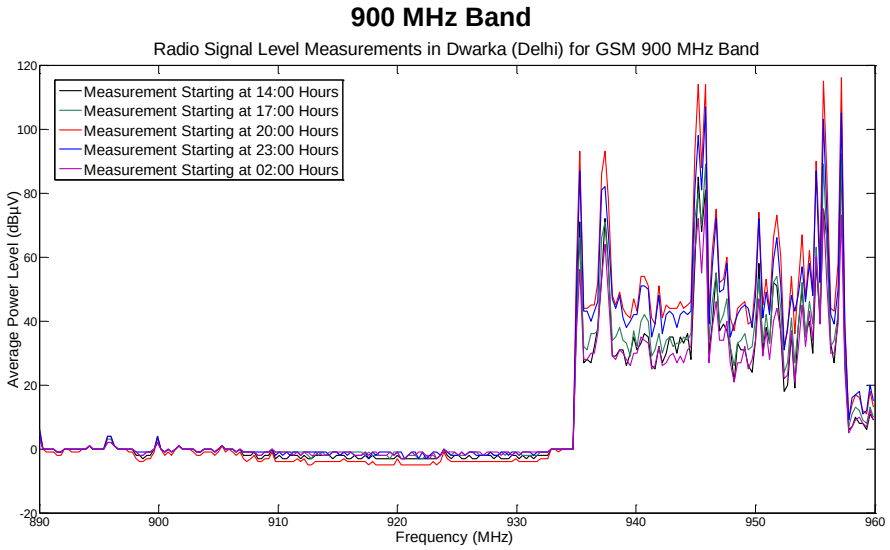

Figure 2-3-11: Average Power Level Measurements in Dwarka (Delhi) for GSM 900MHz Band

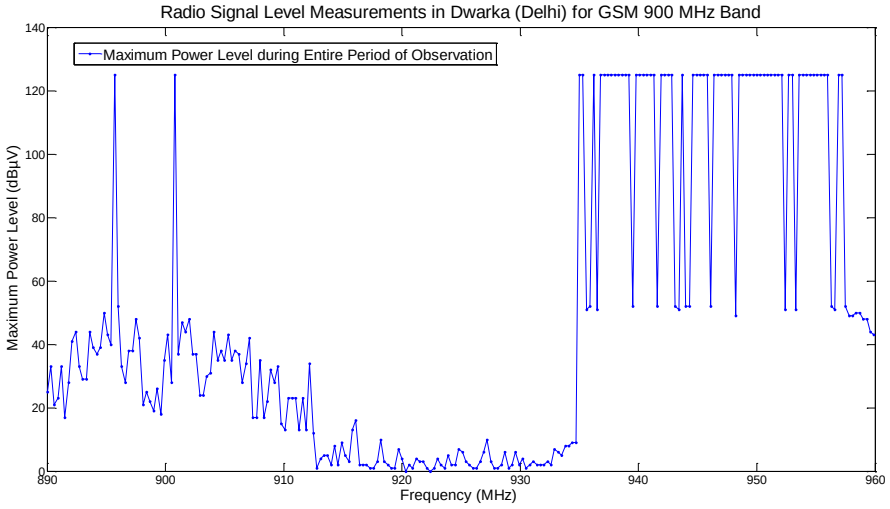

Figure 2-3-12: Maximum Power Level Measurements in Dwarka (Delhi) for GSM 900MHz Band

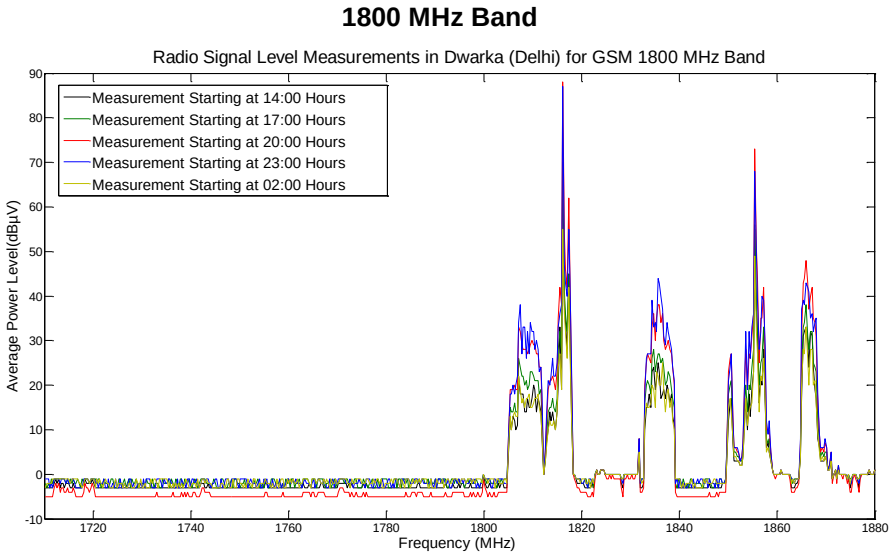

Figure 2-3-13: Average Power Level Measurements in Dwarka (Delhi) for GSM 1800MHz Band

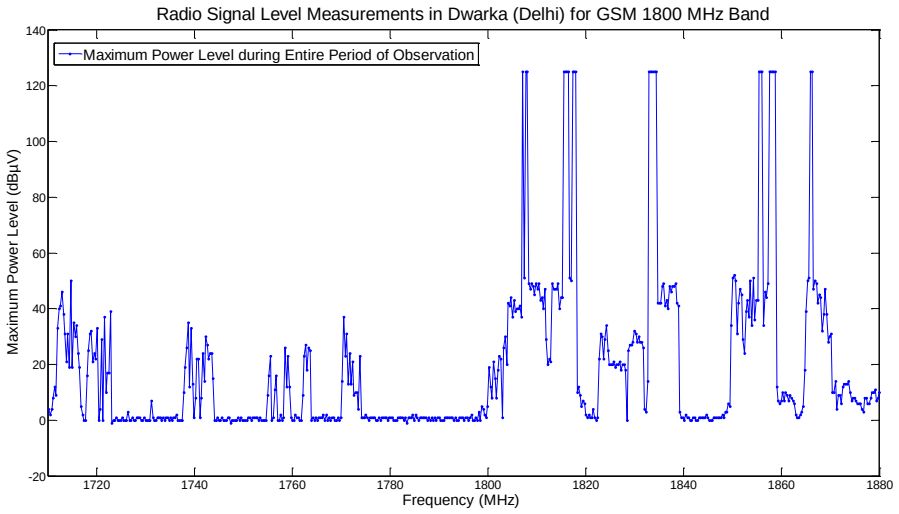

Figure 2-3-14: Maximum Power Level Measurements in Dwarka (Delhi) for GSM 1800MHz Band

Analysis of Spectrum Figures 2-3-9 to 2-3-14

While analyzing the results for the selected frequency bands (800, 900 and 1800 MHz), the following observations were made:

(i) Figures 2-3-9 (800 MHz), 2-3-11 (900 MHz), and 2-3-13 (1800 MHz) show that 2 pm is the second least utilized hour. This is a bit obvious due to the fact that most of the people are away from their residences for their daily works and other outdoor commitments;
(ii) 8 pm is the busiest hour among all of them. Most of the people, who have left their workplaces during 5-8 pm are gradually arriving their home. Also, most people prefer going for shopping during this period. Hence, this duration sees the mixture of traffic generated from entering subscribers and subscribers visiting markets. Therefore, 8 pm sees a lot of traffic generated from these activities;
(iii) The period of 5 pm sees the transition from least activity to the most activity in a single area and while measuring at the same point. The values of the 5 pm measurements coincide with the situation;
(iv) Figures 2-3-9 (800 MHz), 2-3-11 (900 MHz), and 2-3-13 (1800 MHz) also show that 11 pm has a very significant utilization pattern as compared to that of 8 pm. This is a bit surprising as subscribers are expected to cut down their activities as night progresses. However, it is not so surprising if the tariff plans of service providers are thoroughly investigated. Most of the service providers offer lower charges between 11 pm to 5 am, which they call as night plans. It may be seen that subscribers are using this facility to the fullest around 11 pm before closing for the day;
(v) The 2 am period sees a significant drop in the power level of radio signals in all the frequency bands except for CDMA 800 MHz band. This is due to the fact that in CDMA technology the data rate increases when active subscribers are low. The CDMA subscribers use this opportunity for internet activities such scheduled downloads, blogging etc; and,
(vi) Figures 2-3-10 (800 MHz), 2-3-12 (900 MHz), and 2-3-14 support the above observation by showing a significant maximum levels in the frequency bands of respective carriers.

Comparing the results for the measurement sites of CP and Dwarka together, it can be seen that during the hours when workplaces have higher average utilization, the residential places have a lower average utilization and vice-versa. Therefore, it can be interpreted that there is a shift of quanta of capacity between these two locations at different times. Despite that the quantum of capacity has left the location, the carrier configurations of the base stations remain unchanged. As a base station may allocate a channel to the subscriber among the available configured carriers, therefore, the average utilization of the entire set of carriers drops in cooling time (when the capacity quanta have left the location). This is an example of wastage of

carriers when viewed from a broader perspective and combinatorial analysis of two areas. The comparison also shows that how two distinct areas of two distinct behaviours may influence each other in carrier utilization. The service providers plan sites of the configuration that would be needed to cater the local subscribers; however, this combinatorial analysis proves that a big chunk of capacity is not there during a considerable length of time even though the base stations have been configured for them. This is the effect of '***Place-Time-Capacity (PTC)***' [24] that will be detailed in **Chapter 3, section 3.6** of this thesis. As a conclusion, that is drawn from this analysis:

(i) The service providers plan their base stations according to the maximum traffic generated in an area. However, the average utilization may be significantly poor in these areas; and
(ii) It is possible that multiple base stations that are placed at various locations may be serving the same set of subscribers at different times. Therefore, a number of base stations may depend on the subscribers' mobility as discussed in 'Place-Time-Capacity (PTC)' in chapter 3 of this thesis.

The above analysis is an example when people (subscribers) move from one place to another at different times. The next analysis will elaborate a case when there is a net influx of huge subscribers.

B. City of Mumbai

The city of Mumbai is the commercial capital of India (see, figure 2-3-15).

Figure 2-3-15: City of Mumbai

- Population/Area: 12,479,608/603.4 sq. km
- Co-ordinates: $19^{o}04'22"$ N, $72^{o}52'57"$ E
- Terrain: Mumbai lies at the mouth of the Ulhas River on the western coast. Mumbai is bounded by the Arabian Sea to the west. Many parts of the city

lie just above sea level, with elevations ranging from 10 m to 15 m, and the city has an average elevation of 14 m.

- Climate: Tropical climate, specifically a tropical wet and dry climate (AW) under the Köppen climate classification.
- Demography: Very high dense population and high humidity.
- Morphology: Mostly high-rise buildings, it is the city with the 12th highest number of skyscrapers in the world.

Motivation for conducting measurements: It is well known that a very famous carnival Lord Ganesh Visarjan (Visarjan means immersion) during September-October month of every year takes place in Mumbai (including other parts of the State of Maharashtra, India). On this festive occasion, millions of people all over participate in the procession; go for immersion of Lord Ganesh Idol into the sea (see, figure 2-3-16).

Figure 2-3-16: Crowd Gathering During Ganesh Immersion Festival

This huge gathering, accumulation and congestion of mobile subscribers, throw a challenge to the service providers for ensuring cellular services ubiquitously. A location known as 'Royal Opera House', Charni Road (1895'42" N, 7281'15"E) close to the immersion place was selected for taking measurements. The measurements were taken by recording average and maximum power levels for both the DL and UL frequency bands, under the conditions of pre and post procession periods.

It is important to note here that, in anticipation of huge subscriber influx, the service providers have installed many temporary base stations, which are known as "Cell on Wheels" (CoW) sites for the religious procession. A CoW site consists of a vehicle that has enough flat space to accommodate a base station, wireless backhaul unit, a mount for placing antennas (both serving and backhaul antennas), and, battery pack for powering the base station and backhaul units. The CoW site is placed where there is a temporary requirement of coverage or capacity and backhauled to the nearest point of interconnecting through a microwave antenna. As the spectrum availability is very thin in Indian Cities, the addition of CoW sites

disrupts the frequency plan and increases Signal to Noise plus Interference Ratio (SINR). However, to accommodate the booming subscribers this tradeoff is accepted by many service providers.

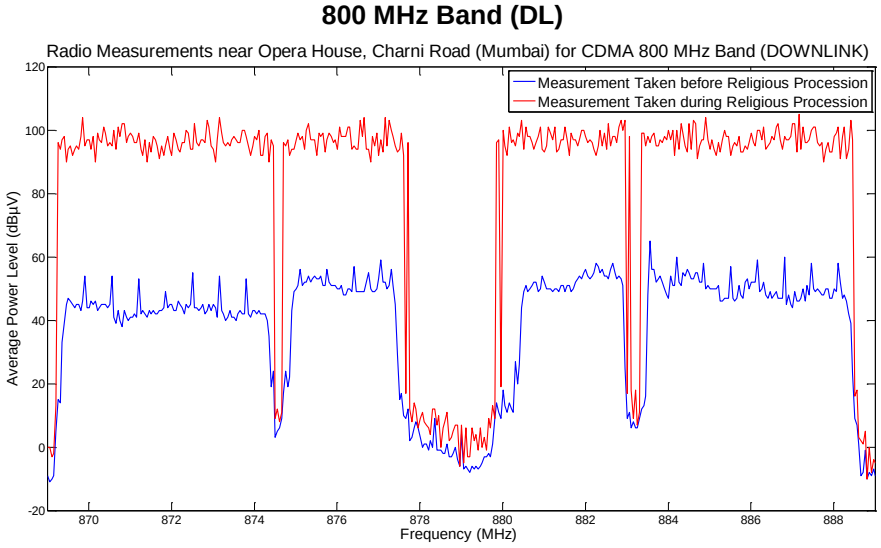

Figure 2-3-17: Average Power Level Measurements in Mumbai for CDMA 800MHz Band (Downlink)

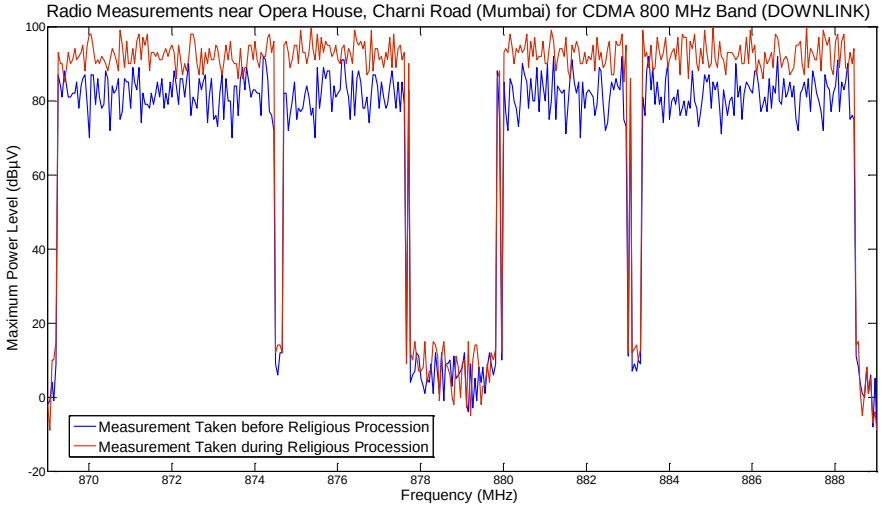

Figure 2-3-18: Maximum Power Level Measurements in Mumbai for CDMA 800MHz Band (Downlink)

In figures 2-3-17 and 2-3-18, the measurements of the average and maximum signal respectively are shown for the DL sub-band of the 800 MHz band for both pre and during the procession. The analysis of these figures is as follows:

(i) It may be observed that some portion of the entire downlink spectrum remains indifferent from the situations and remain insignificant during the measurements. The base stations were static during the entire course of measurement (including the CoW sites). Therefore, the carriers that were observed belonged to the service providers that have their base stations in the Area in Question (AiQ). It was found that this particular area has predominantly been served by a single service provider and it had a monopoly in this area and have many base station to cover this area. Hence, the sub-band that is allocated to this service provider shows the significant variations in the measurements whereas others remain quiet.

(ii) Figure 2-3-17 shows that the average of the duration for which a base station would radiate carrier power is higher during the time of passing of the procession than before the procession taking place. As a huge number of subscribers accumulate in the common vicinity, as shown in figure 2-3-16, the probability of a channel getting accessed is higher than any other normal time. This results in a higher utilization of the channel thereby increasing the average level of the signal which is clearly depicted in figure 2-3-17.

(iii) During the procession, the number of subscriber per unit area increase is hundreds-fold wise. Therefore, the higher the subscriber count, the higher is the chance of accessing a channel. This leads to poor SINR, and the base stations may have to transmit at higher power. These increased radiated powers were captured by the measurement apparatus that was installed in the **V/U**MMS and is presented in figure 2-3-18.

Occupancy statistics in Mumbai in 800 MHz (DL): *CDMA service in India uses a broader channel bandwidth than GSM 900 and 1800; the occupancy values are closely associated with each other. Before the procession, the average utilization of the downlink spectrum (869-889 MHz) is* ***77.2 %,*** *whereas during the procession it is 98.8 %, highest being 100% (see, the discussion on spectrum occupancy* ***in chapter 1****, referring formulations in the equations 1.1 and 1.2).*

The normal occupancy in the measurement of 77.2% shows that the area in mostly busy and amply utilized by the users. It is to be mentioned here that CDMA subscribers are lesser than that of GSM in India and mostly are used for data services.

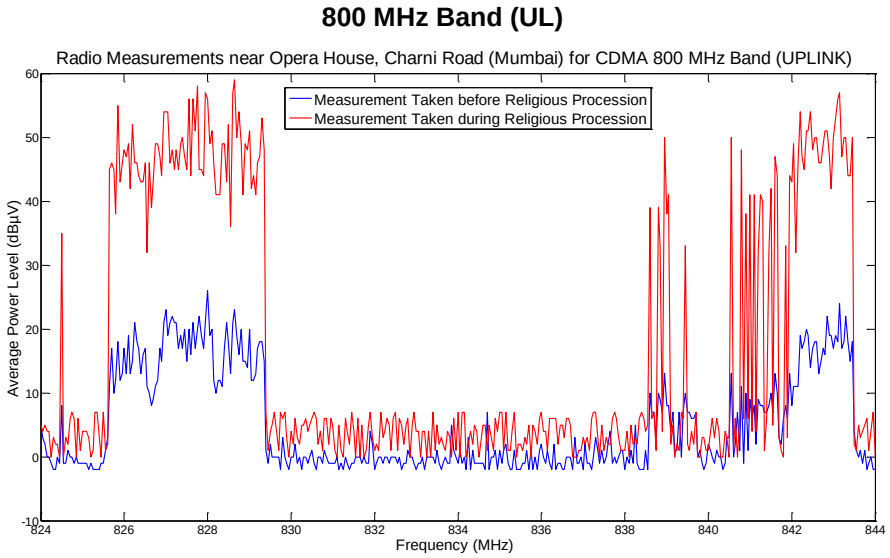

Figure 2-3-19: Average Power Level Measurements in Mumbai for CDMA 800MHz Band (Uplink)

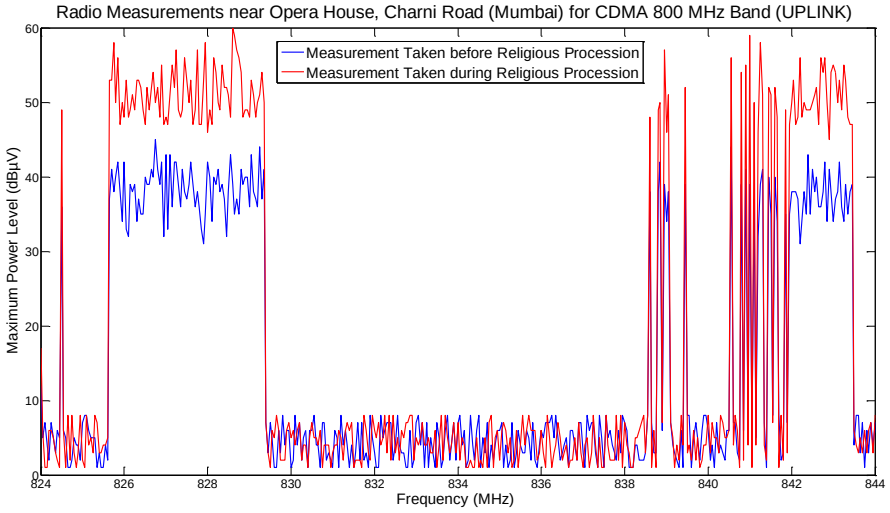

Figure 2-3-20: Maximum Power Level Measurements in Mumbai for CDMA 800MHz Band (Uplink)

In figures 2-3-19 and 2-3-20, the measurements of average and maximum signal respectively are shown for the UL portion of the 800 MHz band for both the pre and during the procession time. It can be seen that both maximum and average levels show a significant jump from "before" to "during" measurements. The analysis of figures 2-3-19 and 2-3-20 is as follows:

(i) The V/UMMS is stationary and observes the signal levels in its vicinity. Therefore, the subscribers who are moving closer to MMS may be subjected to 'multipath' and 'shadowing' fadings and thus, would generate higher maximum amplitudes of the particular carrier. Hence, the maximum amplitudes will be recorded higher for more subscribers. From figure 2-3-16, it can be deduced that during the procession, the probability of finding an active subscriber (subscriber making a call) of a carrier is higher than any other normal time. Also, as the density of active subscribers increases, the SINR in that area decreases, which may force a mobile handset to perform at higher power. These effects are very much visible in the figure 2-3-20, which shows why the maximum signal levels of "during" measurement are higher than that of "before" measurements.

(ii) Similarly, in a situation comparable to what is shown in figure 2-3-16, the probability of a UL channel to be used for a longer time is higher than any other normal situation. This is very much visible in figure 2-3-19, where the average utilization increases from "before" to "during" measurements.

Occupancy statistics in CP in 800 MHz (UL): The uplink CDMA band (824 - 844 MHz) is 72.6 % average utilized (*see, discussion on spectrum occupancy in chapter 1 referring formulations in equations 1.1 and 1.2) before the procession, highest being 81.1%. The occupancy during the period when a procession is taking place is measured to be 92.4%, the highest being 98.2%. This is not surprising as the accumulation instances lead to multiple call initiation for both data access and, data and voice calls.*

The explanations and analysis of figures 2-3-21 and 2-3-22 hold the same justifications as mentioned for the 800 MHz band except for few variations as discussed below:

(i) Comparing figures 2-3-18 and 2-3-22, it can be seen that the maximum power of GSM base stations is higher than that of the CDMA base stations. This is because the GSM channels are narrow band channels and, therefore, have to operate at a higher level to overcome the noise.

(ii) CDMA is a wide band channel service, and can operate at lower power to sustain against the noise. Unlike that of CDMA, all GSM bands operate in AiQ, as seen by comparing figures 2-3-17, and 2-3-18 with 2-3-21 and 2-3-22. When the area was investigated, it was observed that the GSM service providers have installed more CoW sites than that of CDMA

service providers. This can be linked to the fact that the GSM subscribers are significantly higher than the CDMA ones. Also, because the CDMA technology can operate at lower power to sustain against noise than that of GSM; this has brought down the need for CoW sites for the CDMA service providers. The accumulation of all GSM carriers in the same area through CoW sites (and overloading base stations) may have affected the frequency reuse plan and reduced the SINR.

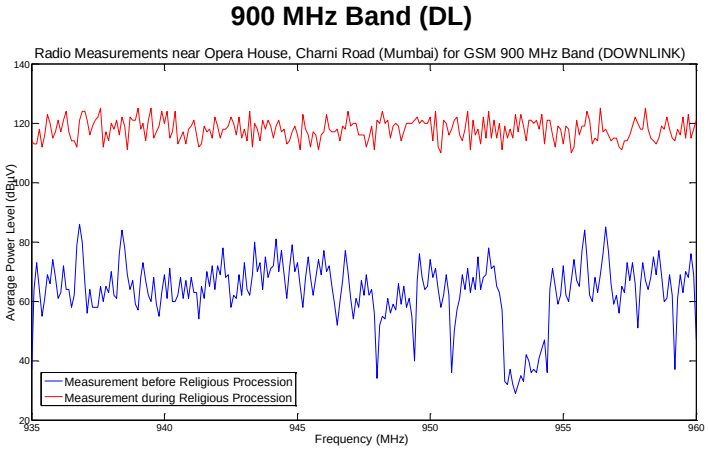

Figure 2-3-21: Average Power Level Measurements in Mumbai for GSM 900MHz Band (Downlink)

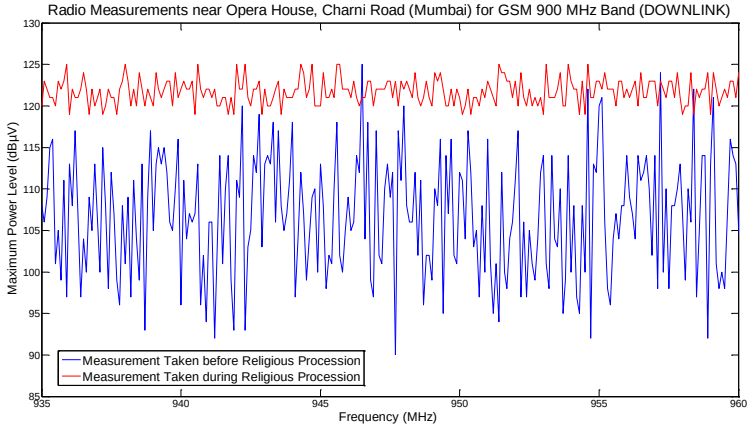

Figure 2-3-22: Maximum Power Level Measurements in Mumbai for GSM 900MHz Band (Downlink)

Similarly, figures 2-3-23 to 2-3-28 can be explained with the above-mentioned reasoning.

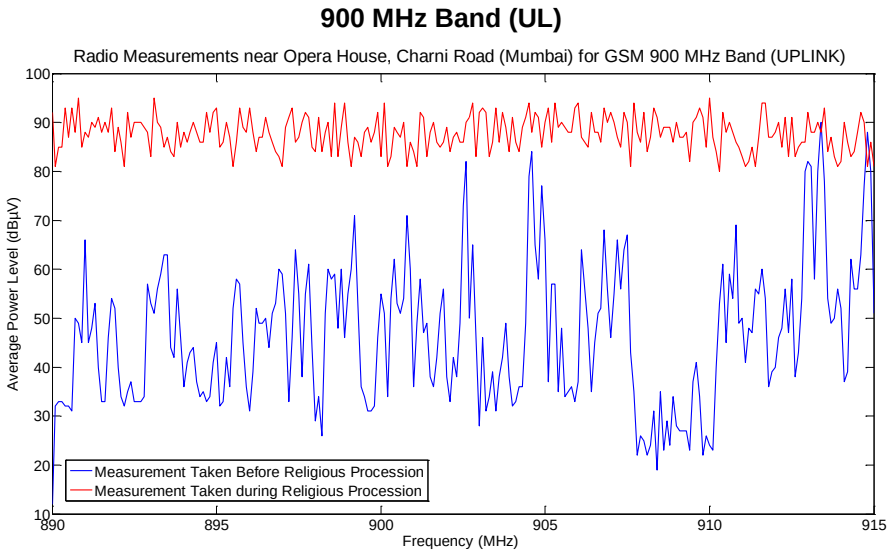

Figure 2-3-23: Average Power Level Measurements in Mumbai for GSM 900MHz Band (Uplink)

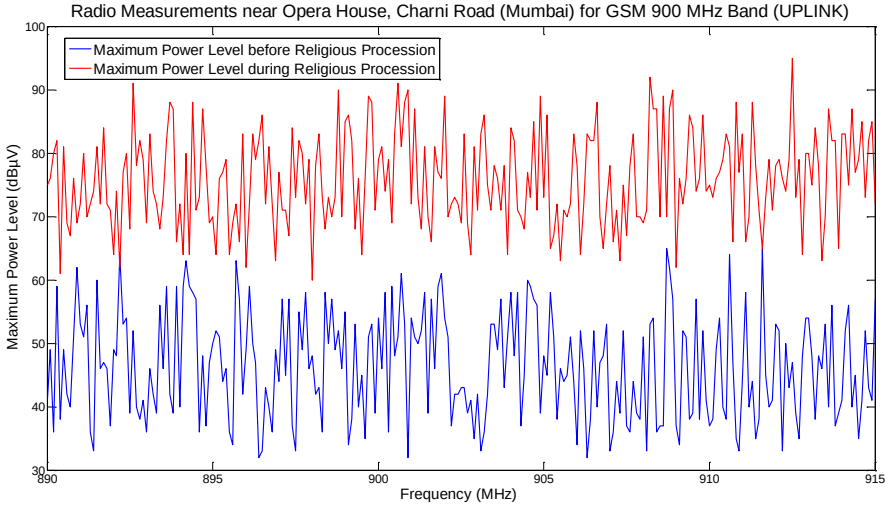

Figure 2-3-24: Maximum Power Level Measurements in Mumbai for GSM 900MHz Band (Uplink)

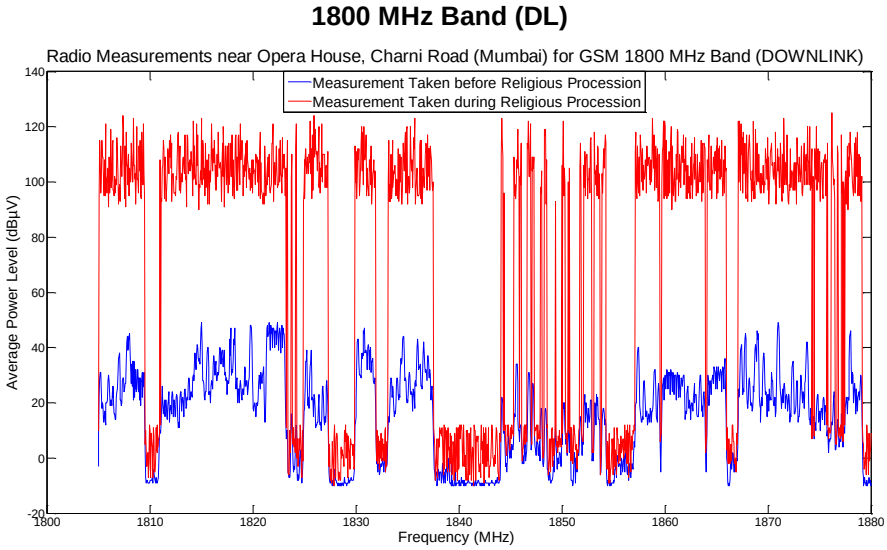

Figure 2-3-25: Average Power Level Measurements in Mumbai for GSM 1800MHz Band (Downlink)

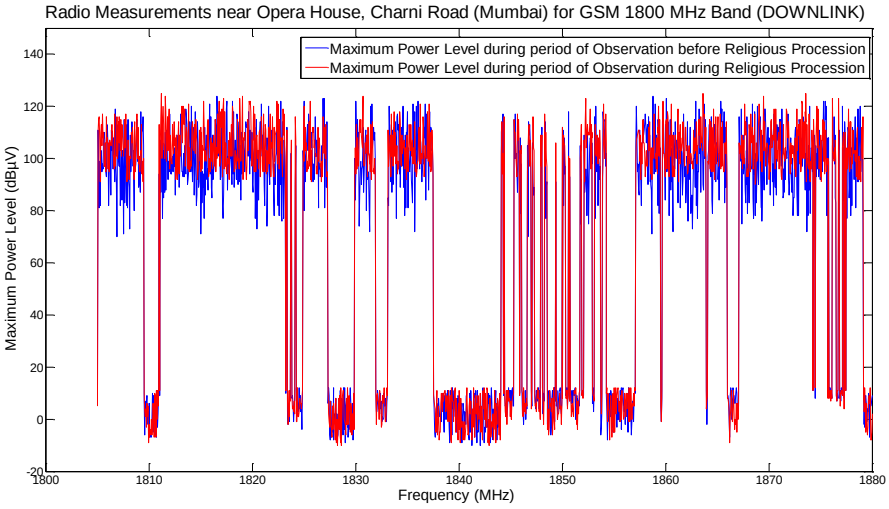

Figure 2-3-26: Maximum Power Level Measurements in Mumbai for GSM 1800MHz Band (Downlink)

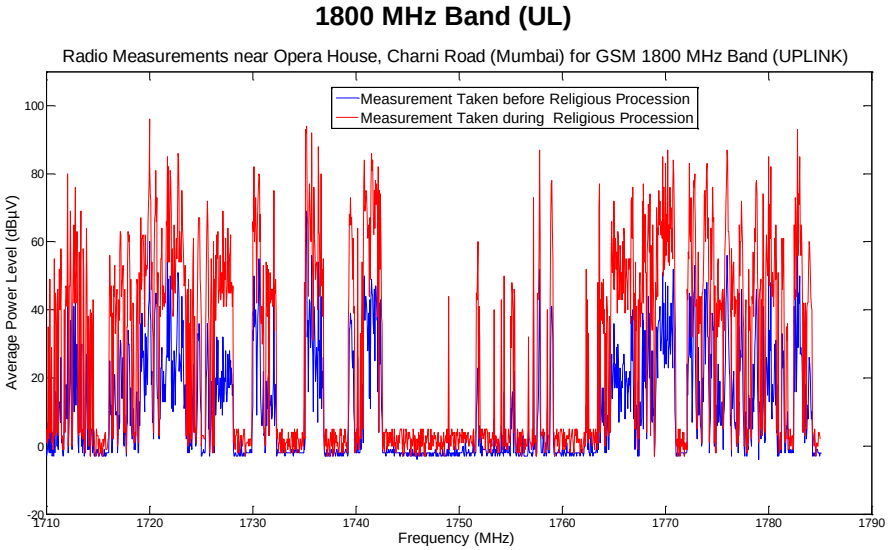

Figure 2-3-27: Average Power Level Measurements in Mumbai for GSM 1800MHz Band (Uplink)

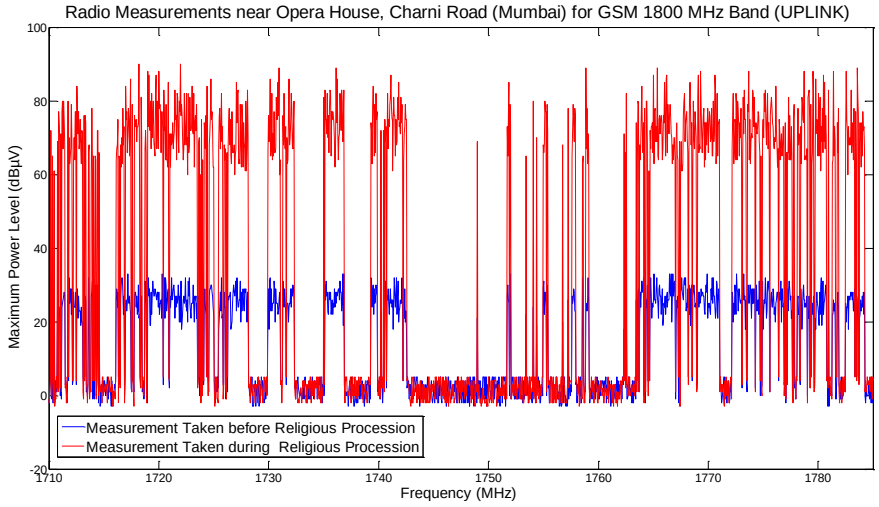

Figure 2-3-28: Maximum Power Level Measurements in Mumbai for GSM 1800MHz Band (Uplink)

Occupancy statistics in Mumbai in 900 MHz (DL): *Unlike the CDMA band, the GSM band is more fragmented with each carrier being 200 KHz wide for GSM 900 and GSM 1800. Being a more favoured service, the spectrum utilization in the GSM*

band is higher than that of CDMA. The average utilization of the GSM 900 downlink band is measured to 89.7% and, highest being 96.6% before the procession and 100% during the procession. However, during the procession, the GSM 900 experienced higher call drops than that of CDMA. A detailed discussion of call success rates is also presented in ***chapter 6*** *of this thesis (in reference to figures 2-3-21 and 2-3-22).*

Occupancy statistics in Mumbai in 900 MHz (UL): *The channel occupancy for GSM 900 uplink (890-915) was observed as 92.2% before the procession, highest being 98.2% being the highest and 100% during the procession (in reference to figures 2-3-23 and 2-3-24).*

Occupancy statistics in Mumbai in 1800 MHz (DL): *Service providers in 1800 MHz face problems due to higher propagation loss and higher absorbtion. The number of sites per area is higher than GSM 900 whereas the carrier bandwidth still being 200 KHz. The spectrum utilization is sharper than GSM 900 and average utilization is 86.2 %, highest being 97.8% before procession and 100% during procession (in reference to figures 2-3-25 and 2-3-26).*

Occupancy statistics in CP in 1800 MHz (UL): *The average UL utilization for GSM 1800 uplink is observed as 88.3%, highest being 92.7% before procession and 100% during the procession (in reference to figures 2-3-27 and 2-3-28).*

Apart from the previous explanations that have been applied to figures 2-3-25 to 2-28, it can also be seen that the deviation from "before" to "during" average values is higher than other technologies. This is because being a narrow band and higher carrier frequency service, the service provider utilizing the 1800 MHz band sees the quicker power dissipation as compared to 800 and 900 MHz bands. Therefore, the number sites needed to cover an area by an 1800 MHz service provider is higher than that of the lower bands. However, it was found that the 1800 MHz has fairly lesser sites than what is required; therefore, the existing base stations have to over perform to compensate the loss. This can be seen in the DL figures (2-3-25 and 2-3-26) of the 1800 MHz band.

2.4. PATH LOSS VARIATION IN AN INCREMENTAL GATHERING OF PEOPLE: A STUDY IN 1400 MHZ FREQUENCY BAND.

In section 2.2 above, the status of the frequency band 470-698 MHz, recommended by ITU, as one of the potential candidate frequency bands for IMT applications was described. Further, section 2.3 above, full details about the status with respect to measurements relating to occupancy and its analysis in the frequency bands 800, 900 and1800 MHz currently being used for commercial mobile services (IMT applications) was given. Summing this, a detailed study was carried out for both the categories of IMT bands.

The analysis reveals that besides the 470-698 MHz, there is another frequency band namely the 1400 MHz that has also among others been recommended by ITU for IMT applications. As per the International Table of Frequency Allocations, out of about 90 MHz in this frequency band, a major portion stands earmarked only for FIXED (FX), and MOBILE (MO) services on primary basis globally. However, presently there are no commercial mobile services in this frequency band; there might be some point-to-point terrestrial fixed (FX) wireless links. The National Frequency Allocation Plan-2011 of India has made a provision in this band for experimental/trial/pilot-study purposes for indigenously developed technologies for point-to-point backhaul and point-to-multipoint access systems [see, IND 53, page 155 of Reference 15]. Since there are no commercial mobile operations, hence no signal from any other BTSs is expected to be transmitted, for this reason, this band has been chosen for clean measurements and analysis regarding variation in path-loss of radio signals due to huge crowd gathering. The results of these analyses shall be useful for endorsement of further work reported in this Thesis.

This Section gives a detailed analysis about the impact of the accumulation of people in an open area, on the propagation of radio wave at 1400 MHz. A theoretical discussion relating to propagation loss due to the random accumulation of people is presented in **Appendix 2.4**. These accumulations of crowd occur in the event of any carnival or other similar events like sports meet in any stadium etc. In the present study, an advantage of a very famous Goa Carnival that takes place every year normally in the month of February, in selecting a suitable site for measurements was taken. This Carnival is attended by thousands and thousands of people, and they accumulate either for recreation or procession.

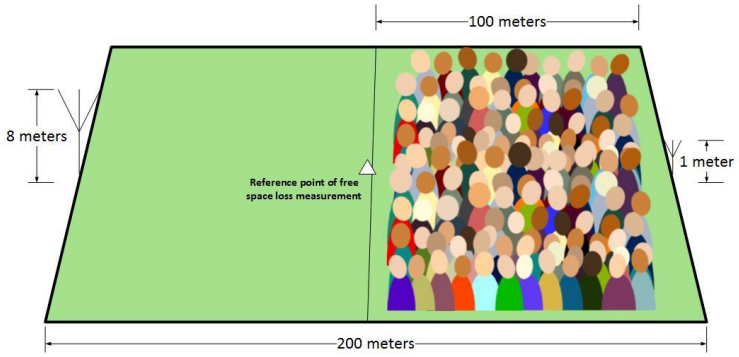

Figure 2-4-1: Experiment setup

For the path-loss measurements, an open area, far away from dwellings and water bodies, measuring 10,000 (200 meters x 50 meters) square meters, in Goa was selected, where it was ensured that there are no terrestrial wireless point-to-point links operating in the 1400 MHz frequency band active within 1000 meter radius to

create any interference. This location was divided into two portions, each one measuring 5000 (100 meters x 50 meters) square meters demarcated as 'X' and 'Y' respectively. A transmitter unit (TXU) is positioned at one corner of the location and receiving unit (RXU) is placed at another corner, as shown in figure 2-4-1.

It may be mentioned that the free space loss was measured, when the TXU was placed at 'A' and RXU at 'B', in the area of 'X', which are separated by a distance of 100 meters. Thereafter, for the purpose of all the measurements, TXU remain at 'A', whereas, RXU is shifted to 'C'. Peoples were requested to enter through a gate 'G', in another portion 'Y'. After entering the area, they were expected to scatter and randomly move across the Area in Question (AiQ).

2.4.1. MEASURING SETUP AND PROCEDURES

The measuring setup consists of a Transmitting Unit (TXU) and a Receiving Unit (RXU). TXU consisting of a sweep oscillator, a microwave frequency counter and a source synchronizer for locking the desired frequency are assembled and installed on the base platform. The transmitting half-wave dipole antenna is attached, which is at a height of 8 meters from the ground level. The transmitter is tuned to radiate a power of 10 watts i.e. 40 dBm. A CW signal from the oscillator is fed to the transmitting antenna through the directional coupler, which provides directivity of typical 23 dB. RXU encompassing a Spectrum Analyzer (SA) capable of receiving radio signals from 30-3000 MHz and a Personal Computer were installed on a fixed platform attached to a receiving antenna of a total height of 1 meter above the ground level. The maximum gain for this frequency band is 13 dBi for both transmitting and receiving antennas. In the first instance, the transmitter was tuned to radiate a signal power of 10 Watts at 1400 MHz and the measurements were performed in the following steps:

(i) The measurements were taken for each sample from 1 second to 1200 seconds in steps of 100 seconds i.e. for a total of 20 minutes.
(ii) Initially, the free space loss was measured at both positions 'B' and 'C' with no people on the ground.
(iii) Then, a group of 10 people was allowed to enter the area, scatter and almost randomly move within the area. The measurements were taken for 20 minutes while they were wandering in the area.
(iv) Similarly, the measurements were taken for a group of 50 and 100 people respectively, each for 20 minutes.
(v) Thereafter, the measurements were taken for each of the group of people counting from 100 to 1000 in steps of 100 in the similar fashion.

The first set of measurements, recording receive signal levels, were taken each with group 0 people to 1000 people count for the time of sample from 1 to 1200 seconds. The results are depicted in figure 2-4-2.

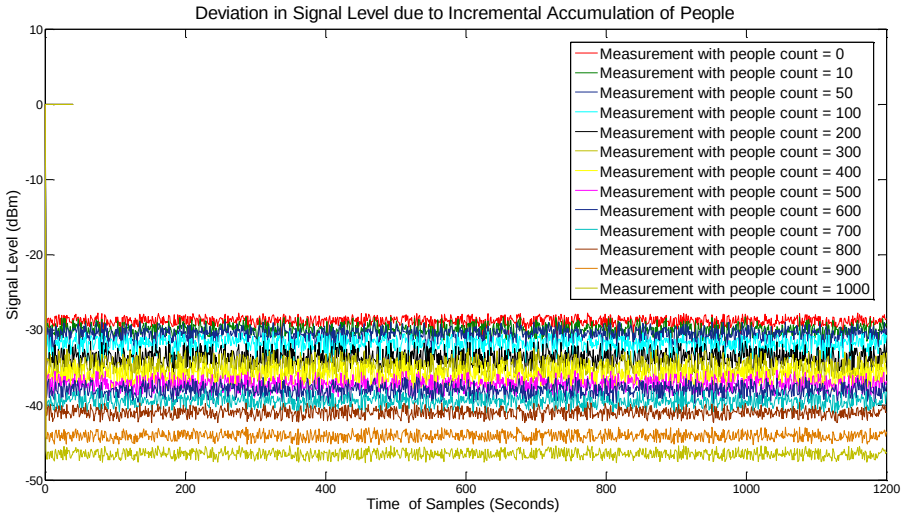

Figure 2-4-2: Deviation in the Signal Level due to Incremental Accumulation of People

Measurement Set-1 depicts the pattern of the received signal power (figure 2-4-3) when the people's gathering range from 10 to 1000, scattered in 5000 square km area and time of samples was 100th second in all kinds of gathering. Similarly, Measurement Set-2 depicts the pattern of the received signal power (figure 2-4-4) when the people's gathering range from 10 to 1000, scattered in 5000 square km area and time of samples was 200th second in all kinds of gathering.

Measurement Set-3 depicts the pattern of the received signal power (figure 2-4-5) when people's gathering range from 10 to 1000, scattered in 5000 square km area and time of samples was 300th seconds in all kinds of gathering. Similarly, Measurement Set-4 depicts the pattern of the received signal power (figure 2-4-6) when people's gathering range from 10 to 1000, scattered in 5000 square km area and time of samples was 400th second in all kinds of gathering.

Measurement Sets-5 and 6 depict the pattern of the received signal power (figures 2-4-7 and 2-4-8) when the people's gathering range from 10 to 1000, scattered in 5000 square km area and time of samples were 500th and 600th second in all kinds of gathering.

Measurement Sets-7 and 8 depict the pattern of received signal power (figures 2-4-9 and 2-4-10) when the people's gathering range from 10 to 1000, scattered in 5000 square km area and time of samples were 700th and 800th second in all kinds of gathering.

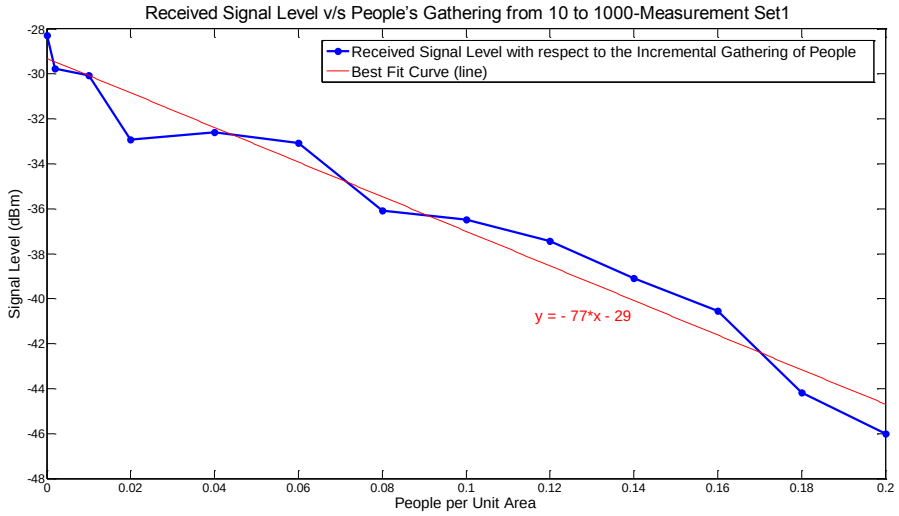

Figure 2-4-3: Measurement Set 1, Received Signal Level v/s People's Gathering

Figure 2-4-4: Measurement Set 2, Received Signal Level v/s People's Gathering

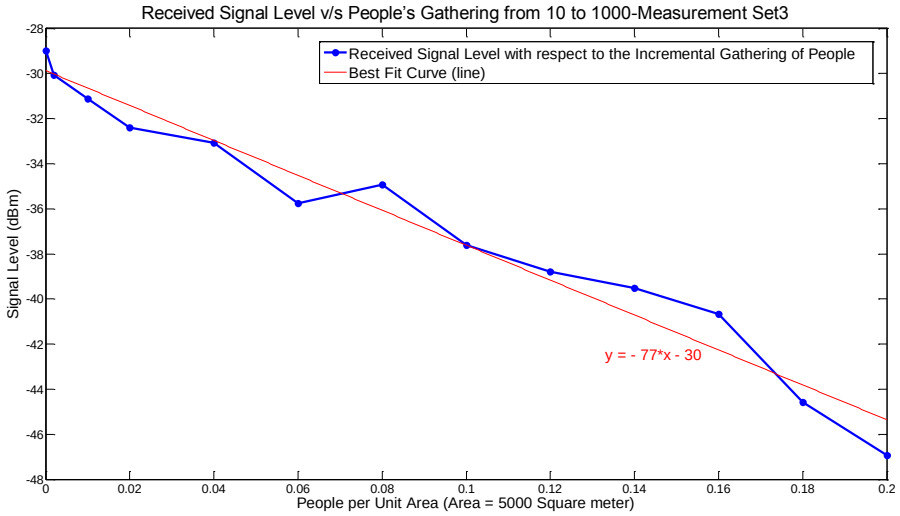

Figure 2-4-5: Measurement Set 3, Received Signal Level v/s People's Gathering

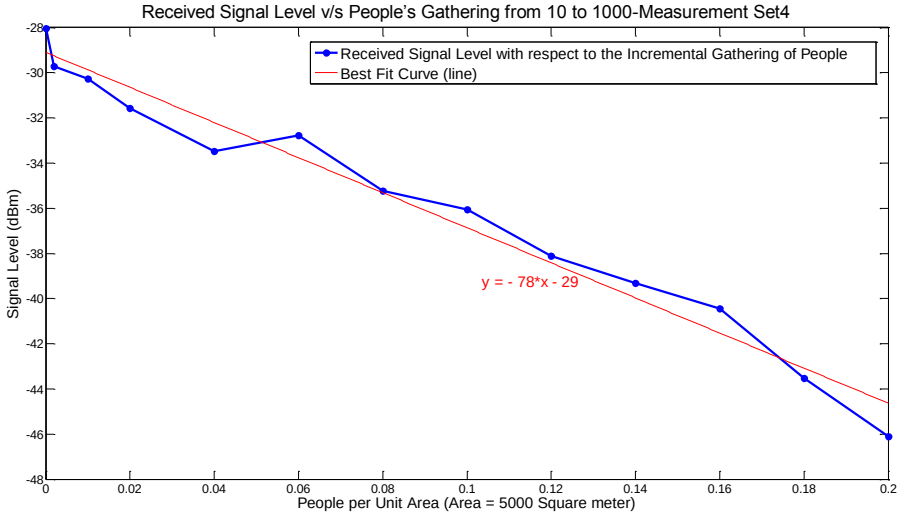

Figure 2-4-6: Measurement Set 4, Received Signal Level v/s People's Gathering

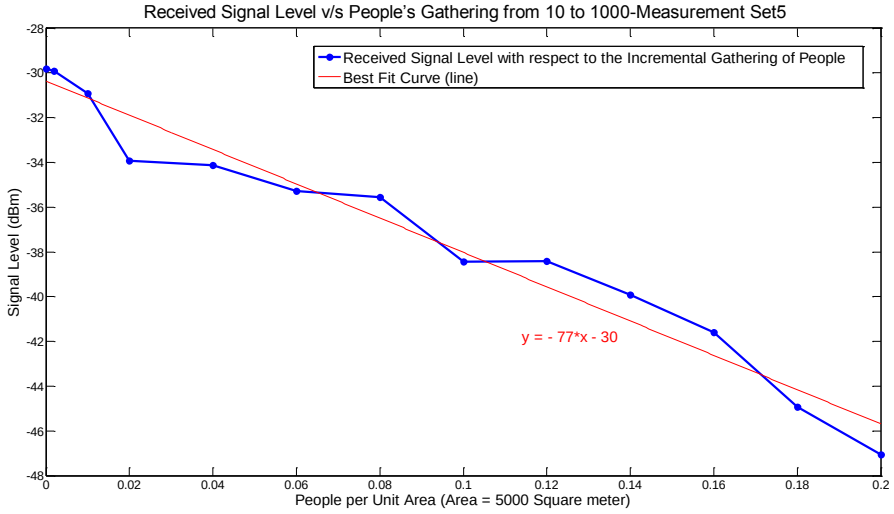

Figure 2-4-7: Measurement Set 5, Received Signal Level v/s People's Gathering

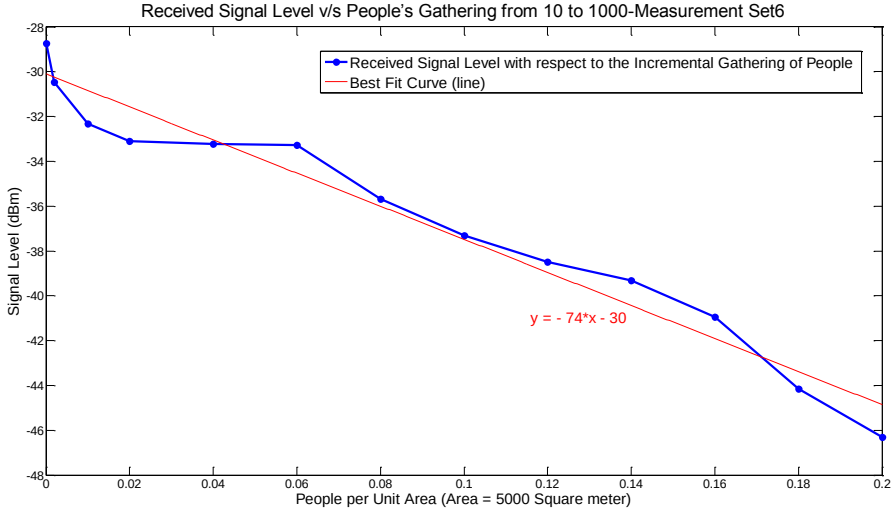

Figure 2-4-8: Measurement Set 6, Received Signal Level v/s People's Gathering

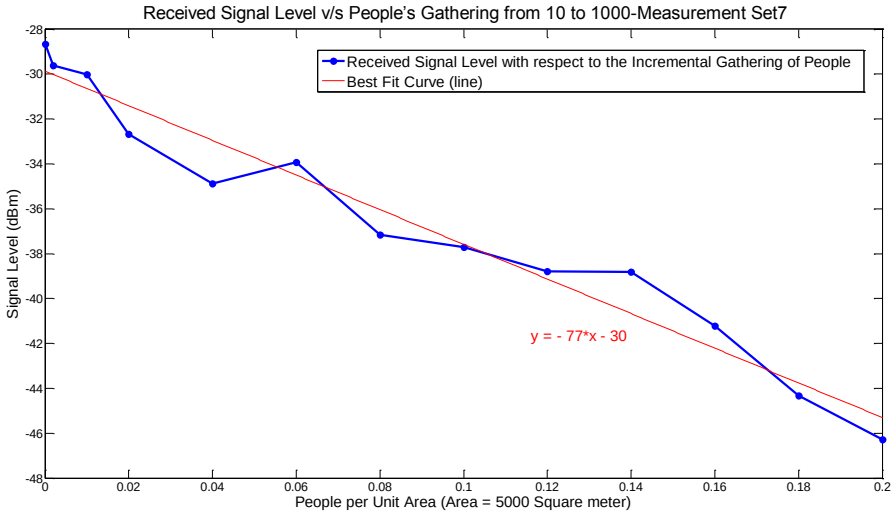

Figure 2-4-9: Measurement Set 7, Received Signal Level v/s People's Gathering

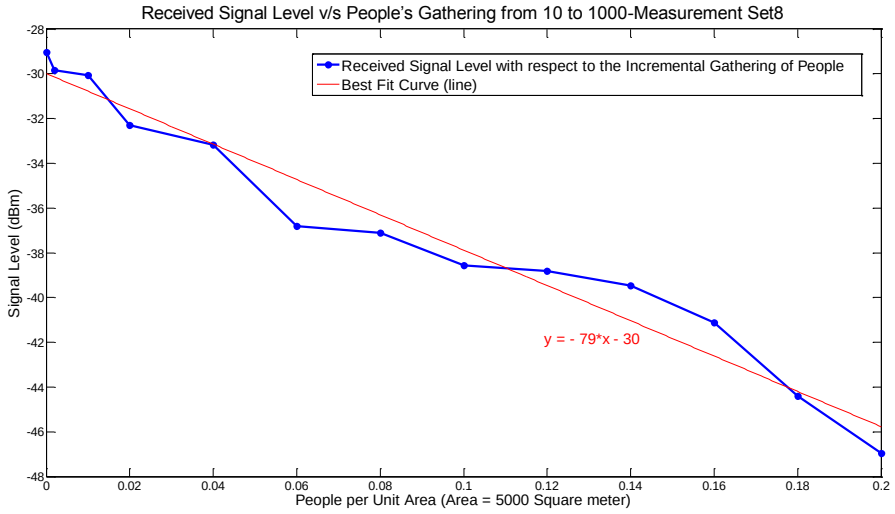

Figure 2-4-10: Measurement Set 8, Received Signal Level v/s People's Gathering

Similarly, measurement Sets-9 and 10 depict the pattern of received signal power (figures 2-4-11 and 2-4-12) when the people's gathering range from 10 to 1000, scattered in 5000 square km area and time of samples were 900^{th} and 1000^{th} second in all kinds of gathering.

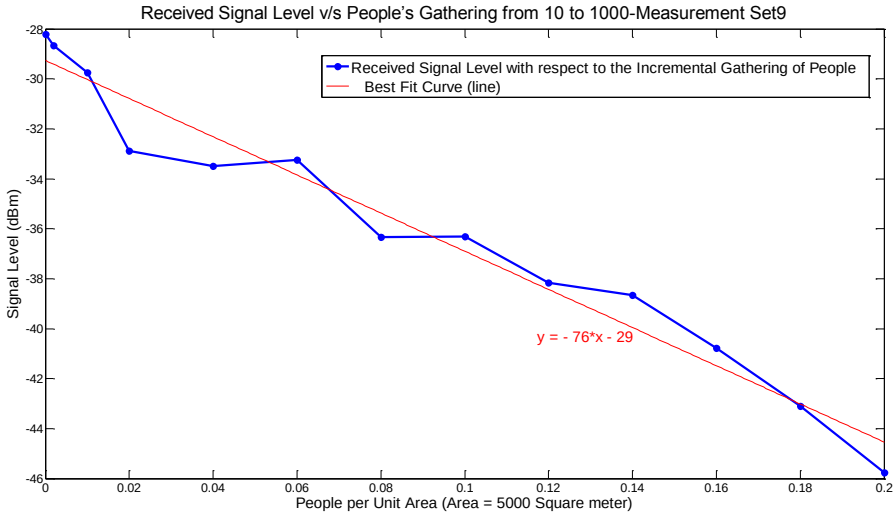

Figure 2-4-11: Measurement Set 9, Received Signal Level v/s People's Gathering

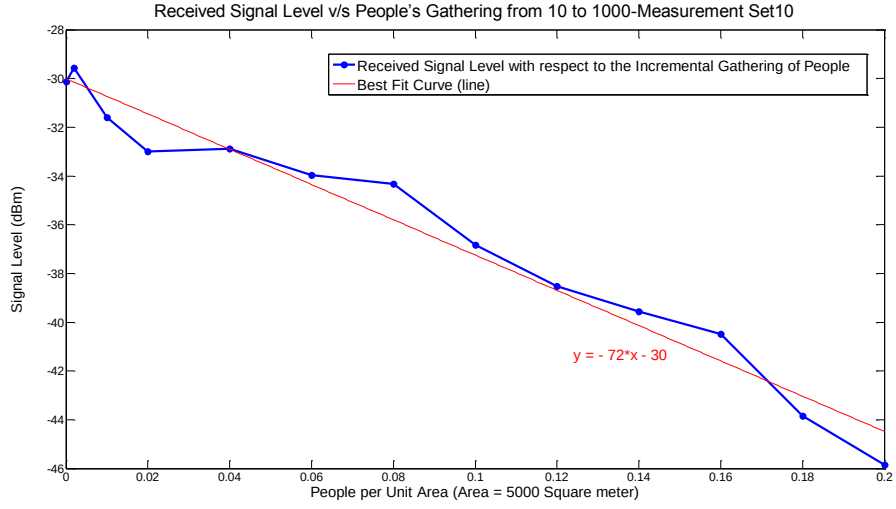

Figure 2-4-12: Measurement Set 10, Received Signal Level v/s People's Gathering

A summarized picture showing the signal level variation due to the accumulation of 10 to 1000 people in 5000 square meter area is depicted in figure 2-4-13

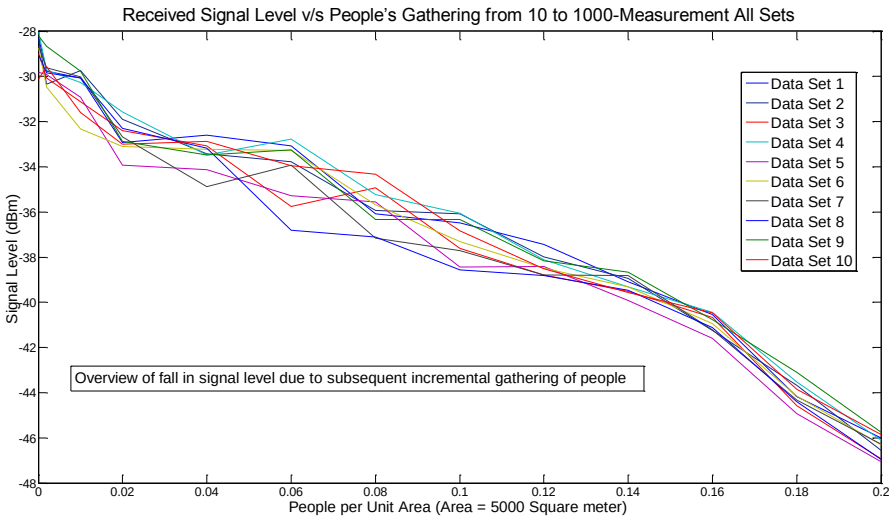

Figure 2-4-13: Received Signal Level v/s People's Gathering, a summarized picture

The mean value of the received power level v/s the number of people per unit area as evaluated is shown in figure 2-4-14.

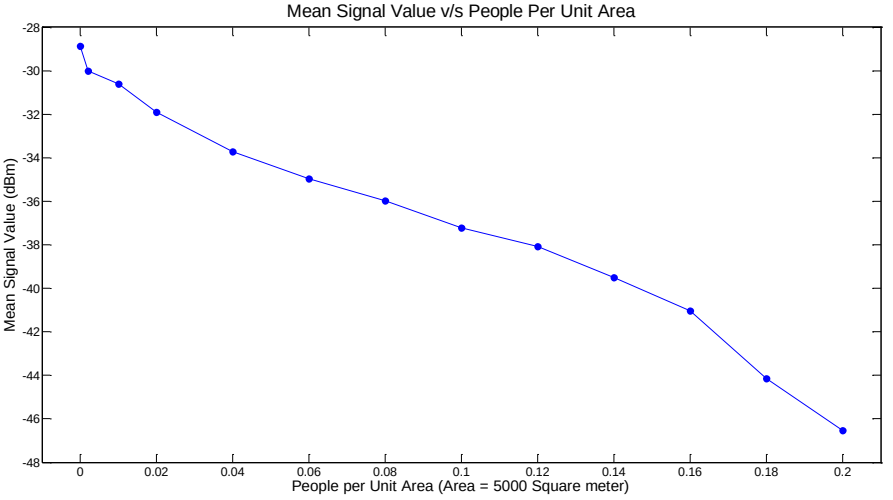

Figure 2-4-14: The mean value of Received Signal Level v/s Number of People per Unit Area

The maximum distance, from the mean and standard deviation values of the received power level v/s the number of people per unit area, as evaluated, are presented in figure 2-4-15.

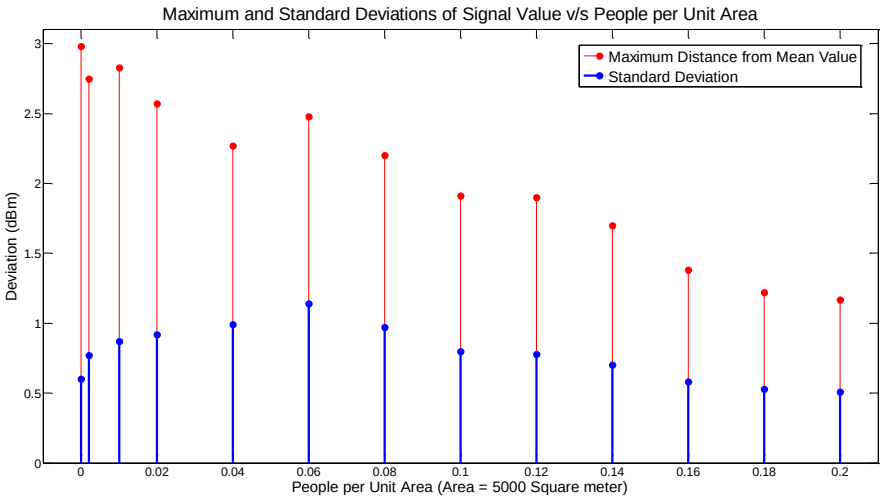

Figure 2-4-15: Mean and Standard Deviation

2.4.2. RESULTS AND ANALYSIS

It can be seen from the measurement results of Set 1 to Set 10, which had been taken at different samples of time that the pattern of signal power remained the same. However, the signal power varied with an increase in the number of people per unit area. It has been observed that when there are no people, the received signal power for all the sets (1 to 10) of measurements vary between -28 to -30 dBm. This signal level drops by -18 to -20 dBm when people per 5000 square meter are 0.2 i.e. 1000 people gathered and randomly moving in the area of 5000 square meters. However, from the measurement Sets 1 to 10, it is evident that for any time of sample say from 100th to 1000th, variation in signal level remains constant. The analysis of the measurements taken, in a fixed area that is the position of transmitting and receiving units remaining unchanged, reveals that the value of 'path-loss exponent' varies with people's assembly. With the increase in a number of people, the value of 'path-loss exponent' increases and drift away from the 'free space path-loss exponent of value- 2'. From figure 2-4-14, it can be seen that the mean signal level v/s people population density, lies in the range of -28 to -48 dBm. The figure 2-4-15, showing the maximum distance from the mean and standard deviation (SD) values of received power level v/s number of people per unit area, demonstrates that maximum value of 'SD' of the mean signal value is little over 1 dBm. Further, the maximum distance from the mean value touches a value of approximately 3 dBm.

2.5. RESEARCH QUESTIONS (RQ) ADDRESSED IN CHAPTER 2

For the future development of IMT for 2020 and beyond, the study shall be directed to evolve technical and operational characteristics including protection criteria in various deployment scenarios for use in sharing/interference studies in the frequency range 24.25-86 GHz.

RQ 1- Efficient Use of Already Assigned Radio Spectrum for IMT Applications

The measurement campaign in the frequency bands 800 MHz, 900 MHz and 1800 MHz as presented in this Chapter revealed that the assigned spectrum is not fully utilized at certain locations in a service area and time.

- What technologies and methodologies should be deployed to potentially tap the unutilized portion in that geographical area?

RQ 2- Sharing Studies and Protection Criteria in the additional frequency bands for IMT application allocated by WRC-15

In this chapter, it was mentioned that to implement an Agenda item 1.1 of WRC-12, a Joint Task Group was formed to study and recommend additional frequency bands for IMT applications (see, 2.1.4 of Appendix 2.1). The recommendations were considered by WRC-15, which earmarked few frequency bands starting from 470 MHz to below 6 GHz. Through experimental studies in the frequency band 470-698 MHz, it has been demonstrated that how the sharing parameters impact both operations of IMT and Broadcasting applications.

- What are the detailed studies required relating to sharing and protection criteria in other similar additional frequency bands earmarked for IMT applications?

RQ 3- Challenges in providing uninterrupted mobile services in a highly populated traffic areas

It was presented that random and dynamic movement of people, in highly demanding areas namely a carnival, huge sports events or natural/man-made disasters, pose a severe challenge to the service providers for meeting their demands. In such situations, the existing network deployment models to cater the static mobile users fail to predict and plan for such eventualities. In this chapter, detailed measurements were carried out for a carnival-like situation in the frequency band of 1400 MHz.

- What simulation models should be developed in several existing and proposed frequency bands for IMT applications that shall take care of random and dynamic movement of people?

RQ 4- Deployment of the frequency bands 24.25 GHz -86 GHz for IMT-2020 (5 G)

a) What are the requirements of the potential users for the further development of IMT?
b) What are the spectrum-related issues including its efficient usages for the further development of IMT that need to be provided within the time line of 2020?
c) What studies are required in the modelling and simulation of IMT networks for use in analysis of sharing and protection criteria?

RQ 5- Change in the path-loss exponent with subscriber density.

With an objective to analyse the impact of the subscriber accumulation, the discussions in the section 2.5 covey that the subscriber's accumulation significantly impacts the propagation losses measured at receiver ends.

a) The granularity of the subscriber also results in multiple fluctuations of the decaying path-loss.
b) The area planned according to certain model is thus likely to fail in providing services to the benchmark level.
c) The path-loss regressing identified due to the accumulation of people is provided by an approximated equation:

$$y = -76x - 28 \quad (2.5.1)$$

A detailed analysis in relation to the impact of the accumulation on the Path Loss Model is given in **Chapter 3** of this thesis.

2.6. CONCLUSIONS

The performed measurements and their outcome, gave the incentive to propose an innovative architecture that could cater for the irregularities that are generated due to the random accumulation of the subscribers. India was chosen as a suitable scenario due to its richness in both 'kind of services', and 'kind of user behaviours'. The spectrum issues require functionalities that must incorporate all kind of services; hence, an overall picture of the spectrum utilization was needed and performed as a detailed measurement campaign. To obtain the collective sense of the spectrum utilization by various services in a single area, a series of measurements were conducted for ensuring the actual utilization of the spectrum bands earmarked for IMT applications. The spectrum bands included those already assigned or proposed for future assignments. The spectrum utilization is not as per norms and tends to vary at different time slots. The issue of introducing IMT applications in the proposed bands is quite complex as these identified frequency

bands are shared by various radio services; hence co-existence of those services with IMT applications is a challenging task.

During the measurements, it was observed that (i) channel occupancies increase significantly in all bands and kinds of services due to accumulations. Even in the busiest area, the variation in occupancies before and during occupancy is well around 5-15%. This means that either the Network Service Provider (NSP) may overplan the network for such issues or, the area faces severe call drops during the event. (ii) The receive signal level may drop by more than 10 dBm due to the accumulation of people in an area. This means that areas served with low powered radios or at cell edges may get levels below receive sensitivity just when people are accumulating in higher amounts. Further, the frequency band 470-698 MHz investigated to allow for the co-existence possibilities in an Indian scenario. In this frequency band, there are a large number of existing operations of broadcasting (TV) and other fixed wireless networks. Hence, it is a challenging task before the planners to protect the existing operations and at the same time make room for the future commercial IMT applications. For the sake of understanding the vacancy and occupancy of the radio signals in this frequency band, extensive on-site field measurements were carried out in the City of Delhi (India). These measurements revealed that the 470-698 MHz band is fully occupied with the existing wireless operations. Therefore, with a view of opening this band for future IMT applications, either some of the existing usages need to be re-located to other frequency bands or enough room is made available for co-existence of radio services. Further, in order to find how the assigned spectrum for commercial mobile applications i.e. 2G (CDMA and GSM) is being utilized, a 24- hour spectrum usage pattern was studied. The cities/locations selected for the measurements were Delhi and Mumbai. This assessment was necessary from the point of view of their future deployment, where there are low or no active usages. It has been observed that the average utilization of these signals is strongly correlated with the subscriber behaviour. It has been established that the average utilization of the entire set of carriers drops in cooling time.

It has been observed from the measurement plots that the spectrum occupancy of the UL and DL are not the same. On the UL, poor visibility of the occupancy was noticed. It was observed that for every case, there is a significant reduction in the average utilization of the carriers and the average utilization has fallen by more than 40%. In an another study, measurements at 1400 MHz in a city of Goa, India were performed to assess the pattern of received signal power due to the accumulation of a large number of people in an open area. The measurements were taken at different time intervals, but it has been observed that whatever time is chosen, it had no impact on the deviation of the signal power, however, it is only the number of people per unit area that impacted the received power levels. In this situation, the 'Path Loss Exponent' of the propagation path varied with an increase in people's population even though the transmitter and receiver positions remained stationary in

an open area. With the increase in a number of people, the value of 'path loss exponent' increases and drifts away from the '*free space path-loss exponent of value '2*'. From the measurement studies, it could be concluded that when there are no people, the received signal power vary between -28 to -30 dBm. However, the mean signal level v/s people population density lies in the range of -28 to -48 dBm.

REFERENCES

[1] "Cisco Visual Networking Index: Global Mobile Data Traffic Forecast Update, 2013-2018" Report.

[2] "GSMA, The Mobile Economy 2014", https://gsmaintelligence.com/research/-?file=bb688b369d64cfd5b4e05a1ccfcbcb48&download.

[3] Kwang-Cheng Chen, Ramjee Prasad, "Cognitive Radio Networks", published by Wiley, 2009, 372 pages.

[4] Haykin S, "Cognitive Radio: Brain-Empowered Wireless Communications", IEEE Journal on Selected Areas in Communications, 23, No 2, February 2005.

[5] P.S.M. Tripathi, Ashok Chandra, Ambuj Kumar, K. Sridhara, "Dynamic Spectrum Access and Cognitive Radio' Presented at the 2nd International Conference on Wireless Communications, Vehicular Technology, Information Theory, Aerospace & Electronic System Technology, 28th February to 3rd March 2011.

[6] "Definitions of Software Defined Radio (SDR) and Cognitive Radio System (CRS)", Report ITU-R SM.2152. (09/2009).

[7] National Telecom Policy -2012, Department of Telecommunications, Government of India. www.dot.gov.in

[8] "Future spectrum requirements estimate for terrestrial IMT", M Series- Mobile, radio determination, amateur and related satellite services", Report ITU-R M.2290-0 (01/2014).

[9] Radio Regulations Articles of ITU, Edition 2012.

[10] Chairman's Reports of the Joint Task Group 4-5-6-7 meeting held in July and October 2013. http://www.itu.int/md/R12-JTG4567-C-0584/en.

[11] "Prediction procedure for the evaluation of interference between stations on the surface of the Earth at frequencies above about 0.1 GHz", Recommendation ITU-R P.452-15 (09/2013). http://www.itu.int/rec/R-REC-P.452/en.

[12] "System parameters and considerations in the development of criteria for sharing or compatibility between digital fixed wireless systems in the fixed service and systems in other services and other sources of interference", Recommendation ITU-R F.758-5 (03/2012).

[13] "Necessary and occupied bandwidths and unwanted emissions of digital fixed service systems", Recommendation ITU-R F.1191. http://www.itu.int/rec/R-REC-F.1191/en.

[14] "General methodology for assessing the potential for interference between IMT-2000 or systems beyond IMT-2000 and other service", https://www.itu.int/dms_pubrec/itu-r/rec/m/R-REC-M.1635-0-200306-I!!PDF-E.pdf.

[15] "National Frequency Allocation Plan-2011", http://www.wpc.dot.gov.in/Docfiles/-National%20Frequency%20Allocation%20Plan-2011.pdf.

[16] "Monte Carlo simulation methodology for the use in sharing and compatibility studies between different radio services or systems", ITU-R SM.2028. http://www.itu.int/dms_pub/itu-r/opb/rep/R-REP-SM.2028-1-2002-PDF-E.pdf.

[17] Federal Communications Commission, Spectrum Policy Task Force, November 2002, Report. ET Docket No. 02-135.

[18] Aguilar-Gonzalez, R. ; Fac. de Cienc., et al, "Spectrum Occupancy Measurements below 1 GHz in the City of San Luis Potosi, Mexico", IEEE 78th Vehicular Technology Conference (VTC Fall), 2-5 September 2013, pages 1-5.

[19] Hoyhtya, M. ; Matinmikko, M. ; Xianfu Chen ; Hallio, J., "Measurements and analysis of spectrum occupancy in the 2.3–2.4 GHz band in Finland and Chicago", 9th International Conference on Cognitive Radio Oriented Wireless Networks and Communications (CROWNCOM), 2014, 2-4 June 2014, pages 95 – 101.

[20] Kliks, Adrian; Kryszkiewicz, Pawel ; Perez-Romero, Jordi ; Umbert, Anna, "Spectrum occupancy in big cities, Comparative study, Measurement campaigns in Barcelona and Poznan", 10th International Symposium on Wireless Communication Systems (ISWCS 2013), 27-30 Aug. 2013, page 1–5.

[21] Barnes, S.D.; Maharaj, B.T. "A comparison of spectrum occupancy in the South African 900 MHz GSM cellular bands", AFRICON, 2013, pages: 1–5.

[22] Pedraza, L.F.; Molina, A.; Paez, I., "Spectrum occupancy statistics in Bogota-Colombia", IEEE Colombian Conference on Communications and Computing (COLCOM), 2013, pages 1 – 6.

[23] Palaios, A.; Riihijarvi, J.; Mahonen, P.; Atanasovski, V.; Gavrilovska, L.; van Wesemael, P.; Dejonghe, A.; Scheele, P., "Two days of European spectrum: Preliminary analysis of concurrent spectrum use in seven European sites in GSM and ISM bands ", IEEE International Conference on Communications (ICC), 2013, pages: 2666 – 2671.

[24] Ambuj Kumar, P. L. Mehta, and R. Prasad, "Place Time Capacity- A Novel Concept for Defining Challenges in 5G Networks and Beyond in India", Presented at the 2014 IEEE Global Conference on Wireless Computing and Networking (GCWCN)': December 2014.

[25] Rahim, A, Dresden, et al, "Impact of People Movement on Received Signal in Fixed Indoor Radio Communications" The 17th IEEE International Symposium on 'Personal, Indoor and Mobile Radio Communications, 2006' , September 11-14, 2006, pages 1-5.

[26] S. L. Cotton & W. G. Scanlon, "Channel characterization for single and multiple antenna wearable systems used for indoor body to body communications," IEEE Trans. Antennas & Propagation, Special Issue on Antennas & Propagation on Body-Centric Wireless Communications, vol. 57, no. 4, pp. 980–990, Apr. 2009.

[27] Turner, J.S.C.; Ramli, M.F.; Kamarudin, L.M.; Zakaria, A., "The study of human movement effect on Signal Strength for indoor WSN deployment", IEEE Conference on 'Wireless Sensor (ICWISE), 2013', 2-4 December. 2013, pages 30-35.

CHAPTER 3. PLACE-TIME COVERAGE AND CAPACITY

In Chapter 2 we showed how the random accumulation of subscribers affects the network environment, which eventually poses a challenge to the network dimensioning. Network dimensioning is a consequence of judiciously placing and configuring the network equipment while, considering the predictions made by the Probability Density Functions (PDFs). However, the networks that are not able to handle such situations face three major challenges (i) PDFs are not apt enough, (ii) the network architecture is not competent enough and, (iii) accumulations are not appropriately evaluated. This chapter investigates and analyzes why the present form of the probability, which is termed here as ***Unostentatoius Probability*** *or* Simple Probability that contributes to evaluating network dimensions, is not appurtenant. This chapter proposes the concept of **Ostentatious *Probability***, *as a means to* redefine and formulate the coverage and capacity issues of a *Mobile Wireless Communication Network* (MWCN). Actually, this can be seen as a study of the *polymorphic* nature of the probability, the results, of which are given in terms of the *Place Time Effect* (PTE) and the *Place-Time Repercussion* (PTR). The ostentatious probability allows for studying and evaluating the phenomena of random accumulations as *Ostentatious Events to show the impact of* accumulation on the coverage and the capacity of the network. The coverage and the capacity are now place and time-dependent events, and are defined as *Place Time Coverage* (PTC_o) and *Place Time Capacity* (PTC). The formulations of PTC and PTC_o incorporate and extend the work towards PTC [1] and evaluation of the impact of the subscriber accumulation on the Path Loss Model (Coverage)[2]. Through these deep investigations in this chapter, we can understand that the factors that the supporting network architecture must consider, in terms of PTE and PTR, so that it's dimensioning is more pertinent to such challenges. *This chapter investigates the conventional challenges of an MWCN with an unconventional approach encompassing the impact of Place and Time on network attributes such as Coverage and Capacity.* The term Place Time Capacity (PTC) was conceptualized in our previous work ([1]). Here, this phenomenon is elaborated further to surface the challenges that will be taken care of by the proposed solution as discussed in chapter 4 of this thesis. The impact of the environmental dynamics on the path-loss models was analysed in our another previous work (abovementioned), [2]. As the positions of the network sites depend on the path-loss models that are static (unostentatious) for most of the cases, severe changes may lead to eccentric site behaviour. This section elaborates these challenges envisaging the impact on the network dimensioning. The challenges described in this section will be pivotal to designing the proposed architecture in chapter 4.

This chapter formulates the challenges that arise due to ostentaniety in the MWCN arena. These formulations will be utilized to design and compare the solution that is proposed in Chapter 4. As a contribution, these investigations hold sumptuous importance by diverting the focus of a network design from ***location specific*** to ***event specific***. This chapter shows that standard network designs based on standard path-loss models are not sufficient for modern and future MWCNs. We redefine the network planning approach by reshaping the network attributes such as of HOTSPOTs, Coverage Holes, and Capacity Congestions.

This chapter is organized into ten sections. **Section 3.2** introduces the concept of place time independent or "UNOSTENTATIOUS" incidences. **Section 3.3** introduces the place and time dependent or "OSTENTATIOUS" events. It is shown how the outcomes of an experiment can be classified as place and time dependent events. **Section 3.4** defines the relationship between the subscribers of NSPs and Place &Time Dependency. Based on relationship, the concepts of *Place Time Capacity* and *Place Time Coverage* are defined in **Section 3.5** and **Section 3.6** respectively. In [3], it is discussed that various network parameters are the function of Probability Density Functions (PDFs). **Section 3.7** takes a step ahead of [3] by analysing the ostentatiousness in a PDF formulating the ostentaneity through certain derivations. **Section 3.8** analyzes the fallbacks in present the network dimensioning when facing ostentaniety. **Section 3.9** discusses the scientific contributions of this chapter. **Section 3.10** concludes the chapter.

3.1. INTRODUCTION

This section is mainly dedicated to coining the unconventional form of probability that is defined here as *Ostentatious Probability*, which has been found to play a major role in redefining and formulating the coverage and capacity issues of a *Mobile Wireless Communication Network* (MWCN).

3.1.1. THE NATURE OF THE PROBABLE EVENTS

Constitutionally, it has been observed that Nature is a certain entity [4]. The natural behaviour and properties are predominantly intact and impassive, so profound that we recognize them as "laws". However, within this resolute aura of certainty, there is an abstruse opulence of randomness and unpredictability about all the events encapsulated in the observable domain. This amalgamation of indeterminable certainty is the natality of the concept of the "probability". With reference to probability, every action that is taking place is the "Event" or "Experiment" whereas the result of that action is "outcome", "score", or "causatum" [5] [6].

In general, the probability of occurrence of an outcome 'O' is defined as,

$$P(O) = \frac{\text{Number of desired outcomes}}{\text{Total number of outcomes}} \quad (3.1.1)$$

Here, P(O) is the probability of occurrence of a set of outcomes [5]. The probability of occurrence of all outcomes of any event is unity [7]. This kind of probability is simple in nature, defined here as *Unostentatious Probability* and is unaffected by position and time of observations. *A detailed discussion about nature of events can be found in* **Appendix 3.1** *of this thesis.*

However, not all incidences are unostentatious. Certain experiments/events when viewed from wider and detailed perspective show obscurity in being an independent event. Such events are discussed here as *Place and Time Dependent Incidences/Events* or Resilient Events and the impact of Place and Time on any seemingly unostentatious even is called here as Place and Time effect. We postulate that the that the Place and Time effects are not exclusive phenomena but a collective impact, therefore, we regard them as Place-Time Incidence (PTI) and Place-Time Effect (PTE).

3.1.2. PROBLEM DEFINITION: PLACE-TIME REPERCUSSIONS ON AN MWCN PLANNING

Any wireless communication technology revolves around the two basic axes of a network, the "Coverage" and the "Capacity" [8]. These two entities are the foundation of a successful wireless network design and depend on how well the sites of the network cover the area and how much capacity the covered area can provide. These two factors are inevitably a simultaneous and a persistent challenge for every MWCN at all times and at every network location [9] and are termed here as *Network Parametric Duos* (NPD). An NPD is associated with the cohesive demand of the subscriber of the MWCN and, therefore, it is not incorrect to say that this duo is actually the two sides of the challenges posed by the network subscribers. More subscribers mean more capacity demand and more scattered subscribers mean more coverage demand [10]. And, more data per subscriber means more capacity of the catering base stations [11]. All challenges of a mobile wireless network are sorted to answer the two categories of questions which are, (i) where to cover, and (ii) how much to cater, to deal with NPD challenge [12].

While analysing these questions, it can be observed that often a unanimous approach is followed while planning and deploying a mobile wireless network. This approach considers that (i) an AoI can be subsequently divided into challenge based sub-sections, and, (ii) the network design and deployment ineluctably have strong belongingness to their respective sub-sections; the network solutions are inevitabley deterministic and location specific. Or simply, we can say that while planning a network, an NSP assumes that the network and the subscriber behaviour are subject to the location. The division and categorization of an AoI in terms of propagation

characteristics (Dense Urban, Urban, Suburban, and Rural, etc.) is based on the static nature of the network environment. This is a primary assumption to decide, which would be the coverage sites of the network. Similarly, the high capacities demands are assumed to be located in hotspots (Airports, train stations, cafe bars, etc.), commercial areas and office complexes [13].

The network conditions are not static at all. Arcanely, the PTE has been impacting the network environment of any MWCN with subscriber mobility and were never taken as a challenge before this research [14]. This chapter postulates that it is inappropriate to consider the network environment as a static entity, and analyses the factors that lead the network to defy from its static nature and how PTE can be investigated in an MWCN. Also, in this chapter, we will see how certain events are place and time dependent, and, what are the implications for the network planning and operations of an NSP?

3.2. UNOSTENTATIOUS EVENTS

An unostentatious event can be defined as follows:

Definition 1: Any event whose outcomes are the set of consequences of an action that is allowed to perform freely in nature has the capability to incur the same chance of occurrence to any particular outcome irrespective of when and where the action takes place.

Where, the outcomes are a set of consequences, also known as *Sample Space* (SS).

3.2.1. MULTIFARIOUSNESS IN UNOSTENTATIOUS PROBABILITY

The condition of unostentatiousness is that an action is allowed to perform without any obstruction, suggesting that all outcomes are equally likely to happen, however, this is not the case. The freedom to generate outcomes is allowed only after the stimulant (i.e. the device on which the experiment is performed; see, **Appendix 3.1)** has stimulated the action and not before that. Therefore, the way the outcomes have likelihood to appear is also dependent on the initial and boundary condition of the stimulant. Further, the study of the outcome depends on the range of the sample space that is under consideration. Accordingly, an unpretentious event can be discrete and continuous with each of it being biased and unbiased. **Appendix 3.2** gives details of the various categories of unostentatious probability that are defined here in this chapter as follows:

- Discrete and Unbiased (see, **Sections 3.2.1** and **3.2.3** of **Appendix 3.2),**
- Continuous and Unbiased, (see, **Sections 3.2.2** and **3.2.3** of **Appendix 3.2),**

- Discrete and Biased (see, **Sections 3.2.3** and **3.2.4** of **Appendix 3.2),**and,
- Continuous-biased (see, **Sections 3.2.3** and **3.2.5** of **Appendix 3.2).**

3.2.2. UNSOTENTIOUSNESS: PLACE & TIME INDEPENDENCY

The experiments, pertaining to the probabilities that are discussed in section 3.2.1, are *Simple Experiments*. These are the "omni occurrent" events and are discussed in detail in **Appendix 3.2**. Before moving any further, it is important to mention here that the term "Omni" is being used strictly to refer to the physical dimensions of the time and location (see, figure 3-2-1). The experiments or events that are discussed till now produce the outcomes of the same probability of occurrence irrespective of the time and location and, therefore, are place and time independent and are termed here as "unostentatious" events. As an example, the rolling of a die will show the same probability of occurrence (see, **Appendix 3.1**) whether it is tossed now or a minute later and whether Copenhagen or Aalborg cities of Denmark. The nature of the probability expressed by these experiments is flat and unchangeable with place and time.

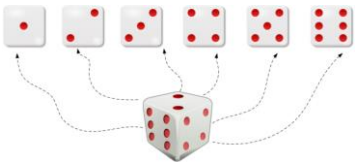

Figure 3-2-1: An example of Unostentatious Probability; all outcomes are equally likely and are Omni Occurant [Source of dice: openclipart.org]

Most of the probability studies are made under the constant "frame of reference" and, therefore, the probability does not change with time. However, when the perspective is widened, the independent outcomes of these experiments may turn out to be a partial projection of the wider phenomenon which incorporates the situational variance. In such cases, not only the experiments rely on the varying physical place and time conditions but also the stimulant itself. The place-time dependent behaviour of the stimulant may also impose the variant nature of the outcomes exhibited by the respective experiment.

3.3. OSTENTATIOUS EVENTS: PLACE & TIME DEPENDENT EVENTS

There are certain events that have the capability to act in exactly the same way in all places and at all times as was explained in the previous section. We have recognized such events as *unostentatious event*. However, the events, in reality, change their behaviours with place and time. This section discusses the *ostentatiousness* of an event.

3.3.1. PLACE-TIME PERPLEXITY

Let us consider again (see, **Appendix 3.2)**, the rolling of a dice, but this time, from an ostentatious point of view. The outcomes of the experiment of rolling a dice are equally likely. This unostentatiousness is relevant to our consideration that "*the experiment is absolutely fair*". However, the degree of unpretentiousness is somewhat abstruse. We can be honest to certain extent by obtaining a fair dice (all faces smooth, and center of gravity coinciding center of the cube of which dice is made of) or by not seeing the initial face of the dice while throwing it or by throwing the dice randomly, however, we cannot control how physical properties affect a dice.

Ironically, although we know that an event is an action that generates some outcomes, we ignore the fact that the outcome itself appears when the action is impeded itself to form the outcome. As an example, the rolling of a dice generates outcome only when it comes to rest, and this rest is obtained because certain undesirable physical phenomena are acting on it such as friction due to the table on which it is rolled and viscosity of air in which it rotates. Therefore, if somehow, a gambler comes to know the deceleration produced by an edge of the dice, then, knowing the initial upward face of the dice, he/she can estimate in how many rotations, a particular face will appear up. Therefore, although for a nascent observer, it will still be a blatant even, however, with the fact that the actor "knows" how to estimate the outcome makes it "*ostentatious."* Hence, a simple looking event can become a conundrum when the nature of stimulant (dice) and the initial conditions are known. This is an example where the actions complete in a very short duration and the displacement and deeper investigation is tedious and not within the present scope. In further sections, let us discuss this effect in more details in relation to its impact on an MWCN.

Let us put the above example in relation to the Place-Time dependency. While throwing a dice, the gambler knows with what force he/she should throw the dice, so that desired outcome is obtained every time. The applied force may change depending on the initial face of the dice. However, this initial force is not perceivable unless it is expressed in tangible quantities such as position and time. A dice, therefore, will terminate its motion at a certain position and after a certain time to display the outcome and varying position and time with respect to the initial state will vary the outcome.

This place-time dependency is just not limited to the "gambling" field. If we replace "rolling of dice" with "finding a user" or "finding a signal", the degree of uncertainity remains the same. We have discussed the subject from "gambling" point of view as this is the first time when "degree of uncertainity" is introduced to show the challenges of commuication systems that are seemingly extrinsic to the system.

3.3.2. OBSERVING AN EVENT IN THE VIEW OF PLACE AND TIME

An event that might look simple may show place time impact when viewed with a wider consideration. Figure 3-3-1 shows the extension of a simple event in the place-time domain. The outcome of any action will be varying when sampled in different time and/or place. Figure 3-3-1 also shows that place-time is considered as a composite entity and presumably, an event that varies with time must also vary with place simultaneously. However, there are certain incidences when each place and time should be considered separately. This can be understood by dissecting the previously considered example. Suppose that, before throwing the dice the gambler let the dice swirl in his palm for a certain time. In such a case, while the position of the dice remains unchanged, it is the action taking place strictly in the time domain to produce variation in outcomes. In such cases treating place and time separately and not as a single entity is required as shown in figure 3-3-2.

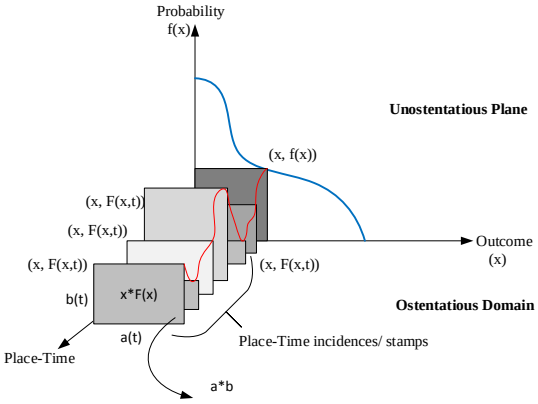

Figure 3-3-1: Place-Time Projection of an Unostentatious Event

Figure 3-3-2 shows that both place and time may impose an effect exclusively in certain events. In the above example, the duration in which only the time is the imperator and the contribution due to the position is null, is said to have a *Positional Latency*. As we can see, this place-time event is a multidimensional resolution of an observable event. This means that an event that is being observed in real-time is a superposition of its place and time projections.

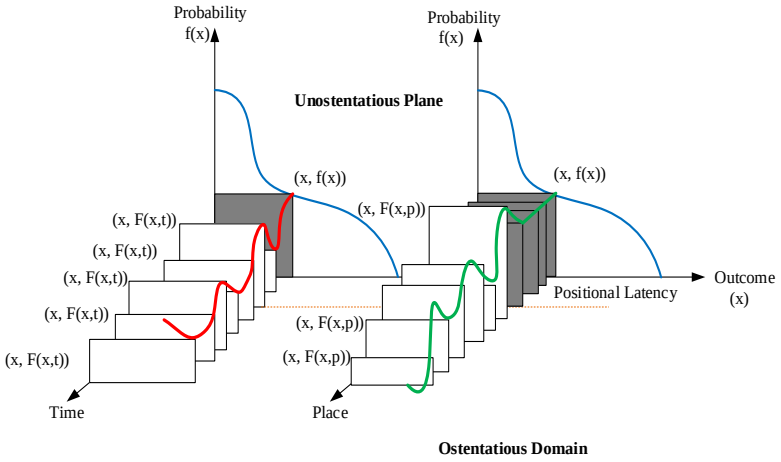

Figure 3-3-2: Place and Time as Separate Entity in evaluating the Ostentatiousness

In the following section and onwards it will be discussed the practical implication of place time effect on a usual network design and operations.

3.4. DILEMMA IN MOBILE WIRELESS NETWORK PLANNING

Referring to figure 3-4-1, let us consider that an NSP plans to set up a network in the Area of Interest (AoI), starting from green field to a mature network as discussed in **Chapter 1, Section 1.2** of this thesis. Considering that the entire AoI has a uniform and constant morphology, let us also consider the assumptions in relation to the planning of the network as per below:

- n_{th} Base Transceiver Station (BTS) transmitter : T_{nx}
- n_{th} Receiver : R_{nx}
- Transmit power of n^{th} BTS : P_{ntx}
- Receive Power of n^{th} receiver antenna : P_{nrx}
- Maximum capacity per subscriber : C_{sub_max}
- Subscriber density per unit area : σ_s
- Area of the AoI : A_{AoI}
- Sensitivity of the R_{nx} : $S_{R_{nx}}$

For the present discussion, the BTS is considered as the generic name of the transmitter-receiver station and is not an exclusive term for any particular technology such as GSM. The BTS along with its infrastructure is termed here is site and will be used adequately as the building block of a network.

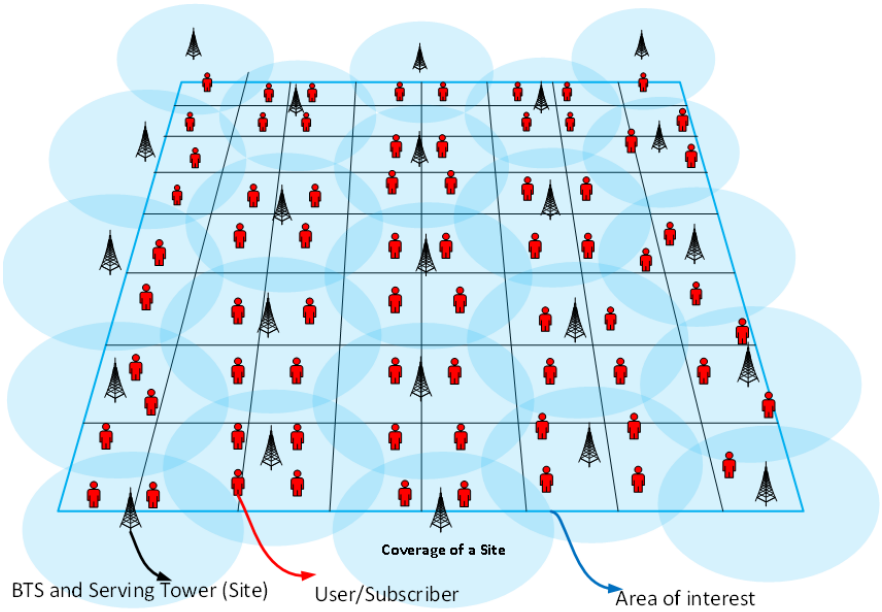

Figure 3-4-1: A Simple Network Deployment Scenario

The usual network planning begins with the assumption that the subscribers are homogenously distributed across the AoI in continuums of evenly distributed chunks of subscribers. If we assume that all receiver units have the same sensitivity, which means that for all n, $S_{R_{nx}} = S_r$ and, the coverage plan must assure that the entire AoI will be covered at least with a level above S_r. Presently we are ignoring the environmental variations of the network and therefore, the area covered by T_{nx} is constant for all n, say A_c.

Therefore, considering the fact that the subscribers are uniformly distributed along the AoI, the number of subscribers served per T_x will be [15] [16]:

$$N_{sub} = \sigma_s A_C \tag{3.4.1}$$

Hence, the capacity that is needed to be served by every site can be derived as,

$$C_{PB} = N_{sub} C_{sub\_max} \tag{3.4.2}$$

Therefore, while planning the network, the NSP has to design a network in which each site has a BTS with serving capacity of C_{PB} and a coverage area of A_c with the total number of sites as [15]:

$$N_{BTS} = \frac{A_{AoI}}{A_c} \tag{3.4.3}$$

This is the much-simplified illustration of a bit complex network design process. However, the present discussion is unabatedly valid even when most of the oddities of a network design are omitted here. For the present discussion, however, we also assume that according to the design of BTS, it has a limit to cater capacity. Let us assume this maximum serving capacity of BTS as C_{PB_max}. Therefore, for all BTS present in the network,

$$C_{PB} < C_{PB\_max} \tag{3.4.4}$$

The strategy mentioned above is followed by most of the network designers to plan, design and deploy a network. However, what is important to notice here is that while designing, the network designer "considers the network as an unostentatious event". This means that a designer assumes that (i) during any time of the network operation, there will not be a moment when the capacity demand of any site will never go above C_{PB_max}, and, (ii) in whatever way the subscriber permute them in the AoI; the subscriber density σ_s shall always remain constant. This is somewhat an unostentatious event as the possibility of a subscriber served by any site always remains the same although the subscriber may change the permutation. Hence, the event is not affected by the time and position of the subscriber. This seems a very delightful situation as the AoI is presumed "catered" once all the sites are deployed and the network is made operational. Nonetheless, this comes out to be fairy tale when observed in the place-time domain. The next subsection discusses the frustration that an NSP may face post deploying a seemingly well-planned network.

3.4.1. PLACE &TIME ENTRANCED NETWORK DYNAMICS

Although, the network is assumed homogeneous, in reality, this is not the eternal situation and with time, the network grows and matures. In such situation, the density of subscribers per unit area σ_s, the subscribers count per site N_{sub}, and the capacity served by the BTS C_{PB} would vary from site to site and for the n^{th} site can be written as:

(i) The subscriber density per unit area under site n: σ_{n_s}
(ii) The subscriber count under site n: N_{n_sub}
(iii) The capacity served by BTS of site n: C_{n_PB}

Therefore, for initial deployment scenario, equation (3.4.4) can be restated as:

$$C_{n\_PB} < C_{PB\_max} \text{ for all n} \tag{3.4.5}$$

Thus, the site count is subject to the coverage requirement of the AoI which means that the required number of sites is limited by the area that is needed to be covered as obtained by equation (3.4.3). This kind of planning where the coverage is the driving factor of planning sites is known as *Coverage Driven Network* and the sites dedicated to providing coverage are the coverage sites of the network. As, the subscriptions of a network grow, so do the subscribers. Thus, this seamless distribution tends to collapse under the uneven distribution of the subscriber density. This is mainly because the realistic subscription is more occurant in a densely populated area than otherwise. Then, the condition expressed by equation (3.4.6) turns around to:

$$C_{n\_PB} > C_{PB\_max} \tag{3.4.6}$$

Where, {n: n^{th} site satisfies the condition of the expression 3.4.6}

For all those areas, where the sites satisfy expression (3.4.6), the network planner adds more sites to abate the raised capacity demand. Ergo, the total site count of the network will be:

$$N_{BTS\_ADD} = \frac{\sum_{n=1}^{N_{BTS}} C_{n_{PB}} - C_{PB\_max}}{C_{PB\_max}} \tag{3.4.7}$$

This means that the site count is limited by the growing capacity of the network, and hence, the Coverage Driven Network turns into a Capacity Driven Network. These sites, that are deployed exclusively to cater for the raised capacity, are the *Capacity Sites* of the network. From here on, the network keeps growing and the total subscriber count keeps on increasing to the point, when the new subscribers are strictly marginal, and network gains *Maturity*.

Such kind of planning considers the "STATIC" nature of the subscriber. This means that while configuring and deploying a site, the average traffic demand of the location is considered, and not the actual mobility of the subscribers. Nonetheless, the subscribers eventually are humans and are cognitive entities, and, are likely to mobilize from place to place. In networks where the subscriber count is in millions, as described in Table 3-1 referring to the subscriber count and growth in the past decade in Delhi, India, such dynamics may lead to a baffling situation for an otherwise well-planned network. Referring to figure 3-4-1, let us consider a state when the subscribers dynamics develop a condition where after a certain time 't', somehow they find themselves in distributed quantized form as shown in figure 3-4-2.

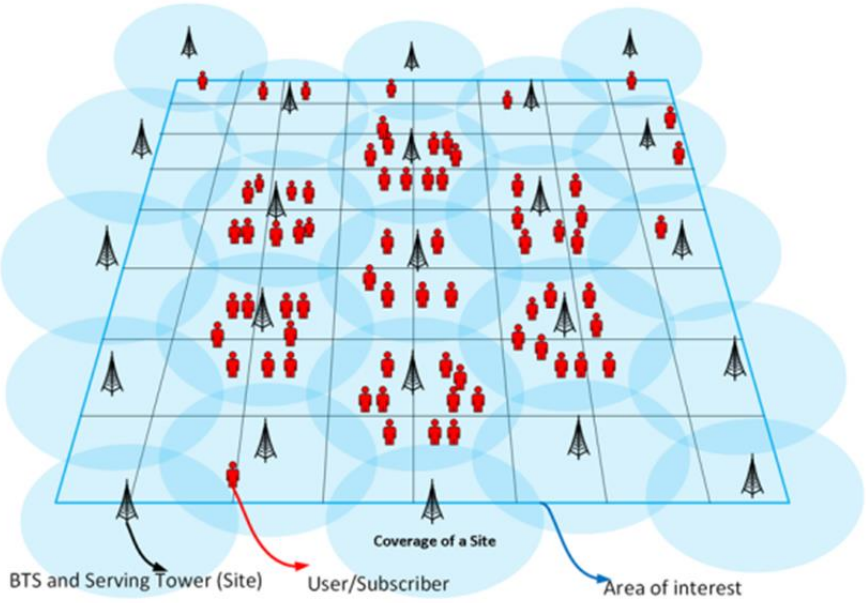

Figure 3-4-2: Status of a dynamic network at a certain time't'

From figure 3-4-2 we can see, that the value of *increased* $\boldsymbol{\sigma_s}$ *increases* the value of $\mathbf{N_{Sub}}$. Therefore, equations (3.4.1) to (3.4.3) are now time dependent events. Therefore, for any particular site, the subscriber count, and total capacity demand can be expressed as:

$$N_{sub}(t) = \sigma_s(t)A_C \tag{3.4.8}$$

and, $$C_{PB}(t) = N_{sub}(t)C_{sub\_max} \tag{3.4.9}$$

Referring to figure 3-4-2, let us consider that there are two sites A and B in the AoI and that the subscriber from site B has moved to A. This brings two simultaneous events, one being site A where the subscribers are accumulating and another site B from where the subscribers are churning out.

For the first case, equation (3.4.8) can be rewritten as:

$$N_{A\_sub}(t) = \sigma_{A\_s}(t)A_{A\_C} \tag{3.4.10}$$

Also, the capacity expressed in equation (3.4.9) can be rewritten for site A as:

$$C_{A\_PB}(t) = N_{A\_sub}(t)C_{sub\_max} \tag{3.4.11}$$

Which means, for $t_1<t_2$,

$$N_{A\_sub}(t_1) < N_{A\_sub}(t_2) \tag{3.4.12}$$

and, $$C_{A\_PB}(t_1) < C_{A\_PB}(t_2) \tag{3.4.13}$$

In case, the subscriber count is increasing for site A.

Similarly, for the site B, the above equations can be written as:

$$N_{B\_sub}(t) = \sigma_{B\_s}(t) A_{B\_C} \tag{3.4.14}$$

Also, the capacity for site B can be rewritten as:

$$C_{B\_PB}(t) = N_{B\_sub}(t) C_{sub\_max} \tag{3.4.15}$$

Which means, for $t_1<t_2$,

$$N_{B\_sub}(t_1) > N_{B\_sub}(t_2) \tag{3.4.16}$$

and, $$C_{B\_PB}(t_1) > C_{B\_PB}(t_2) \tag{3.4.17}$$

In case, the subscriber count is decreasing for site B moment by moment.

However, $$N_{BTS\_ADD\_GATHER} = \frac{\sum_{n=1}^{N_{BTS}} C_{n_{PB}} - C_{PB\_max}}{C_{PB\_max}} = 0 \tag{3.4.18}$$

Hence, as seen in equation (3.4.18) the net increment in the subscriber count in the entire network is zero. This means that the entire traffic variation is due to non-uniform distribution of subscribers in the entire AoI and not due to net increment in subscriber growth.

In a subscriber mobility environment, the subscribers are deemed to mobilize within the network area. Anticipating such situations, the BTSs are configured with higher capacity (traffic) also known as *Busy Hour Traffic* to cater for such dynamics. For certain known regions, where the subscriber density goes extreme on a regular basis, the area is planned with additional sites known as capacity sites. However, in a certain situation, this is a heartbreaking condition. The NSP is in ambivalence when the flux is intolerably high which is very much visible in densely populated areas such as metropolitan cities (e.g. Delhi and Mumbai in India, New York in the United States, Tokyo in Japan, and Copenhagen in Denmark, etc.). This often brings up a choking situation where the required capacity surpasses C_{PB_max} in multiple sites. On the other hand, there are sites that are underutilized due to the

churning of its subscribers to other sites. This is highly momentarily, and therefore, the usual solutions are not feasible.

Figure 3-4-3: Momentary huge gathering of Potential Subscribers. Left: Procession of Immersion Ceremony of Lord Ganesh in Mumbai, India. More than 4 million city residents are involved in the celebration every year[4]*. Right: 35rd Berlin Marathon Sunday, Sept. 28, 2008, in Berlin, Germany. Around 40,000 runners from 100 countries took part in the event*[5]

Such accumulations are very much occurrent in the daily life in India as shown in figure 3-4-3. Although the problem has been taken up numerous times by the network planners, this research provides a novel view point for the analysis. It sets up a platform for the "need of self-configurable systems".

3.5. THE PLACE TIME CAPACITY [1]

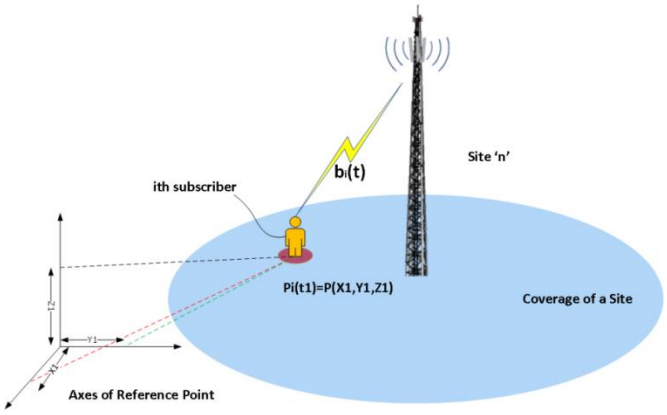

Figure 3-5-1: A subscriber in place -time domain

[4]*Resource: Lord Ganesha Immersion Ceremony, Indian Express, September 25, 2015*

[5] *Resource: www.berlin.de*

Referring to figure 3-5-1, let us assume that at any arbitrary instantaneous time ʻtʼ:

(i) There is a subscriber ʻiʼ.
(ii) The position of a subscriber with respect to an arbitrary reference plane at instantaneous time ʻtʼ is $p_i(t)$.
(iii) The *instantaneous* throughput demand of the subscriber at the instantaneous time ʻtʼ is $b_i(t)$.

While the subscriber is in the coverage area, its demand is catered by the n^{th} site of the network (see, figure 3-5-1).

However, when the subscriber decides to move from a position p_1 to p_2, carrying the capacity demand along with, the network is bound to subside the need everywhere the subscriber traverses. Conventionally, it is deemed that the moving subscriber, while moving with the same coverage area, can be catered by the same site, yet, the subscriber may find some coverage holes against which the NSP may have to install additional coverage site to cater for the deficiency (see, figure 3-5-2) [17].

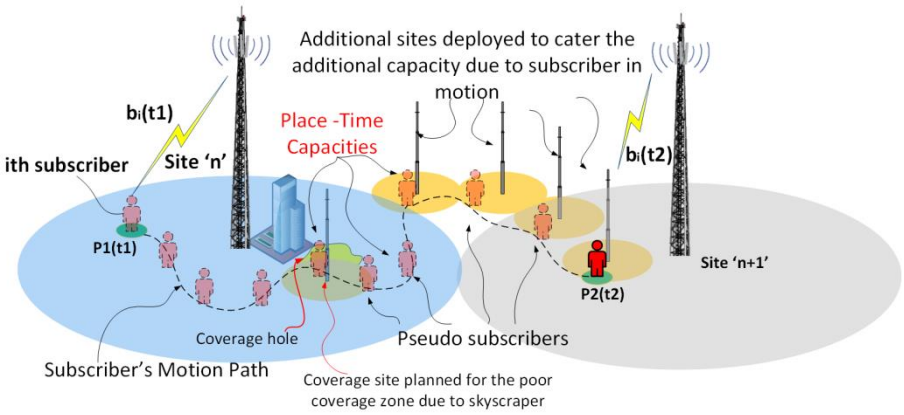

Figure 3-5-2: Place Time Capacity generated by a moving subscriber

Consequently, the subscriber creates the need for the capacity throughout the path it traverses, which is termed as the *Place Time Capacity (PTC)* [1]. *The PTC is an eminent example of an ostentanious event and the ostentaneity is described in equation (3.5.2).*

3.5.1. INSTANTANEOUS PLACE TIME CAPACITY

Assuming that this i^{th} subscriber has instantaneous velocity of $v_i(t)$, we have:

- When $v_i(t) = 0$, then the demand for capacity at the position $p_i(t)$ is $b_i(t)$ (3.5.1).
- And, when $v_i(t) \neq 0$, which means that subscriber is changing the position, then the rate at which the subscriber generates the demand will be the instantaneous place time capacity.

The rate of PTC is the velocity of the subscriber times the capacity demand of the subscriber. This rate is the *Instantaneous Place Time Capacity* (iPTC) and is given by:

$$\overrightarrow{PTC_i^i} = \frac{d}{dt}\{p_i(t)b_i(t)\}$$

or,
$$\overrightarrow{PTC_i^i} = b_i(t)\frac{d}{dt}\vec{p}_i(t) + \vec{p}_i(t)\frac{d}{dt}b_i(t) \quad (3.5.2)$$

From the definition of velocity, $\vec{v}_i(t) = \frac{d}{dt}\vec{p}_i(t)$ (3.5.3)

Therefore,
$$\overrightarrow{PTC_i^i} = b_i(t)\frac{d}{dt}\vec{v}_i(t) + \vec{p}_i(t)\frac{d}{dt}b_i(t) \quad (3.5.4)$$

Where, the superscript 'i' indicates that it is an instantaneous value, and, the subscript 'i' denotes that it belongs to the 'i^{th} 'subscriber. Also, it is important to note that iPTC is a vector quantity with direction pointing towards the direction of motion (velocity).

The relation of PTC and iPTC can be understood as:

$$\overrightarrow{PTC_i^i} = \frac{d}{dt}(\overrightarrow{PTC_i}) \quad (3.5.5)$$

Therefore, equations (3.5.4) and (3.5.5) when putting together, yields:

$$\overrightarrow{PTC_i^i} = \frac{d}{dt}\left(\overrightarrow{PTC_i}\right) = b_i(t)\vec{v_i}(t) + \vec{p}_i(t)\frac{d}{dt}b_i(t) \quad (3.5.6)$$

Hence, we can say that the instantaneous PTC depends on the instantaneous velocity of the subscriber. Further, the second term also reveals that the varying

data rate $b_i(t)$ can also contribute to unprecedented capacity demand at any position $p_i(t)$.

Planning a network for maximum throughput 'b' per user, we can consider $b_i(t)$ =b for all the time instants.

Therefore, $$\frac{d}{dt}\left(\overrightarrow{PTC_i}\right) = b\frac{d}{dt}\vec{p}_i(t) + \vec{p}_i(t)\frac{d}{dt}b \tag{3.5.7}$$

Being a constant, $\frac{d}{dt}b = 0$ that reduces equation (3.5.5) to:

$$\frac{d}{dt}\left(\overrightarrow{PTC_i}\right) = b\frac{d}{dt}\vec{p}_i(t) + 0 \tag{3.5.8}$$

Hence, $$\frac{d}{dt}\left(\overrightarrow{PTC_i}\right) = b\vec{v}_i(t) \tag{3.5.9}$$

The iPTC for the i^{th} subscriber can be derived by integrating equation (3.5.9) to have,

$$\overrightarrow{PTC_i} = b\int \vec{v_i}(t)dt \tag{3.5.10}$$

Again from 3.5.3, we have:

$$\overrightarrow{PTC_i} = b\{\vec{p}_i(t) + l_i\} = b\vec{p}_i(t) + b.l_l \tag{3.5.11}$$

Where l_i is constant that we term as *Length of Impact*.

To avoid the above equation to be understood only as the net displacement dependent process, equations (3.5.10) and (3.5.11) are rewritten as:

$$\overrightarrow{\dddot{PTC}_1} = b\dddot{\int} \vec{v_1}(t)dt \tag{3.5.12}$$

and, $$\overrightarrow{\dddot{PTC}_1} = b\{\vec{p}_i(t) + l_i\} = b\vec{p}_i(t) + b.l_l \tag{3.5.13}$$

This signifies that the quantity is the forward integral of the displacements, and the reverse paths are omitted.

Equation (3.5.11) conveys that when the data rate is considered constant, the instantaneous PTC has two terms. The first term imparts the amount of capacity demand imposed at every positional instance and throughout the path that is traversed by the user and the second term reveals the capacity demand imposed on

the system while the subscriber is stationary. Figure 3-5-3 pictorially shows the difference between the two terms and their contribution to the instantaneous PTC.

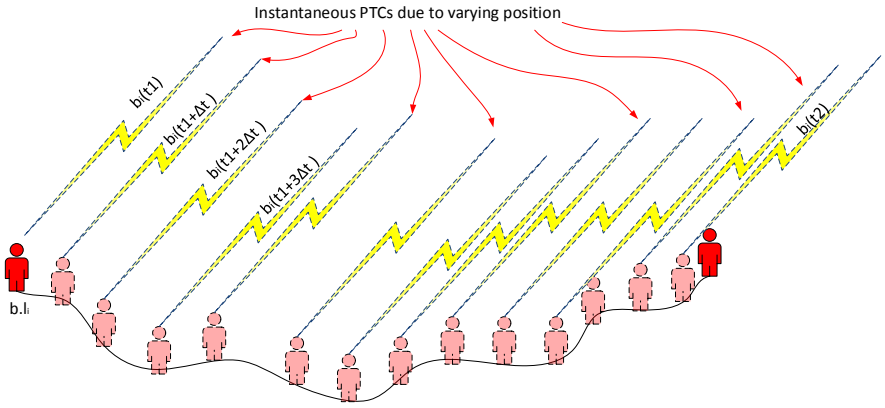

Figure 3-5-3: Instantaneous Place Time Capacity

The Length of Impact: Figures 3-5-1and 3-5-2, give an insight that the user (subscriber) may not be moving every time and will be static for some time. In such a situation, there would be no change in the position with time. Nonetheless, the need for a capacity catering is inevitable. In the case when the capacity demand is consumed (fully or partially) by a temporary site, also known as Cell on Wheels (CoW) at the target position, the CoW site has to remain active until the user becomes static at the very position. Hence, the capacity demand is generated by the virtue of time and is with respect to the position of the user, hence the stimulant is termed here as the length of impact which is equivalent to the amount of PTC generated if the user would have moved to a certain additional length.

The '$b\vec{p}_i(t)$ ': The first term is a place dependent entity; however, as everything that is changing is associated with time, it is a function of time. The dual dependency signifies that it is not only the duration of the event that signifies the capacity challenges but also the position of the stimulant. This means that for a user who has traversed a distance 'd' from point A to point B (see, figure 3-5-4) as a single event and then sometimes later travels from P to R with the same distance, the amount of PTC generated in the two events may be the same but the net PTC will be the accumulation of the PTCs by the two events. This is because the locus of the traversed path will be different. Hence, the same user can create enough disturbances in a network by placing capacity demands arbitrarily and unevenly. The present discussion is limited to a single user, however for an ample user density; such dynamics can strongly impact in a negative way the performance of a network.

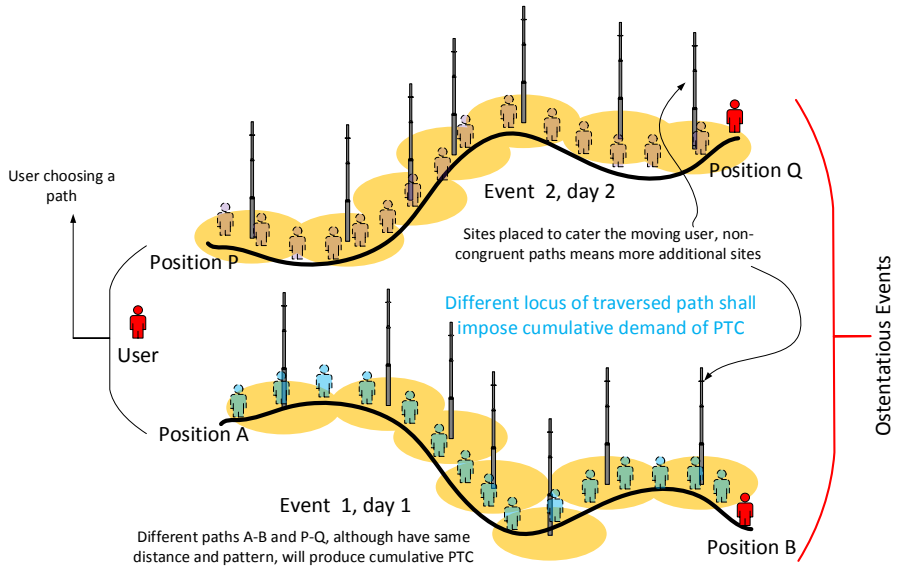

Figure 3-5-4: Cumulative Place Time Capacity illustration

Both the iPTC and PTC, are dependent on the position and time, and can be represented as vector quantities.

3.5.2. NET AND CUMULATIVE PLACE TIME CAPACITY

The appended PTC generated during time interval (t_1, t_2), equation (3.5.10) is integrated over the period (t_1, t_2) to have:

$$\mathrm{PTC_i}\big|_{t_1}^{t_2} = \mathrm{b}\int_{t_1}^{t_2} \vec{v_i}(t)\,dt$$

or, $$\mathrm{PTC_i}\big|_{t_1}^{t_2} = \mathrm{bp_i}(t)\big|_{t_1}^{t_2} + \mathrm{bl_i}\,\big|_{t_1}^{t_2} \qquad (3.5.14)$$

The above equation can be solved for varying place and time separately. As the second term is time invariable, hence, for the itinerant user,

$$\mathrm{bl_i}\,\big|_{t_1}^{t_2} = 0 \qquad (3.5.15)$$

Therefore, $$\mathrm{PTC_i}\big|_{t_1}^{t_2} = \mathrm{bp_i}(t)\big|_{t_1}^{t_2}$$

$$= b\{p_i(t_2) - p_i(t_1)\}$$

$$= b\Delta p \tag{3.5.16}$$

Therefore, the change of PTC or Δ PTC is the capacity demand placed due to the mobility of the user *and is defined here as*:

$$\Delta PTC_i = b\Delta p \tag{3.5.17}$$

Net PTC: The net PTC or nPTC is, however, the cumulative PTC that incorporates the PTC due to motion and place latency (length of impact) and is defined here as:

$$n\ PTC_i = \Delta PTC_i + bl_i = b\nabla p + bl_i \tag{3.5.18}$$

Sections 3.5.1 and 3.5.2 discussed the PTC situations for a single user. However, in any live network, there are huge magnitudes of the user. Section 3.5.3 shall discuss the PTC phenomena is a more realistic scenario, i.e. when the user count in the network is a huge number.

3.5.3. GROSS PLACE TIME CAPACITY

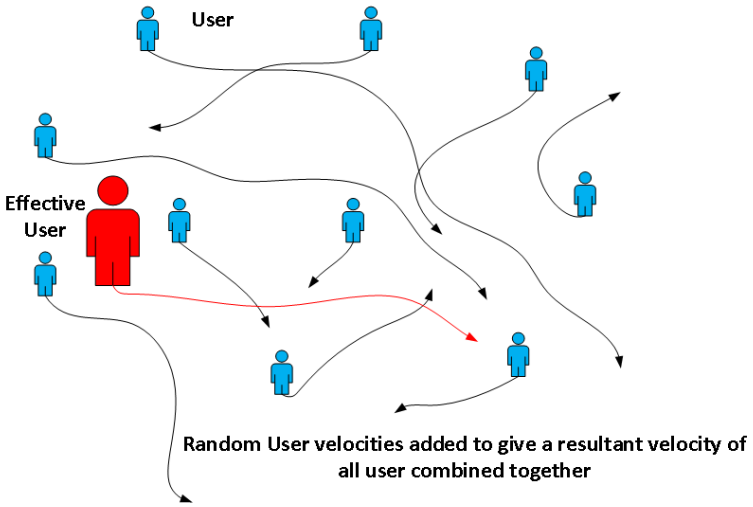

Figure 3-5-5: Gross Place Time Capacity generated by an effective user

In reference to figure 3-5-5, let the user 'i' has an instantaneous velocity of $v_i(t)$ then, within a certain progressive interval, the resultant velocity for all $S=N_{BTS}$ users can be determined as:

$$\overrightarrow{\overrightarrow{V_r}}(t) = \sum_{i=1}^{S} v_i(t) \tag{3.5.19}$$

The $V_r(t)$ is the net instantaneous velocity of the users of the AoI. This means that although the users can move randomly within the AoI, at any time instant when all the velocities are added together, it is possible to estimate how much a resultant drift of the subscribers would be.

Therefore, when $V_r(t) = 0$, this means that the subscriber distribution is unchanged since the last instance. In the case when $V_r(t) \neq 0$, this means that there is a huge resultant drift in the subscriber position. If we combine all the velocities as $V_r(t)$, then we can consider this net change as the movement done by an effective user U_{eff} such that:

$$b_{u_{eff}}(t) = \sum_{i=1}^{S} b_i(t) \tag{3.5.20}$$

or, $$b_{u_{eff}}(t) = S.b \tag{3.5.21}$$

Considering $b_i(t) = b$ for all users.

Hence, revisiting the concept of PTC from equation (3.5.14), the Gross PTC or GPTC during a time interval (t_1, t_2) is defined as:

$$GPTC(t_1, t_2) = S.b \int_{t_1}^{t_2} V_r(t)dt \tag{3.5.22}$$

This is certainly an enormous amount of PTC generated with the subscriber count of the order of 10^6 (million).

3.5.4. PLACE TIME CAPACITY AND NETWORK DIMENSIONING

Let us assume a mature network in an AoI (see, figure 3-5-6), where,

(i) A_{AoI} is the area of the AoI,
(ii) C is the capacity offered by each site,
(iii) the total number of sites required to satisfy the capacity requirement of AoI at any time instant 't' is n(t),
(iv) the area served by the j^{th} site is a_j,
(v) total number of subscriber of the network is S,
(vi) the capacity demand of the i^{th} subscriber is b_i bps,

and,

(vii) the network under consideration is a Capacity Driven Network (CDN), which means that capacity site requirement is more than that of coverage sites.

Then, the total number of capacity sites required to cater for the AoI is:

$$n(t) = \frac{\sum_{i=1}^{S} b_i(t)}{C} \tag{3.5.23}$$

Therefore, at any given time $t = t_1$, the total capacity sites requirement will be:

$$N = n(t_1) = \frac{\sum_{i=1}^{S} b_i(t_1)}{C} \tag{3.5.24}$$

Considering, that the AoI is morphologically homogeneous meaning that the propagation loss of AoI is uniform at all points in the AoI, each site will serve the geographical area of the same size of value given as:

$$\{ a_j : a_j = \frac{A_{AoI}}{N} = a, \text{for } 1 \leq j \leq S\} \tag{3.5.25}$$

Hence, each site will confine its coverage to a value 'a' as mentioned in equation (3.5.25). Figure 3-5-6 describes this scenario where the A_{AoI} is divided among N coverage areas where a_j is a coverage area that belongs to a j^{th} site. In this way, A_{AoI} contains N subareas each of having magnitude of 'a' and position of site j which are the squares marked sequentially from 1 to N.

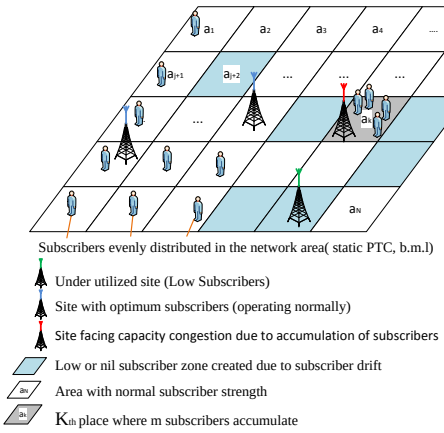

Figure 3-5-6: Accumulation of subscribers in a network

Now, as we can see from figure 3-5-6, a subscriber can choose to be in any area (from 1 to N), and chances are equally likely. Therefore, the probability of finding an i^{th} subscriber at an arbitrary location a_k is:

$$P_i = \frac{1}{N} \tag{3.5.26}$$

As the event of choosing a position by any subscriber is mutually independent of any other subscriber, the probability that 'm' subscribers choose to visit an arbitrary location a_k is given as:

$$P_m = \frac{1}{N^m} \tag{3.5.27}$$

Therefore, the place time capacity generated in the duration (t_1, t_2), when m subscribers chose to move from their original location to an arbitrary location a_k, can be defined as:

$$\overrightarrow{\overrightarrow{PTC}}_m(t_1, t_2; a_i, a_k) = b\sum_{i=1}^{m}\left(\int_{t_1}^{t_2}\vec{\vec{v}}_i(t)dt\right) + (bm)\sum_{i=1}^{m}\vec{\vec{l}}_i \tag{3.5.28}$$

As all subscribers arrive at a_k, therefore, l_i for all subscribers is the unit vector pointing a_k. Therefore, in this case, the amount of the new demand will be [1]:

$$PTC_m(t_1, t_2; a_i, a_k) = b\sum_{i=1}^{m} p_i(t)|_{t_1}^{t_2} + bm \tag{3.5.29}$$

This is the PTC accumulated when each of the m subscribers decide to approach a_k with a certain definite path which is unique in itself. Therefore, combining equations (3.5.27) and (3.5.29) the probability of accumulation is determined as [1]:

$$P(PTC_m) = P_m = \frac{1}{N^m} \tag{3.5.30}$$

This means that the growth of the PTC due to m subscribers accumulating at a single location is $1/N^m$. This is certainly a very low probability when m is large, and it decreases with the growth of the subscribers. If such a situation occurs, the offered capacity of the site, which is serving the location a_k will not be enough. Further, in equation (3.5.30), it is assumed that the network has 'm' subscribers.

Nonetheless, when the user count is larger than those who are visiting the location a_k, the situation changes drastically.

Let,

(i) S be the total users of the network,
(ii) m are the subscriber count visiting location a_k such that m< S.

Then, the probability of m subscribers visiting location a_k will be as mentioned in equation (3.5.30). However, the number of ways in which these 'm' subscribers can be chosen out of S is given by the formula:

$$ {}^{S}_{m}C = \frac{S!}{m!\,(S-m)!} \tag{3.5.31} $$

Where the superscript denotes the total choices and the subscripts denote the number of choices that can be made. Therefore, combining equations (3.5.30) and (3.5.31), we can define the *probability that the PTC generated by m subscribers out of S subscribers of the network is observed at a given instant of time as*:

$$ P(PTC_m|\,S) = {}^{s}_{m}C \times P_m $$

$$ = \frac{S!}{m!\,(S-m)!} \times \frac{1}{N^m} \tag{3.5.32} $$

Therefore, there might be a case when,

$$ \frac{S!}{m!\,(S-m)!} \times \frac{1}{N^m} > 1 \tag{3.5.33} $$

and the probability of accumulation is more than 100% a_k, which means that at any instant of time, the site serving a_k will always experience additional *m* subscribers and will always be congested.

The complex individual behaviour of a user can have a big impact on the above-discussed scenario. Let us consider that; there are [1]:

(i) S subscribers in the network are under consideration,
(ii) categories of likings, to which users are inclined to, are numbered as {1, 2, 3, ..., q}. For example, category 1 being set of those users who like shopping and category 2 of those who like a marathon and so on,
(iii) and, S1, S_2, S_3... S_q are user sets with a subscript indicating the category to which they belong. As an example, S_1 are the users who like watching movies and, therefore, belong to category 1.

Further, let us assume a period such as “Black Friday” in the city of the AoI and the shops and malls declare a major discount. Such incidences often provide ample opportunities to people to accumulate in the destinations of common interest. In such incidences, whether willingly or unwillingly, users form groups that tend to remain together. Therefore, the users of common interest may accumulate at the mall at position ‘O’. Finally, they decide to ‘stick’ and move together along the paths OA, AB and BC to reach the final mall at the position C (or a_k in relation to previous discussions, see, figure 3-5-7).

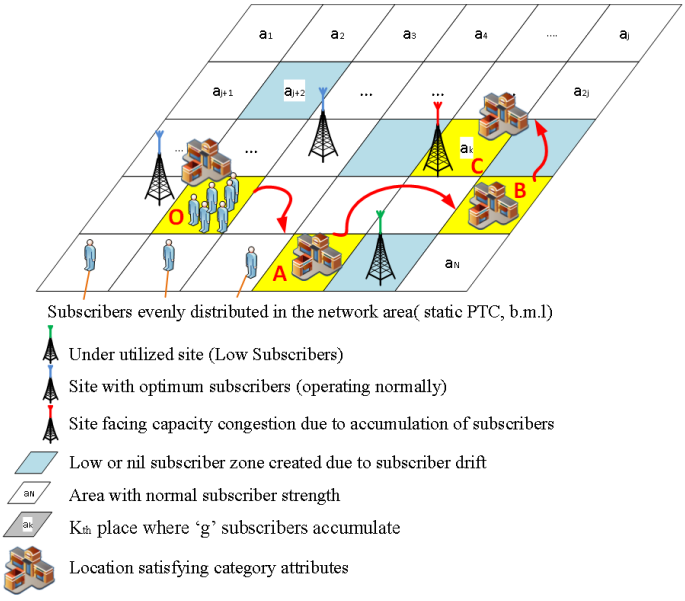

Figure 3-5-7: Subscriber accumulation in a biased situation

Then,
$$S = \sum_{i=1}^{q} |S_i| \tag{3.5.34}$$

Where, $|S_1|$ is the number of elements in group S_1. Considering that users have now formed a group and tend to be together throughout the exploration, we can say that the probability of this group visiting any location in the geographical area of AoI, as per equation (3.5.26) will be:

$$P_{S_1} = \frac{1}{N} \tag{3.5.35}$$

This is far greater than when m subscribers traverse the location in an unbiased manner as given in equation (3.5.30). The PTC generated by g_1 is:

$$|\overrightarrow{\overrightarrow{\overrightarrow{PTC}}}_{S_1}(t_1, t_2)| = ||S_1|b(\vec{\vec{\vec{P}}}_{S_1}(t)|_{t_1}^{t_2}) + |S_1|b.\vec{\vec{\vec{l}}}| \quad (3.5.36)$$

This is the additional, although temporal; demand that any NSP should take into consideration. This is an inevitable and frequent phenomenon in a densely occupied network where the users are amply available to create such collisions where the capacity demands boom up the serving capability of the ruling site. However, as a network contains an ample amount of site to fulfill the coverage and the capacity needs, the portion of the generated PTC is absorbed by the sites that have surplus capacities and may fall in the traversed path. This is the fundamental objective of an MWCN to cater for the mobile subscribers and the surplus capacity is planned to serve this mobility when a subscriber traverses multiple zones served by different sites.

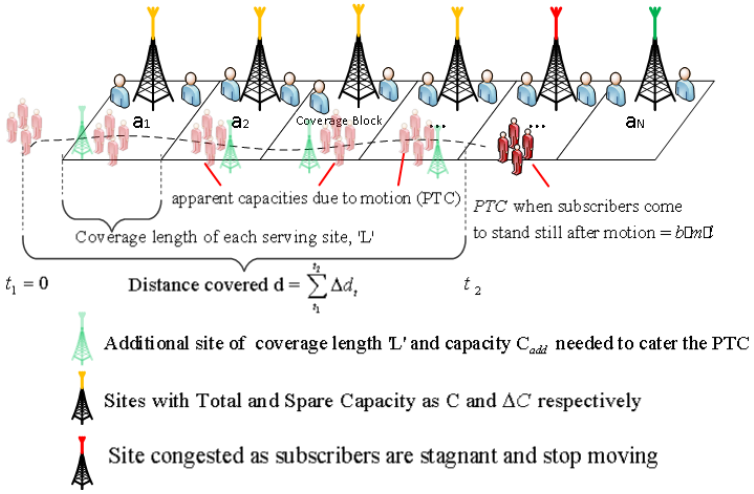

Figure 3-5-8: Additional Capacity Planning[1]

Figure 3-5-8 shows a case where a service provider may have to plan additional sites or add capacity radios in the serving sites to absorb the generated PTC. Therefore, to evaluate the network dimensioning to absorb the generated PTC, referring to figure 3-5-8, let us again assume that,

- the network is covered by N sites,
- initially, the subscribers are uniformly distributed across network so that every site has same static subscribers,
- each site has a spare capacity of ΔC,
- each site has capacity C,
- and, each site has a coverage length L (for simplicity, linear mobility analysis).

While planning a network, there is always a tradeoff between the expenses and ARPU. Therefore, the coverage and the capacity are not 100 percent assured. If it is a question of a handful of wobbling, an NSP will ignore the event. Nonetheless, if the ample subscriber strength demands an additional need, the NPS is bound to cater the additional event even though the ARPU gain is negligible.

Figure 3-5-9: An AoI that is subjected to a complex network environment where multiple iterations may lead to the cumulative PTC-generating need of additional coverage and/or capacity sites

Let us suppose that a group g_1 spends a time interval (t_1, t_2) and traverses a distance 'd' in discrete steps of Δd_t. Now, if in this duration, the group travels in an uncovered area of AoI, the additional 'coverage' sites needed to cater this path (shown as red curve in figure 3-5-9) [1]:

$$N_{add} = \frac{\sum_{t_1}^{t_2} \Delta d_t}{L} \tag{3.5.37}$$

Extending the present scenario in equation (3.5.36), we have:

$$|\overrightarrow{\overrightarrow{\overrightarrow{PTC}}}_{g_1}(t_1, t_2)| = Bd + |B.\ddot{\hat{l}}|| \tag{3.5.38}$$

Where $B = |S_1|b$ is the collective capacity of the subscribers in the group g_1 and 'd' is the magnitude of the distance traversed by the group.

The RHS of equation (3.5.38) has two terms which describe the nature of the sites deployed in this scenario. The first term represents the temporary sites or *Short Sites* that can remain for a short time and can be removed. The second term represents the *Length of Impact* site or *Long Sites* as we have termed it here that bounds the site to be active for a considerably prolonged period.

The capacity demand of the moving subscribers can be absorbed by these additional N_{add} only if there PTCs match. Therefore,

$$|\overrightarrow{\overrightarrow{\overrightarrow{PTC}}}_{g_1}(t_1, t_2)| = C_{new}d$$

or,
$$C_{new} = \frac{|\overrightarrow{\overrightarrow{\overrightarrow{PTC}}}_{g_1}(t_1, t_2)|}{d} \tag{3.5.39}$$

Then, the absorbable PTC by a site while traversing the coverage length L of a site will be [1],

$$PTC_{absorb} = \Delta CL \tag{3.5.40}$$

Therefore, the additional PTC in the form of reconfiguring the existing sites or adding new capacity sites will be [1]:

$$C_{add} = \frac{|\overrightarrow{\overrightarrow{\overrightarrow{PTC}}}_{g_1}(t_1, t_2)| - \Delta CL|S_1|}{d} \tag{3.5.41}$$

In this section, we have discussed the impact on the capacity requirements due to the mobility of potentially high data demanding subscribers or groups. Such dynamics in capacity demand may compel an NSP to expand or update the present network to compensate the additional demand. The next section will discuss the coverage impact due to place-time dynamics of the users. The goal is to provide the holistic overview of the place time impact on the network dimensioning.

3.6. THE PLACE TIME COVERAGE [2]

The Path Loss Model (PLM) plays a key role in the planning of a site for a chosen AoI. The Signal propagation characteristics define the limit of the extent, to which the signals can be received by a receiver above its respective sensitivity that we call

as Coverage Area or coverage radius of sites for a particular location in AoI. Needless to say that every location in AoI is different, therefore, may have a different radio propagation environment.

3.6.1. CONVENTIONAL COVERAGE PLANNING OF A NETWORK

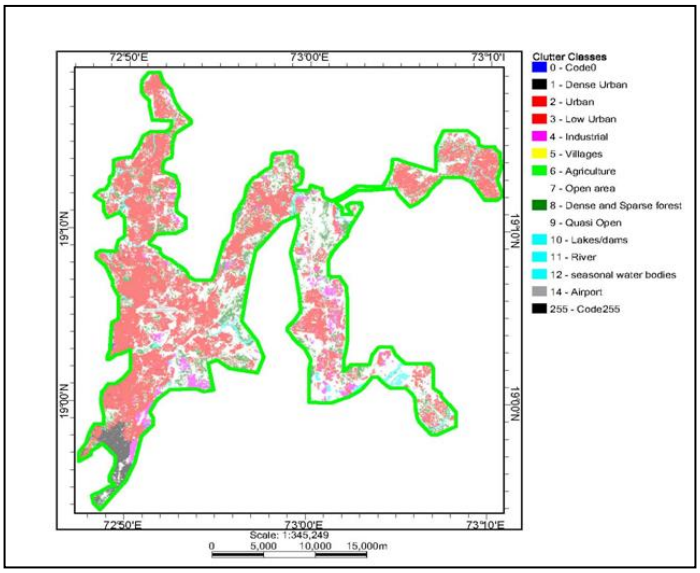

Figure 3-6-1: City of Mumbai, India clutter class based on propagation environment [18]

For the analysis, the City of Mumbai, India, was chosen for the coverage planning strategy of an AoI (Here in the City of Mumbai). Figure 3-6-1 shows the digital map of the City of Mumbai, which is resolved into areas based on the propagation environment, also known as clutter. This classification is based on the electric properties of the materials that come across when a signal traverses from a transmitter (T_x) to a receiver (R_x) flows. The denser the medium, the harder it is for the signal to maintain its strength (power), which leads to a drop in the power strength more quickly in a Dense Urban (DU) environment than in a Urban (U) or Sub Urban (SU). The rate of this drop with respect to the distance from the transmitter is known as *Path Loss* (PL). The minimum power required by a receiving unit to perceive a signal is often called as Receive Sensitivity (RS) and, based on the transmit power of a T_x, the maximum PL that can prevail in a communication system, corresponding to a propagation environment, without receiver failing to detect the signal, is known as Maximum Allowed Path Loss (MAPL). The value of MAPL decides the maximum inter-site distances in a particular area and varies area to area and is useful for a Coverage Driven Network. Table 3-1 shows the MAPL considerations for DU, U, SU and Rural (R) areas of

the City of Mumbai. For a tentative projection of coverage sites, this data is fed into a planning tool to run prediction based on the input parameters, some of these are mentioned in Table 3-1. As additional information, apart from the 1 to 14 clutter classes that are described here in figure 3-6-1, Class 0 means the site location and class/code 255 means no data (both are immaterial in the present discussion).

Table 3-1: Network Design coverage considerations for various clutter types for the City of Mumbai

System Gain (dB)	**163.4**	**154**
Handoff gain (dB)	2.5	2.5
Interference margin (dB)	3	3
Availability margin (dB)	-	-
System Gain within network (dB)	**162.9**	**153.5**
Shadow margin (dB)	11.6	
Indoor penetration (dB)	22	
Other margin (dB)	0	
MAPL (dB)	**129.3**	**120**

Dense Urban (DU)

System Gain (dB)	**163.4**	**154**
Handoff gain (dB)	2.5	2.5
Interference margin (dB)	3	3
Availability margin (dB)	-	-
System Gain within network (dB)	**162.9**	**153.5**
Shadow margin (dB)	8.7	
Indoor penetration (dB)	18	
Other margin (dB)	0	
MAPL (dB)	**136.2**	**126.9**

Urban (U)

System Gain (dB)	**163.4**	**154**
Handoff gain (dB)	2.5	2.5
Interference margin (dB)	3	3
Availability margin (dB)	-	-
System Gain within network (dB)	**162.9**	**153.5**
Shadow margin (dB)	5.9	
Indoor penetration (dB)	12	
Other margin (dB)	0	
MAPL (dB)	**145**	**135.7**

Sub-Urban (SU)

System Gain (dB)	**163.4**	**155.8**
Handoff gain (dB)	2.5	2.5
Interference margin (dB)	3	3
Availability margin (dB)	-	-
System Gain within network (dB)	**162.9**	**155.3**
Shadow margin (dB)	5.9	
Indoor penetration (dB)	8	
Other margin (dB)	0	
MAPL (dB)	**149**	**141.4**

Rural (R)

The network is to be designed in such a way that the user in an indoor location can receive the signal above the sensitivity level of the user device. It can be seen in Table 3-1 that the indoor penetration and shadowing margin are the main contributors to the loss. The MAPL value obtained here will decide the radius of a cell that belongs to a particular site. With these considerations, when the planning tool is operated on the given digital map, it generates the site predictions so that there are minimum coverage sites for the maximum area covered with a probability of 95% and above. Figure 3-6-2 shows the site predictions and their location with respect to the digital map data. As we can see, the site count is higher where the digital map data shows DU or U areas the lowest in the vegetation and rural areas. This is because the indoor loss in DU is higher than any other clutter. Although vegetation also contributes to the path-loss, however, as the subscriber expectancy is negligible and the indoor loss as well, the site counts are fairly low in these areas. It is important to mention that COST-231 propagation model is chosen here for evaluating the coverage sites of the given area.

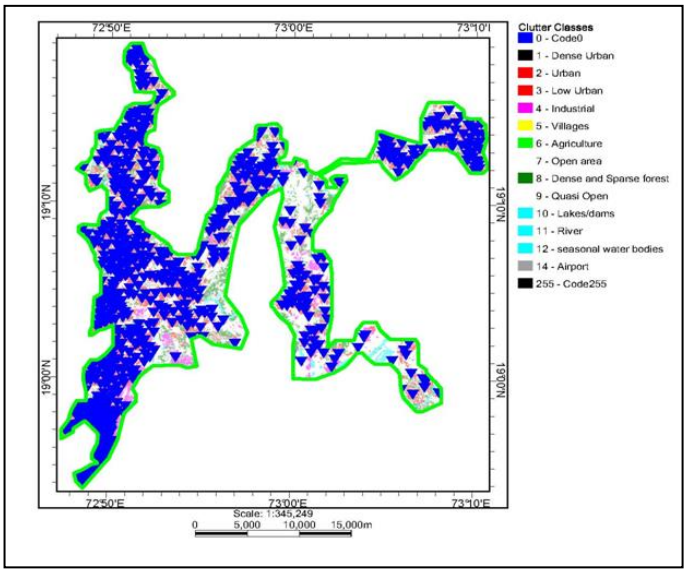

Figure 3-6-2: Site Predictions based on assumptions in Table 3-1[6][15]

Further, based on the estimated sites, the coverage prediction of the area is also analysed by the tool. Figure 3-6-3 shows the coverage of the predicted sites for the given area. To avoid irregularities and to narrow down the operation time of the planning tool, the coverage is categorized into four groups namely, based on the clutter types DU (Best Signal Level ≥ 60.3), U (Best Signal Level ≥ 70.2), SU (Best Signal Level ≥ 79.0) and R (Best Signal Level ≥ 83.0). The coverage prediction is done considering 95% coverage probability. This means that if an area is coloured with Best Signal Level >=60.3 dBm, for 95% of the time, a user within this area will receive a signal strength equal or above 60.3 dBm. This will ensure that a user in an indoor environment, as described by the indoor loss value for DU clutter in Table 3-1, will receive the signal level at least above the receiver sensitivity 95% of the total time.

The network is planned to inscribe the subscriber mobility throughout the AoI notwithstanding, the planned network is essentially static in nature which means that once the sites are deployed, they are strictly dedicated to the area surrounding that particular location where the site is installed. Table 3-1 is an endorsement of this statement as the MAPL values are essentially global within the clutter area. Despite being the universal method of the network deployment strategy on the global scale, yet, as the MNC are progressing to the new futuristic paradigm, such approach shall not be a viable solution in future.

[6] Predictions obtained from Atoll® Planning Tool

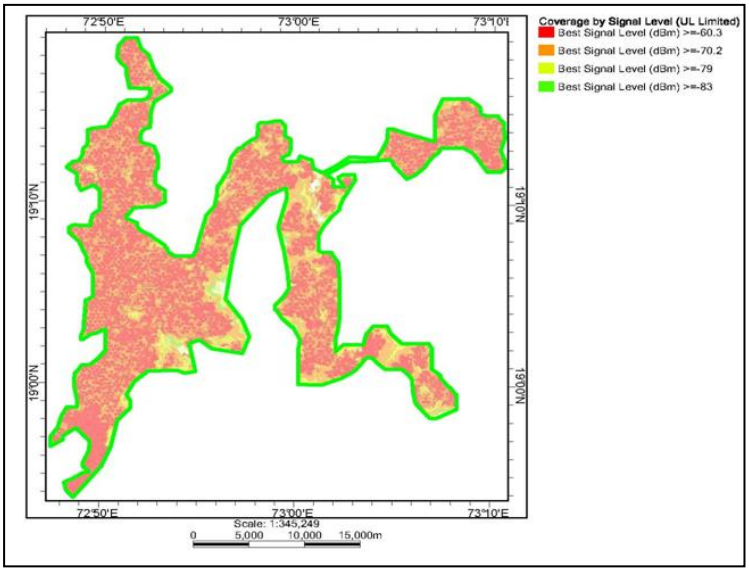

Figure 3-6-3: Coverage plot of the site predictions for the City of Mumbai[7] [18]

PLMs are mathematical models that are used to predict the received signal strength at some distance D from a T_x based on some empirically obtained reference values at some reference distance D_0. Based on environment type and the frequency of operation, certain predefined PLMs are developed. As an example and as already been discussed in this section, the PLM that was used by the planning tool to predict coverage sites in the City of Mumbai is COST 231. The next subsection describes problems associated with this static nature of PLMs.

3.6.2. RELATED WORKS: STATIC PATH LOSS MODELS

Generally, a path-loss is expressed as the ratio of transmitting power to the received power, that is [19]:

$$\mathrm{PL}(a,b) = \frac{P_t(a)}{P_r(b)} \tag{3.6.1}$$

Where, 'a' and 'b' are transmit and receive geographical positions respectively, and, PL(a, b) represents the path-loss between them.

[7] Predictions obtained from Atoll® Planning Tool

The above equation can be expressed in decibel form as below:

$$P_{r(dB)}(b) = P_{t(dB)}(a) - PL_{(dB)}(a, b) \quad (3.6.2)$$

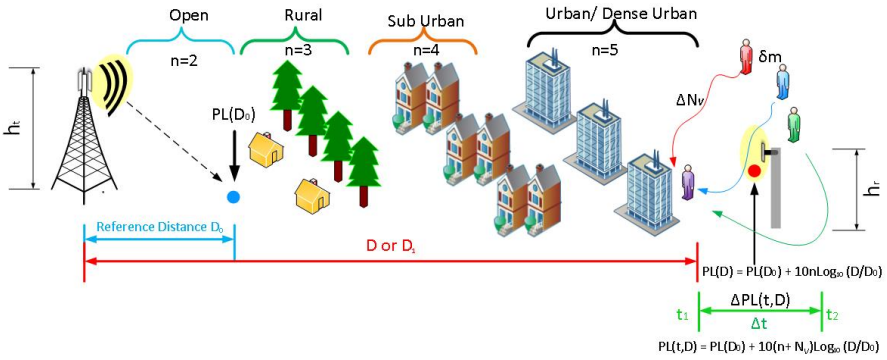

Figure 3-6-4: Path-loss Contributors with respect to the path-loss coefficient

Figure 3-6-4 shows the path-loss contributors that collectively define a clutter type. Each clutter type can be represented by the Path Loss Exponent (PLE) with its value increasing from 2 to 5 depending upon the combined properties of materials which a clutter is composed of.

The least square regression PLM can be expressed in decibels (dB) as:

$$PL(D) = PL(D_0) + 10\log_{10}\left(\frac{D}{D_0}\right)^n \quad (3.6.3)$$

Where, D_0 is the distance from T_x where the reference received signal of T_x is measured, D is the distance from T_x where the signal needs to be predicted, and PL(D): Total Path-loss at a distance D from T_x. For the convenience of calculations, D_0 is usually the unit distance from a T_x. The PLE, being the clutter indicator, takes an appropriate value from the empirically obtained list. Usually, PLE takes values such as n=2 (free space) which increases to 3 for flat rural, 3.5 for rolling rural, 4 for SU, 4.5 for U and, 5 for DU. Although PLE has a very limited domain varying from 2-5 or 6, yet being an exponent, the slight variation may lead to significant impact.

Popular PLMs

(i) Friis PLM [19]:

This PLM considers the loss in the signal strength due to the dissipation of energy in the free space and is often formulated as:

$$\frac{P_r}{P_t} = G_t G_r \left(\frac{\lambda}{4\pi D}\right)^2 \tag{3.6.4}$$

Where,

- λ: Operating Carrier Wavelength of the signal,
- T_x : Antenna of the Transmitting Module,
- R_x : Antenna of the Receiving Module,
- P_t : Power Transmitted from a T_x,
- P_r : Power Received by a R_x,
- G_t : Gain of T_x,
- G_r : Gain of R_x,

Considering the antenna gains as unity, i.e. $G_t=G_r=1$, from equations (3.6.2) and (3.6.4), we have:

$$PL_{friis}(D) = PL_{FS}(D) = \left(\frac{4\pi D}{\lambda}\right)^2 \tag{3.6.5}$$

This is a non-decibel form of the PLM equation, and the decibel form can be derived by using $10\log_{10}(.)$ operator on either side. The other PLMs discussed below are in decibel form.

(ii) Okumura-Hata PLM [19]:

This is a very popular model for most of the Terrestrial Mobile Communication planning, and its formula is as per given below:

$$\begin{aligned} PL_{OH} = {} & 69.55 - 26.16\log_{10}(f) - 13.82\log_{10}\left(\frac{h_t}{h_0}\right) - C_H \\ & + \left[44.9 - 6.55\log_{10}\left(\frac{h_t}{h_0}\right)\right]\log_{10}\left(\frac{D}{D_0}\right) + A_\alpha \end{aligned} \tag{3.6.6}$$

Where, $C_H = 0.8 + [1.1\log_{10}(f) - 0.7]h_{mt} - 1.56\log_{10}(f)$

For smaller cities, and,

$$C_H = \begin{cases} 8.29(\log_{10}(1.54h_m))^2 - 1.1, & \text{if } 150 \le f \le 200 \\ 3.2\left(\log_{10}(11.75h_m)\right)^2 - 4.97, & \text{if } 200 \le f \le 1500 \end{cases}$$

For large cities

(iii) Cost-231 Hata PLM [19]:

This is again a popular model and is well suited for 1.5-2 GHz and is as per below.

$$PL_{cost231} = 46.3 + 33.9\log_{10}(f) - 13.82\log_{10}(h_t) - a(h_r) + [44.9 - 6.55\log_{10}(h_t)]\log_{10}(D) + C \quad (3.6.7)$$

Where, $a(h_r) = (1.1log_{10}(f) - 0.7)h_{r-}(1.56log_{10}f - 0.8)$

and,

- T_x / R_x: Antenna of the Transmitting/ Receiving Module,
- D: Distance between T_x and R_x,
- P_t / P_r : Power Transmitted / Received from/by a T_x/R_x,
- G_t/ G_r : Antenna gain of T_x/R_x,
- A_α: Area adjustment factor,
- C_H: Receiver antenna height correction factor,

and, the parameters in Table 3-2 below.

Table 3-2: Common PLM parameters between Okumura-Hata and Cost 231with different values

Parameter	Okumura-Hata	Cost 231
f : Operating Carrier frequency of the signal	150≤ f≤ 1500	1500 ≤f≤2000
h_t : Height of T_x (BS) with respect to ground	20-200	20-200
h_r : Height of R_x (MS) with respect to ground	1-1.5m	1-1.5m
h_0 : BS antenna height (length)	1m	1m
C: Receiver antenna height correction factor	C_H	$C = \begin{cases} 0 \text{ for SU} \\ 3 \text{ for} > U \end{cases}$

These PLMs are commonly used by planning tools at an industrial level to predict the site count and positions of any geographical portion. It can be seen from all three examples that the factors that account for the dynamics in PLMs are the operational frequency f, the antenna heights of both the BS and the MS, h_t and h_r etc. It may be seen from Table 3-2, that h_t is the height of T_x (BS) with respect to ground and h_r is the height of R_x (MS) with respect to ground. These parameters are essentially uniform and predominantly unchangeable during the certain course of time. Therefore, the Place-Time events are unaccounted for, while planning a network. Of course, with a large coverage radius (> 250m to a few kilometers), high site counts, especially in a metro city like Mumbai (India), and with the current voice-oriented communication technologies, the Place-Time events are often insignificant. However, for a throughput sensitive demand, this can lead to a

scorching situation. The next subsection will discuss the dynamics in a PLM due in a Place-Time event.

3.6.3. DYNAMIC PATH LOSS MODEL [2]

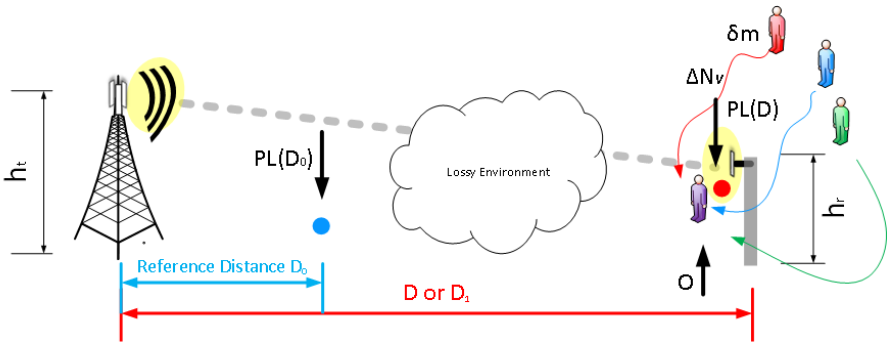

Figure 3-6-5: Dynamics in Path-loss Model (PLM)

The dilemma of a Static Network Design: Let us assume the scenario as described in figure 3-6-5 where the T_x and R_x are separated by distance D_1. Therefore, as discussed in section 3.6.2, an observer with a receiving antenna at O will obtain a signal level as per equation 3.6.1 as rewritten below [20] [21] [22] [23]:

$$PL(D_1) = PL(D_0) + 10\log_{10}\left(\frac{D_1}{D_0}\right)^n = PL(D_0) + 10n\log_{10}\left(\frac{D_1}{D_0}\right) \quad (3.6.8)$$

Let us also assume that this observer is continuously observing the received signal for a considerable period of time, say during the interval (t_1, t_2). Therefore, any discrete change during this period in the observed signal levels can be expressed as:

$$\Delta PL(D_1)|_{t_1}^{t_2} = \Delta PL(D_0)|_{t_1}^{t_2} + \Delta 10n\log_{10}\left(\frac{D_1}{D_0}\right)|_{t_1}^{t_2} \quad (3.6.9)$$

Where, Δ signifies a discreet change in the observed values.

In our previous discussion, we have considered the network environment to remain unchanged at every instance of time. Extending this assumption to the present scenario, we may assume that all relevant physical parameters would remain unchanged for the present discussion. This means that there will be no change in the observed values and, Right Hand Side (RHS) of equation (3.6.9) reduces to zero and therefore:

$$\Delta \mathrm{PL}(\mathrm{D}_0)|_{t_1}^{t_2} = 0$$

and,

$$\Delta 10\mathrm{nlog}_{10}\left(\frac{\mathrm{D}_1}{\mathrm{D}_0}\right)|_{t_1}^{t_2} = 0 \tag{3.6.10}$$

From equations (3.6.8), (3.6.9) and (3.6.10) we have:

$$\Delta \mathrm{PL}(\mathrm{D}_1)|_{t_1}^{t_2} = 0 \tag{3.6.11}$$

It can be seen from equation (3.6.11) that for the presumably static environment the observed values must be unchanged. Hence, as per assumptions, the observer (user) will not experience any change in path. Nonetheless, this is a hypothetical truth and, in reality, users do experience the variations in the signal levels. Although, long term and short term fadings are incorporated in evaluating the losses, yet, they are limited to the individual mobility of the user.

Dynamic PLM: Assuming that the user is strictly static at a distance D from T_x, we can incorporate the variation by negating equation (3.6.11) as:

$$\Delta \mathrm{PL}(\mathrm{D}_1)|_{t_1}^{t_2} \neq 0 \tag{3.6.12}$$

Rewriting equation (3.6.12) in its normal form, we have:

$$\overline{\overline{\mathrm{PL}}}(\mathrm{D}_1) = \overline{\overline{\mathrm{PL}}}(\mathrm{D}_0)\left(\frac{\mathrm{D}_1}{\mathrm{D}_0}\right)^{\mathrm{n}} \tag{3.6.13}$$

Where, the accent indicates the path-loss in non-decibel format. From equation (3.6.5), we have the value of $\overline{\overline{\mathrm{PL}}}(\mathrm{D}_0)$ as mentioned in equation below where,

$$\overline{\overline{\mathrm{PL}}}(\mathrm{D}_0) = \left(\frac{4\pi \mathrm{D}_0}{\lambda}\right)^2 \tag{3.6.14}$$

As per assumption, this is a scenario when the received signal has traversed through the static environment as modeled by a static PLM mention in equation (3.6.13).

Firstly, let us assume that the environmental conditions are stagnant during the period of observation which holds equation (3.6.11) true. As a next step, let the medium between T_x and R_x densify in small increments of a material δm that is entering into the medium. This δm can be any material or object including human beings. Therefore, the static path which previously had invariable environment will now react to the incremental change in the material property of the medium. As the medium densifies or rarifies in steps of **δm**, the propagation behaviour will also

change. Hence, now, *the static expression of the medium modifies to a place and time dependent entity* and the path-loss behaviour of medium depends *on the rate with which* ***δm*** *changes and the position that it acquires* in the AoI.

This Place-Time dependency is incorporated here in this chapter by modifying equation (3.6.14) to a place and time varying entity shown in equation below as:

$$\overline{\overline{PL}}_{\omega}(D,p,t) = \overline{\overline{PL}}(D_0)\left(\frac{D}{D_0}\right)^{n+N_{AR}(m,p,t)} \tag{3.6.15}$$

Where N_{AR} is the ***Augmented Repercussive Exponent*** and is the function of time, position, and properties of the material of the changing medium. The constant n is not absorbed in N_{AR} to indicate that the observation is made at a point D, and it is different from the reference point. As N_{AR} is dependent on certain parameters, therefore, the variation of N_{AR} w.r.t time can be written as:

$$\frac{d}{dt}[N_{AR}(m,p,t)] = \frac{d}{dt}[N_{AR}]\left[\frac{d}{dt}(m) + \frac{d}{dt}(p)\right]$$

Which yields,

$$\frac{d}{dt}[N_{AR}(m,p,t)] = \widehat{N_{AR}}\left[p(t)\frac{d}{dt}(m) + m(t)\frac{d}{dt}(p)\right] \tag{3.6.16}$$

The second term in RHS of equation (3.6.16), $p(t)\frac{d}{dt}(m)$, represents the change in the material properties with time for a position p(t). This means that if the property of the material changes with time rather than with the position, this term will be determining. Similarly, the third term $m(t)\frac{d}{dt}(p)$ is considered when the change in the medium is due to a positional disturbance of a material.

Let, $$\frac{d}{dt}(m) = \rho_m$$

and, $$\frac{d}{dt}(p) = v_m \tag{3.6.17}$$

Where ρ_m is the material property and v_m is the velocity of the incremental δm. For a three-dimensional space, it is possible that a material may show polymorphism. Therefore, equation (3.6.17) will transform into a Cartesian expression as per below:

$$\frac{d}{dt}(m) = \rho_{mx}\frac{dx}{dt} + \rho_{my}\frac{dy}{dt} + \rho_{mz}\frac{dz}{dt}$$

and, similarly,

$$\frac{d}{dt}(p) = v_{mx}\frac{dx}{dt} + v_{my}\frac{dy}{dt} + v_{mz}\frac{dz}{dt} \tag{3.6.18}$$

From equation (3.6.15), we have:

$$\overline{\overline{PL}}_{\omega}(D, p, t) = \overline{\overline{PL}}(D_0)\left(\frac{D}{D_0}\right)^{n+N_{AR}(m,p,t)}$$

or, $$\overline{\overline{PL}}_{\omega}(D, p, t) = \overline{\overline{PL}}(D_0)\left(\frac{D}{D_0}\right)^{n}\left(\frac{D}{D_0}\right)^{N_{AR}(m,p,t)}$$

or, and from equation (3.6.13), we have:

$$\overline{\overline{PL}}_{\omega}(D, p, t) = \overline{\overline{PL}}(D)\left(\frac{D}{D_0}\right)^{N_{AR}(m,p,t)} \tag{3.6.19}$$

Therefore,

$$\frac{d}{dt}\overline{\overline{PL}}_{\omega}(D, p, t) = \frac{d}{dt}\overline{\overline{PL}}(D)\left(\frac{D}{D_0}\right)^{N_{AR}(m,p,t)}$$

or, $$\frac{d}{dt}\overline{\overline{PL}}_{\omega}(D, p, t) = \overline{\overline{PL}}(D)\frac{d}{dt}\left(\frac{D}{D_0}\right)^{N_{AR}(m,p,t)}$$

or, $$\frac{d}{dt}\overline{\overline{PL}}_{\omega}(D, p, t) = \overline{\overline{PL}}(D)\frac{d}{dt}\left(\frac{D}{D_0}\right)^{N_{AR}} \tag{3.6.20}$$

It is already known that:

$$\frac{d}{dx}(a^x) = \frac{a^x}{\log_e(a)} \tag{3.6.21}$$

and, $$\frac{d}{dx}f(y) = \frac{d}{dy}f(y)\frac{dy}{dx} \tag{3.6.22}$$

Therefore, joining equations (3.6.20), (3.6.21) and (3.6.22), would give:

$$\frac{d}{dt}\overline{\overline{PL}}_{\omega} = \frac{\overline{\overline{PL}}(D)\left(\frac{D}{D_0}\right)^{N_{AR}}}{\log_e\left(\frac{D}{D_0}\right)}\frac{d}{dt}(N_{AR})$$

or, and from equation (3.6.16), we have:

$$\frac{d}{dt}\overline{\overline{PL}}_{\omega} = \frac{\overline{\overline{PL}}(D)\left(\frac{D}{D_0}\right)^{N_{AR}}}{\log_e\left(\frac{D}{D_0}\right)}\widehat{N_{AR}}\left[p(t)\frac{d}{dt}(m) + m(t)\frac{d}{dt}(p)\right] \qquad (3.6.23)$$

Replacing (3.6.17) in (3.6.23) we have:

$$\frac{d}{dt}\overline{\overline{PL}}_{\omega} = \frac{\overline{\overline{PL}}(D)\left(\frac{D}{D_0}\right)^{N_{AR}}}{\log_e\left(\frac{D}{D_0}\right)}\widehat{N_{AR}}\left[p(t)\rho_m + m(t)v_m\right]$$

or, $$\widehat{\overline{\overline{PL}}_{\omega}} = \frac{\overline{\overline{PL}}(D)\left(\frac{D}{D_0}\right)^{N_{AR}}}{\log_e\left(\frac{D}{D_0}\right)}\widehat{N_{AR}}\left[p(t)\rho_m + m(t)v_m\right] \qquad (3.6.24)$$

Or, when expressed in dB, equation (3.6.24) yields:

$$\widehat{PL_{\omega}} = \widehat{PL}(D) + 10\,N_{AR}\log_{10}\left(\frac{D}{D_0}\right) + 10\log_{10}\widehat{N_{AR}}\left[p(t)\rho_m + m(t)v_m\right] \qquad (3.6.25)$$

Where the reference power ratio $\widehat{PL} = \frac{PL(D)}{\log_e\left(\frac{D}{D_0}\right)}$; and, similarly, the decibel expression of equation (3.6.15) yields:

$$PL_{\omega}(D,p,t) = PL(D_0) + 10\,n\log_{10}\left(\frac{D}{D_0}\right) + 10\,N_{AR}\log_{10}\left(\frac{D}{D_0}\right)$$

or,
$$PL_{\omega}(D,p,t) = PL(D) + 10\,N_{AR}\log_{10}\left(\frac{D}{D_0}\right) \qquad (3.6.26)$$

Equation (3.6.24) is the time differential form of equation (3.6.26).

Both equations, (3.6.25) and (3.6.26) can be understood as: *the PLM of a radio environment contains two factors, one (which are the first terms in both equations) that represents the loss due to composition, although static, of the medium and another (which are the terms other than the first term) represent the change in the environmental behaviour due to dynamics of some or all composition within the environment*.

Hence, it can be seen that the Position and Time of a material can impact the propagation characteristics of a seemingly static environment. Although, some cushion is provided to compensate the real-time variations in the network but that is not optimal, and it will be discussed in the next section. As, the path-loss of an environment decides the coverage radius of a cell, this kind of phenomenon where the radio environment of a channel is affected with time and position of the type of material (dielectric compositions) in the propagation path is termed here as Place Time Coverage (PTCo).

3.7. OSTENTATIOUS PROBABILITY DENSITY FUNCTION

In section **3.2.5** of **Appendix 3.2**, provides details about the Gaussian probability distribution function for the unostentatious events. In this section, the ostentatiousness in the PDF that may alter the smooth bell-shaped curve of a PDF into a time-based pattern is discussed. The PDF, as discussed in section 3.2.5 predicts the probability of an output (such as the arrival of a signal value) of a biased probability in which the output inclines towards a median value (such as the center of an antenna lobe). Therefore, in this section, the change in the predictability of an event with time is endorsed to elaborate the PDF in a time and place domain.

Let us assume that an experiment is sampled at a point P which is inclined to a median value μ with deviation σ, as shown in figure 3-7-1. The experiment may be an arrival of a signal or an arrow that was slinged from a bow. For all such unsotetatious experiments, the PDF can be described as (see, equation 3.2.8):

$$f_R(r) = \frac{1}{\sqrt{2\pi}\,\sigma} e^{\left[-\frac{(r-\mu)^2}{2\sigma^2}\right]} \tag{3.7.1}$$

Where 'r' is the domain of a Random Variable R. This equation describes the probability of finding a sample at a certain distance and inclining to a certain value. Plotting all the probabilities will generate a bell-shaped PDF as shown in figure 3-7-1.

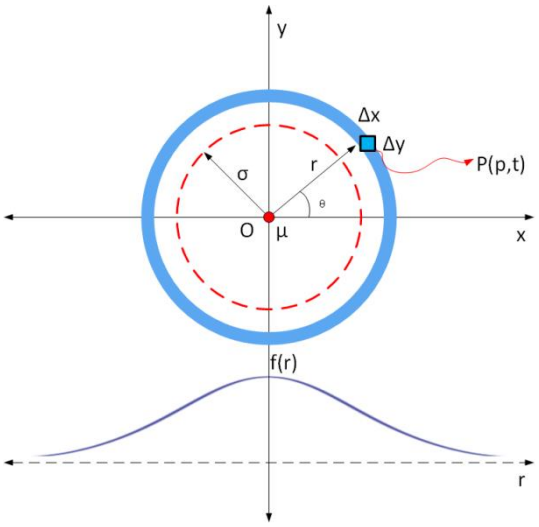

Figure 3-7-1: Sampling an outcome at a point A

Let, in equation (3.7.1), f(r) be the probability of finding a user at a point P with the median at a point 'O' which describes the point of interest, say an idol of Lord Ganpati, of all the users in that area. However, this event is not flat in the time domain and the subscribers, being an itinerant entity, tend to move closer or away from the point of interest. Also, for every time instant, the location of a subscriber may be at the different position for the same time instant. Similarly, the point of interest that is situated at 'O' may also change its position with time and may attain different positions for same time stamps. Therefore, both standard deviation 'σ' and mean 'μ' are the time and place dependent functions.

This means that the same PDF f(r) would have appeared differently in the present time under different circumstances. Therefore, having a PDF for an experiment itself is a matter of chance. The same thing is applicable for any future moment. Nonetheless, if this would have been an unostentatious event, then the PDF in equation 3.7.1 would yield:

$$\frac{d}{dt} f_R(r) = 0 \tag{3.7.2}$$

However, for f(r) behaving ostentatiously, we have:

$$f_R(r,p,t) = \frac{1}{\sigma(p,t)\sqrt{2\pi}} e^{\left[-\frac{(r-\mu(p,t))^2}{2\sigma(p,t)^2}\right]} \tag{3.7.3}$$

or, $$f_R(r,p,t) = \frac{1}{\ddot{\sigma}\sqrt{2\pi}} e^{\left[-\frac{(r-\ddot{\mu})^2}{2\ddot{\sigma}^2}\right]} \tag{3.7.4}$$

Where, $\ddot{\sigma}$ and $\ddot{\mu}$ represents the Place-Time format of σ and μ respectively.

Differentiating equation (3.7.4) in place and time:

$$\frac{d}{dt}\left(\frac{d}{dp} f_R\right) = \frac{d}{dt}\left(\frac{d}{dp}\left[\frac{1}{\ddot{\sigma}\sqrt{2\pi}} e^{\left[-\frac{(r-\ddot{\mu})^2}{2\ddot{\sigma}^2}\right]}\right]\right) \tag{3.7.5}$$

Let, $A(p) = \frac{1}{\ddot{\sigma}\sqrt{2\pi}} e^{\left[-\frac{(r-\ddot{\mu})^2}{2\ddot{\sigma}^2}\right]}$, $\ddot{\sigma} = w$, and, $\ddot{\mu} = v$

Then, $$A(p) = \frac{1}{w\sqrt{2\pi}} e^{\left[-\frac{(r-v)^2}{2w^2}\right]} \tag{3.7.6}$$

Therefore,

$$\frac{d}{dt}A(p) = \frac{d}{dt}\left[\frac{1}{w\sqrt{2\pi}} e^{\left[-\frac{(r-v)^2}{2w^2}\right]}\right]$$

or, $$A'(p) = \frac{1}{w\sqrt{2\pi}}\frac{d}{dt}\left[e^{\left[-\frac{(r-v)^2}{2w^2}\right]}\right] + e^{\left[-\frac{(r-v)^2}{2w^2}\right]}\frac{d}{dt}\left[\frac{1}{w\sqrt{2\pi}}\right]$$

or, $$A'(p) = \frac{1}{w\sqrt{2\pi}} e^{\left[-\frac{(r-v)^2}{2w^2}\right]}\frac{d}{dt}\left[-\frac{(r-v)^2}{2w^2}\right] + e^{\left[-\frac{(r-v)^2}{2w^2}\right]}\frac{d}{dt}\left[\frac{-w'}{w^2\sqrt{2\pi}}\right]$$

or, $$A'(p) = -\frac{1}{w\sqrt{2\pi}} e^{\left[-\frac{(r-v)^2}{2w^2}\right]}\left[\frac{d}{dt}\left\{\frac{(r-v)^2}{2w^2}\right\} + \frac{w'}{w}\right]$$

or, $$A'(p) = -\frac{1}{w\sqrt{2\pi}} e^{\left[-\frac{(r-v)^2}{2w^2}\right]}\left[\frac{2(r-v)(-v')w^2 - (r-v)^2(2w)w'}{2w^4} + \frac{w'}{w}\right]$$

or, $$A'(p) = -\frac{1}{w\sqrt{2\pi}} e^{\left[-\frac{(r-v)^2}{2w^2}\right]}\left[\frac{(r-v)(-v')w^2 - (r-v)^2(w)w'}{w^4} + \frac{w'}{w}\right]$$

or, $$A'(p) = \frac{(r-v)}{w\sqrt{2\pi}} e^{\left[-\frac{(r-v)^2}{2w^2}\right]}\left[\frac{(v')(w^2) + (r-v)(w)(w')}{w^3} + \frac{w'}{w}\right] \tag{3.7.7}$$

Substituting (3.7.6) in (3.7.7), we have:

$$A'(p) = A(p)(r-v)\left[\frac{(v')(w^2)+(r-v)(w)(w')}{w^3}+\frac{w'}{w}\right] \quad (3.7.8)$$

Now let,

$$B = A' \quad (3.7.9)$$

Therefore,

$$\frac{d}{dt}B = \frac{d}{dt}A' \quad (3.7.10)$$

Substituting A' from (3.7.8) in (3.7.10), we have:

$$\frac{d}{dt}B = \frac{d}{dt}\left\{A(t)(r-v)\left[\frac{(v')(w^2)+(r-v)(w)(w')}{w^3}+\frac{w'}{w}\right]\right\}$$

or,

$$B' = \frac{d}{dt}\left\{A(t)(r-v)\left[\frac{(v')(w^2)+(r-v)(w)(w')}{w^3}+\frac{w'}{w}\right]\right\} \quad (3.7.11)$$

Let,

$$G(t) = (r-v)\left[\frac{(v')(w^2)+(r-v)(w)(w')}{w^3}+\frac{w'}{w}\right] \quad (3.7.12)$$

When differentiated with position and,

$$H(t) = (r-v)\left[\frac{(v^*)(w^2)+(r-v)(w)(w^*)}{w^3}+\frac{w^*}{w}\right] \quad (3.7.13)$$

When differentiated with time.

Therefore, from equations (3.7.11) and (3.7.12), we have:

$$B' = \frac{d}{dt}\{A(t)G(t)\}$$

or,

$$B' = G(t)\frac{d}{dt}A(t) + A(t)\frac{d}{dt}G(t)$$

or, $$\boxed{B' = G(t)A'(t) + A(t)G'(t)} \quad (3.7.14)$$

Interpreting (3.7.7) in terms of time, and substituting with (3.7.13), we have:

$$A'(t) = A(t)H(t) \quad (3.7.15)$$

Therefore, from (3.7.14) and (3.7.15), we have:

$$B' = G(t)A(t)H(t) + A(t)G'(t)$$

or, $$B' = A(t)\{G(t)H(t) + G'(t)\} \quad (3.7.16)$$

From equations (3.7.16) in (3.7.5), we have:

$$\frac{d}{dt}\left(\frac{d}{dp} f_R\right) = A\{GH + G'(t)\}$$

or, $$\boxed{U(f_R) = A\{GH + G'(t)\}} \quad (3.7.17)$$

When place and time are independent parameters, then equation (3.7.8) is the rate at which the PDF varies with either place or time, that is:

$$\boxed{Q(f_R) = \frac{d}{dp} f_R = AG} \quad (3.7.18)$$

for a change due to the position, and,

$$\boxed{T(f_R) = \frac{d}{dt} f_R = AH} \quad (3.7.19)$$

for a change due to time, and, equation (3.7.17) is the influence of one parameter on the rate with respect to another. In case, these two parameters are related (as for most of the cases), equations are complemented with the derivatives of other entity such as:

$$\boxed{T(f_R) = AH\frac{dp}{dt} = AH\vartheta} \quad (3.7.20)$$

and, $$\boxed{U(f_R) = A\{GH + G'(t)\}\frac{dp}{dt} = A\{GH + G'(t)\}\vartheta} \quad (3.7.21)$$

Where, ϑ is the velocity with which the stimulant is moving in space (place).

3.8. ANALYSIS OF PTC IN THE NETWORK DEPLOYMENT

Referring to figure 3-8-1, let us consider that a network has to be planned where,

(i) there is only one subscriber in the network,
(ii) the subscriber needs ξ carriers/ Subcarriers to satisfy its capacity demand,
(iii) the subscriber transit from point A to B and vice versa (considering A as home and B as the workplace) through various paths and, APB, AQB, and ARB are three of them,
(iv) each site has a cell radius of λ,
(v) κ is the total carriers required by the network to satisfy subscriber needs.

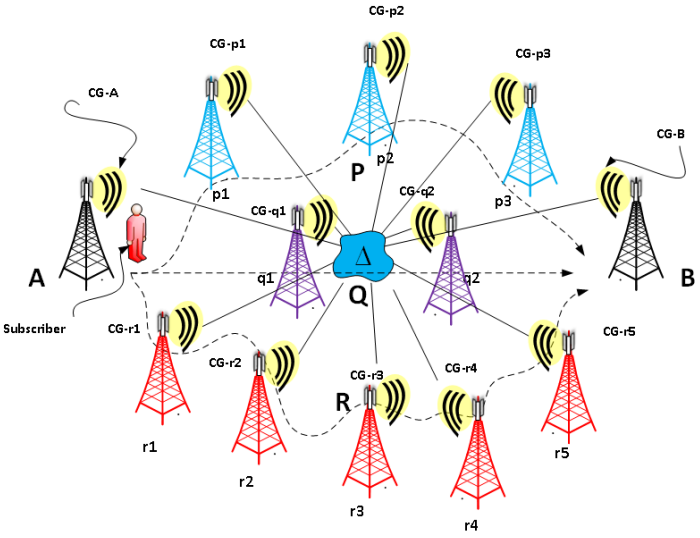

Figure 3-8-1: A conventional deployment scenario

Then, with conventional strategy, the network will be planned as follows:

(A) Phase 1: Initially, the sites are deployed where the subscriber spends a considerable duration of time. This initial deployment is what is discussed in section 1.1 of this thesis as Green Phase.
  (i) In this case, Point A and B are such locations and the sites are deployed at both locations.
  (ii) Then, these sites are allocated with ξ carriers grouped as (carrier group A) CG-A and CG-B. Such that, | CG-A| = |CG-B| = ξ. Where, |.| operator denotes the number of elements of a set.

Ideally, to avoid co-channel interference, {CG-A} and {CG-B} should be distinct or orthogonally separated[15]. For the present discussion, let us consider the prior condition, that is:

$$\{CG\text{-}A\} \cap \{CG\text{-}B\} = \phi \quad (3.8.1)$$

Therefore, $\kappa = 2\xi$ (3.8.2)

(B) Phase 2: The intermediate paths that are traversed by the subscriber are now addressed.

(i) There is a need for a new site the moment subscriber crosses the distance κ from the center of serving the site. The new site is deployed in such a way that inter-site distance is 2κ.

(ii) Starting from point A, the next site position is either of p1, q1 or r1 if subscriber follows either of AQB, APB or ARB respectively.

(iii) Step (A-ii) is followed to allocate carriers to this new site and therefore, from equations (3.8.1) and (3.8.2), we have:

$$\{CG\text{-}A\} \cap \{CG\text{-}p1\} = \phi \quad (3.8.3)$$

and, $\kappa = 3\xi$ (3.8.4)

(iv) As, sites at position p1, q1 and r1 are neighbours to A and, to each other as well therefore, the condition of (B-iii) also applies here. Hence,

$$\{CG\text{-}A\} \cap \{CG\text{-}p1\} \cap \{CG\text{-}q1\} \cap \{CG\text{-}r1\} = \phi \quad (3.8.5)$$

and, $\kappa = 5\xi$ (3.8.6)

(v) Assuming that the service provider is extremely pessimist about the spectrum, the next sites can be planned by allocating the same CGs among the sites such that no CG of same carrier sets is an immediate neighbour to each other. Such as:

$$\{CG\text{-}q2\} = \{CG\text{-}A\}; \{CG\text{-}r2\} = \{CG\text{-}q1\};$$

$$\{CG\text{-}q2\} = \{CG\text{-}r1\} \quad (3.8.7)$$

and, $\kappa = 5\xi$ (3.8.8)

(vi) Steps (B-iv) and (B-v) can be repeated for covering all the paths where the service provider ever needs to deploy a site to cater the subscriber mobility.

(vii) While performing step (B-vi), in case the permutations of CGs are exhausted, then more spectrum demand is raised. Thus, for a completely planned network,

Let, $\kappa = C\xi$, (3.8.9)

$R_u = \sqrt{C}$, (3.8.10)

and, $\gamma = \frac{A_{AoI}}{\lambda}$ (3.8.11)

Where, C is the cluster size of the network that is repeated across the entire network to form a Honey Comb-like cellular structure, R_u is the reuse distance[24], and, γ is the number of sites in the network of area A_{AoI}.

Such sites, as discussed in Chapter 1 of this thesis, are the Coverage Sites and are intended to provide mobility to the subscriber.

(C) Phase 3: The above two steps involve only single subscriber. Now considering that one more subscriber adds up in the network, depending upon the condition, two situations arise:

(i) BSs of each site still have the capacity to add ξ more carriers, then, equation (3.8.9), would yield:

$\kappa = 2C\xi$, for 2 subscribers

or, $\kappa = SC\xi$, for S subscribers (3.8.12)

while, $R_u = \sqrt{C}$ (3.8.13)

and, $\gamma = \frac{A_{AoI}}{\lambda}$ (3.8.14)

(ii) One or more sites of the network are saturated, and BSs cannot accommodate more carriers. Therefore, more sites are required to compensate the demand. Hence, extending the equations from (3.8.12) to (3.8.14) to incorporate more subscribers, we have:

$\kappa = SC_\varepsilon\xi$, for S subscribers (3.8.15)

while, $R_u = \sqrt{C_\varepsilon}$ (3.8.16)

and, $\gamma_\varepsilon = \kappa/\Omega$ (3.8.17)

Where, Ω is the maximum BS capacity, C_ε is the cluster size in the capacity scenario and, γ_ε is the total sites in the capacity network. It is quite inevitable that the cluster size may change due to the intrusion of more sites within the 2λ (inter-site) distance and number of sites in the network now depend on the capacity of the network; and hence, this is the capacity phase of the network.

3.8.1. OSTENTATIONS CARRIER UTILISATION: A MARKOV PROCESS

Now, we analyze the carrier utilization in an ostentanious network. This section highlights the problem of underutilization of channels due to the PTC impact.

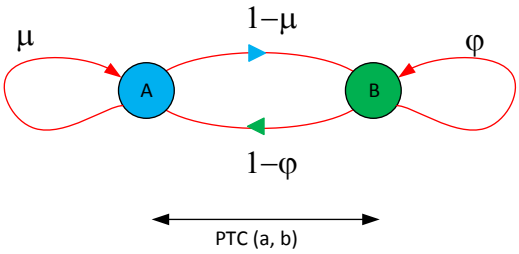

Figure 3-8-2: State transition diagram for Phase 1

Referring to the discussion in (A) of this subsection let, at any instant of time,

(i) The probability that the single subscriber stays at home or point A is μ,
(ii) The probability that the single subscriber stays at workplace or point B is φ Then, considering that the subscriber initially traverses only these two locations, and that
(iii) The probabilities of the subscriber transiting from A to B and from B to A will be 1-μ and 1- φ, respectively [25].

Let us describe the above scenario with state transition diagram as shown in figure 3-8-2. The transition probability matrix notation is (Using Markov Process) [26] [27]:

$$P_\Psi(S = 1)\begin{bmatrix} \mu & 1-\mu \\ 1-\varphi & \varphi \end{bmatrix} \tag{3.8.18}$$

Therefore, to obtain the Eigen values, let,

$$\det(P_\psi - \theta I) = 0 \tag{3.8.19}$$

That yields, $(\theta-1)(\theta-\mu-\varphi+1) = 0$

or, $\theta=1$; and $\theta=\mu+\varphi-1$ (3.8.20)

Roots of θ are the Eigen values of P_Ψ (for a single subscriber) that are 1 and $\mu+\varphi-1$. Hence, using similarity transformation, P_Ψ can be written as [28] [27]:

$$P_\Psi(S=1) = M\begin{bmatrix}1 & 0\\ 0 & \mu+\varphi-1\end{bmatrix}M^{-1} \quad (3.8.21)$$

Where, M is the Eigen vector matrix.

And therefore, for the probability of a subscriber staying at point A after n iterations can be written as[25] [29] [30]:

$$P^n{}_{\Psi AA}(S=1) = \alpha + \beta(\mu+\varphi-1)^n \quad (3.8.22)$$

Where α and β are arbitrary values.

From our assumptions, we know that,

(i) $P^{n=0}{}_{\Psi AA}=1$; as there is no transition, so it is still an absorbing state.
(ii) $P^{n=1}{}_{\Psi AA}=\mu$; the probability of subscriber staying at A after the first iteration (see, figure 3-5-2).

Putting these value sets of n and $P^n{}_Y$ in equation (3.8.22), we have

$$\alpha + \beta(\mu+\varphi-1)^{n=0}=1; \text{ or, } \alpha+\beta=1 \quad (3.8.23)$$

and, $\alpha + \beta(\mu+\varphi-1)^{n=1}= \mu$;

or, $\alpha + \beta(\mu+\varphi-1)= \mu$ (3.8.24)

Solving equations (3.8.23) and (3.8.24), for α and β, we have:

$$\alpha = \frac{\varphi-1}{\mu+\varphi-2} \quad (3.8.25)$$

and,
$$\beta = \frac{\mu-1}{\mu+\varphi-2} \quad (3.8.26)$$

And therefore, substituting (3.8.25) and (3.8.26) in (3.8.22), we have:

$$P^{n}{}_{\Psi AA}(S=1)=\frac{\varphi-1}{\mu+\varphi-2}+\frac{\mu-1}{\mu+\varphi-2}(\mu+\varphi-1)^{n} \tag{3.8.27}$$

Similarly, the other state transitions can be calculated to obtain:

$$P^{n}{}_{\Psi}(S=1)=\begin{bmatrix}\frac{\varphi-1}{\mu+\varphi-2}+\frac{\mu-1}{\mu+\varphi-2}\Lambda^{n} & \frac{\mu-1}{\mu+\varphi-2}-\frac{\mu-1}{\mu+\varphi-2}\Lambda^{n}\\ \frac{\varphi-1}{\mu+\varphi-2}-\frac{\varphi-1}{\mu+\varphi-2}\Lambda^{n} & \frac{\mu-1}{\mu+\varphi-2}+\frac{\varphi-1}{\mu+\varphi-2}\Lambda^{n}\end{bmatrix} \tag{3.8.28}$$

Where, $\Lambda = \mu+\varphi-1$.

Extracting the matrix in (3.8.28) according to transitions, we have:

$$P^{n}{}_{\Psi AA}(S=1)=\frac{\varphi-1}{\mu+\varphi-2}+\frac{\mu-1}{\mu+\varphi-2}(\mu+\varphi-1)^{n} \tag{3.8.29}$$

$$P^{n}{}_{\Psi BB}(S=1)=\frac{\mu-1}{\mu+\varphi-2}+\frac{\varphi-1}{\mu+\varphi-2}(\mu+\varphi-1)^{n} \tag{3.8.30}$$

$$P^{n}{}_{\Psi AB}(S=1)=\frac{\mu-1}{\mu+\varphi-2}-\frac{\mu-1}{\mu+\varphi-2}(\mu+\varphi-1)^{n} \tag{3.8.31}$$

$$P^{n}{}_{\Psi BA}(S=1)=\frac{\varphi-1}{\mu+\varphi-2}-\frac{\varphi-1}{\mu+\varphi-2}(\mu+\varphi-1)^{n} \tag{3.8.32}$$

$P^{n}{}_{\Psi AA}$ and $P^{n}{}_{\Psi BB}$, as in equations (3.8.29) and (3.8.30) respectively, are the probabilities of the subscriber retaining the same position (A and B) and similarly, $P^{n}{}_{\Psi AB}$ and $P^{n}{}_{\Psi BA}$ are the probabilities of the subscriber transiting from A to B and B to A respectively, as in equations (3.8.31) and (3.8.32).

Referring to section 3.5, we can say that, *equations (3.8.29) and (3.8.30) are the probabilities that a subscriber would demand capacity due to the time that the subscriber has spent at a point, and similarly, equations (3.8.31) and (3.8.32) describe the probabilities of PTC due to the transit in positions and time*. Revisiting figure 3-8-2, we can say that the probability of the subscriber acquiring any state is always 1, as ultimately, the subscriber will choose whether to say at the same point of the move. Therefore, according to equation (3.5.36) and replacing b with ξ, the PTC ratio, after n iterations, can be formulated as:

$$\widehat{PTC}_{S}\,(t_{A1}, t_{A2}) =$$

$$S\xi(\overrightarrow{\overrightarrow{P_S}}(t)|_{t_{A1}}^{t_{A2}})\left[\frac{\mu-1}{\mu+\varphi-2}-\frac{\mu-1}{\mu+\varphi-2}(\mu+\varphi-1)^n\right]+\ S\xi\left[\frac{\varphi-1}{\mu+\varphi-2}+\frac{\mu-1}{\mu+\varphi-2}(\mu+\varphi-1)^n\right]$$

For the position A and, (3.8.33)

$$\widetilde{PTC}_S\,(t_{B1}, t_{B2}) =$$

$$S\xi(\overrightarrow{\overrightarrow{P_S}}(t)|_{t_{B1}}^{t_{B2}})\left[\frac{\varphi-1}{\mu+\varphi-2}-\frac{\varphi-1}{\mu+\varphi-2}(\mu+\varphi-1)^n\right]+\ S\xi\left[\frac{\mu-1}{\mu+\varphi-2}+\frac{\varphi-1}{\mu+\varphi-2}(\mu+\varphi-1)^n\right]$$

For the Position B, where accent shows the weighted PTC. (3.8.34)

Being probabilities, both $0 \leq \mu$ and $\varphi \leq 1$

Therefore, considering both μ and φ are non-absorbing states, $\mu+\varphi-1 < 1$, then, for a large n (iteration), we can say that

$$\lim_{n\to\infty}(\mu+\varphi-1)^n \cong 0 \tag{3.8.35}$$

Also, as we have assumed that the subscriber transits linearly and smoothly from A to B or B to A, therefore,

$$|\overrightarrow{\overrightarrow{P_S}}(t)|_{t_{A1}}^{t_{A2}}| = d = \text{distance between A and B} \tag{3.8.36}$$

Accommodating (3.8.35) and (3.8.36) in (3.8.33) and (3.8.34), we have, for large number of steps (iterations),

$$\widetilde{PTC}_S\,(A) = S\xi d\left[\frac{\mu-1}{\mu+\varphi-2}\right]+\ S\xi\left[\frac{\varphi-1}{\mu+\varphi-2}\right] \tag{3.8.37}$$

$$\widetilde{PTC}_S\,(B) = S\xi d\left[\frac{\varphi-1}{\mu+\varphi-2}\right]+\ S\xi\left[\frac{\mu-1}{\mu+\varphi-2}\right] \tag{3.8.38}$$

For the single subscriber, S=1; hence, the above equations reduce to:

$$\widetilde{PTC}_1\,(A) = \xi d\left[\frac{\mu-1}{\mu+\varphi-2}\right]+\ \xi\left[\frac{\varphi-1}{\mu+\varphi-2}\right] \tag{3.8.39}$$

$$\widetilde{PTC}_1\,(B) = \xi d\left[\frac{\varphi-1}{\mu+\varphi-2}\right]+\ \xi\left[\frac{\mu-1}{\mu+\varphi-2}\right] \tag{3.8.40}$$

Assuming that the subscriber likes to stay more at the native position, and tend to transit less, then, when subscriber is at position A, we can say that, $1 \cong \mu > \varphi >> 0$.

So, for equation (3.8.39), we can say that,

$$\widetilde{PTC}_1(A) = \xi d\left[\frac{\mu-1\cong 0}{\mu+\varphi-2}\right] + \xi\left[\frac{\varphi-1}{\mu-1\cong 0+\varphi-1} \cong \frac{\varphi-1}{\varphi-1}\right]$$

or, $\widetilde{PTC}_1(A) = \xi d\,[\cong 0] + \xi[\cong 1\,]$; for a single subscriber

or, $\widetilde{PTC}_S(A) = S\xi d\,[\cong 0] + S\xi[\cong 1\,]$; for S>>1 subscribers (3.8.41)

Equation (3.8.36) points out that *in the case,* when *the subscriber tends to spend more time at destinations rather than traveling, then, during a course of time, the effective capacity demand converges to the point A and B than the transit path*. Therefore, referring to figure 3-8-1, we can say that all sites that are deployed to cater for the subscriber mobility, i.e. sites at p1, p2, p3, till r5 (excluding A or B, depending on the place of retention), have very less contribution in capacity absorption. This situation is deeper when the subscribers accumulate in groups. Therefore, from equations (3.8.15) and (3.8.41), we can say that *the percentage carrier utilization dedicated for states other than self-retention at position A is u(A)*100,* where u(A) is*:*

$$u(A) = \left[\frac{\mu-1}{\mu+\varphi-2}\right] \quad (3.8.42)$$

And similarly,

$$u(B) = \left[\frac{\varphi-1}{\mu+\varphi-2}\right] \quad (3.8.43)$$

Figures 3-8-3 and 3-8-4 describe the resource utilization pattern as formulated in equations (3.8.39) and (3.8.40). Referring to points 1, 2, and 3 in figure 3-8-4, we can see that with a high value of μ, the resource utilization is fairly low even with the increase in the value of φ. Therefore, the resource abundance with respect to the subscriber priority will be the probability of subscriber NOT retaining the position A, and is formulated as:

$$UR(A) = (\kappa - \xi).\left[\frac{\varphi-1}{\mu+\varphi-2}\right] \quad (3.8.44)$$

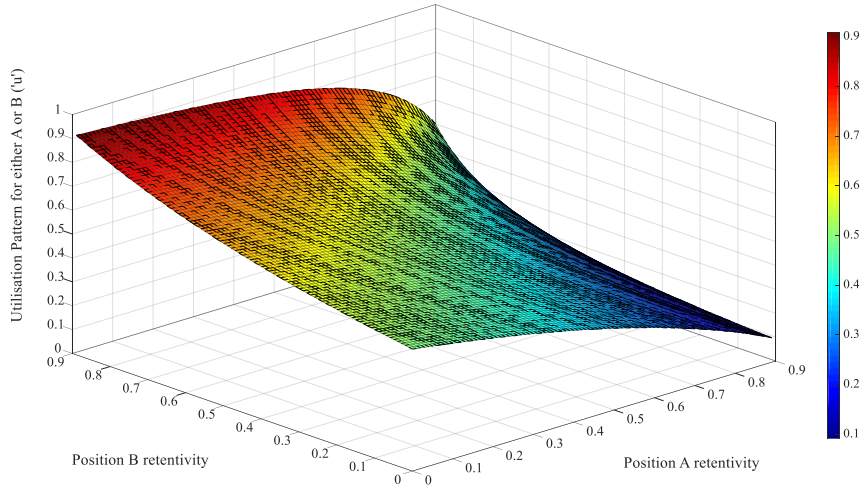

Figure 3-8-3: Resource utilisation pattern by a subscriber with position 'A' as homing location

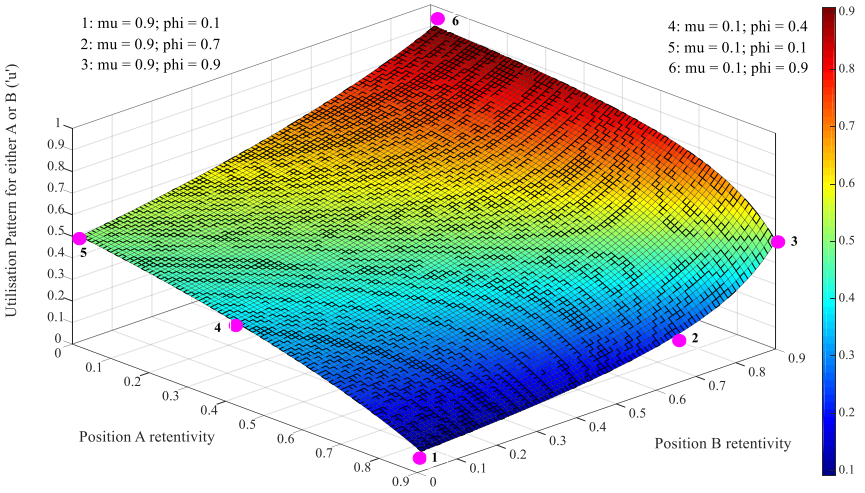

Figure 3-8-4: Resource utilisation pattern with some values of mu (μ) and phi (φ)

Where, **UR(.)** is defined as the **resource abundance ratio** with respect to the position A and κ is the total spectrum demand in deploying the network (see, figure 3-8-1). As subscriber at point A is using ξ channels, hence they are subtracted from the total carrier count in equation (3.8.39). *Therefore, the percentage utilization 'u',*

as mentioned in (3.8.39), is negligible and, assuming that $\kappa >> \xi$, spectrum utilization per subscriber is very low.

3.8.2. OSTENTATIOUS CARRIER UTILISATION IN THE EFFECT OF PTC

Section 3.8.1 may be a seemingly conflicting discussion as the argument may be that while the network is serving the subscriber at point A, it also serves another subscriber at point B. In that case, the network utilization is much larger than what is expressed by equation (3.8.41). This is valid while the subscribers are separated by either place and time or, both. So, when there are two subscribers having affinities to positions A and B respectively, then, when both subscribers are not moving, the resource utilization in the above case will be much higher (ideally, 100 percent).

However, as discussed in sections 3.5.3 and 3.5.4, the severity arises when the subscribers meet at common interests (locations serving the specific needs). From section 3.8.1, we have, for a long succession, the respective transition matrix for both subscribers will be (see, equation 3.8.28):

$$P^{n}{}_{\Psi}(X,A) = \begin{bmatrix} \frac{\varphi_X - 1}{\mu_X + \varphi_X - 2}(AA) & \frac{\mu_X - 1}{\mu_X + \varphi_X - 2}(AB) \\ \frac{\varphi_X - 1}{\mu_X + \varphi_X - 2}(BA) & \frac{\mu_X - 1}{\mu_X + \varphi_X - 2}(BB) \end{bmatrix} \tag{3.8.45}$$

$$P^{n}{}_{\Psi}(Y,A) = \begin{bmatrix} \frac{\varphi_Y - 1}{\mu_Y + \varphi_Y - 2}(AA) & \frac{\mu_Y - 1}{\mu_Y + \varphi_Y - 2}(AB) \\ \frac{\varphi_Y - 1}{\mu_Y + \varphi_Y - 2}(BA) & \frac{\mu_Y - 1}{\mu_Y + \varphi_Y - 2}(BB) \end{bmatrix} \tag{3.8.46}$$

In equation (3.8.28), there was only one stimulant; therefore, probabilities of A and B were independent. However, in present case, there are two stimulants and both can exist either at A or B, Hence, being at A and B are now not exclusive and the new sample space for X will be the product of outcomes given below as [31]:

$$SS(X,Y|S=2) = \sum_{i,j,k,l=1}^{i,j,k,l=2} \overline{X_{ij}}\ \overline{Y_{kl}}$$

$$= 4(\varphi_X - 1)(\varphi_Y - 1) + 4(\varphi_X - 1)(\mu_Y - 1) + 4(\varphi_Y - 1)(\mu_X - 1)$$

$$+4(\mu_X - 1)(\mu_Y - 1) \tag{3.8.47}$$

Where, the bar above X and Y indicates the numerator of the vector value. The probability of such two variables (subscribers), X and Y at position A, creating a wobble can be formulated as:

When X and Y gather at A,

P(X, Y| A) = P(X|A)* P(Y|B') + P(Y| A)* P(X| B') + P(X| A)* P(Y| A)

Or simply, = {P(X|A)+ P(X|B')}* {P(Y|A)+ P(Y|B')}- P(X|B')* P(Y|B')

And, when subs transit together,

P(X, Y| A') = P(X| A') * P(Y| B')+ P(Y| A')* P(X| B')+ P(X| A') *{P(Y| A')

Or simply, = {P(X|A')+ P(X|B')}* {P(Y|A')+ P(Y|B')}- P(X|B')* P(Y|B')

Where,

- $P(\alpha \mid \theta)$ is the probability when subscriber α is at θ,
- $P(\alpha \mid \theta')$ is the probability when the subscriber α is not at θ,
- $P(\alpha, \beta \mid \theta)$ is the probability when subscriber α and β is at θ,
- $P(\alpha, \beta \mid \theta')$ is the probability when subscriber α and β is not at θ, and,
- Variables α and β can be X or Y and θ can be A or B.

So, P(X,Y| A) =

$$\frac{\varphi_X - 1}{SS(X,Y)} * \frac{\varphi_Y - 1}{SS(X,Y)} + \frac{\varphi_Y - 1}{SS(X,Y)} * \frac{\varphi_X - 1}{S(X,Y)} + \frac{\varphi_X - 1}{S(X,Y)} * \frac{\varphi_Y - 1}{S(X,Y)} \quad (3.8.48)$$

and, P(X,Y| A') =

$$\frac{\mu_X - 1}{SS(X,Y)} * \frac{\mu_Y - 1}{SS(X,Y)} + \frac{\mu_Y - 1}{SS(X,Y)} * \frac{\mu_X - 1}{SS(X,Y)} + \frac{\mu_X - 1}{SS(X,Y)} * \frac{\mu_Y - 1}{SS(X,Y)} \quad (3.8.49)$$

For simplicity, if we assume that both X and Y has the same affinity towards positions A and B, we have $\mu_X = \mu_Y = \mu$ and, $\varphi_X = \varphi_Y = \varphi$. We have from equation (3.8.47):

$$SS(X,Y|S=2) = \sum_{i,j,k,l=1}^{i,j,k,l=2} \overline{X_{ij}}\ \overline{Y_{kl}} = \{2(\varphi - 1) + 2(\mu - 1)\}^2 = \{2(\varphi + \mu - 1)\}^2$$

or, $$SS(X,Y|S=2) = \{2(\varphi + \mu - 2)\}^2 \quad (3.8.50)$$

Then, solving equations (3.8.48) and (3.8.49), we have:

$$P(X,Y|\ A) = \frac{3(\varphi - 1)^2}{\{2(\varphi + \mu - 2)\}^2} \quad (3.8.51)$$

and, $$P(X, Y|\ A') = \frac{3(\mu - 1)^2}{\{2(\varphi + \mu - 2)\}^2} \quad (3.8.52)$$

And similarly, $$P(X, Y|\ B) = \frac{3(\mu - 1)^2}{\{2(\varphi + \mu - 2)\}^2} \quad (3.8.53)$$

$$P(X, Y|\ B') = \frac{3(\varphi - 1)^2}{\{2(\varphi + \mu - 2)\}^2} \quad (3.8.54)$$

Equations (3.4.51) to (3.4.54) are for two subscribers transiting in groups between two locations. Generalizing above terms for 'S' subscribers with respect to two locations (A and B), we have for S >1:

$$P^s(X, Y|\ A) = \frac{(2^S - 1)(\varphi_1 - 1)(\varphi_2 - 1) \dots (\varphi_S - 1)}{2^S(\varphi + \mu - 2)^S}$$

$$= \frac{(2^S - 1)(\varphi - 1)^S}{2^S(\varphi + \mu - 2)^S} \quad (3.8.55)$$

and ,

$$P^s(X, Y|\ A') = \frac{(2^S - 1)(\mu_1 - 1)(\mu_2 - 1) \dots (\mu_S - 1)}{2^S(\varphi + \mu - 2)^S}$$

$$= \frac{(2^S - 1)(\mu - 1)^S}{2^S(\varphi + \mu - 2)^S} \quad (3.8.56)$$

And similarly,

$$P^s(X, Y|\ B) = \frac{(2^S - 1)(\mu - 1)^S}{2^S(\varphi + \mu - 2)^S} \quad (3.8.57)$$

$$P^s(X, Y|\ B') = \frac{(2^S - 1)(\varphi - 1)^S}{2^S(\varphi + \mu - 2)^S} \quad (3.8.58)$$

Now, putting the values from above equations in equations (3.8.39) and (3.8.40), we have, for S, subscribers:

$$\widehat{PTC}_S\ (A) = S\xi d\left[\frac{(2^S - 1)(\mu - 1)^S}{2^S(\varphi + \mu - 2)^S}\right] + S\xi\left[\frac{(2^S - 1)(\varphi - 1)^S}{2^S(\varphi + \mu - 2)^S}\right] \quad (3.8.58)$$

$$\widetilde{\widetilde{\mathrm{PTC}}}_{\mathrm{S}}(\mathrm{B}) = \mathrm{S}\xi\mathrm{d}\left[\frac{(2^{S}-1)(\varphi-1)^{S}}{2^{S}(\varphi+\mu-2)^{S}}\right] + \mathrm{S}\xi\left[\frac{(2^{S}-1)(\mu-1)^{S}}{2^{S}(\varphi+\mu-2)^{S}}\right] \tag{3.8.59}$$

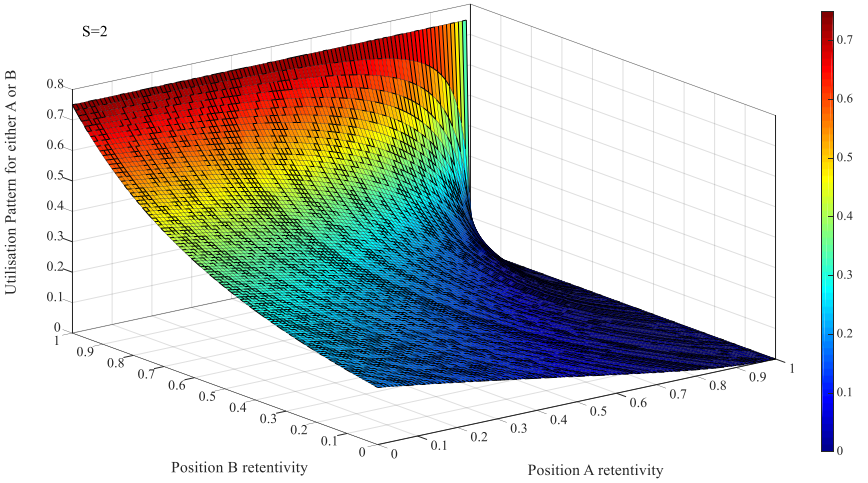

Figure 3-8-5: Utilization pattern with two subscribers forming a group

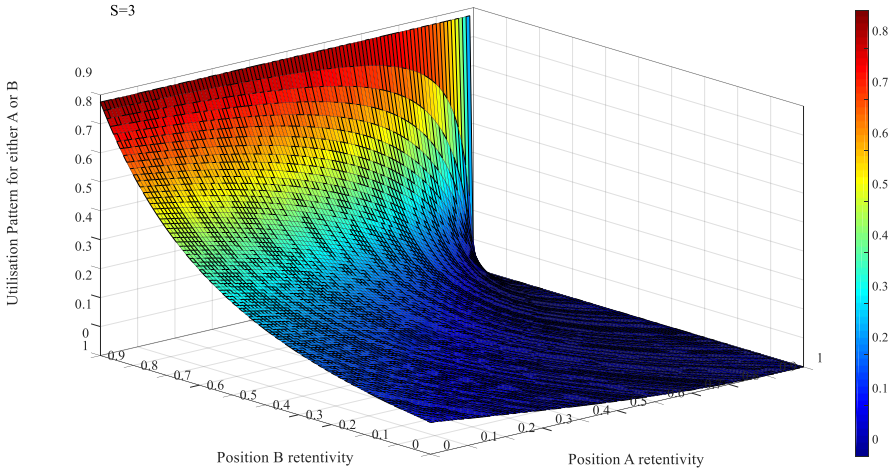

Figure 3-8-6: Utilization pattern with three subscribers forming a group

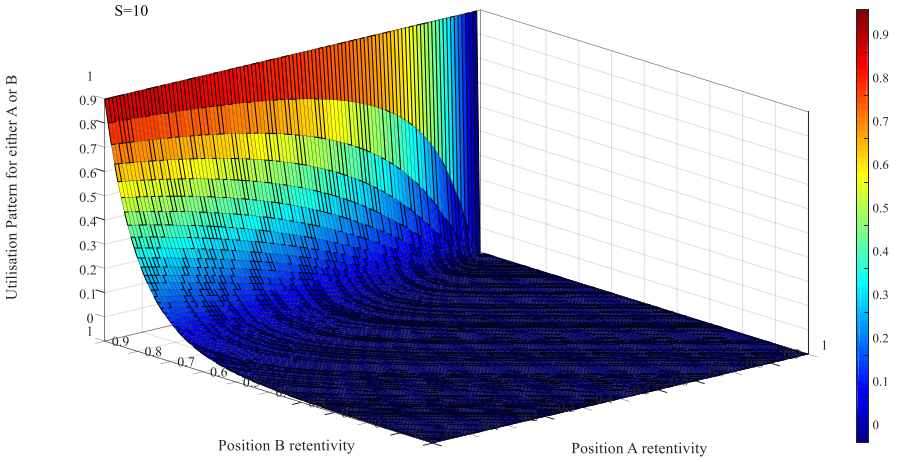

Figure 3-8-7: Utilization pattern with ten subscribers forming a group

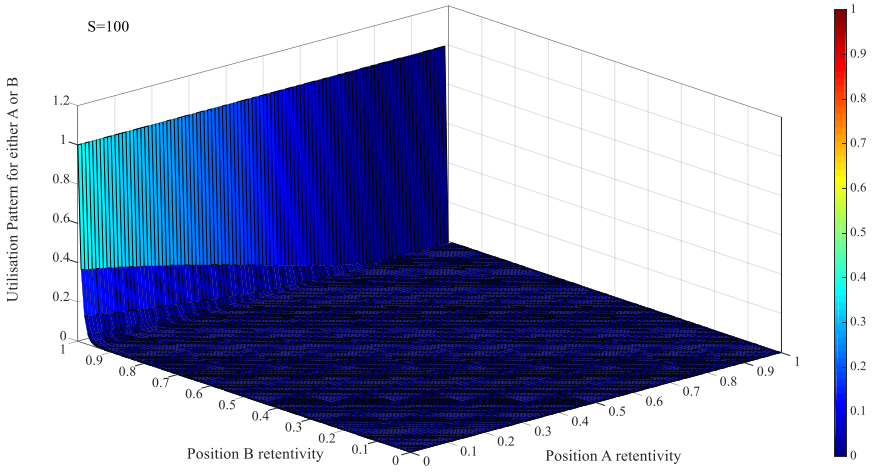

Figure 3-8-8: Utilization pattern with a hundred subscribers forming a group

Figures 3-8-5 to 3-8-8 clearly show that with an increase in the subscriber count, the probability that a channel is utilized converges to blue colour, which as per colour bar is less than 0.3 (or 30 percent).

3.9. RESEARCH QUESTIONS ADDRESSED IN CHAPTER 3

This section highlights the Research Questions (RQs) that are addressed in this chapter (Chapter 3) of this thesis. The RQs highlighted here are the summary of the formulations derived and discussed in this chapter and will play a prime role in defining the working of the innovative architecture conceived in Chapter 4.

3.9.1. RQ 1: LOCUS OF CAPACITY DEMANDS CREATED DUE TO MOVING HUGE GROUPS OF SUBSCRIBERS (PLACE TIME CAPACITY)

When the subscribers accumulate at random locations and traverse a path, the capacity demand generated throughout their journey can be given by the Place Time Capacity as derived in equation (3.5.36) and written again below as:

$$|\overrightarrow{\dddot{\mathrm{PTC}}}_{S_1}(t_1, t_2)| = ||S_1|b(\overrightarrow{\dddot{P}}_{S_1}(t)|_{t_1}^{t_2}) + |S_1|b.\ddot{\hat{l}}| \tag{3.9.1}$$

The conventional network deployment approach usually does not incorporate such dynamics and often fail to cater these conditions. The imbalance in the resource utilization created due to such accumulation is discussed in section 3.8 and derived in equations (3.8.58) and (3.8.59) written below again as:

$$\widetilde{\mathrm{PTC}}_S(A) = S\xi d\left[\frac{(2^S-1)(\mu-1)^S}{2^S(\varphi+\mu-2)^S}\right] + S\xi\left[\frac{(2^S-1)(\varphi-1)^S}{2^S(\varphi+\mu-2)^S}\right] \tag{3.9.2}$$

$$\widetilde{\mathrm{PTC}}_S(B) = S\xi d\left[\frac{(2^S-1)(\varphi-1)^S}{2^S(\varphi+\mu-2)^S}\right] + S\xi\left[\frac{(2^S-1)(\mu-1)^S}{2^S(\varphi+\mu-2)^S}\right] \tag{3.9.3}$$

For any two points of inclinations A and B.

These equations will be used by an intelligent system to mitigate the wobble and run the network smoother than the conventional network approach.

3.9.2. RQ 2: DIP AND RISE IN SIGNAL STRENGTHS AT MACRO, MICRO AND PICO LEVEL AREAS IN A DYNAMIC NETWORK

A network dynamics involves densification or rarefication of medium modifiers such as dielectrics, reflectors, diffractors, etc. that affect the path-loss of the propagation medium. Accumulation of people and vehicles in traffic jams are such phenomena that cause such effects. This variation is due to the fact that in the path of a traveling signal, reflections, diffractions, and absorption from these modifiers are additive as interferers that affect the median path-loss to get modified as given below [3]:

$$\mathrm{PL_{mod}(d)} = \mathrm{PL_{median}(d)} + \mathrm{G}(\sigma) \tag{3.9.4}$$

Where $\mathrm{PL_{median}(d)}$ is the median path-loss at a distance 'd', G is the zero mean Gaussian distributed random variable and is expressed in dB, and $\mathrm{PL_{mod}}$ is the modified path-loss. This equation incorporates the variations in the propagation environment due to refractions and diffractions also known as shadowing effect.

In section 3.6, we have derived the Place and Time dependent path-loss model, given in equation (3.6.26) and written again below as:

$$\mathrm{PL_{\omega}(d,p,t)} = \mathrm{PL(d)} + 10\ \mathrm{N_{AR}log_{10}}\left(\frac{\mathrm{d}}{\mathrm{D_0}}\right) \tag{3.9.5}$$

where, $$\mathrm{PL(d)} = \mathrm{PL(D_0)} + 10\ \mathrm{nlog_{10}}\left(\frac{\mathrm{d}}{\mathrm{D_0}}\right) \tag{3.9.6}$$

Considering $\mathrm{PL}\omega = \mathrm{PL_{median}}$ to accommodate PTR in equation (3.9.4), we have:

$$\mathrm{PL_{mod}(d)} = \mathrm{PL}\omega\mathrm{(d)} + \mathrm{G}(\sigma) \tag{3.9.7}$$

In section 3.7, it is discussed how the PDF function varies when median and variance of the PDf function $\mathrm{f_R}$ are ostentatious. The expression (3.7.21) describes the relation and is written again as:

$$\mathrm{U(f_R)} = \mathrm{A\{GH + G'(t)\}}\vartheta \tag{3.9.8}$$

Therefore, referring to section 3.7, we can say that,

$$\mathrm{f_R} = \iint \mathrm{A\{GH + G'(t)\}}\vartheta\ \mathrm{dpdt} \tag{3.9.9}$$

In equation (3.9.7), the random variable $G(\sigma)$ distributes with variance σ and median=0. With median point and σ are under place time influence, equation (3.9.7) should further be modified as per equation (3.9.9), expressed below as:

$$PL_{PT-DIS}(d) = PL\omega(d) + f_G \quad (3.9.10)$$

Where $PL_{PT\text{-}DIS}$ indicates the path-loss modified for shadowing and under place and time influence. The two RQs that are discussed in this section generate multiple other phenomena that pose a challenge to conventional networks. In the next chapter, we will discuss some of them and our innovative approach to catering them.

3.10. CONCLUSIONS

Today, the network dimensioning is done based on the probability of arrival of the signals at various locations in the AoI. However, while dimensioning the network, for the portion of the AoI with a probability of an event, the common irregularities that happen in the network during its actual implementation and operation are neglected. The change in the nature of the probability of outcomes, as described by a probability density function (PDF), from time to time and place to place due to random nature of stimulant, is defined here as *Ostentaneity* and the event generating such outcomes are *Ostentaneous Events*. In this chapter, the irregularities due to hefty and random accumulations of subscribers within the AoI, and their impact on normal operation of a network are deeply investigated. This random dynamics in the network is defined here as Place Time Event. The random accumulation of subscribers, causing the random rise in capacity demands and random coverage jitters are defined individually as the Place Time Capacity (PTC) and the Place Time Coverage (PTC_o) and collectively as PTC^2. Further, the impact of PTC^2 on the coverage and capacity dimensioning is mathematically analysed and expressed as Ostentanoues Coverage and Capacity. Lastly, this chapter discusses the PTC^2 challenges and defines it as contributions through Research Questions (RQs) that can be a concern to any present and future network dimensioning. This chapter lays a platform for the innovative architecture to be discussed in the upcoming chapter.

REFERENCES

[1] A. Kumar, P. L. Mehta, and R. Prasad, “Place Time Capacity- A novel concept for defining challenges in 5G networks and beyond in India,” in *2014 IEEE Global Conference on Wireless Computing and Networking (GCWCN)*, 2014, pp. 278–282.

[2] A. Kumar, A. Mihovska, and R. Prasad, "Dynamic Pathloss Model for Future Mobile Communication Networks," in *18th International Symposium on Wireless Personal Multimedia Communications (WPMC) of the Global Wireless Summit-2015*, Hyderabad, India, 2015, Presented.

[3] T. S. Rappaport, *Wireless Communications: Principles and Practice*, 2 edition. Upper Saddle River, N.J: Prentice Hall, 2002.

[4] H. Tijms, *Understanding Probability: Chance Rules in Everyday Life*, 2 edition. Cambridge: Cambridge University Press, 2007.

[5] W. Feller, *An Introduction to Probability Theory and Its Applications, Vol. 1, 3rd Edition*, 3rd edition. New York: Wiley, 1968.

[6] C. Ash, *The Probability Tutoring Book: An Intuitive Course for Engineers and Scientists*, 1 edition. New York: Wiley-IEEE Press, 1996.

[7] M. H. DeGroot and M. J. Schervish, *Probability and Statistics*, 4 edition. Boston: Pearson, 2011.

[8] V. J. Arokiamary, *Cellular and Mobile Communications*. Technical Publications, 2009.

[9] Anjan Ghosh, Vikas Aggarwal, and Nidhi Marwaha, "'Telecom Infrastructure Industry in India,'" ICRA Limited, Gurgaon, India, Survey, Mar. 2009.

[10] C. Ohanami, G. Onoh, E. Ifeagwu, and I. Eneh, "Improving Channel Capacity of Cellular System Using Cell Splitting," *Int. J. Sci. Eng. Res. Retrieved Httpwww Ijser Orgresearchpaper 5CIMPROVING-CHANNEL-CAPACITY---Cell.-Syst.-CELL-Split. Pdf*, 2012.

[11] L.-C. Wang and K. K. Leung, "A High-Capacity Cellular Network by Improved Sectorization and Interleaved Channel Assignment," in *Multiaccess, Mobility and Teletraffic for Wireless Communications: Volume 3*, K. K. Leung and B. Vojcic, Eds. Springer US, 1999, pp. 43–58.

[12] M. F. Catedra, *Cell Planning for Wireless Communications*, First Edition edition. Boston, Mass: Artech Print on Demand, 1999.

[13] M. F. Catedra and J. Perez, *Cell Planning for Wireless Communications*, 1st ed. Norwood, MA, USA: Artech House, Inc., 1999.

[14] P. | M. 17, 2016, and 05 53 Pm Ist, "Call drops: Ravi Shankar Prasad to personally go on 'drive tests,'" *The Economic Times*. [Online]. Available: http://economictimes.indiatimes.com/industry/telecom/.

[15] *Cell Planning and Channel Assignment for Cellular Mobile Communication System*. 2000.

[16] A. R. Mishra, *Advanced Cellular Network Planning and Optimisation: 2G/2.5G/3G...Evolution to 4G*. John Wiley & Sons, 2007.

[17] E. Yaacoub and Z. Dawy, *Resource Allocation in Uplink OFDMA Wireless Systems: Optimal Solutions and Practical Implementations*. John Wiley & Sons, 2012.

[18] RMSI, India, "Digital Map of Indian Cities," RMSI, India, 2013.

[19] V. S. Abhayawardhana, I. J. Wassell, D. Crosby, M. P. Sellars, and M. G. Brown, "Comparison of empirical propagation path loss models for fixed

wireless access systems," in *Vehicular Technology Conference, 2005. VTC 2005-Spring. 2005 IEEE 61st*, 2005, vol. 1, pp. 73–77 Vol. 1.

[20] C. C. Pu, P. C. Ooi, B. G. Lee, and W.-Y. Chung, "Analysis of path loss exponent error in ranging and localization of wireless sensor network," in *International Conference on Frontiers of Communications, Networks and Applications (ICFCNA 2014 - Malaysia)*, 2014, pp. 1–6.

[21] X. Zhang and J. G. Andrews, "Downlink Cellular Network Analysis With Multi-Slope Path Loss Models," *IEEE Trans. Commun.*, vol. 63, no. 5, pp. 1881–1894, 2015.

[22] Z. Nadir, "Empirical pathloss characterization for Oman," in *Computing, Communications and Applications Conference (ComComAp), 2012*, 2012, pp. 133–137.

[23] Y. I. Gabrousenko, I. A. Machalin, and A. G. Taranenko, "Radiowaves propagation model of unmanned aerial system data," in *Actual Problems of Unmanned Aerial Vehicles Developments (APUAVD), 2015 IEEE International Conference*, 2015, pp. 254–256.

[24] J.-P. Linnartz, *Narrowband Land-Mobile Radio Networks*. Boston: Artech House Publishers, 1993.

[25] L. Rabiner and B. Juang, "An introduction to hidden Markov models," *IEEE ASSP Mag.*, vol. 3, no. 1, pp. 4–16, Jan. 1986.

[26] X. g Yu, Y. h Liu, D. Wei, and M. Ting, "Hybrid Markov Models Used for Path Prediction," in *15th International Conference on Computer Communications and Networks, 2006. ICCCN 2006. Proceedings*, 2006, pp. 374–379.

[27] D. W. Stroock, *An Introduction to Markov Processes*, 2005 edition. Berlin; New York: Springer, 2005.

[28] A. O. Allen, *Probability, Statistics and Queueing Theory with Computer Science Applications*. New York: Academic Press Inc, 1978.

[29] J. H. Wilkinson, *The Algebraic Eigenvalue Problem*, Revised ed. edition. Oxford : Oxford ; New York: Clarendon Press, 1988.

[30] B. N. Parlett, *The Symmetric Eigenvalue Problem*. Philadelphia: Society for Industrial and Applied Mathematics, 1987.

[31] P. Billingsley, *Probability and Measure*, 4 edition. Hoboken, N.J: Wiley, 2012.

CHAPTER 4. SELF CONFIGURABLE INTELLIGENT DISTRIBUTED ANTENNA SYSTEM (SCIDAS) ARCHITECTURE

In Chapter 3, we discussed how simple looking random variables can produce different outcomes when it becomes a place and time dependent event. We also discussed the impact of place-time phenomenon on the coverage and capacity dimensioning of an ergodic network. This chapter proposes an innovative and open framework, based on the conventional *Distributed Antenna System* (DAS) architecture that twines around the place time variabilities. Further, we propose a mechanism that operates on this framework to mitigate the PTC^2 challenge (see, **Chapter 3**, and [1] [2]). The findings of this chapter have been partially published in [3], where we introduced it as *Self Configurable Intelligent Distributed Antenna System (SCIDAS).* This chapter also highlights the major limitations of the state-of-the-art concepts such as the Cloud-Radio Access Network (C-RAN) and the Self Organising Networks (SON). *SCIDAS* surmounts the challenges associated with the present state-of-the-art by separating the technology from its infrastructure and permeating intelligence as a separate layer in the architecture. The immense reachability of a DAS has motivated us to base SCIDAS on the DAS architecture. In this chapter, we have explained PTC^2 motivation for an intelligent and responsive architecture, in order to track the place-time variations. This chapter discusses the architectural components of SCIDAS. The logical functionalities are examined in Chapter 5.

4.1. INTRODUCTION

Initially, the Mobile Wireless Communication Networks (MWCNs) were based on a localized radio access architecture where the BTS was closely collocated to the radiating elements. Therefore, with every newer technology upgrades or change of vendors, the entire infrastructure needed to be sanitized, and the processes were called ‘revamping’ or ‘swapping’. The major challenges related to the MWCN architecture were identified in Chapter 1. Here, these are summarized again for clarity.

- The transportation of the BTS equipment to different destinations can be more expensive than the deployment cost of the site.

- The repair and replacement process demand a lot of time, money and manpower (more for difficult terrains and reachability).
- The architecture is granule or independent in nature, and therefore, a complete overhauling is needed at every location separately for even minor changes. As an example, if there are some carrier upgrades in one site, the carrier reuse groups of all neighbouring sites would be required to be changed. Hence, a lot of time would be consumed for one single adjustment to be completely accommodated in the network system.
- The need to indulge infrastructure for revamping or swapping the network is always there. This means that the trade-off of cost versus effort versus revenues is high.
- It could be difficult to place "everything" at every desired location (reachability).
- Some equipment (such as an antenna) would be sturdier than other (electronics and battery banks etc.).

Pertaining to the above challenges, this research adopts the distributed network approach.

4.1.1. THE DISTRIBUTED ANTENNA SYSTEM ARCHITECTURE

If one could separate the antennas from the BS so that only the radiating elements could be placed at the point of demand, then the above problems can be mitigated. DAS emerged as a compelling technology to revolutionize the network architecture, and boosts its ability and efficiency [4] [5]. Technically speaking, "*DAS is a network of spatially separated antenna buds, connected to a common source via a transport medium that provides wireless service within a geographic area or structure*" [6] [7]. Future generations such as 5G [8] are looking forward to resilient architectures that could support these data-centric technologies. Network architectures with DASs have emerged as promising solutions that have shown commensurateness towards upcoming challenges. In the recent years, DASs have gained a lot of attention worldwide owing to the latest advancements in communication technologies.

DAS architecture:

Presently, most of the DAS networks prefer optical medium for data transport (backhauling). The Master Optical Unit (MoU) and the Remote Optical Unit (RoU) follow Boss and the Subordinate hierarchy, which is one of the primary reasons for the success of adaptation of fiber optics in DAS network layer [6]. The modulation and demodulation of RF-to-Optical and Optical-to-RF (RF/Optical/RF) are the fundamental principles behind the working of MoU-RoU system. A Wideband Optical Carrier (WOC) is linearly modulated corresponding to the RF signals with No-Phase-distortion method [5]. The WOC can travel considerably long distances

through an optical medium, such as glass fiber cables where, at the remote end, it can be demodulated back to RF signal. The optical medium can be sliced and spliced for both converged and distributed signal transport (see, figure 4-1-1).

Figure 4-1-1: RF over Optical

MoU is an RF-to-optical and vice-versa converter with two main participating units i.e. the Antenna Interface Unit (AIU) and the Optical Interface Unit (OIU) (see, figure 4-1- 2). RoU has a reverse role, and its architecture is almost similar to that of the MoU with a Low-Noise-Amplifier (LNA) in the uplink direction as an extra module (see, figure 4-1-2).

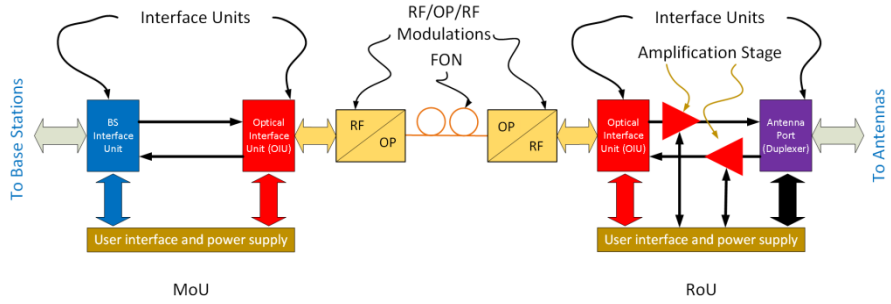

Figure 4-1-2: Diagram showing MoU(Left) and RoU (Right) and their connectivity [9]

By virtue of its innovative architecture, a DAS network allows several base stations to be connected to its MoU, which allows service providers to collocate their equipment at a convenient location. From this site, known as BTS hub or BTS Hotel, the RF signals, which are modulated over an optical carrier, are distributed across the network and terminate at various RoUs. At the RoU end, these RF signals are retrieved and fed to a duplexer of an antenna to be radiated in the radio environment [6] [5] [10]. The duplexer separates downlink and uplink paths, and an LNA amplifies the uplink signal. The enhanced uplink signal is modulated over the optical carrier to get transported over optical medium back to MoU, where it is retrieved back to RF signal to be fed to the BS (see, figure 4-1-2).

A traditional DAS [11] can be utilized rigorously to extend the network without additional spectrum resources [12][13]. In a traditional DAS network, firstly, the locations of the serving sites (BTS/Nodes/Buds and the Antenna System combined together is referred as a network site) in a target area are calculated [14]. Then, as

shown in figure 4-1-3, instead of placing BTS/Nodes/Buds at the site locations, they are collectively placed in an enclosure known as the BTS Hub. This saves space, is easy to manage, and easy to maintain yielding a lower operational expenses (OpEx). Here, in the BTS Hub, the RF output from each BTS is fed into an MoU that converts the RF input into Optical output. The optical output of the MoU is fed into a fiber cable that eventually joins the main FON network. As shown in figure 4-1-4, the main fiber of this FON is spliced with fiber threads at multiple locations. These fiber threads, also known as optical feeder cables, carry the optical signal from the main FON to the various remote equipment or RoUs. These RoUs convert the optical signal into RF signal and feed the RF signal into respective antennas. Hence, the RF signals that are fed into an MoU at the BTS Hub are distributed in the entire region through all the antennas that are connected to this MoU via respective RoUs.

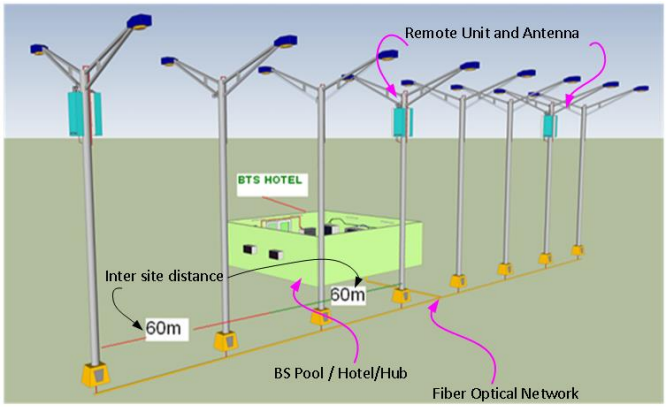

Figure 4-1-3: BS hotel and antenna array on public utility (Streetlight Poles)

A DAS network distributes the radio frequency signals from a central location to remote antennas. This simplifies the design of the remote antennas by concentrating the BS at a centralized BS. Because, at the site end, only the antennas are the major equipment, they can be mounted in any convenient place such as public utility, building structures, and, even street-light poles. These antennas can be connected with BSs by fiber optic cables. DAS is an efficient way to utilize the carrier usage either by spreading the same carriers at different locations or by increasing the carrier footprint by feeding the same carrier in adjacent antennas. Multiple BSs may be connected to the single MoU that can send the signals by multiplexing the signals from various BSs as a separate Wave Channel for each BS. Such kind of multiplexing is known as Wave Division Multiplexing (WDM) (see, Section 4.1.2). The WDM is considered very important for the proposed SCIDAS architecture because it can bring in a new layer of sub-architecture, carrying intelligence over the conventional architecture through a separate wave channel. Both WDM and

DAS are well-known concepts that have been in use for a long time in various telecommunication applications.

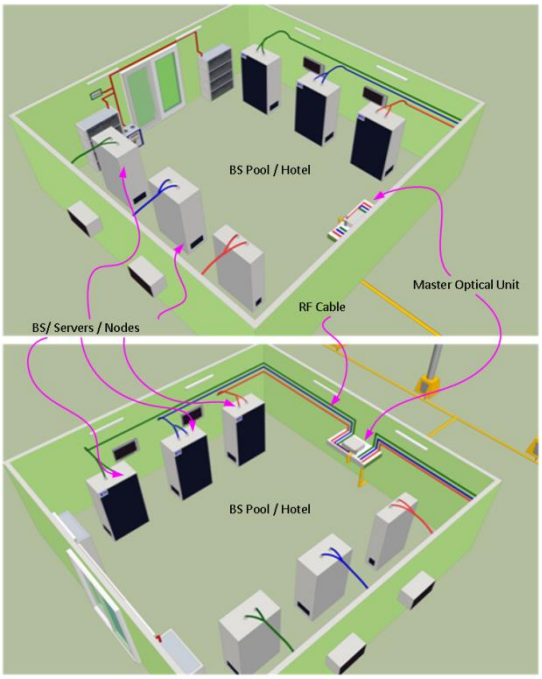

Figure 4-1-4: Inside a BS Hotel/ Hub/Pool

Later in this chapter, we will see how we have utilized the combination of WDM over a DAS as an opportunity to influence a control on the entire network by disseminating the intelligence as a separate layer that propagates through a WDM channel. In the next subsection, it is explained how the WDM multiplexes multiple BSs on a common Fiber Optic Network (FON) enabling a DAS network in distributing carriers of a multiple BSs.

4.1.2. WAVE DIVISION MULTIPLEXING FOR PARALLEL COMMUNICATION

The SCIDAS architecture discussed in this chapter involves intelligence and data to flow and distribute parallerly. A popular method to enable this uses the property of light splitting into its components when passed through a prism and can be recombined to form the white light as shown in figure 4-1-5. The prism, in this case, is both a filter and a combiner when used for different purpose. This allows multiple waves to traverse the same path (with a slight phase difference), thereby,

densifying the rate of information. This method of multiplexing the data over waves (primarily optical) is well known as Wave Division Multiplexing (WDM) [15].

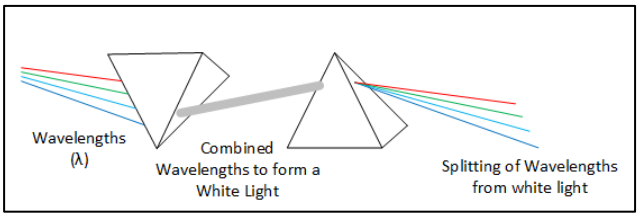

Figure 4-1-5: The idea of WDM-based communication system

The architecture of the DAS can take the advantage of combining and splitting of a white or mixed coloured light using a simple prism as shown in Figure 4-1-5. The simple phenomenon shown in figure 4-1-5 can be utilized to create WDM-based communication as shown in figure 4-1-6 as the transmitting side and figure 4-1-7 as the receiving side [16]. Here, each optical wavelength is a carrier that propagates through fiber optic medium with enough band gap so as not to interfere significantly with its colleagues as shown in figures 4-1-5 and 4-1-6 [17]. WDM technique helps in densification of bits over an FON.

In figure 4-1-7, it is shown that a signal from a certain input source (channels) is fed to an optical modulator such as Laser LED which modulates the electrical signal over a particular colour of the visible spectrum (including infrared). Similarly, signals from other sources are collected and are combined and fed to an FON for it to propagate to a destination. Figure 4-1-7 shows that the mixture is collected at a destination from the FON and is systematically filtered to get back the original components. In order to extract information, this mixture of optical components is allowed to fall on Thin Film Filters (TFF) [18] in a systematic manner that reflects a particular wavelength and passes others through it. The passed on optical mixture has now one component less than what was before TFF and so on, till all the components are sequentially separated. The reflected optical component is collected by a corresponding matched photodetector that converts optical signal to an electrical signal that can be received by electrical receivers. By the systematic collection of the optical components, the information of all the sources can be obtained by optical channel receivers [19] [20]. This kind of arrangement has been used for over a decade for increasing the efficiency and capacity of a Fiber Optic (FO) based network. Such system allows the parallel propagation of the optical signal over the same FON that enhances the system scalability with more redundancy and without upgrading the FO network. Many of the FO based DAS networks use a similar arrangement to establish communication between BSs/Nodes/Buds and the far located remote units.

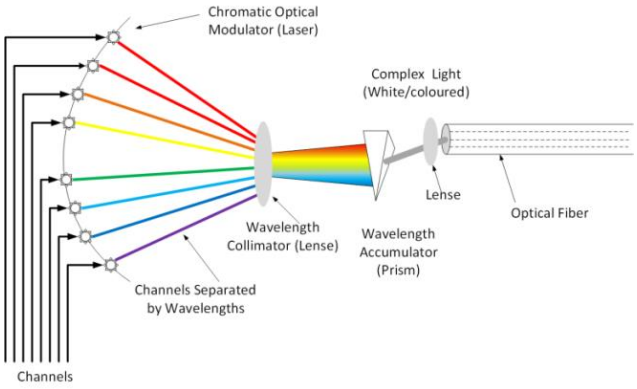

Figure 4-1-6: Transmitting end of the WDM-based communication system

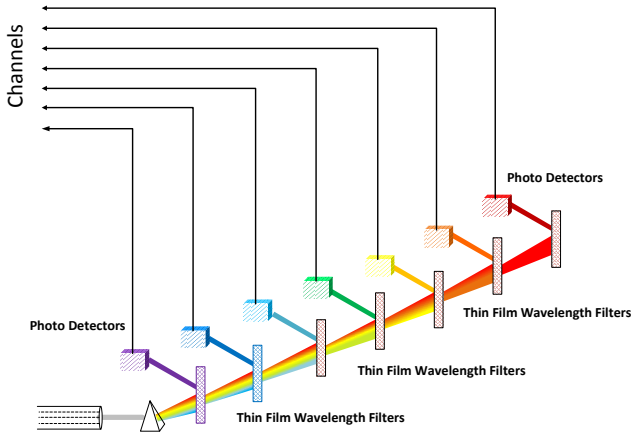

Figure 4-1-7: Receiving end of the WDM-based communication system

The structuring of the various modules in the DAS architecture empowers it to accommodate any RF technology making it an open architecture as mentioned in [5] and [21]. In this chapter, this property of DAS is extended to accommodate intelligence and self-healing capabilities in the communication system. The open architecture enables it to perform in a multi-technology environment and the distributed nature capacitates system to be controlled and managed centrally. Through this chapter, we will see how this conventional and proven architecture model is used to for a more resilient and futuristic conception.

This chapter is further organized as follows. **Section 4.2** discusses the state of the art and relevant works in the area of distributed and self-organizing networks. **Section 4.3** proposes the WDM and the DAS integration and evolution of SCIDAS architecture along with its various modules and their coordinated functioning.

Section 4.4 discusses a set of mechanisms defined as *Amoebic PTC^2 Response* (APR) to serve PTC^2 challenge. The APR mechanism, in this section, is discussed from the point of view of the superiority of the SCIDAS architecture, in terms of its flexibility and dexterity to handle multitude of variations in the Area of Interest (AoI). This section also complements **Chapter 5** of this thesis, in which the APR is discussed from the algorithmic point of view, and C**hapter 6** of this thesis**,** in which the SCIDAS deployment analysis in a hotspot region is discussed to study the interference management in the dense urban area. **Section 4.5** concludes the chapter.

4.2. RELEVANT WORKS AND STATE-OF-THE-ART

The major attributes of the proposed architecture are Intelligence, Reconfigurability, and Distribution. The reconfigurability is also associated with dynamic cell management to reduce the SINR and increase data rates. [22] discusses the importance of DAS in today's fast growing data demand, pointing the main advantage as the minimum access distance from the users. This paper argued about the need of a scalable signal processing framework to incorporate the computational cost and channel measurement overhead in the line of rate gains in data rate due to the massive amount of distributed antennas in an area. The authors have assumed the concept of a user virtual cell, by choosing neighboring base stations. The investigation focussed on studying the effect on virtual cell size on the average user rate with respect to the downlink direction of DAS with a large number of users and uniformly distributed BSs in the AoI. It was shown that by increasing the virtual cell size and grouping the users with overlapped virtual cells, the average user rate can be improved considerably. However, this may lead to higher signal processing complexity. The limitations of using ZFBF is addressed in this chapter. We have proposed an algorithm that creats virual cell as per the PTC^2 behaviour. Therefore, it was necessary to understand the limitations of cell virtualisation, as provided in this paper.

[23] investigated the possibility to improve the performance of space shift keying (SSK) with reconfigurable antenna (RAs). The authors have attempted to use the reconfigurability in attracting a higher degree of freedom in enhancing the performance of SSK in terms of throughput, system complexity, and error performance. The authors proposed several SSK-RA schemes, taking advantage of the effect of RAs on the multipath channel, that considered correlated and nonidentically distributed Rician fading channels with the antenna-state selection. The performance of the proposed SSK-RA schemes was evaluated over Rician fading channels in terms of average spectral efficiency (ASE) and bit error rate (BER).

In [24], the authors investigated the interference management through multi-antenna cell constellation in dense urban areas. The paper proposed a multi-antenna

cell concept to provide a uniform signal-to-noise plus interference ratio (SINR) distribution over the entire cell coverage area. To keep the cell size small, the antenna height was reduced to street lamp post level. At such antenna height, propagation behaviours are severely affected by the surrounding environment like building, electric wire, and traffic, etc. The waves are highly sensitive towards reflection, diffraction, scattering, etc. from the surrounding walls at such height. Such situation is known as 'Urban street canyon effect'. This is similar to line of sight (LoS) propagation. The interference effect can be controlled by strategically placing the transmitter antennas and using small horizontal half-power beam width antennas. The simulation was carried out at 2100 MHz with a system bandwidth of 20 MHz and 10 dBm transmit power. After computing the signal strength of individual cells at each receiver location, the dominant cell can easily be found. The SINR can be computed by using the formula:

$$\mathrm{SINR} = 10\log_{10}\left(\frac{\mathrm{P\_ri}}{\sum_{j=1}^{N}\mathrm{P\_rj}}\right) \qquad (4.2.1)$$

Where, P_ri is the received signal strength from the dominant cell, and P_rj is the received signal strength from the other cells, which considered as an interfering signal, N is the total number of the first-tier interfering cell.

The findings suggest that the line of sight effect can be generated, while lowering the receiver antenna height at street lamp level but with a high amount of interference due to reflection, diffraction and scattering effect from the walls and other objects present within the cell area. However, this interference effect and almost constant SINR in most of the cell area can be achieved using the multi-antenna system with at least more than 8 receivers in a cell.

Another method to minimize interference is discussed in [25] that presented a sectorized distributed antenna to minimize the "inter-cell interference". Under the proposed method, power adjusted beam switching has been introduced to support the various transmission modes based on UE geographic locations and channel conditions including blanket and selection transmission via dynamic power allocation. The idea of power adjusted beam is that a fixed beam pattern is designed for each transmitter along with its remote units. This beam pattern could be more than one for a cell. With multiple beam patterns, the entire cell area including cell edge is covered and can thus be extended for entire AoI. When users enter in the cell, all terminals listen to user-specific reference signal and report signal strength to BS to decide the best beam combination. The paper also suggested dynamic power allocation to all receiver and base transmitter using the maximum ratio transmitter (MRT) principle to optimize the diversity gain. The power adjustment is based on channel strength. The entire concept was simulated with the typical LTE parameters for conventional DAS (C-DAS) and sectorized DAS (S-DAS) together

with centralized antenna system. The result showed that the SINR improved mainly in certain close areas to the remote antennas. The capacity is slightly lower for high SINR due to limited transmit power and at low SINR inter-cell interference increases. On the other hand, optimal power allocation provides better SINR across the cell, which results in a better capacity. However, inter-cell interference is still an issue at low SINR at the cell edge. While investigating our novel SCIDAS architecture, we observed that it already considers C-DAS and S-DAS concepts. We have mentioned this paper to highlight the advantage of our architecture over the state-of-the-art.

While proposing a suitable architecture for PTC^2, an overview of downlink performance and capacity of a DAS network was obtained from [26] where the authors had analyzed the realistic potential gains of a downlink DAS in a multi-cell environment. As a result, DAS can achieve lower symbol error probability and higher capacity than conventional cellular systems. The authors also quantified that DAS can reduce the cost of the installing system and simplify maintenance because DAS can reduce the required number of base stations within a target service area. This paper endorses our choice of DAS paradigm as base concept of the SCIDAS.

A capacity analysis, using cooperative transmission schemes, was reported in [27]. A scenario of a full frequency reuse operation leading to severe signal quality degradation near the antenna coverage boundaries was shown to occur when more users are to be served simultaneously; similar to the "cell-edge problem" of conventional cellular systems. If the signal transmission would be performed cooperatively among the remote antenna units, both the alleviation of the problem and further capacity enhancement could be achieved by an appropriate transmission mode selection according to the location and channel condition of the receiver. The authors observed that cooperation is not always beneficial; that is, for geographical user positions close to one of the RoUs it is better to use non-cooperative transmission (serve the user with only one RoU), and for cell coverage boundaries cooperation is beneficial. Based on those results, the authors propose to adaptively optimize the network operation mode (i.e., the number of cooperative RoUs) to combine the advantages of cooperative and non-cooperative schemes to maximize the system throughput. Results show that adaptive cooperation becomes more significant when shadowing effects increase, with more than 20 percent cell-average gain for up to three RoUs' cooperation. The mechanism to manage PTC^2 challenge, which we proposed in this chapter, incorporates adaptive cooperation, although with a different approach.

In [28], it was identified that selecting a cluster of antennas from all the distributed antennas is a key problem in DAS and proposed an uncomplicated antenna selection algorithm based on the upper bound of multi-users sum rate to achieve comparable uplink throughput. The proposed algorithm provides better signal strength for both the users as compared to conventional antenna selection method.

Energy efficient gains may also be an outlook of a new approach in architecture. Authors, in [29], explained that user distribution within the cell coverage area is rarely uniform. About 50% of network traffic is carried by 10% of BTS, and these places are known as a hotspot. The author investigated the energy efficiency gains of DAS in the case of non-uniform user distributions for outdoor hotspot scenarios and compared that performance with the case of macrocell deployment.

An Efficient Uplink User Selection algorithm is discussed in [30] where, authors proposed a dominant-antenna-least-correlation (DALC) algorithm which utilizes the channel characteristics of DAS and set simulation environment considering a single cell with one base station (BS) with several numbers of mobile stations (MSs) which are randomly distributed in the cell. The authors introduced three basic user selection algorithms, which are exhaustive search algorithm (ESA), incremental selection algorithm (ISA) and greedy selection algorithm (GSA). Simulation results show that the DALC algorithm reaches more than 98.5 % of the spectral efficiency of optimal cases, i.e. ESA, ISA, and always outperforms GSA. The algorithm is very simple and suboptimal since the interferences between users are not considered; the performance is severely degraded in a multiuser environment. A scenario of a full frequency reuse operation leading to severe signal quality degradation near the antenna coverage boundaries was shown to occur when more users are to be served simultaneously; similar to the "cell-edge problem" of conventional cellular systems. If the signal transmission would be performed cooperatively among the remote antenna units, both the alleviation of the problem and further capacity enhancement could be achieved by an appropriate transmission mode selection according to the location and channel condition of the receiver

[29] and [30] are utilised as benchmarks for evaluating the working of SCIDAS architecture.

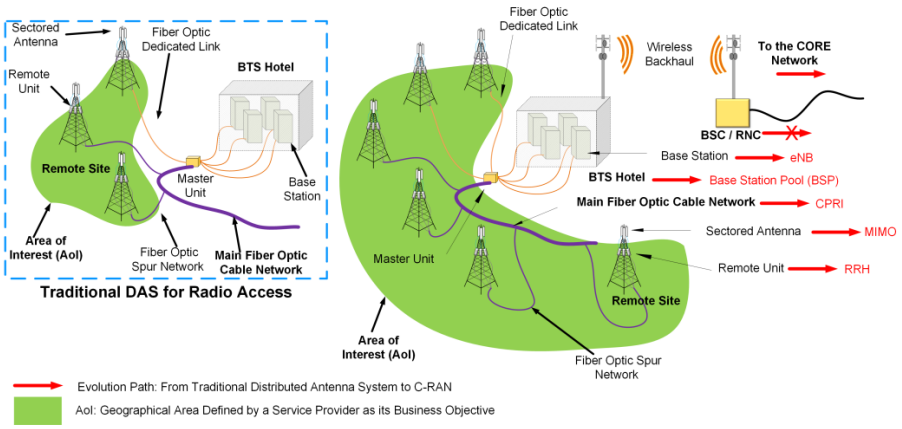

Figure 4-2-1: Evolution of C-RAN from Traditional DAS Architecture

Apart from the related works discussed above, here we discuss two major industrial state-of-the-art works that hold a close relevance to the present chapter.

C-RAN: Latest technologies such as LTE [31] are the promising step in next generation of mobile communication and can boost the carrier utilisation like never before [32] [33]. However, they are not just sufficient for efficient spectrum utilisation, but the how the dissemination of the resources is performed is equally important. Figure 4-2-1shows the evolution of Cloud-RAN (C-RAN) [34][35] that form the conventional DAS architecture. Where the conventional DAS architecture involves multiple BSs to reside at the BTS Hotel, the C-RAN is primarily for LTE systems and multiple BSs are collectively functional and are called as BS Pool. Associating distributive property in the existing LTE technology, a C-RAN can thus enhance resource utilization significantly.

SON: Another LTE-oriented innovative *Self Organizing Network (SON)* [36] [37] [38] architecture is conceived by Nokia Siemens Networks (NSN). As per NSN, SON is leapfrog to a higher level of automated operations in Mobile Networks [39], and the SON architecture manages the major network operations at the core level. The description of the architecture is taken from the NSN online white paper that says "*SON has potential ability to tune and adjust parameters in real time can cope with problems on the fly, acting fast before performance suffers. Human response, entailing site visits and drive testing, is slower and costlier. SON can minimize and, in many cases, eliminate both. For example, it detects handover failures, prompting the BTS to adjust HO parameters on its own while preventing ping-pong oscillations. Congested and overloaded cells invite complaints because users get less bandwidth than they expect. Promising results with the current SON implementation suggest that this will soon change owing to its load-balancing powers. SON monitors the BTS, and when one cell is overloaded, hands over users at the cell's edge to a neighboring cell. This resolves the traffic problem and, under typical cell load conditions, decreases the number of dissatisfied users from about 10 to 2 percent.*" This shows that they are targeting similar concerns that are picked up in this thesis.

The state-of-the-art has several limitations that are addressed with our novel SCIDAS architecture. Some of them are as follows: (a) state-of-the-art architectures are convolved around the respective technology,and therefore, cannot accommodate future technologies, such as 5G, (b) they tightly bind the technology to their infrastructures, and therefore, less flexibility in upgrading either of them while other is undisturbed, (c) intelligence is more oriented in managing the network than managing users, (d) heterogeneous networks are not true heterogeneous as all macro, micro, and pico cells belong to same technology, and for true heterogeneous environment, multiple Base Stations (BSs) of various technologies needs to be co-located, and (e) present state-of-the-art architectures have a limited control at site ends.

The SCIDAS is an intelligent network system that has the following capabilities:

- to understand the varying physical conditions that impact the communication network environment in both optimistic and pessimistic ways and to identify the epicenter of problems in case network conditions deteriorate, and
- to plan and decide the changes, whether mechanical or electrical, which should be implemented across the network to cope up with the deteriorating conditions so that the network performs at or above a certain health benchmark in every condition and at every time,

and, by Self-Configurable, we mean, the capability to adapt and behave as per the decisions made by network intelligence.

4.3. THE SCIDAS ARCHITECTURE MODEL

Future communications will be voracious for data [8]. A lot of research has been ongoing for improving the data rates. Several studies have been performed in recent times considering the distributed nature of the system models.

In [40], a comparison of asymptotic user rates between standard co-located antenna (CA) and distributed antenna (DA) models is performed assuming that the ratio of the number of antennas and users tend to a definite value. The paper showed that for a large number of antennas, the DA's performance is much better than CA.

In a newsletter published by Bell Labs [41], authors assumed a system model where the antennas were presumed to coordinate for enhanced spectral efficiency. Recent researchers have considered Poisson Point Process (PPP) models for their investigations.

The network topology is obtained through stochastic geometry. In [42], authors consider a system model where the locations of BSs, comprising N antennas are installed according to a homogeneous PPP model to evaluate the spectral efficiency of Dynamic Coordinated Beamforming. The C-RAN architecture in considered for investigating the optimizing antenna selection and achieve combined power from these antennas.

A Large-Scale DAS is investigated for its energy efficiency in [43] where authors assume the numbers of DAs are larger than users and, energy efficiency in multiple user scenarios is investigated. However, the architectural description is limited to the radio access with connectivity to their respective BS serves/ Pool.

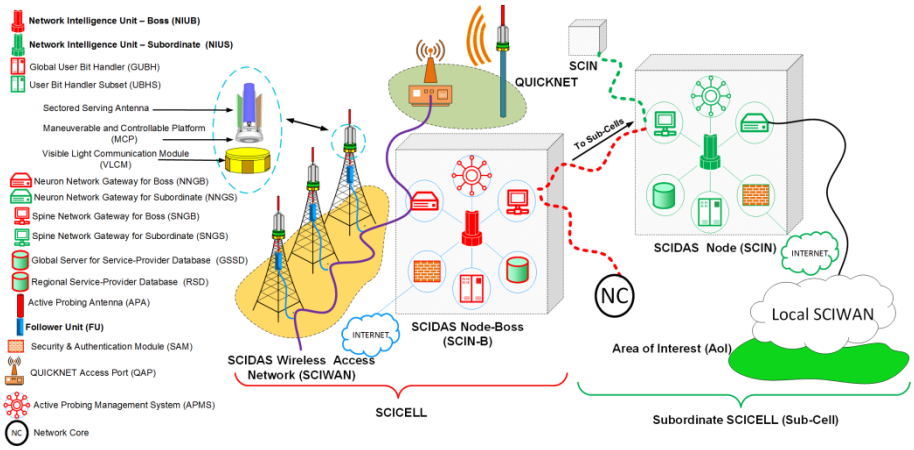

Figure 4-3-1: the SCIDAS: two step Architecture [1]

In this section a holistic architecture is proposed that may accommodate many of, if not all, presumptions made for various investigations. This architecture is based on the DAS concept and has been designed to support Cell Virtualization [22], Coordination [44], Cooperative Transmissions [27], Reconfigurability [23], Random and organized clustering[45] [46], and multi-cell environment [47]. The architecture can accommodate PPP and Stochastic Geometry topologies of cell formations through its simple design model. The initial SCIDAS concept was conceived in our previously reported work in [1] and is elaborated here in terms of its architectural attributes, making it superior to presently existing architectures. The SCIDAS architecture is in line with the traditional DAS and C-RAN paradigm. However, it is provided with intelligence and other functional modules layered above the DAS architecture for it to be responsive to variations in a network environment. The following subsection discusses the salient features of the proposed SCIDAS architecture.

4.3.1. SALIENT FEATURE 1: TWO TIER FORMAT

Referring to figure 4-3-1, the following are the architectural details of SCIDAS.

(i) *Boss and Subordinate Hierarchy*:

SCIDAS focuses on simplifying the deployment of a network, and therefore, is proposed to be in two tiers, namely BOSS and SUBORDINATE defined in [1]. It is similar to the mother (Boss) and daughter (Subordinate) analogy with the condition that daughter can inherit all properties of the mother in certain duration of time. An SCIDAS network can have a maximum of one Boss, however, may have more than one Subordinate. Each Boss and Subordinate is an independent network. However,

the Subordinate must inherit the parameters from the Boss and also, the Subordinate must rely on and "obey" for inter-subordinates management. A network can be deployed with Boss at a central/ strategic location and Subordinates covering the rest of the AoI. It seems similar to conventional network planning where the core resides at the center, and the BS subsystem spreads across the area, however, technically, the approach is quite different in the case of SCIDAS. Figure 4-3-2 shows the hierarchical deployment structure of an SCIDAS network. We have defined this architecture as two-tier system, as the SCIDAS network has two tiers of deployments, namely, BOSS and SUBORDINATE. The architectural hierarchy is maintained so that the intelligence, which begins with BOSS, is properly disseminated across all the SUBORDINATES of the network. As, mentioned earlier, a SUBORDINATE can only be a sub-set of BOSS, hence all controls remains at with BOSS, though, depending upon the situation, a temporary "power of attorney" may be granted to one or more SUBORDINATES to avoid unnecessary protocol delays (in seeking access, authentications, and handovers, etc.) while managing PTC[2].

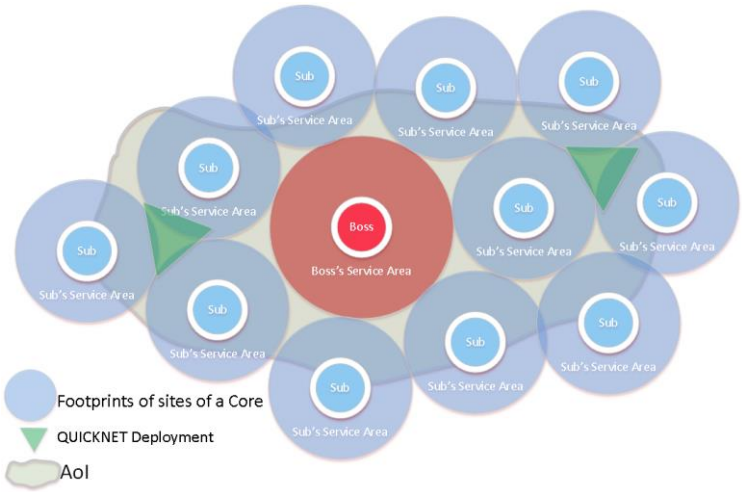

Figure 4-3-2: SCIDAS Two tier deployment strategy

(ii) The SCIDAS Node (SCIN):

Just like conventional DAS/C-RAN, a container is needed to encapsulate the working system of the SCIDAS network. However, SCIDAS has two categories of these containers. Hence, categorically, the SCIDAS's BSP or BTS Hub (as in DAS) system is proposed to be in two forms each belonging to the Boss and Subordinate respectively. The container can be a logical node in a computer system or a physical structure such as room to hold necessary equipment. The SCIDAS Nodes are termed here as SCIN-S (or simply SCIN), and the node that is dedicated for Boss is termed as SCIN-B.

(iii) *Location Based Equipment Hierarchy:*

Both the Boss and the Subordinates are the containers, logical and/or physical, that contains GUBH, Neuron Network Gateway for Boss/Subordinate (NNG-B/S), Spine Network Gateway fo Boss/Subordinate (SNG-B/S), Security and Authentication Module (SAM), Active Probing Management System (APMS), Global/Regional Server for Service Provider Database (G/RSSD), etc. handling the mobility management, authentication and security roles of the network. In most ways, both the Boss and Subordinate are similar to a conventional network core except for one "major" difference, the Network Intelligence Unit. From the hierarchical point of view, the components of the Boss'sub-architecture have more privilages than to the ones of the the Subordinates.

(iv) *Neuron Network:*

Similar to the conventional DAS networks, the sites in SCIDAS are connected to the network core (Boss or Subordinate) through Optical Fiber Backhaul Network (OFBN). Notwithstanding with the usual DAS/C-RAN backhaul network, the SCIDAS backhaul is in two scales, a local and a global one. The convenience of the deployment decides whether a site would belong to a Core, SCIN-B or SCIN-S. The connectivity of sites grouped for a particular core is managed through a certain set of OFBN defined here as Neuron Network (NN) and shown in figure 4-3-1. The sites, therefore, are first grouped at the Boss level and then, when the geographical separation between the sites and the Core are significantly large enough, the next core is chosen.

(v) Spine Network:

For a complete network interconnection, it is important that all Subordinate Cores are connected to the Boss. This is proposed here by connecting cores to a high capacity backhaul network that is defined as SPINE. For complete network operations, it is important that eventually, all the network cores must be connected to the Boss. This can be done in star, ring, and/or distributed kind of deployments as shown in figure 4-3-3.

(vi) *Neuron and Spine Network Gateways*:

The port through which the Core connects to the NN is the Neuron Network Gateway (NNG). At the Boss/ Subordinate level, it is defined as the Neuron Network Gateway for Boss/ Subordinate (NNG-B/S). Similarly, the Spine network connects to a Core through the Spine Network Gateway for the Boss/ Subordinate SNG-B/S.

(vii) *SCIWAN:*

All sites (SRUs) that are connected to a specific SCIN through NNG are the part of a common network termed here as SCIDAS Wireless Access Network (SCIWAN). Hence, in a geographic sense, an SCIWAN is the area covered by a single SCIN.

(viii) *SCICELL:*

The SCIWAN sites disseminate the carriers of the common BSs or UBH, hence, all sites with its SCIN are termed here as SCICELL. It is the SCICELL 'block' that repeats in the entire AoI for complete services.

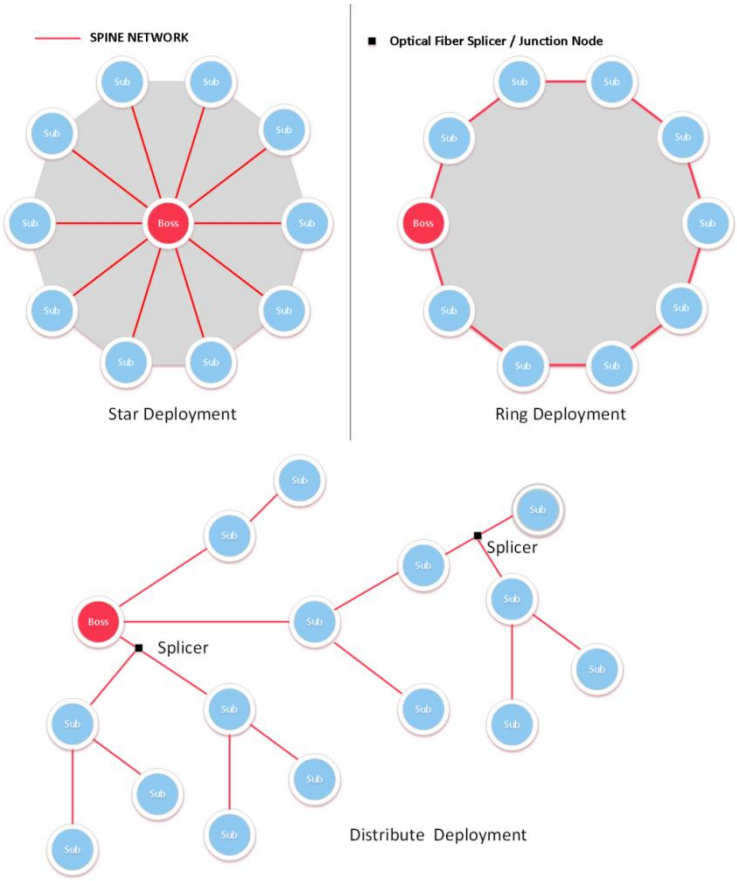

Figure 4-3-3: Spine Network Connectivity Types

.

4.3.2. SALIENT FEATURE 2: INTELLIGENT SUB-ARCHITECTURE

This subsection discusses the most important feature of the proposed architecture, namely, the intelligence. We call this layer of intelligence the Intelligent Sub-Architecture (ISa). The Components of ISa are as follows:

(i) *Network Intelligence Unit (NIU):*

An NIU is the intelligent unit of the SCIDAS system that handles all the intelligent activities in the network management, such as gathering, prediction, scheduling, coordination, etc. The NIU is located at the SCIN-B. The NIU obtains the network information from the Active Probing Management System (APMS) and all Smart Remote Units (SRUs), processes the information, send the decision over a reserved channel to be followed at the remote end by *SRU, MCP,* and *VLC* (discussed later). This process is iterative and the time period of the iterations depends on the dynamics of the network environment. This intelligent unit makes the SCIDAS architecture more robust and efficient than contemporary network architectures because of the following capabilities:

- NIU works independently to the underneath technology. Hence it can manage the multi-technology environment more efficiently than the LTE dedicated technology;
- The decisions are based on the dynamics of the subscribers and propagation of EM waves. Hence, SCIDAS is more resource efficient;
- The two-tier architecture can be extended more flexibly than the C-RAN or similar architectures; and,
- The NIU is an imminently independent intelligent unit and therefore is a programmable, upgradeable and expandable unit. This makes SCIDAS superior to SON and similar technologies.

(ii) *Smart Master Unit:*

The SMU is the upgraded version of the standard traditional MU and resides in the NNGB or NNGS. Besides the standard RF/Optical conversion as its predecessors are doing, an SMU has the additional features that enable it to assist and follow the NIU. As shown in figure 4-3-4, the BSs of the service providers connect to the RF stage of the SMU. The RF stage provides a dedicated circuit channel for both the Transmission (T_x) and the Reception (R_x), separately and, further, all BSs are grouped in separate T_x and R_x modules. Each circuit channel of the RF stage is interfaced with the T_x and R_x modules of the Optical Stage where the circuit channel is converted to the optical channel for further stages. Each optical channel of the Optical Stage is modulated over separate wavelengths by the WDM module

that is cascaded to the Optical stage of the SMU so that the T_x output of the Optical Stage drives the WDM optical transmitters and similarly, the WDM optical receivers drive the R_x module of the Optical Stage.

In figure 4-3-4, it is shown that the NIU resides in the SCIN and directly connects to the Optical Stage of the SMU. This is due to the fact that, firstly, the NIU is not providing services over the air interface, secondly, unlike the BSs, the NIU is not to be a variable component of the system and, therefore, can communicate over a fixed circuit channel that is dedicated to it permanently as shown by the deep red arrow flow in figure 4-3-4. Also, both RF and Optical stages are controlled by the NIU (as shown as control bus in figure 4-3-4) for improvising the efficiency of both network and electronics.

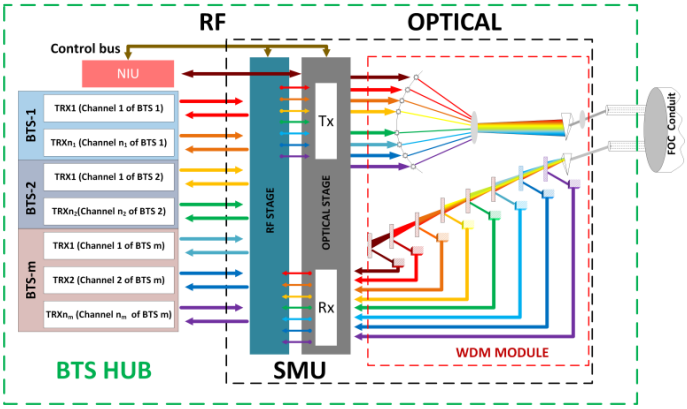

Figure 4-3-4: Smart Master Unit (SMU)

(iii) *Smart Remote Unit (SRU)*:

Similar to the SMU, the SRU is the upgraded version of the traditional standard remote unit. *The SRU along with its remote site infrastructure is defined here as* **BUD** *to differentiate with usual Nodes/BSs*. Although, the function of the SRU should be reverse to that of the SMU, the internal architecture of the SRU is not a mirror image of the SMU. Figure 4-3-5 shows that the optical stage is cascaded to the WDM Module where the output of the T_x module of the Optical stage drives the WDM optical transmitters and R_x module of the SRU is driven by the optical receivers of the WDM module.

Here, we can see that the instructions from the NIU that have reached a particular SRU via the FON network over dedicated optical wavelength are sent to the Follower Unit (FU) of the SRU where the instructions are decoded to be followed by other modules of the SRU. At the Optical Stage, there is a conversion of

Optical/Digital and Digital/Optical and each optical wavelength has a dedicated circuit channel.

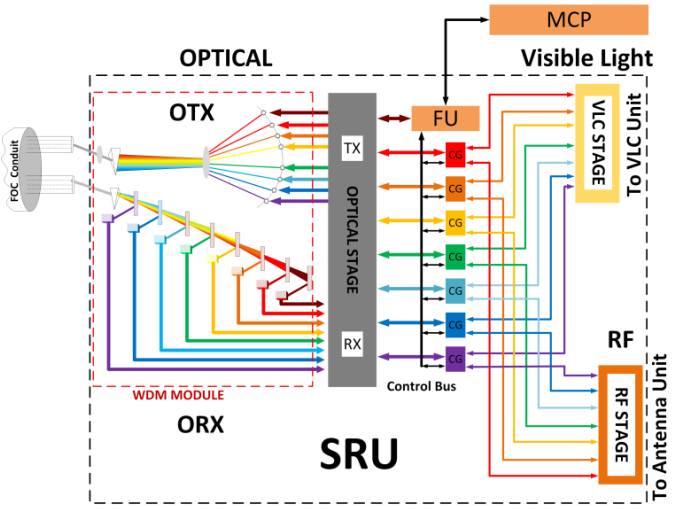

Figure 4-3-5: SRU (supporting RF and VLC Ports) with MCP at the bud

The digital interface of the optical stage is connected to a controllable sub-module that we call as Carrier Gate (CG) and is controlled by FU. This CG will send the digital signals to the two separate output modules (i) The RF Stage that converts the digital signal to an RF signal that is fed to the RF antennas and (ii) The VLC Stage that converts the digital signal into the visible light pattern as discussed in [48]. The FU also interacts with the MCP Module of ISa that will modify the physical parameters of the antenna by performing three-dimensional (3D) motions. The working of the RF stage is the reverse of what has been discussed for the SMU. Hence, the SMU-SRU setup will act as a bridge between the NIU-MCP, NIU-VLC STAGE and NIU-RF STAGE for controlling the configuration of SCIDAS for efficient resource management.

(iv) *Active Probing Management System (APMS)*

Active Probing is the process of observing a system by measuring the variation in the observed state of the system, which is created by injecting a stimulant, in such way that the system is least deviated from its present state. In SCIDAS, this is achieved by impinging tiny signal bursts from one bud and then sensing the variations by various buds to obtain the holistic view of the network. The APMS belongs to ISa and is controlled by the NIU via an intelligent layer, and is intended to monitor the entire SCIDAS network activity. Through APMS, the NIU can

gather information about the network and take necessary decision. APMS is discussed in detail in Chapter 5.

(v) *User Bit Handlers*

The SCIDAS architecture endorses that *when the access technology is accessed by the user, the information should be modulated at the user end*. Hence at the SCIN, we have placed a generic BS that we call the User Bit Handler (UBH), which is a type of BS/eNB with its access technology separated out from the module. Thus, a UBH will process the user/subscriber bits in terms of handling the user packets (such as addressing, sending and receiving, etc.) and the security/parity coding. Here, the SRU plays an important role in modulating the right access technology on the user bits. This enables SCIDAS to function on various technologies (such as RF and VLC) simultaneously without compromising the processing power. Figure 4-3-5 shows the SMU when each service provider proposes their own BS. The same can be modified with one single UBH with multiple channels for parallel transmission. UBH at SCIN-B rules all other UBHs and thus is defined as Global UBH or GUBH. The unique property of GUBH is that they can share modify or delete the user properties among each other thereby making the resource management more efficient.

4.3.3. SALIENT FEATURE 3: ENACT SUB-ARCHITECTURE

Following are the components of the sub-architecture which is responsible for all actions of the SCIDAS network.

(i) *Follower Unit (FU):*

As shown in figure 4-3-5 and discussed in the SRU section, the FU resides in the SRU to (a) convert the optical information into the desired access technology carrier, and, (b) to optimize the antenna system with MCP. Unlike the conventional Remote Radio Head (RRH) [32], the FU has two lines of information to deal with, data and intelligence, both flowing through same connectivity route. Data line mainly contains user bits exchange between GUBH and user equipment and the intelligent line contains address and control. FU deciphers the information streams and deals accordingly.

(ii) *Maneuverable and Controllable Platform (MCP):*

Out of all the components of SCIDAS, MCP shall be the part that will support motions and displacements. An MCP resides at the remote end (bud) and provides a support system for the mounting antennas. Figure 4-3-6 shows one of the many ways in which the MCP can be designed; however, the most important is its capability to enable the changing of the orientations and tilts of the antennas to

confine or expand, and to follow/track the target within the vicinity of the site.The MCP, proposed in the present architecture can play a significant role in clustering, cell virtualisation and managing SINR. Apart from the physical orientations, the MCP can also accommodate electrical supplements such as electrical tilts, physical and electrical diversities, etc.

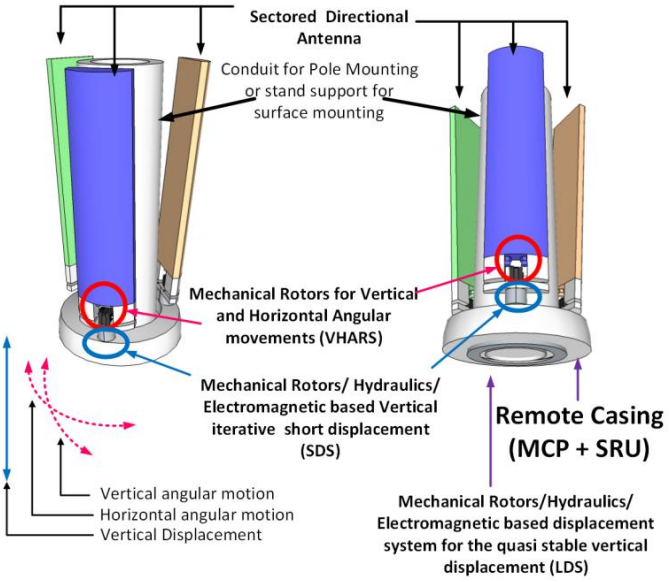

Figure 4-3-6: A closer look of Remote MCP and SRU integrated together.

.

4.3.4. SALIENT FEATURE 4: PLUG AND PLAY SUPPORT

A DAS network can distribute any resource that can be impregnated at the BS Hub of the network. SCIDAS is based on a plug and play principle. In SCIDAS the users reside at the access end, therefore, we consider the wireless technology only from the point of view of access. We propose SCIN to be a generic hub, and various technologies may be accommodated through plug and play provisions.

(i) *Multi-Technology Ports:*

In [48], we discussed the importance of VLC for Ambient Assisted Living (AAL) and the advantages of using visible light (VL) for indoor data services. We also proposed a unique architecture that can work hand-in-hand with the present systems for environments where VLC is more preferable. Figure 4-3-7 shows the VLC working in parallel and in distributed mode along with the International Mobile

Telecommunications (IMT) carriers. As mentioned, the SRU can accommodate multiple technologies to modulate the user bits from the UBHs simultaneously. Therefore, a VLC unit, which connects to the SRU by the VLC port, is proposed here; it can easily blend in the SCIDAS system with the SRU module. As proposed earlier in [48], the VLC system has a Visible Light Transceiver (VLTRX) System that resides at both, the user and the base ends. It uses Visible Light (VL) portion of the EM spectrum as an air interface. The VLCTRXs can be activated by the instructions sent from the NIU that can work in parallel or as a complementary unit for any network environment. Figure 4-3-8 shows the working of VLC along with the IMT services with an intelligent network layer managing the VLC network system. This intelligent network layer can be taken over by NIU of SCIDAS when plugged into the system.

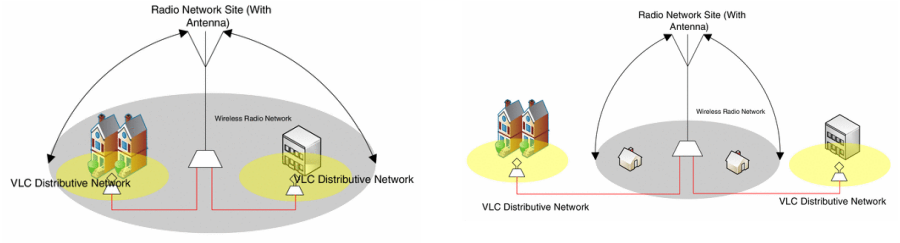

Figure 4-3-7: VLC in parallel (Left) and Distributed (Right) Mode [48]

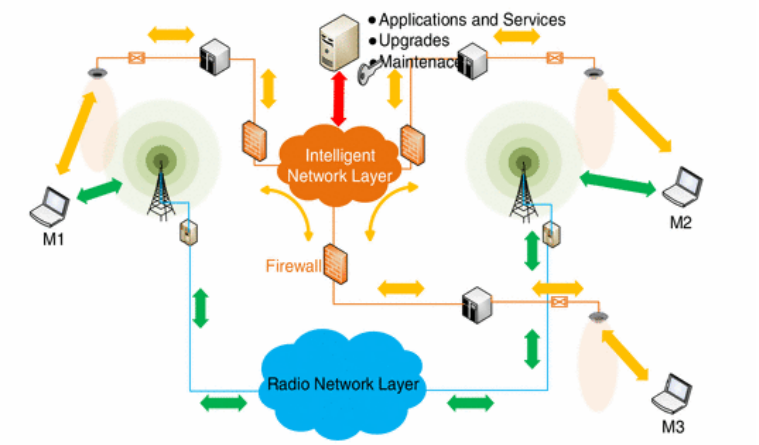

Figure 4-3- 8: M2M Communication in different scenarios of multilayered network [48]

(ii) *QUICKNET:*

QUICKNET is sub-architecture that is an SRU without NN. The NNGB or NNGS connects with the SRU through a wireless access port or QUICKNET Access Port (QAP). This is used for the case where the deployment is difficult, laying the optical cable is not feasible, or, the deployment needs are quick and temporary. The QUICKNET is also introduced here to accommodate the densification and clustering of the cellular architecture. It can be quickly deployed in the areas to enforce a stochastic approach.

4.3.5. DEPLOYMENT LAYOUT: PRESENT AND FUTURISTIC

Figure 4-3-9 shows a deployment layout of an SCIDAS model. The type of architectural layout shown in figure 4-3-9 is what was partially implemented in a hotspot area and is discussed in Chapter 6 of this thesis. Here, the SCIN/ SCIN-B contain discrete BSs (in contrary to the GUBH) to show the multifarious possibility in deployment. The intelligent layer, containing NIU, SMU, SRU and APMS is shown to work parallelly on the existing DAS network by replacing the Master and Remote modules with SMU and SRU respectively. SCIDAS can thus be implemented with the present DAS based network architectures and can make them intelligent.

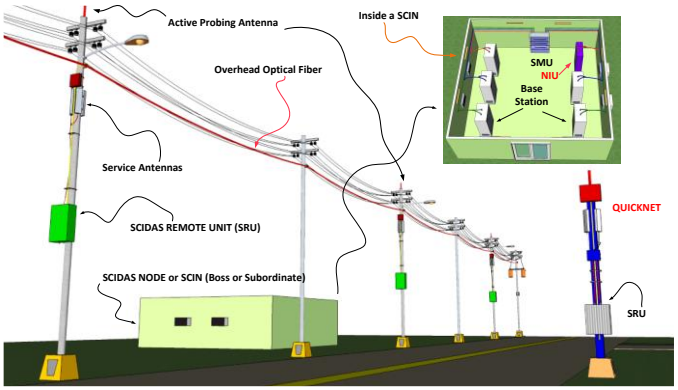

Figure 4-3-9: SCIDAS Architecture in compatible with present DAS /CRAN Architecture

Figure 4-3-9 is a deplyoment example of SCIDAS in a real scenario. It shows the APMS antennas and QUICKNET in an AoI. Figure 4-3-10 shows the location of the equipment in the SCIDAS architecture in more details.

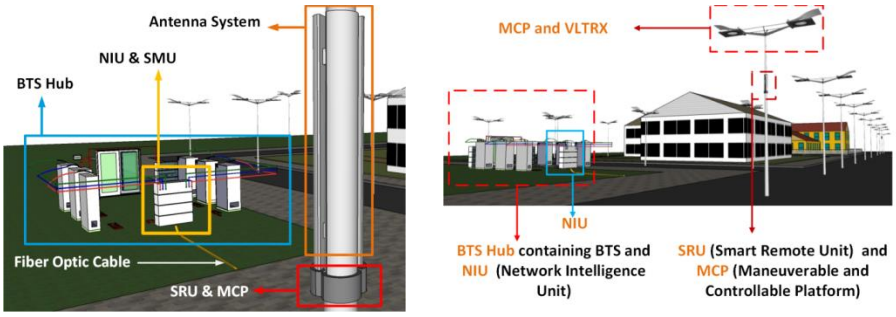

Figure 4-3-10: SCIDAS Network Architecture –closer view

Similarly, figure 4-3-11 shows a typical SCIDAS deployment in a HOTSPOT area.This deployment scenario is considered for our discussion in Section 4.4, Chapter 5, and Chapter 6 to analyse the working of the algorithms and their performance. The buds (remote units) are deployed on the street poles to form a square patted deployment. This kind of deployment is considered to represent the SRU in an (x,y) positioning system and for the ease of discussions.

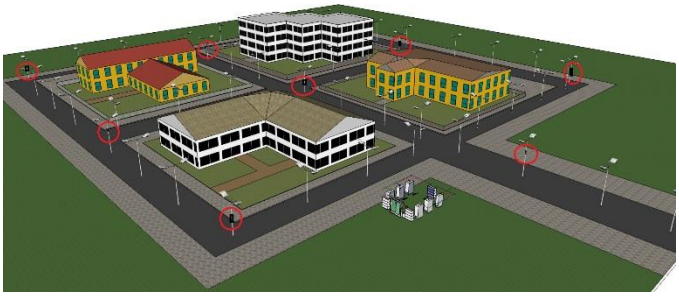

Figure 4-3-11: SCIDAS Deployment Scenario

Figure 4-3-11 is a typical example of an experiment performed in Okhla, Delhi, India where the basic model of SCIDAS was installed to sense the network. The details about this experiment is discussed in Chapter 6 of this thesis.

FUTURE APPLICABILITY OF THE SCIDAS ARCHITECTURE

The radio spectrum is assigned to the Telecom Service Providers (TSPs) through market driven pricing method (may be auction), for providing the mobile services to the subscribers in a service-area. The service-area (AoI) is not uniform from the traffic density point of view. It is normally divided into three categories i.e., Most

Dense Traffic Area (MDA), Dense Traffic Area (DTA) and Normal Traffic Area (NTA). The traffic density is also dependent on the hour of operation, i.e., busy hour, normal hour and light hour. To cater for the subscribers in an MDA and during a busy time is a challenging task. The TSPs face a further challenge to service some special occasion like New Year's Eve, any major festival, major accidents, natural calamity, etc. During such incidences, the call demand, as well as the call duration, increase sharply and can be attributed to location, time, and event. The increase in demand leads to a heavy call congestion demanding additional spectrum. The demand for additional spectrum for a short duration to tackle the heavy traffic requirements and the call congestion, a different approach to spectrum management is needed. In the previously published research in [49], proposed an innovative auction method that can allow temporary spectrum allocation on demand. However, such a process still cannot solve the wobbling as discussed in Chapter 3.

The SCIDAS architecture, defined and discussed in this chapter can aptly cater for the on-demand requirement by shifting the network resources to the place of requirement. Further, the architecture allows various technologies to operate in different layers. Also, a separate sensing sub-architecture is accommodated in the SCIDAS to offload the unnecessary paging and beaconing during mobility. Because it is based on the traditional DAS architecture, SCIDAS can easily adapt to the existing FONs with a provision of QUICKNET for difficult areas. This makes SCIDAS a suitable candidate for the future network architecture. The novelty of the architecture is in the logical functionalities that are detailed in Chapter 5.

In 4.3.4, we discussed the plug and play property of SCIDAS allowing it to accommodate future technologies, such as the most recent upcoming technology, Light Fidelity or Li-Fi [50]. In this sub-section, we discussed how SCIDAS can support a VLC system by plugging in the access module to the SRU. The VLC, when applied for data access, becomes Li-Fi. Hence, the architecture has immediate relevance to the Li-Fi based operations.

4.4. SCIDAS FUNCTIONING: AMOEBIC PTC^2 RESPONSE MECHANISM (APR)

In section 4.2, it was discussed that the SCIDAS architecture has an intelligent core, defined earlier as the NIU that resides in BOSS, and has the ample capability to control each and every bud in the network. This attribute allows SCIDAS to breakdown the Fixed-Cellular paradigm of the present networks' frequency resue pattern. Here, we elaborate the functioning of this new paradigm, defined as TISSUE structured reuse pattern by using the architectural attributes of SCIDAS. This section discusses the set of algorithms, defined here as Amoebic PTC^2 Response (APR) mechanism, through which an SCIDAS network manages and mitigates the PTC^2 challenge. The mechanism is termed as Amoebic because the

processes resemble the amoeba life cycle and, just like amoeba tames the food, APR never leaves PTC wobble untreated. APR has five processes as per below:

a) Prompt
b) Ingestion,
c) Digestion & Absorption,
d) Fission and Assimilation, and,
e) Egestion.

Presently, the APR mechanism is discussed in terms of the architectural flexibility of SCIDAS. It will be shown how the SCIDAS intelligence can control various buds of the network to form an individual cell or need-based group of cells, or TISSUES, to create a network environment that harmonizes with the PTC^2 dynamics. The APR's iterative management enables SCIDAS to follow the accumulations by grouping the cells (buds) to form Tissues or disintegrating from tissues to cells as per demand till they dissipate.

4.4.1. DESCRIPTION OF THE APR PROCESS

Here, we describe the six processes that collectively define the APR mechanism. The processes appear in the description in the same sequence they are expected to perform in the PTC^2 situation.

A. Prompt Mechanism

Figure 4-4-1 shows an SCIWAN area where the SRUs have divided the area into a Honeycomb pattern. We have already discussed that the NIU can choose the specific carriers/ sub-carriers that can be radiated by a sector antenna by enabling SRU of the specific sector. Therefore, among the total spectrum allocated to the service provider, NIU selects which of them should be radiating through a specific SRU. Hence, each SRU can enable its own sets of carriers as individual Carrier Groups (CGs). Each dot in figure 4-4-1 refers to an SRU with location (i, j) and k is the sector as shown by three colours of the dense pattern. The CGs can thus be allocated in three ways, (i) continuous pattern, where a same CG is shared by adjacent SRUs till a condition is met, (ii) alternate pattern, where, two sets of CGs are allocated alternately to adjacent SRUs and repeated till a condition is met, and, (iii) dense pattern, where the sectors of SRU are allocated with different set of CGs to fulfill certain conditions.

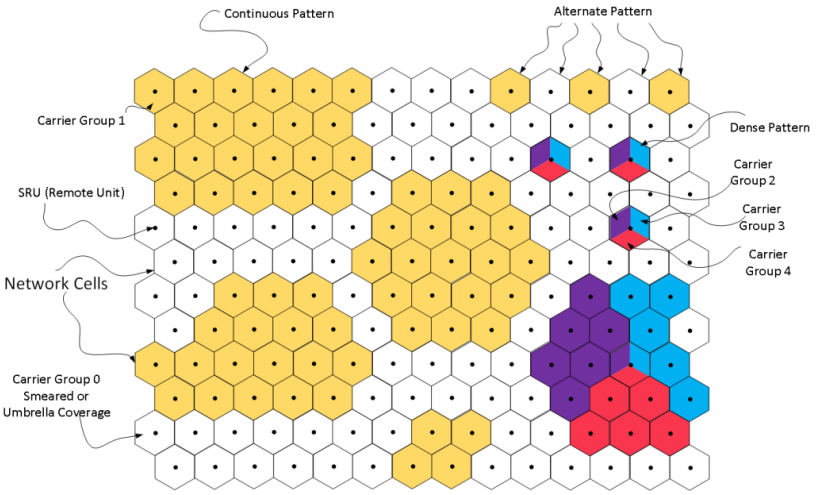

Figure 4-4-1: A typical Prompt State

We propose a novel algorithm, called PROMPT that iteratively monitors the network to keep track of wobbles in the network. The intensity of wobbling can be in two ways, one when the crowd moves from one place to another and, another when people come closer to each other in the same subject area. This is calculated by iteratively scanning the network in the position and time domains (see, Chapter 5 for position and time-based scanning). There is always some tolerance limit that all networks offer to cater for such dynamics. Here, the limits are fed to the algorithm as the time and position base tolerances. As the PROMPT algorithm takes the assistance of APMS, it can proactively identify the approaching wobble, as shown in figure 4-4-2, without involving the real network resources.

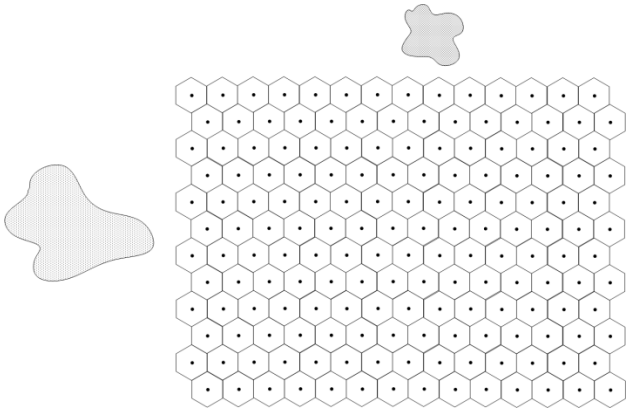

Figure 4-4-2: A typical PTC^2 situation

B. Ingestion Mechanism

Figure 4-4-3 shows the proposed INGESTION process when a wobble is welcomed in the SCIDAS network. Ingestion follows PROMPT. As the wobble approaches a SCIDAS network, the SRU iteratively allocates the carriers to cells (Sub-bud area) that are affected by the accumulation. Figure 4-4-3 shows two wobbles approaching a network from two different directions. The intelligence of SCIDAS is encashed in this process when the carrier allocations are significantly localized. Hence, when distance apart, the same Carrier Group (CG) can cater for different accumulations, until they collide at a common point. At the point of collision, the smaller user group is allocated a new CG as shown in figure 4-4-3 with distinct colours. As shown in figure 4-4-3, the process of ingesting a wobble is accomplished by series of algorithms discussed in section **5.2 of Chapter 5**. As we can see in figure 4-4-3, PTC^2 is a dynamic network and tends to collide at a common place, and a new CG is assigned to the smaller group. This is part of a process when a limited set of carriers are dynamically allocated to accommodate more and more wobbles. This process is defined here as DIGESTION and ABSORPTION mechanism.

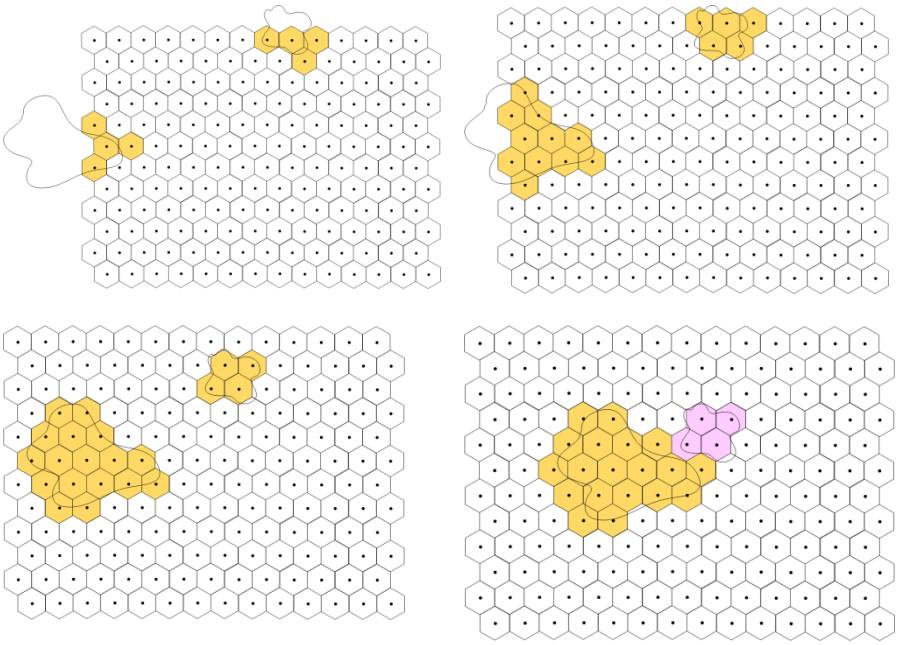

Figure 4-4-3: Ingestion Process

C. Digestion and Absorption Mechanism

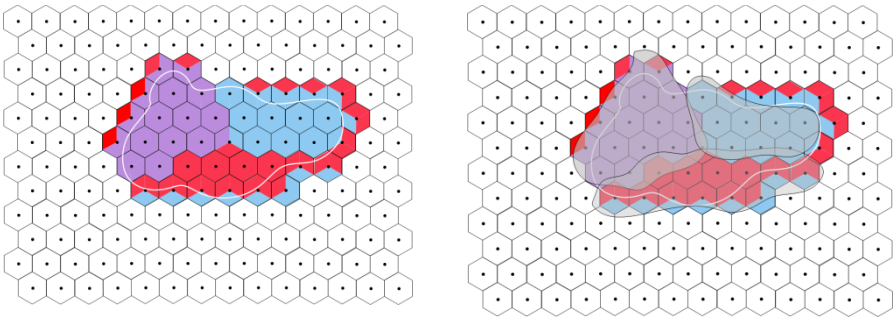

Figure 4-4-4: Digestion and Absorption Mechanism

In the DIGESTION and ABSORPTION mechanisms, are shown in figure 4-4-4. The bigger groups are broken into smaller groups (in terms of CGs) in such a way that the frequencies belonging to various CGs must not decrease the SINR beyond a tolerance limit (receive sensitivity). The smaller groups are also formed based on the tendency of the departing or dissolving (this process is monitored by algorithm discussed in section 4.5.2).

D. Fission and Assimilation Mechanism

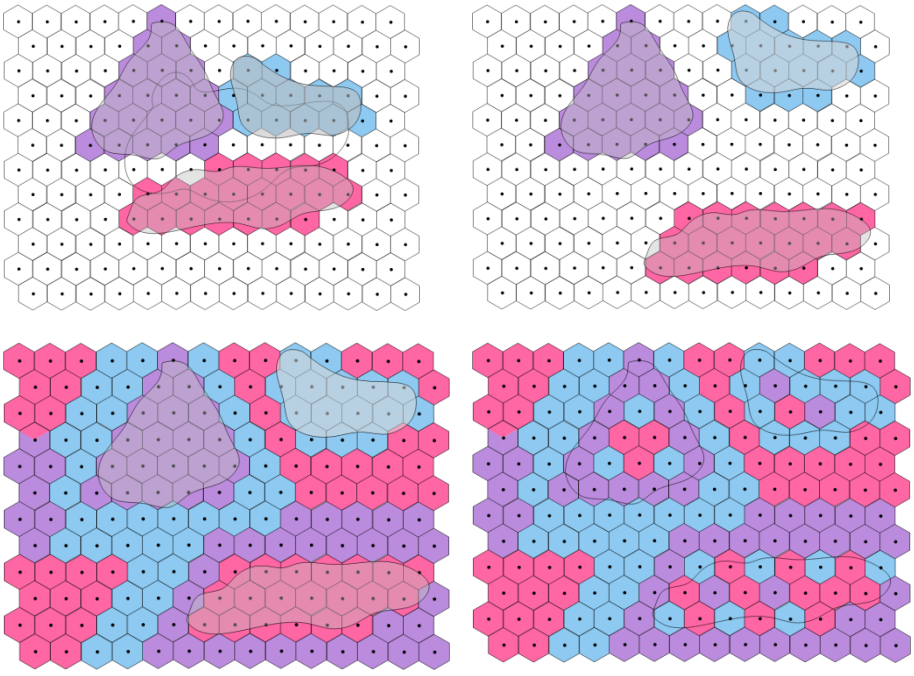

Figure 4-4-5: Fission & Assimilation Mechanism

As accumulations are dynamic (PTC^2), it is very much possible that users from a common place depart with different density and strengths than to what it was when they accumulated at the time of arrival. This challenge is abated with the FISSION and ASSIMILATION mechanism, which distributes the accumulation by disintegrating tissues into smaller chunks of cells, catering of sub-groups, and treating individual sub-groups as a separate PTC^2 challenge. This can be viewed as multiple iterations of the DIGESTION and ABSORPTION mechanism.

Figure 4-4-5 shows the FISSION & ASSIMILATION mechanism where the top two figures show the Fission Process and the lower two figures are the Assimilation Process. As we can see in the Assimilation Process, only three sets of CGs are intelligently used to dynamically cater the PTC^2. Once the ranges of neighboring cells that can accommodate the common carriers are evaluated, the configuration floats on the network architecture by iteratively allocating the subsequent cells.

E. Egestion Mechanism

This mechanism is shown in figure 4-4-6. The process can be seen as the reverse of the INGESTION mechanism. However, SCIDAS must keep serving the departing accumulations till the forthcoming network welcomes them. The EGESTION Mechanism is also important for the mutual coordination among the various SCINS of the network. Suppose, the group leaves one SCIWAN to another SCIWAN, then the two SCINS can coordinate for a smooth handover of the wobble. For the new SCIN, these five processes follow till the wobble departs from that SCIWAN and so on. It is also important to note that, in the case, when the service provider reserves some carriers for catering the additional wobbles, the grouped formed with such carriers can be passed on to other SCIWANS iteratively to till the accumulations are below the tolerance limit. Thus, a CG can thus be repeated in neighbor SRUs till it reaches some limits.

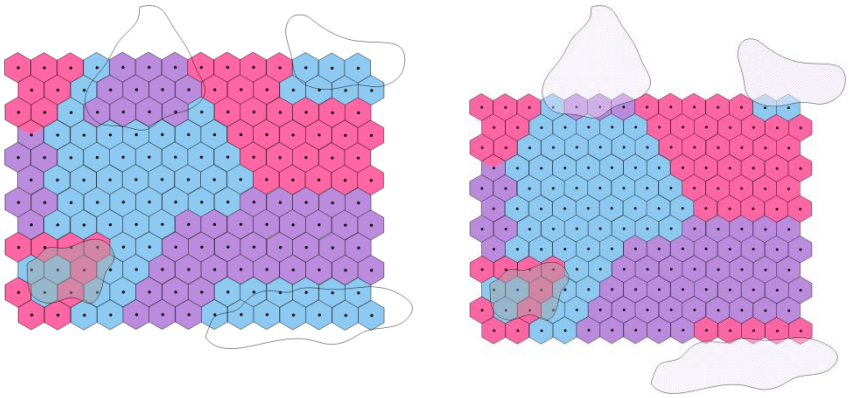

Figure 4-4-6: Egestion Mechanism

The mechanisms discussed in this section is to show the capability of an SCIDAS architecture. With these mechanisms, the SCIDAS can make accumulations float above the base network till it dissipates or exists. The algorithmic formation and evaluation of these mechanisms are discussed in detail in the next chapter (Chapter 5) of this thesis.

4.5. CONCLUSIONS

Chapter 4 defined and detailed the SCIDAS architecture in terms of its flexibility, adaptability, heterogeneity, expandability, and deployability. All these attributes are possible due to the proposed independent, intelligent module that was defined as the *Network Intelligence Unit* (NIU) that uses underlayed *Distributed Antenna System* (DAS) to disseminate both intelligence and service in accordance with the PTC^2 distribution, discussed in Chapter 3 of this thesis. The responses to the PTC^2 challenge, which we expect from SCIDAS, are performed through collaborative coordination of three more modules introduced here as *Smart Master Uni*t (SMU), *Smart Remote Unit* (SRU) and, *Maneuverable and Controllable Platform* (MCP). We also introduced *Active Probing Management System* (APMS) that is the sensory part of the intelligent system.The proposed architecture is supported by several algorithms that also we introduced in this chapter. These algorithms bring in intelligence within the SCIDAS architecture that spreads parallerly along with the carriers, as an independent layer, through the inherited distributed network. To summarise, in this chapter, we proposed (i) in what way intelligence can be mounted over a communication system to produce situation-based responses for the better management of resources, (ii) once mounted, how its reachability can be extended to every operational site, (iii) how this system will work to mitigate PTC^2 challenge, (iv) what are other advantages of this architecture as a future scope, and (v) how a set of procedures can be executed with ease in the SCIDAS to cater the seemingly diffuclt PTC^2 challenge.

REFERNCES

[1] A. Kumar, A. Mihovska, and R. Prasad, "Dynamic Pathloss Model for Future Mobile Communication Networks," in *18th International Symposium on Wireless Personal Multimedia Communications (WPMC) of the Global Wireless Summit-2015*, Hyderabad, India, 2015, Presented.

[2] A. Kumar, P. L. Mehta, and R. Prasad, "Place Time Capacity- A novel concept for defining challenges in 5G networks and beyond in India," in *2014 IEEE Global Conference on Wireless Computing and Networking (GCWCN)*, 2014, pp. 278–282.

[3] A. Kumar, A. Mihovska, and R. Prasad, "Self Configurable Intelligent Distributed Antenna System for Resource Management in Multilayered Dense-nets," in *Global Wireless Summit, 2015*, Hyderabad, India, 2015, Presented.

[4] Y. Qian, M. Chen, X. Wang, and P. Zhu, “Antenna location design for distributed antenna systems with selective transmission,” in *International Conference on Wireless Communications Signal Processing, 2009. WCSP 2009*, 2009, pp. 1–5.
[5] Y. Zhang, H. Hu, and J. Luo, Eds., *Distributed Antenna Systems: Open Architecture for Future Wireless Communications*. Boca Raton: Auerbach Publications, 2007.
[6] M. Tolstrup, *Indoor Radio Planning: A Practical Guide for GSM, DCS, UMTS, HSPA and LTE*, 2 edition. Chichester: Wiley, 2011.
[7] S. K. Ramachandran, *Distributed Antenna Systems: Establishing a Regulatory Framework*. VDM Verlag, 2009.
[8] R. Prasad, *5G: 2020 and Beyond*. River Publishers, 2014.
[9] “Optical DAS | Shyam Telecom.” .
[10] “Distributed Antenna Systems | Genwave Technologies.” .
[11] J. Zhang and J. G. Andrews, “Distributed Antenna Systems with Randomness,” *IEEE Trans. Wirel. Commun.*, vol. 7, no. 9, pp. 3636–3646, Sep. 2008.
[12] T. Wu, Y. H. Kwon, J. Zhang, and Y. Wang, “Distributed Antenna Systems with Power Adjusted Beam Switching,” in *Vehicular Technology Conference (VTC 2010-Spring), 2010 IEEE 71st*, 2010, pp. 1–5.
[13] Y. Qian, M. Chen, X. Wang, and P. Zhu, “Antenna location design for distributed antenna systems with selective transmission,” in *International Conference on Wireless Communications Signal Processing, 2009. WCSP 2009*, 2009, pp. 1–5.
[14] S. Pato, F. Ferreira, P. Monteiro, and H. Silva, “On supporting multiple radio channels over a SCM-Based distributed antenna system: A feasibility assessment,” in *2010 12th International Conference on Transparent Optical Networks (ICTON)*, 2010, pp. 1–4.
[15] ITU-T G.694.2, “Spectral grids for WDM applications: CWDM wavelength grid.” ITU-T, Dec-2003.
[16] ITU-T G.694.1, “Spectral grids for WDM applications: DWDM frequency grid.” ITU-T, Feb-2012.
[17] W. J. Tomlinson and C. Lin, “Optical wavelength-division multiplexer for the 1–1.4 #x003BC;m spectral region,” *Electron. Lett.*, vol. 14, no. 11, pp. 345–347, May 1978.
[18] “Practical Design and Production of Optical Thin Films,” *CRC Press*, 09-Jul-2002. [Online]. Available: https://www.crcpress.com/Practical-Design-and-Production-of-Optical-Thin-Films/Willey/9780824708498.
[19] M. Nebeling and H. J. Thiele, *Coarse Wavelength Division Multiplexing: Technologies and Applications*. CRC Press, 2007.
[20] “Wiley: Wavelength Division Multiplexing: A Practical Engineering Guide - Klaus Grobe, Michael Eiselt.” [Online]. Available: http://eu.wiley.com/WileyCDA/WileyTitle/productCd-0470623020.html.

[21] A. Conte, “Energy-Efficient Base Stations,” in *Green Communications*, K. Samdanis, P. Rost, Andreaseder, M. Meo, and C. Verikoukis, Eds. John Wiley & Sons, Ltd, 2015, pp. 73–96.

[22] J. Wang and L. Dai, “Downlink Rate Analysis for Virtual-Cell Based Large-Scale Distributed Antenna Systems,” *IEEE Trans. Wirel. Commun.*, vol. 15, no. 3, pp. 1998–2011, Mar. 2016.

[23] Z. Bouida, H. El-Sallabi, A. Ghrayeb, and K. A. Qaraqe, “Reconfigurable Antenna-Based Space-Shift Keying (SSK) for MIMO Rician Channels,” *IEEE Trans. Wirel. Commun.*, vol. 15, no. 1, pp. 446–457, Jan. 2016.

[24] S. F. Yunas, J. Turkka, P. Lähdekorpi, T. Isotalo, and J. Lempiäinen, “Multi-antenna cell constellations for interference management in dense urban areas,” in *2010 7th International Symposium on Wireless Communication Systems (ISWCS)*, 2010, pp. 310–334.

[25] G. Wunder, M. Kasparick, A. Stolyar and H. Viswanathan, "Self-organizing distributed inter-cell beam coordination in cellular networks with best effort traffic," Modeling and Optimization in Mobile, Ad Hoc and Wireless Networks (WiOpt), 2010 Proceedings of the 8th International Symposium on, Avignon, France, 2010, pp. 295-302.

[26] W. Choi and J. G. Andrews, “Downlink performance and capacity of distributed antenna systems in a multicell environment,” *IEEE Trans. Wirel. Commun.*, vol. 6, no. 1, pp. 69–73, Jan. 2007.

[27] J. Park, E. Song, and W. Sung, “Capacity analysis for distributed antenna systems using cooperative transmission schemes in fading channels,” *IEEE Trans. Wirel. Commun.*, vol. 8, no. 2, pp. 586–592, Feb. 2009.

[28] Y. Zhao, X. Su, J. Zeng, Y. You, and X. Xu, “Capacity analysis and antenna selection strategy for multi-user distributed antenna system,” in *2011 11th International Conference on ITS Telecommunications (ITST)*, 2011, pp. 784–787.

[29] J. Serugunda, S. Armour, and M. Beach, “Energy efficiency gains of distributed antenna systems for non uniform user distributions,” in *2013 IEEE 24th Annual International Symposium on Personal, Indoor, and Mobile Radio Communications (PIMRC)*, 2013, pp. 3100–3104.

[30] J. Choi, I. Sohn, S. Kim, and K. B. Lee, “Efficient Uplink User Selection Algorithm in Distributed Antenna Systems,” in *2007 IEEE 18th International Symposium on Personal, Indoor and Mobile Radio Communications*, 2007, pp. 1–5.

[31] T. Nakamura, “LTE and LTE-advanced: Radio technology aspects for mobile communications,” in *General Assembly and Scientific Symposium, 2011 XXXth URSI*, 2011, pp. 1–4.

[32] Christian F. Lanzani, Georgios Kardaras, and Deepak Boppana, “Remote Radio Heads and the evolution towards 4G networks.” Feb-2009.

[33] Alcatel Lucent, “The LTE Network Architecture: A comprehensive tutorial.” 2008.

[34] Y. D. Beyene, R. Jantti, and K. Ruttik, “Cloud-RAN Architecture for Indoor DAS,” *IEEE Access*, vol. 2, pp. 1205–1212, 2014.
[35] J. Huang, R. Duan, C. Cui, and I. Chih-Lin, “Overview of cloud RAN,” in *General Assembly and Scientific Symposium (URSI GASS), 2014 XXXIth URSI*, 2014, pp. 1–4.
[36] “Nokia SON for Mobile Backhaul Executive Summary | Nokia Networks,” *Nokia Solutions and Networks*. [Online]. Available: http://networks.nokia.com/.
[37] “Wiley: Self-Organizing Networks (SON): Self-Planning, Self-Optimization and Self-Healing for GSM, UMTS and LTE - Juan Ramiro, Khalid Hamied.” [Online]. Available: http://eu.wiley.com/WileyCDA/WileyTitle/productCd-0470973528.html.
[38] S. Hämäläinen, H. Sanneck, and C. Sartori, Eds., *LTE Self-Organising Networks (SON): Network Management Automation for Operational Efficiency*, 1 edition. Oxford: Wiley, 2012.
[39] “Self-Organizing Network (SON) | Nokia Networks,” *Nokia Solutions and Networks*. [Online]. Available: http://networks.nokia.com/.
[40] J. Wang and L. Dai, “Asymptotic Rate Analysis of Downlink Multi-User Systems With Co-Located and Distributed Antennas,” *IEEE Trans. Wirel. Commun.*, vol. 14, no. 6, pp. 3046–3058, Jun. 2015.
[41] M. K. Karakayali, G. J. Foschini, and R. A. Valenzuela, “Network coordination for spectrally efficient communications in cellular systems,” *IEEE Wirel. Commun.*, vol. 13, no. 4, pp. 56–61, Aug. 2006.
[42] N. Lee, D. Morales-Jimenez, A. Lozano, and R. W. Heath, “Spectral Efficiency of Dynamic Coordinated Beamforming: A Stochastic Geometry Approach,” *IEEE Trans. Wirel. Commun.*, vol. 14, no. 1, pp. 230–241, Jan. 2015.
[43] J. Joung, Y. K. Chia, and S. Sun, “Energy-Efficient, Large-Scale Distributed-Antenna System (L-DAS) for Multiple Users,” *IEEE J. Sel. Top. Signal Process.*, vol. 8, no. 5, pp. 954–965, Oct. 2014.
[44] H. Dahrouj and W. Yu, “Coordinated beamforming for the multicell multi-antenna wireless system,” *IEEE Trans. Wirel. Commun.*, vol. 9, no. 5, pp. 1748–1759, May 2010.
[45] S. Akoum and R. W. Heath, “Interference Coordination: Random Clustering and Adaptive Limited Feedback,” *IEEE Trans. Signal Process.*, vol. 61, no. 7, pp. 1822–1834, Apr. 2013.
[46] M. Sadeghzadeh, H. R. Bahrami, and N. H. Tran, “Clustered linear precoding for downlink network MIMO systems with partial CSI,” in *2013 International Conference on Computing, Networking and Communications (ICNC)*, 2013, pp. 479–483.
[47] K. Huang and J. G. Andrews, “An Analytical Framework for Multicell Cooperation via Stochastic Geometry and Large Deviations,” *IEEE Trans. Inf. Theory*, vol. 59, no. 4, pp. 2501–2516, Apr. 2013.

[48] A. Kumar, A. Mihovska, S. Kyriazakos, and R. Prasad, “Visible Light Communications (VLC) for Ambient Assisted Living,” *Wirel. Pers. Commun.*, vol. 78, no. 3, pp. 1699–1717, Jul. 2014.

[49] K. Sridhara, P. S. M. Tripathi, A. Kumar, A. Chandra, and R. Prasad, “Multi-users Participation in Bidding Process in a Congested Cellular Network,” in *Globalization of Mobile and Wireless Communications*, Springer Netherlands, 2011, pp. 203–221.

[50] L.-F. Research, D. Centre, Alex, er G. B. Building, T. U. of Edinburgh, K. ’s Buildings, M. Road, Edinburgh, E. 3jl, Scotl, and +44131 650 2766, “What is Li-Fi technology?,” *Lifi Research and Development Centre*. [Online]. Available: http://www.lifi-centre.com/about-li-fi/what-is-li-fi-technology/.

CHAPTER 5. ACTIVE PROBING AND SELF CONFIGURABILITY IN SCIDAS

This chapter elaborates the SCIDAS functionalities. This chapter complements Chapter 4 and proposes a holistic approach for solving the PTC^2 challenge. The research contributions are a continuation of the initially published findings in [1]. This shifts the network architecture paradigm from a conjectural approach to a definite approach. As we know from Chapter 4 the intelligent module, defined as *Network Intelligence Unit* (NIU), senses the network dynamics through the sensing layer of the SCIDAS architecture, defined as *Active Probing Management System* (APMS) [1]. This chapter elaborates the APMS architecture as a sub-architecture, its role in SCIDAS, and its functioning. In Chapter 4, we also introduced a set of mechanism, defined as Amoebic PTC^2 Response (APR) that can be executed by NIU to cater for the PTC^2 problem from its formation to dissipation. Here, we focus on the supporting algorithms of these mechanisms that, when executed by SCIDAS, would make it a *Self Configurable* network. We have shown a scenario of sensing the user accumulations, and execute apt procedures to manage them. Therefore, all algorithms are designed to work with the assistance of the APMS and are discussed as APMS-oriented procedures. This chapter complements Chapter 4 to have a holistic SCIDAS model to resolve the challenges that occur due to random and hefty accumulations.

5.1. INTRODUCTION

In [2] authors discuss diagnosing a large distributed networks in terms of interference localization by using a combination of online and offline active probing. [3] discusses active probing in Wireless Sensor Networks (WSNs), where, authors propose a strategy, using Genetic Algorithm (GA), to identify the right bud that could participate in monitoring the environment of the subject in the WSN. Usually, the active probing is understood as a 'live' monitoring of the system. However, in this chapter, by Active Probing (AcPro) we mean, a technique to monitor a system by sending a small signal and observe the variations produced in the system. Usually, the active probing is used to detect faults in the networks or estimation of the errors. In this chapter we use AcPro in the same way, what is being followed for space observation. Figure 5-1-1 shows an example of active probing, when environmental irregularities (error correction factor) are identified from the relected components of the prob signal that are collected by observing antennas. This is similar to imaging a distance star that needs to be observed by a ground-based observatory. To accommodate the blurredness caused due to scatterers, such as dust and clouds, in the intermediate path between star and aperture, a laser beam, as a probe signal, is sent in the sky to estimate the dust and

cloud density. Once, the 'scatterers' are known, the error is subtracted from the received image to have a clean picture of the distant subject. Later, in this chapter, we will see that the same strategy is used to monitor and estimate PTC^2 values at various locations of the SCIDAS network.

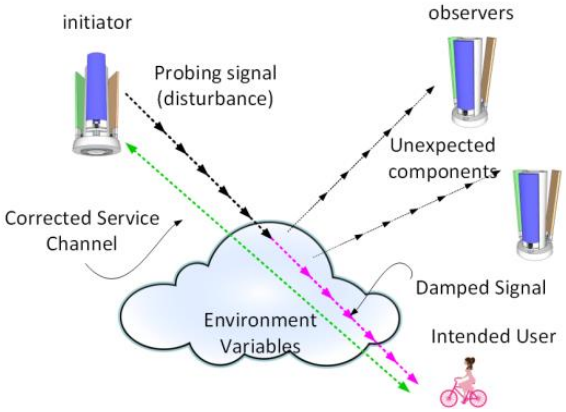

Figure 5-1-1: Active Probing technique

We will also discuss in this chapter that how SCIDAS will use its attributes to accommodate the wobbling, once we know the accumulations, in terms of both position and strength.

This Chapter is further organized as follows. **Section 5.2** elaborates the sensing attribute of the SCIDAS architecture, the Active Probing Technique, in terms of why we chose this technique, where it is accommodated in SCIDAS and how it performs the sensing. **Section 5.3** elaborates "how" by introducing some algorithms and explaining the way they are are executed. To support this aninnovative algorithm that enables SCIDAS to self-reconfigure and respond is proposed. **Section 5.4** proposes the algorithm Amoebic PTC^2 Response mechanism. **Section 5.5** concludes the chapter.

5.2. ACTIVE PROBING TECHNIQUE IN THE SCIDAS

The innovative SCIDAS architecture can impose extremely localised iterations based on the commands of a central controller, the NIU. We propose a sub-architecture of SCIDAS, namely, the *Active Probing Management System* (APMS) that is the core of the intelligent layer to identify the PTC^2 dynamics. In this section, first we discuss why, then what, and then, how, this intelligent sub-architecture acts in the SCIDAS system.

5.2.1. WHY: NEED FOR SENSING THE DYNAMICS

Let us consider a system, as shown in figure 5-2-1 that has an output Y(t) for an input X(t). We say that it as a responsive system since it gives an output for every input. Therefore, we can say that,

$$Y(t) = \Phi[X(t)] \tag{5.2.1}$$

Where $\Phi[.]$ is the response function of the system for an input X(t) [44]. Observing this system in discrete time steps is the same as imposing the system with discrete input values of X(t) such that:

$$X(t) = \{X(n) : n \in N\} \tag{5.2.2}$$

X(n), as a sample of an input signal, can be defined as:

$$X(n) = \int_{-\infty}^{+\infty} X(n-\tau)\delta(\tau)d\tau$$

or
$$X(n) = (X * \delta)(t = n) \tag{5.2.3}$$

Where, $\delta(\tau)$ is the impulse function at time τ and * is the convolution operator.

If this system is Linear Time Invariant (LTI), with an impulse response h(t), then, corresponding to the discrete inputs as mentioned in equation (5.2.3), the output Y(n) can be expressed as:

$$Y(n) = \int_{-\infty}^{+\infty} X(n-\tau)h(\tau)d\tau$$

or
$$Y(n) = (X * h)(n) \tag{5.2.4}$$

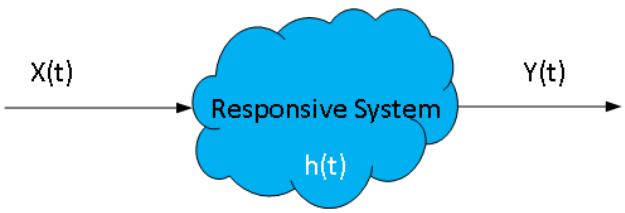

Figure 5-2-1: A responsive system with input, output and transfer function

Equation (5.2.4) is the standard way of expressing the output of an LTI system. This system ought to behave according to the above equation due to the linear and

time invariant nature of the impulse response. This somehow reflects the internal nature of the system, which, as per observation, is either an inevitably invariant system or conducively dynamic to produce favourable output. In either case, h(t) is a convenient impulse response to accompanying the input function.

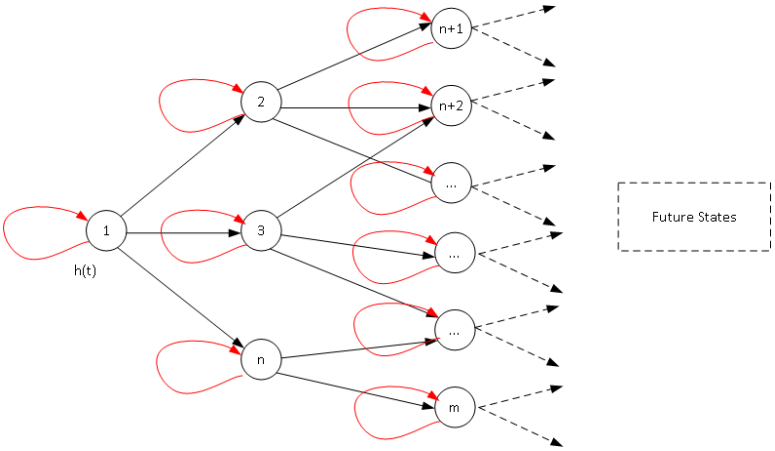

Figure 5-2-2: State diagram of impulse responses in Place-Time influence

Now, for the sake of the present discussion, if we assume that this responsive system is internally subjected to some unfavourable actions so that the LTI behaviour turns into a random nature, the impulse response h(t) will not be consistent. Hence, the response of the system at time t_1 will not be same at time t_2 for the same input sequence. Therefore,

$$h(n)|_{t_1} \neq h(n_k)|_{t_2} \tag{5.2.5}$$

Therefore, equation (5.2.4) will not be a valid statement for such situations. It is important to mention here that equation (5.2.5) does not mean that the system intrinsically is a non-LTI system; rather the system is pseudo-invariant when the stimulant is absent. Therefore, h(t), depending upon the stimulant's nature, can choose a state of invariability till the nature of stimulant varies. Figure 5-2-2 shows this hopping nature of h(t) from one state to another, where h(t) may transit from one state to another (as represented by black arrowhead lines) or can remain in the same state (as represented by red arrowhead curves). The arrowhead represents the next state, and the tail represents the present state. For a set of discrete observations, h(t) can be represented as a time and sample based transition matrix as below, where rows represent time stamp and column represents a sample.

$$h(n,t) = \begin{matrix} h_{11} & h_{12} & h_{13} & \dots & h_{1n} \\ h_{21} & h_{22} & h_{23} & \dots & h_{2n} \\ h_{m1} & h_{m2} & h_{m3} & \dots & h_{mn} \end{matrix}$$

An MWCN, with all of its components, can be viewed as an LTI system as shown in figure 5-2-1. Therefore, the variations in the response function of such systems from time to time, show ostentaniety in the network behaviour.

Let, X(t) be the function of calls generated at a time 't' and Y(t) is the network health status at the same time. The health status corresponds to one or multiple of parameters of the following:

(i) Total call fails (call did not initiate) of the network
(ii) Total call drops in the network (call initiated but dropped)
(iii) SINR status with respect to all BSs in the network

(i) and (ii) are the parameters that correspond mainly to the *Network Congestion* meaning that all the channels of a BS are occupied in various services in which a subscriber is making a call. The parameter (ii) above corresponds to cases when either subscriber is in motion and tries to handover in a congested BS or the signal strength of the serving BS is dropped below R_x sensitivity. The parameter (iii) above corresponds to the interference status of a network and reflects the signal strength ratios of the dominant server to its neighbours. Such measurements will not be consistent due to the dynamic nature of the subscribers. Sometimes the huge accumulation beneath a serving cluster of the BSs can congest these BSs quite significantly, and deteriorate the overall network health report. Hence, equation (5.2.4) cannot describe the network in a broader scope. Although, the total capacity demand and coverage demand of the system as a whole may be consistent throughout these variations, but the way the system challenges are permutated, is the cause that most systems would behave inefficiently, thereby, increasing the computational cost and lowering the system efficiency. The demands, in such conditions, are served with some delay or never served at all. Therefore, an independent layer to detect the PTEs is required to be a part of the SCIDAS architecture. The concept of APMS sub-architecture is proposed to fulfill this requirement. As discussed in Chapter 4, the proposed SCIDAS architecture is deliberately designed in layered form. This means that each of the attributes of SCIDAS, namely, infrastructure, service, intelligence, and probing coexist as independent layers. This enables SCIDAS to modify any of its layers without affecting others, unlike present state-of-the-art where even the civil infrastructures are impacted during technological upgrades. Further, by the virtue of WDM, the intelligence (NIU) and sensing (APMS) can disseminate parallelly and simultaneously across the network without utilising the network resources (such as paging and broadcasting). The ***independent feature*** APMS, under the control of

NIU, allows for monitoring the entire PTC[2] related activity continuously without imposing any burden on the service layer(network resources).

5.2.2. WHAT: THE SYSTEM MODEL

Figure 5-2-3 shows the time ustilised at the various stages of the APMS sub-architecture, residing within SCIDAS architecture. APMS can use either normal service antenna or separate series of top mounted omnidirectional antennas to monitor and triangulate the PTC[2] wobbels, as shown in figure 5-2-3.

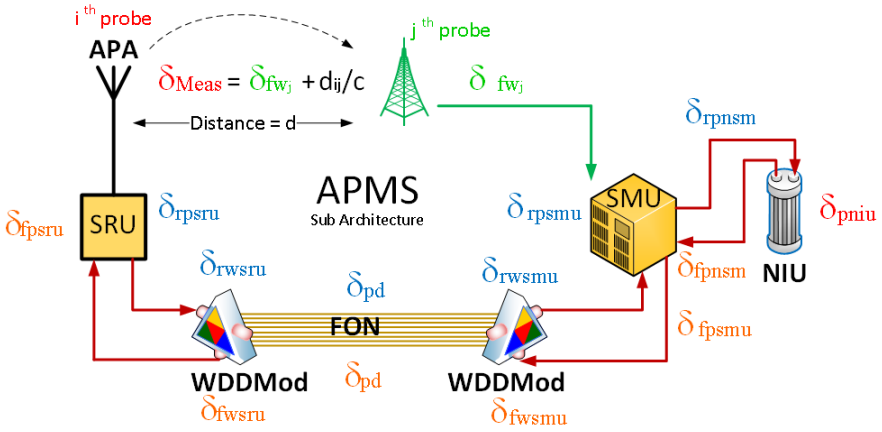

$$t_{repeat} \geq \delta_{meas} + \delta_{rpsru} + \delta_{rwsru} + \delta_{pd} + \delta_{rwsmu} + \delta_{rpsmu} + \delta_{rpnsm} + \delta_{fpsru} + \delta_{fwsru} + \delta_{pd} + \delta_{fwsmu} + \delta_{fpsmu} + \delta_{rpnsm} + \delta_{pniu}$$

Figure 5-2-3: APMS System Model

In figure 5-2-3, the time consumed during the APMS process is also shown. Conventionally, the signal flow from the NIU to APA is considered as a forward path and, similarly, the reverse path for vice versa.

(i) δ_{meas} :Time needed for a signal tap (single set of measurement),
(ii) δ_{rpsru}/ δ_{fpsru} : Processing time of SRU for the reverse/ forward path,
(iii) δ_{rwsru}/ δ_{fwsru} : Time consumed in converting and sending the RF signal to Optical by the *Wavelength Division Demodulator & Modulator* (WDDMod) for the reverse/ forward path at SRU end,
(iv) δ_{pd} : Path delay during signal flow between a distant SRU to SCIN,
(v) δ_{rwsmu} / δ_{fwsmu} : Time consumed the *Wavelength Division Demodulator & Modulator* (WDDMod) for the reverse/ forward path at SMU end,
(vi) δ_{rpsmu} / δ_{fpsmu} : Processing time of SMU for the reverse/ forward path,

(vii) δ_{rpnsm} / δ_{fpnsm} : Delay between SMU and NIU due to system architecture (included to accommodate the limit of the processing time) for the reverse/ forward path, and,

(viii) δ_{niu} : Processing time of NIU.

Hence, the iteration time, t_{repeat}, must be larger than the sum of all the latent times needed for the information flow and the processing, given in equation (5.2.6).

$$t_{repeat} \geq \delta_{meas} + \delta_{rpsru} + \delta_{rwsru} + 2\delta_{pd} + \delta_{rwsmu} + \delta_{rpsmu} + \delta_{rpnsm} + \delta_{niu} + \delta_{fpnsm} + \delta_{fpsmu} + \delta_{fwsmu} + \delta_{fwsru} + \delta_{fpsru} \quad (5.2.6)$$

This system model is considered while describing the working of the system, discussed in section 5.2.3.

5.2.3. HOW: WORKING OF THE APMS ARCHITECTURE

The purpose of APMS is to sense the PTC[2] and Spectrum Occupancy 'Ω'. This is done by two methods defined here as SILENT PROBING and, *WHISPER & LISTEN PROBING.* In this subsection, it will be discussed how the knowledge of Ω helps to generate the Carrier Pool 'Φ' and to pull off the unutilised spectrum from the system. The SRU with the MCP system at the remote ends are termed as Remote Buds (RBs), and each sector in an SRU, that participates in the APMS is termed as probes. Figure 5-2-4 shows a SCIDAS network provisioned with an APMS sub-architecture having 'S' subscriber mobile equipment (ME), 'M' SRUs, and 'N' probes with an APMS antenna, such that, N= M ×number of sectors in each SRU.

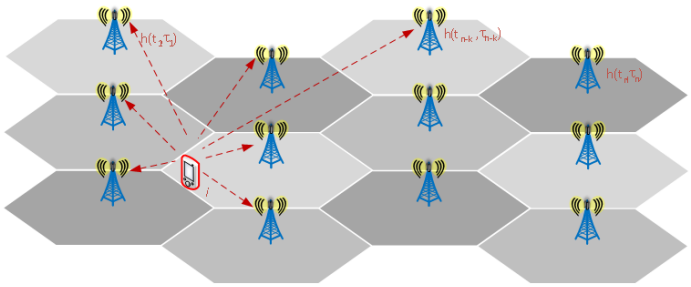

Figure 5-2-4: Listening by APMS Sub-Architecture in an SCIDAS Network.

(i) *SILENT PROBING METHOD (SPM)*: In SPM, the APMS listens to the received signals from the users analysis by tapping the signal samples at each APMS Antenna (AAN). The spectrum scanning is done at each APMS bud (antenna) starting from the least frequency carrier to the

highest frequency carrier. The measurement can start simultaneously or sequentially at all APMS buds depending on the need. [5] described the APMS system in a realistic scenario, which is also detailed in Chapter 6 of this thesis. As APMS only listens to the arriving signals, the method is defined here as *SILENT PROBING METHOD*. Through SPM, a holistic view of the subscriber distribution is attained by recording the arriving signal periodically at each AAN.

(ii) *WHISPER AND LISTEN METHOD (WHISLME)*: In this method, the APMS sends a short duration signal burst from each AAN, which creates a disturbance in the existing network condition. The response of the network environment is then observed by each AAN. This method is performed when the SPM method is not efficient enough. The capability of the APMS to analyse the environment by impinging the disturbance in the subject itself is the reason of nomenclaturing this method as ACTIVE PROBING. By the virtue of SCIDAS's intelligent architecture, the intelligent selection can be performed conveniently, and the APMS would perform measurements both actively and passively in a simultaneous, sequenced and scheduled manner. For the WHISLME process, the service antennas can also be used to utilise the directivity advantage for exclusivity of the measurements.

It is important to mention here that the APMS system can perform all CME measurements in the frequencies that may or may not belong to the licensed or unlicensed bands. Therefore, a lot of network resources can be saved by shifting the PTC^2 estimation to the out-of-band domain. This is one of the biggest advantages of using a separate system for catreing the environmental irregularities.

Through APMS, the sequential and targetted measurements leads to creating a holistic picture of the network environment. The biggest advantage of APMS system is that it provides a global view of the variations at all locations of the network without utilising the real network resources (such as paging and piloting).

The next section will elaboratly describe the proposed supporting algorithms.

5.3. ALGORITHMS: PROCEDURAL APPROACH IN MANAGING PTC^2

This section discusses the SCIDAS approach, in terms of algorithms, to cater for the PTC^2 challenges. We will see how SCIDAS identifies the wobble and then iteratively re-configures the resource distribution for smooth transition of the accumulations. Arranging these algorithms in a systematic way, as discussed in the next section, leads to the complete APR mechanism that is discussed in section 5.4 of this thesis.

The APMS capitalises the channel impulse response of a network environment. If a signal burst is injected into a channel medium, the channel impulse response is the summation of the signals arriving through multiple paths, and can be written as:

$$h_{ij}(t_{ij}, T) = \sum_{g=1}^{N_{ij}} A_{ijg}\delta(t_{ij} - T_g)e^{-j\theta_g} \qquad (5.3.1)$$

Where h_{ij} is the response function between i^{th} initiator probe and j^{th} receptor Probes, A_{ijg} is the amplitude of g^{th} component of the signal generated by i^{th} probe and received by j^{th} probe at time T_g [6] (see, figure 5-3-1).

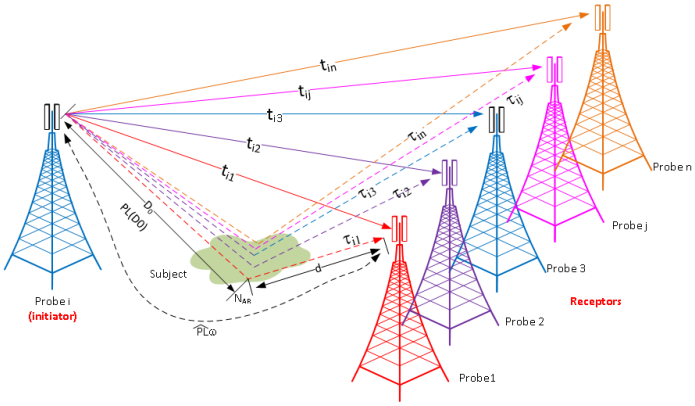

Figure 5-3-1: Active Probing in an SCIDAS: Time Domain

The signal burst, initiated by the i^{th} probe can be received by all probes with some delay, as shown in figure 5-3-2. As these components would arrive after dealing with the network environment, they would contain information about the network composition. For the present discussion, the first two components of the signals, denoted by t and τ, are considered to be recorded by all probes. In the SCIDAS architecture, the RNs are normally low-powered and are closer to than in the usual network sites. Hence, it is assumed that each probe antenna can "see" its neighbours, and, therefore, the first component that arrives after a delay of t_{ij} seconds is considered as a direct signal and the next tap that arrives after a delay of τ_{ij} seconds is the reflection from the subject.

Through MCP, the AANs can be maneuvered and re-oriented in both horizontal and vertical azimuths, therefore, as shown in figure 5-3-2, a subject of interest can be illuminated by any probing antenna (AAN) through minor adjustments. This is required when the PTC^2 needs to be followed, and only a specific portion the covered area is the subject of interest.

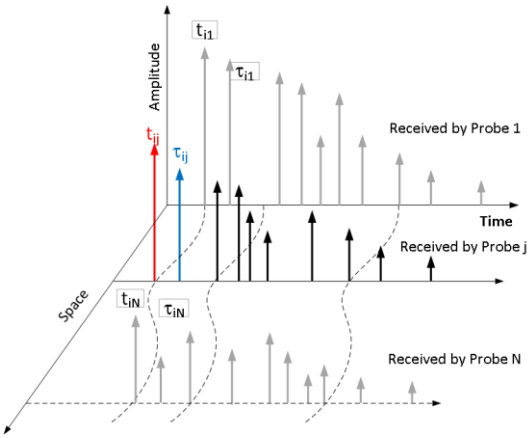

Figure 5-3-2: Channel Response of a signal burst

As mentioned earlier, the prime purpose of the APMS is to estimate the PTC[2] in an SCIDAS network. Both SPM and WHISLME generate a channel matrix, mentioned in (5.3.2) as (see, figure 5-2-4):

$$\begin{pmatrix} \Psi_1 \\ \Psi_2 \\ \Psi_3 \\ .... \\ \Psi_R \end{pmatrix} = \begin{pmatrix} \mathbf{h_{11}} & \mathbf{h_{12}} & \mathbf{...} & \mathbf{h_{1T}} \\ h_{21} & h_{22} & ... & h_{2T} \\ h_{31} & h_{32} & ... & h_{3T} \\ ... & ... & ... & .. \\ ... & ... & ... & \\ h_{R1} & h_{R2} & ... & h_{RT} \end{pmatrix} \begin{pmatrix} \xi_1 \\ \xi_2 \\ ... \\ \xi_T \end{pmatrix} + \begin{pmatrix} \xi_1 \\ \xi_2 \\ \xi_3 \\ ... \\ ... \\ \xi_R \end{pmatrix} \tag{5.3.2}$$

and, can be translated in equation form as mentioned in (5.3.1) given below [7]:

$$\boldsymbol{\Psi = H\chi + \xi} \tag{5.3.3}$$

Where $\boldsymbol{\psi}$ is the receive vector, $\boldsymbol{\chi}$ is the transmit vector and, $\mathbf{H=[}h_{ij}\mathbf{]}$ is the channel matrix and is the $\boldsymbol{\xi}$ noise vector such that:

- R is the number of receiving probes,
- T is the number of transmitting probes,
- $\boldsymbol{\Psi}$ is the received signal vector (values measured by APMS)**,**
- $[h_{ij}]_{R\times T}$ is the complex channel matrix,
- $\boldsymbol{\chi}$ is the transmit signal vector (transmit signals),

- h_{ij} is the channel coefficient between i_{th} base station and j_{th} ME, and,
- ξ is the additive Gaussian noise with covariance of $\mathbf{I}\sigma^2$.

In a varying condition, however, the channel matrix-vector H is also a varying entity. Hence, it is almost impossible to solve equation (5.3.3) in a PTC^2 condition. Hence, the first step towards solving equation (5.3.3) is to find **H**.

5.3.1. WHISPER AND LISTEN METHOD (WHISLME)

In the WHISLME procedure, the APMS uses the intelligence of SCIDAS for its antennas to perform in all modes such as MIMO, MISO, SIMO, and SISO by selecting single or multiple antennas to participate during the operation. To identify the fading between i^{th} transmitter and j^{th} receiver, the SCIDAS allows APMS to operate in SISO mode where the i^{th} activity is heard by all other probes one-by-one at distinct times. The data can be obtained through WHISLME algorithm given below as:

Steps	Function	Description
BEGIN **WHISLME(T,R,D,γ)**		// **T** is the set of Transmitters (T_x), **R** is the set of Receivers (R_x), neighbours distance **D**, and *stamp type* **'γ'**
1	i, j←1;	// *variables are initialised*
2	While **(** i ≤ |**T**|) do	// *perform till i reaches number of T_x elements in **T***
3	Whisper (T_i) = χ_i ;	// *i^{th} probe of set T sends a burst* χ_i **; use eq. (5.3.1)**
4	While (j ≤ |**R**|) do	// *perform till j reaches number of R_x elements in **R***
5	If ($TDO_{ij\gamma}$= True) then	// *limiting the number of neighbors;* ***see, (5.3.22)***
6	Listen(R_{ij}) = Ψ_{ij} ;	// *j^{th} probe records the R_x signal from i^{th} probe*
7	$[m_{ij}]_{T\times R}$ = Ψ_{ij} /χ_i ;	// *calculating the loss between i and j*
8	Else goto next step	// *jump when the number of neighbours exceed*
9	j←j+1; *Else Step 8*	// *condition of terminating While j ≤ |**R**|*
1	Wait (t_{repeat});	// *Wait before next iteration (see, figure 5-2-3)*
1	j←1;	// *initialize the R_x probe count*
1	i←i+1; *Else Step 11*	// *preparing next probe to whisper*
1	i, j←1;	// *reset variables (to avoid conflicts in multiple use*
3		*of same variables)*
END **WHISLME($[M]_{T\times R}$)**		// *output matrix ; Algorithm terminates*

(5.3.4)

The matrix M obtained through (5.3.4) can be in two domains, time, and position. The time –domain decomposition is expressed by M=λ and the iterations are in the time domain and, therefore $m_{ij}(t) = \lambda_{i,j,t}$.

The $\lambda_{i,j,t}$ represents the measurement performed in terms $\boldsymbol{\Psi_j / \chi_i}$ where $\boldsymbol{\chi_i}$ is the transmitted signal from the i^{th} probe, and $\boldsymbol{\Psi_j}$ is the signal received at the j^{th} probe at any time t. Therefore measuring λ at various time intervals shall provide datapoints as given below:

$$(\lambda_{i_1,j_1,t_1}, t_1), (\lambda_{i_2,j_2,t_2}, t_2), (\lambda_{i_3,j_3,t_3}, t_3), \square, (\lambda_{i_\tau,j_\tau,t_\tau}, t_\tau)$$

$$\text{or,} \quad (\lambda_1, t_1), (\lambda_2, t_2), (\lambda_3, t_3), \dots, (\lambda_\tau, t_\tau) \tag{5.3.5}$$

Considering the incidences happening in the time domain, the dynamics can be expressed as a τ-1 degree polynomial function mentioned below [8] [9]:

$$\lambda_{i,j,t} = a_{ij\tau} t^{\tau-1} + a_{ij\tau-1} t^{\tau-2} + \dots + a_{ij1} t^0 \tag{5.3.6}$$

To obtain the function out of measured values, the coefficient 'a' is needed to be obtained. The matrix equation for the expression (5.3.6) describes the channel matrix as a time-dependent entity λ and correspondingly the coefficients are obtained. Later the same will be derived for the position-dependent channel matrix. The two components shall be used to describe both position and time dependent variations in the system. The time variant channel matrix can thus be described as:

$$\begin{pmatrix} t_1^{\tau-1} & t_1^{\tau-2} & t_1^{\tau-3} & \dots & t_1 & 1 \\ t_2^{\tau-1} & t_2^{\tau-2} & t_2^{\tau-3} & \dots & t_2 & 1 \\ \dots & \dots & \dots & \dots & \dots & 1 \\ t_\tau^{\tau-1} & t_\tau^{\tau-2} & t_\tau^{\tau-3} & \dots & t_\tau & 1 \end{pmatrix} \begin{pmatrix} a_\tau \\ a_{\tau-1} \\ \dots \\ a_1 \end{pmatrix} = \begin{pmatrix} \lambda_1 \\ \lambda_2 \\ \dots \\ \lambda_\tau \end{pmatrix} \tag{5.3.7}$$

The coefficient can thus be determined as per below [10] [11]:

$$\begin{pmatrix} a_\tau \\ a_{\tau-1} \\ \dots \\ a_1 \end{pmatrix} = \begin{pmatrix} t_1^{\tau-1} & t_1^{\tau-2} & t_1^{\tau-3} & \dots & t_1 & 1 \\ t_2^{\tau-1} & t_2^{\tau-2} & t_2^{\tau-3} & \dots & t_2 & 1 \\ \dots & \dots & \dots & \dots & \dots & 1 \\ t_\tau^{\tau-1} & t_\tau^{\tau-2} & t_\tau^{\tau-3} & \dots & t_\tau & 1 \end{pmatrix}^{-1} \begin{pmatrix} \lambda_1 \\ \lambda_2 \\ \dots \\ \lambda_\tau \end{pmatrix} \tag{5.3.8}$$

Equation (5.3.8) says that the coefficients are obtainable for a given set of observations, and so a generic equation representing z observations can be formulated as:

$$\lambda_{i,j}(t,z) = a_{ijz}t^{z-1} + a_{ijz-1}t^{z-2} + \ldots + a_{ij1}t^{0} \quad (5.3.9)$$

The complete matrix of time-variant channel matrix λ can be described as:

$$[\lambda_{ij}]_{T\times R}(t,z) = \sum_{k=1}^{z} a_{ijk}\, t^{k-1} \quad (5.3.10)$$

Where, z is the variable on which λ is evaluated and, t is the variable of which the λ is a function matrix. As mentioned earlier, it is assumed that these variations in λ are due to variations in the user position casing variations in long term fading of the channel. Hence,

$$\frac{d}{dt}[\lambda_{ij}]_{N\times N}(t,z) = rate\ of\ variations\ in\ time\ domain \quad (5.3.11)$$

Similarly, the position domain decomposition can be achieved by relating the matrix with measurements performed in the position domain rather than the time domain. Therefore, setting M=σ, ϕ =p, ϕ_l =N, and $m_{i,j,t}$ = $\sigma_{i,j,t}$.. To avoid the complexity in 2-dimensional coordinates to a single dimension, the position is expressed in terms of bud position (total buds =N). The position variant channel matrix can thus be described as:

$$\sigma_{i,j}(p,N) = b_{ijN}p^{N-1} + b_{ijN-1}p^{N-2} + \ldots + b_{ij1}p^{0} \quad (5.3.12)$$

The complete matrix of the position-variant channel matrix σ can be described as:

$$[\sigma_{ij}]_{N\times N}(p,N) = \sum_{k=1}^{N} b_{ijk}\, p^{k-1} \quad (5.3.13)$$

Where, t and z are the variables on which σ is evaluated. As mentioned earlier, it is assumed that these variations in σ are due to the variations in the user position casing variations in fading of the channel.

$$\frac{d}{dt}[\sigma_{ij}]_{N\times N}(p,N) = rate\ of\ variations\ in\ position\ domain \quad (5.3.14)$$

As mentioned in the 3.5.19 (see, section 3.5.3 of Chapter 3 of this thesis), the place time depended must accommodate both the place and time dependent variations. Therefore, place time variant matrix H can thus be defined as:

$$H^{est} = (U\ \lambda)(W\ \sigma);\ \ h_{ij} = \ (u_{ij}\lambda_{ij}(w_{ij}\ \sigma_{ij}) \tag{5.3.15}$$

5.3.2. CHANNEL MATRIX ESTIMATOR (CME)

Here, we define an algorithm *Channel Matrix Estimator* (CME) that uses WHISLME to identify the elements of H. The CME thus, can be described as compound algorithm containing two steps, the first one obtaining the data and the second one estimating the matrix.

This algorithm uses WHISLME to observe the channel matrix at various stamps of the observation. The stamps can be regular or irregular time instances or positions within the AoI. The **CME** algorithm is described in algorithm 5.3.16 and generates the estimated channel matrix for a given set of Transmitters (T_xs) **T**, set of Receivers(R_xs) **R**, set a total number of stamp C.

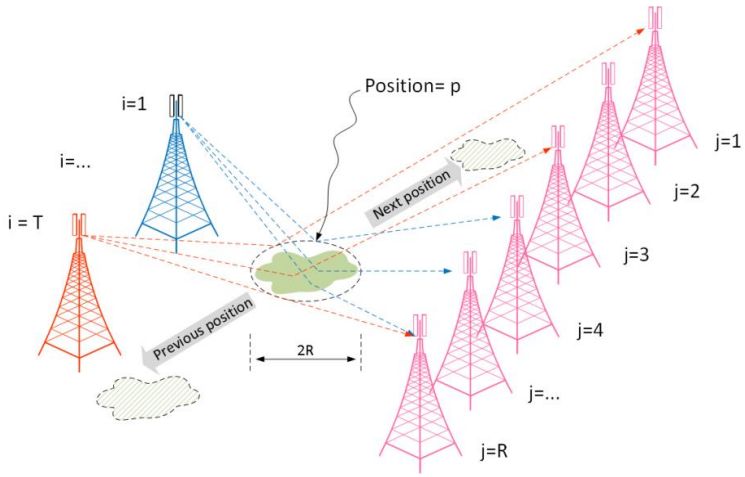

Figure 5-3-3: Active Probing in an SCIDAS: Position Domain

Steps		**Function**	Description
BEGIN CME(R,T,D,C,γ)		*// Set of R_xs & T_xs* **R** ,**T**, *Distance* **D,** *Stamp domain* **C,** *stamp type* **γ**	
1		BEGIN: ACTIVE PROBING TECHNIQUE	*STARTING APT Sub-Algorithm*
2	A1	u, v←1; ω ← 1	*// variables initialised*
3	A2	While (ω ≤ C) do	*//condition for stamps (time or position)*
4	A3	**WHISLME**(T,R,D,M)	*//create measured Matrix at a stamp ω*
5	A4	While (u ≤ |**T**| **)** do	*//do for all elements in set of T_xs **'T'***
6	A5	While (v ≤ |**R**| **)** do	*//do for all elements in set of R_xs **'R'***
7	A6	k← (u-1)R +v	*//2-Dim R×T vector→ 1-Dim vector **'K'***
8	A7	$[\Delta_{\omega k}]_{C\times(T\times R)} \leftarrow [m_{uv}]_{T\times R}$;	*//Matrix with measurement v/s stamps*
9	A8	v←v+1; Else **Next Step (M9)**	*// next R_x; looping condition for **A5***
10	A9	Wait (t_{repeat});	*//breathing period **(see, section 5.2.2)***
11	A10	v←1;	*// Intitailising R_x count for next iteration*
12	A11	u←u+1; **Else Next Step (A12)**	*// Next T_x; looping condition for **A4***
13	A12	j ←1;	*// initialization for stamp matrix*
14	A13	While (j ≤ C) do	*// for creating '**t**' matrix**(see, eq. 5.3.8)***
15	A14	$[TT_{\omega j}]_{C\times C} \leftarrow \omega^{C-j}$;	*// assigning values to each element of '**t**'*
16	A15	j←j+1; **Else Next Step (A16)**	*// looping condition for **A13***
17	A16	u←1;	*// Intitailising T_x count for next iteration*
18	A17	ω ← ω +1; **Else END APT**	*// Next Stamp; looping condition for **A2***
19		END: ACTIVE PROBING TECHNIQUE	*ENDING APT Sub-Algorithm*
20		BEGIN: MATRIX EVALUATION	*STARTING ME Sub-Algorithm*
21	C1	ω, i, j, k ←0;	*// variables initialised*
22	C2	While (i ≤ |**T**|) do	*//considering all Transmitters*
23	C3	While (j ≤|**R**|) do	*// considering all Receivers*
24	C4	k← (i-1)R +j;	*// representing T-R in single dimension*
25	C5	While (k ≤ T×R) do	*// representing T-R in single dimension*
26	C6	While (ω ≤ C) do	*// considering all stamps*
27	C7	$\lambda_{\omega k} \leftarrow [\Delta_{\omega k}]$;	*// assigning measurements to estimator*
28	C8	ω ← ω+1; **Else Next Step (C9)**	*// next stamp*
29	C9	$[a_{\omega k}]_{C\times(T\times R)} = TT^{-1}\,[\lambda_{\omega k}]_{C\times(T\times R)}$;	*// evaluating coefficients **(eq. 5.3.8)***
30	C10	$[\Pi_{ij}(tt)]_{T\times R} = \sum_{z=1}^{C} a_{zk}\, tt^{C-\omega}$	*// evaluating Channel Matrix **(eq. 5.3.9)** elements.*
31	C11	j ←j+1; **Else Next Step (C12)**	*// next R_x is selected for evaluation*
32	C12	i ←i+1; **Else END ME**	*// next T_x is selected for evaluation*
33		END: MATRIX EVALUATION	*ENDING ME Sub-Algorithm*
END CME(Π(tt))		*// ouput matrix* **Π** *with stamp type variable* **'tt'**	

(5.3.16)

Table 5-3-1: list of symbols used in CME algorithm.

1	T	: the set of those probes (or sector-buds if the service antenna is chosen as AAN) that are chosen by SCIN through logical addressing to perform transmit function. It is important to note that, to avoid unnecessary calculations, only specific transmitters can be chosen where the probability of wobbling is likely to happen. T includes all such transmitters.
2	u	: the variable that counts until the number of elements in T (count of elements) denoted here as |T|
3	R	: the set of those probes (or sector-buds if the service antenna is chosen as AAN) that are chosen by SCIN through logical addressing to perform receive function. All transmitters may not perform receive functions and vice-versa, hence receiving probes may be different from those who are chosen in T. Thus, a different set R is chosen to incorporate receivers.
4	v	: the variable that counts until the number of elements in R (count of elements) denoted here as |R|
5		addressing : the logical address that is used by SCIDAS intelligence to choose a particular SRU. This is an essential and imminent feature of SCIDAS where a simple DAS network becomes a selective network.
6	k	: the variable that denotes a pair of i^{th} transmitter and j^{th} receiver. As the measurement's belongingness is the with the T-R pair, it will be appropriate if this pairing is numbered sequentially as it is easier to deal with a two-dimensional matrix by reducing i-j plane to a single dimensional counting. Transforming the i-j plane to a linear numbering is done is similar to counting squares on the chess board with i and j representing row and column respectively using the formula in A6 of (5.3.16).
7	$\boldsymbol{\gamma}$	(Stamp type) is a dimension in which the iterations of measurements are performed. If the stamp type is time, then the measurement is performed at certain time intervals. Like t=1,2,3 seconds and if it is of type 'position', then measurements in performed in certain iterative positions like position1,2, 3 etc.
8	$\boldsymbol{\gamma}$	: the variable that represents stamp type.
9	**C**	: the number of iterations needs to be performed to accomplish measurements.
10	ω	: the variable that counts until a number of iterations, 'C', is complete.
11	**M,** $\mathbf{m_{ij}}$	: the output of a matrix containing measurement performed with a single set of active probing by WHISLME. m_{ij} is an element of M that has measurement when i has transmitted, and j has received the probing signal.

12	$[\Delta_{\omega k}]$	: the matrix that holds the information obtained by all WHISLME iterations. $\Delta_{\omega k}$ is the element of the matrix that holds information obtained at ω^{th} iteration and between k^{th} i-j pair (see, 6 in this list of symbols).
13	**TT**	: the stamp-type matrix as in equations (5.3.7) and (5.3.8). The purpose is to estimate the degree of function which represents the wobbling pattern between any k pair.
14	$TT_{\omega j}$	: the element of $[TT_{\omega j}]$ or TT, that that presents n^{th} degree for the variable type see, A14 of (5.3.16). TT only depends on iteration parameters C and ω.
15	$\lambda_{\omega k}$	: the element of $[\lambda_{\omega k}]$ that holds the value of $[\Delta_{\omega k}]$. This is a copy of $[\Delta_{\omega k}]$ and protects the precious measurement set $[\Delta_{\omega k}]$ from getting altered accidently. Moreover, a different variable λ is chosen to match with equations from (5.3.2) to (5.3.11).
16	$a_{\omega k}$	: the coefficient matrix for ω^{th} iteration and k^{th} i-j pair. To satisfy equation (5.3.8), both $a_{\omega k}$ and $\lambda_{\omega k}$ are evaluated column-wise in such a way that each column of both $[a_{\omega k}]$ and $[\lambda_{\omega k}]$ holds common k, and therefore, evaluates for all iterations of a particular i-j pair 'k'.
17	$[\Pi_{ij}(tt)]_{T\times R}$	: the output matrix with each element $\Pi_{ij}(tt)$ representing the variations in the subject area between i-j pair in the form of a function of stamp type tt. Each element $\Pi_{ij}(tt)$ is obtained as in equation (5.3.10). It is important to note that equation (5.3.10) is for one T-R pair and $[\Pi_{ij}(tt)]$ is obtained by performing the process for all T-R pairs measurements, and therefore, the size of $[\Pi_{ij}(tt)]$ is T× R.

The CME algorithm generates an estimated matrix with respect to the type of stamps used for obtaining the measurements. This relates the channel matrix as a function of the stamp, the time-stamp, and the position stamp. The time domain estimation is shown in figure 5-3-1. Figure 5-3-3 shows the position domain measurements. In the time domain, a time interval is chosen for a set of transmitters and receivers to perform another set of observations, similarly, in the position domain measurement, a position or subject is chosen to perform one set of observation. The sequence of these observations will create a position-dependent channel matrix that eventually will imitate the subscriber distribution in the locus of the path created by integrating the discrete positions. The position based measurement is essential in the case when the users do not move from one place to another and rather come closer thereby, creating an additional loss in the measurement values. This will not be noticed by the time-based iterations when the measurements are done in a short interval.

In figure 5-3-3, we can see that the position based measurements can be used to follow the accumulation path. For analysing the locus of the positions, a distribution of the gathering can be generated. Therefore, while in the time-domain a single location is measured iteratively multiple times to obtain a time-based function, the position domain measurement is generated by observing positions in a process to obtain a position based function of distributions. Next, we analyse the efficiency of the CME algorithm regarding its response time and its utility in network dimensioning.

CME Efficiency Analysis: The CME algorithm is an essential process of understanding the network environment for the intelligent system to deal with. This algorithm can present the environment behaviour at various spot (number of spots defining the complexity in calculations) as a function of the place and time. The H^{est} may not present the exact environmental conditions, however; the rate of change in H^{est} definitely gives an estimation of an influx or outflux to/ from the spot. Undoubtedly, this is an initial stage of evolving any such response algorithm and has an ample scope of redefining and improvising the efficiency, accuracy, and applicability in future works. Figures 5-3-4 to 5-3-11 show the efficiency of the CME algorithm for a network with 500 buds. For the calculation, the buds were deployed as shown in figure 5-3-13 and the inter-bud distance was set to be 200m. The performance is judged on the machine having Intel Core i7-4960X processor, with Nvidia GTX 970 graphics card (248 frames per second), Crucial M4 128GB drive (max speed 316 MB/s) and Random Access Memory (RAM) with 44.9 GB/s speed. These specifications are important as the time of the calculations depends hugely on the processor at the NIU.

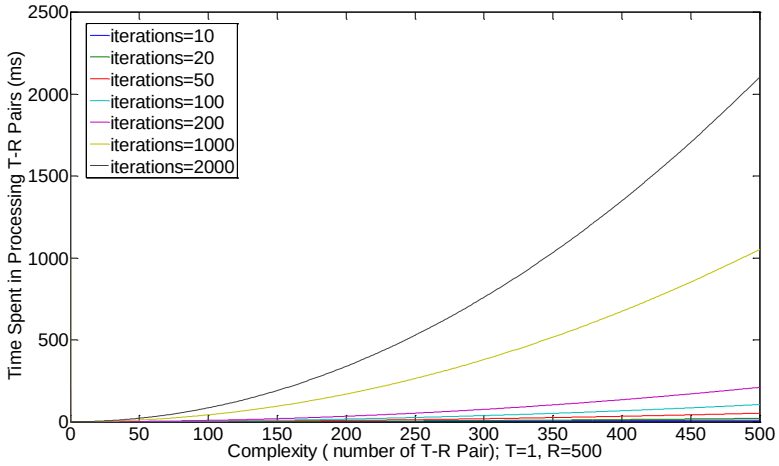

Figure 5-3-4: CME response time for the complexity of 1 Transmitters pairing with all 500 Receiver buds

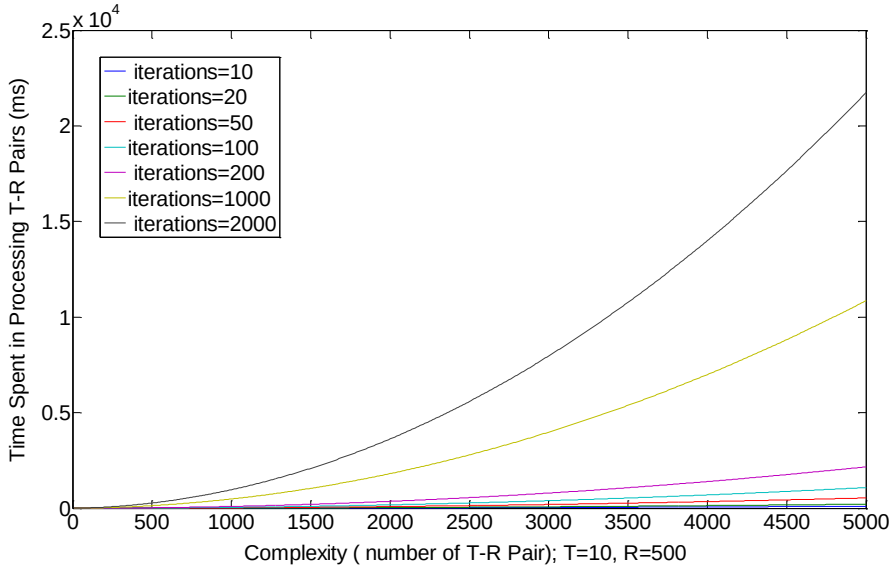

Figure 5-3-5: CME response time for the complexity of 10 Transmitters pairing with all 500 Receiver buds (1to 500)

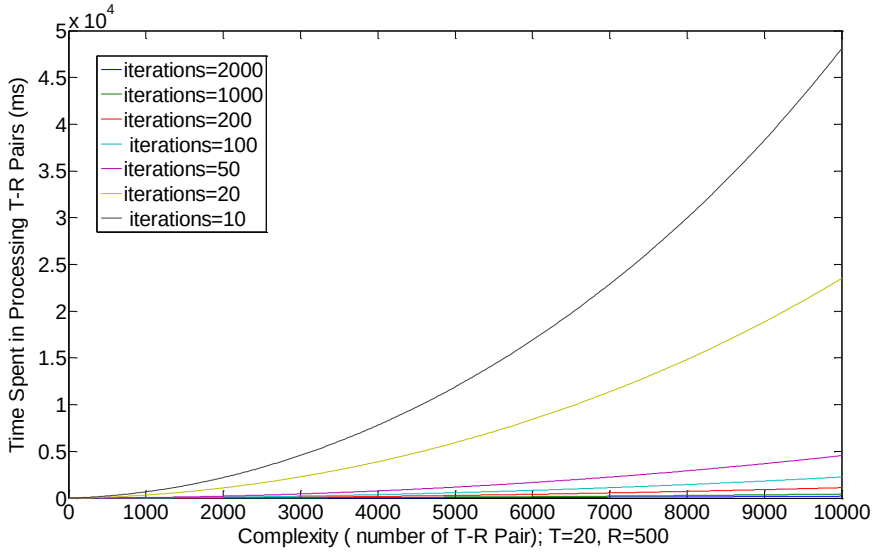

Figure 5-3-6: CME response time for the complexity of 20 Transmitters pairing with all 500 Receiver buds (1to 500)

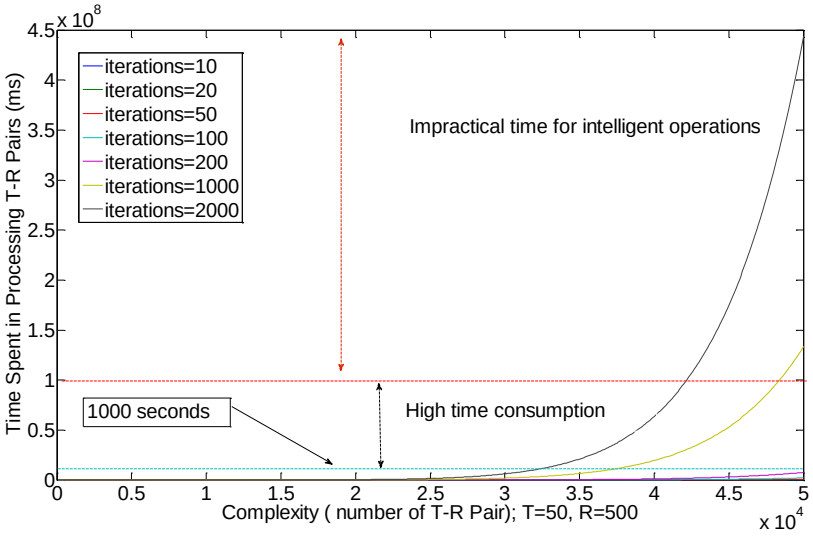

Figure 5-3-7: CME response time for the complexity of 10 Transmitters pairing with all 500 Receiver buds (1to 500)

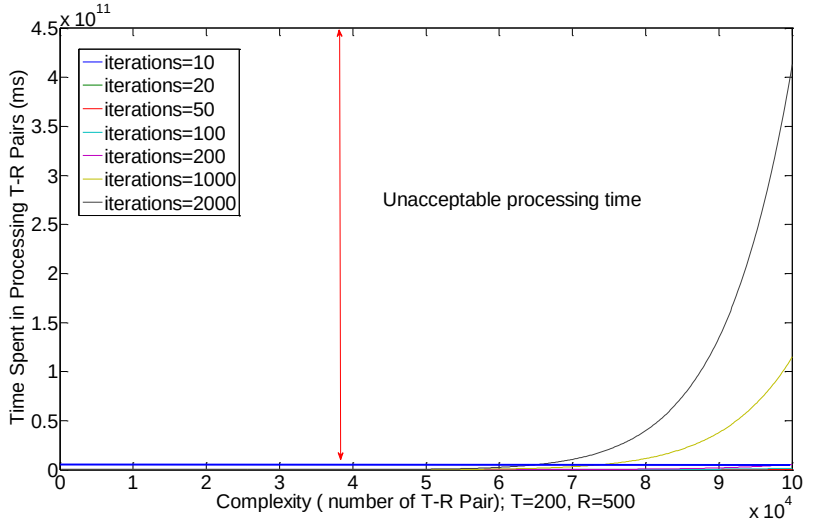

Figure 5-3-8: CME response time for the complexity of 200 Transmitters pairing with all 500 Receiver buds (1to 500)

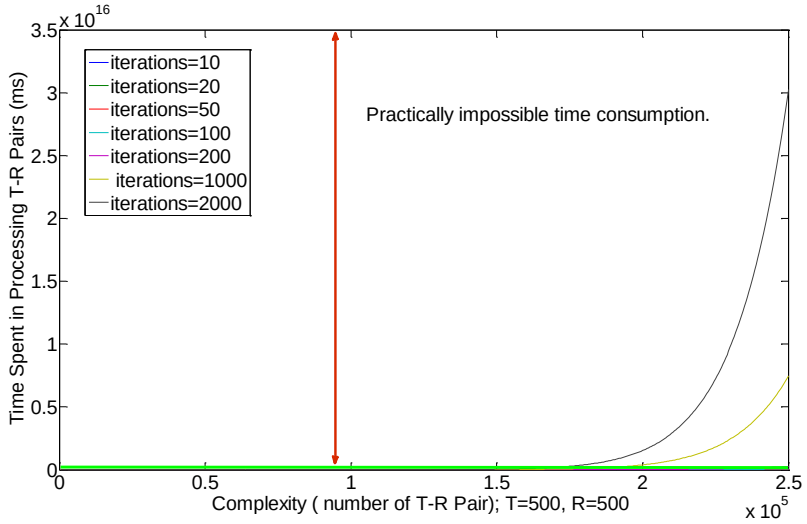

Figure 5-3-9: CME response time for the complexity of 500 Transmitters pairing with all 500 Receiver buds (1to 500)

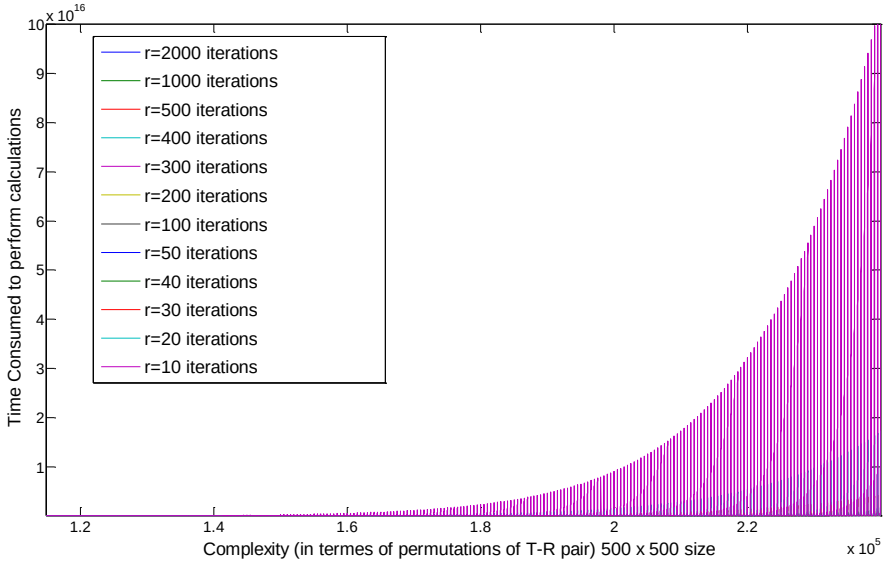

Figure 5-3-10: CME response time for the complexity of 500 Transmitters (1to 500) pairing with all 500 Receiver buds (1to 500)

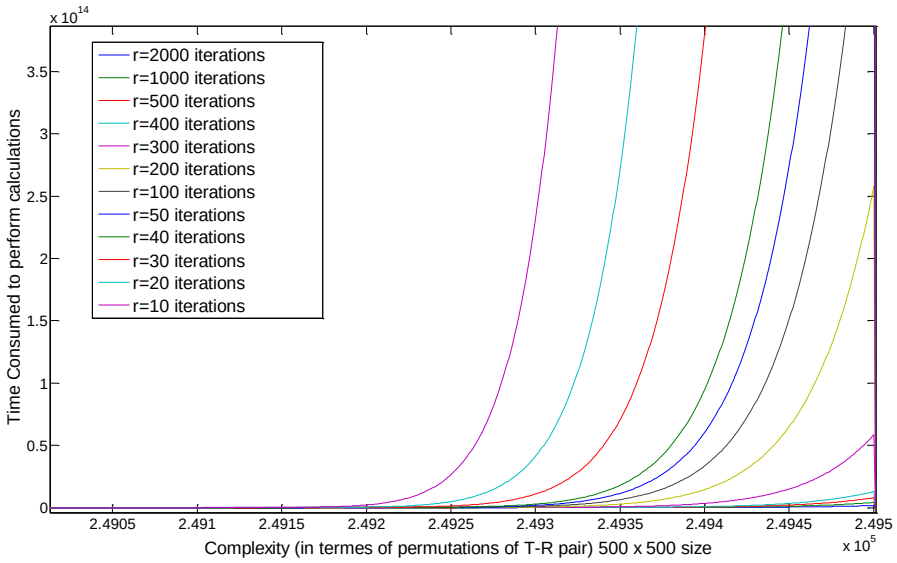

Figure 5-3-11: Zooming in figure 5-3-9 for insight of response pattern for a single transmitter pairing with growing number of receivers

From the results shown in figures from 5-3-3 to 5-3-8, it can be noticed that as the number of elements in the T and R sets increase, the complexity in terms of the number of elements generated by each new addition of T_x and R_x pair would increase drastically. Further, as shown in figure 5-3-12, the location of SCIN is not equidistant from all buds, and hence, the time it takes for the signals to travel to a destination is not uniform as shown in figure 5-3-11. This is incorporated in t_{repeat} and a single unit of addition in the delay can impact a lot if the number of the iterations is huge. Usually, the forward and reverse paths do not pose the same time consumption, therefore, in the case that the reverse path consumes more time, the larger the number of elements in **T**, more severe the curve bends.

When the (number of elements) is large, then the size of matrix 'Π' increases drastically thereby inflating the time consumption. This increases the time to estimate the PTC^2 at various location of the network. Each curve in figures 5-3-4 to 5-3-9 represents the time consumed when |T| probes are transmitting, and the probing R_xs are incremented from 1 to 500. The time consumption increases with an increase in the number of R_xs. Figure 5-3-10 shows the combined pattern when all 500 buds are participating as both, T_x and R_x. Figure 5-3-11 is the zoomed -in version of the figure 5-3-10 to show the individual pattern.

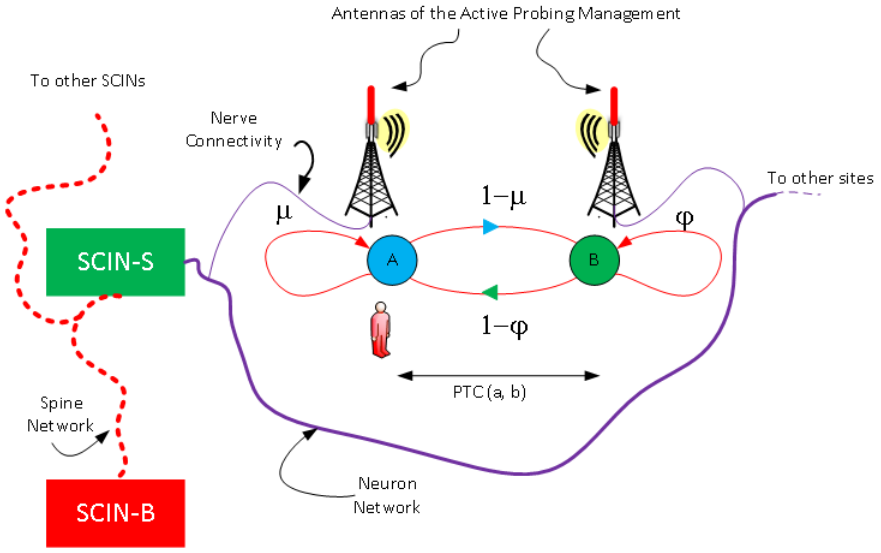

Figure 5-3-12: Probability of finding accumulation at a random place impacts CME performance

From the above discussion, it is very clear that the complexity of the CME algorthim may not be very suitable for SCIDAS for a large number of antennas. With 500 buds, the processing time may be in the order of 10^{16}, which is practically impossible for any network performance. Hence, to assist CME in maintaining the quality of the performance, another algorithm is proposed that is defined here as a T-R Distance Optimiser (see, sub-section 5.3.3), where, the distance is in terms of neighbours of a particular T_x. By choosing the right neighbours as R_x probes, a huge amount of calculations can be avoided. Sub-section 5.3.3 explains how the right neighbours can be obtained. In sub-section 5.3.3, we define the TDO algorithm that can be applied for both the position and time domains and is indicated by the stamp-type variable γ gamma. When γ=1, the algorithm performs in the time-domain else in the position domain. For the position domain, only those neighbors are chosen that are serving the desired position and the condition is given in equations (5.3.17) and (5.3.18) whereas in the time domain measurements only those neighbours, that can receive a signal level above a certain value $P_{criteria}$ would be served. Normally, $P_{criteria}$ is the R_x sensitivity of the system.

5.3.3. T-R DISTANCE OPTIMISER (TDO)

Let (xi, yi) and (xj, yj) be the position coordinates of the transmitter and the receiver probes respectively, and, (xp, yp) be the position of accumulation. For the position-domain observations, the TDO, defined in (5.3.22), chooses the receivers that satisfy the following equations:

$$y = \left(\frac{yj - yi}{xj - xi}\right) x + C$$ Standard line equation between i^{th} transmitter and j^{th} receiver. (5.3.17)

and, $x^2 + y^2 \leq R^2$ Limiting the observation span within the observation zone (5.3.18)

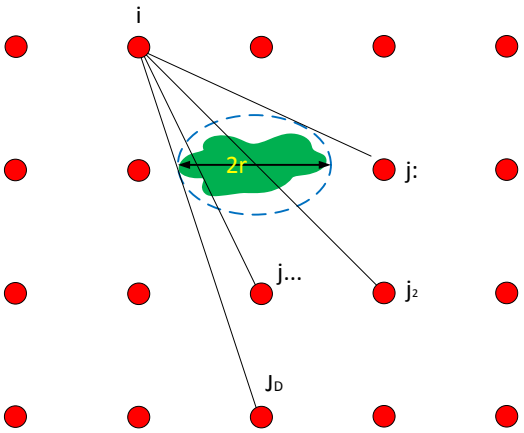

Figure 5-3-13: Position domain measurements: estimating the set of observers

Where, the observation zone is the circular area of radius R that encapsulates the subject area as shown in figure 5-3-13, and 'm' is the rate of line in equation (5.3.17). The condition of observing the probes with x and y as coordinates is identified as:

$$x \leq \frac{-mC \pm \sqrt{(mR)^2 + R^2 - C^2}}{m^2 + 1}$$ (5.3.19)

and, $$y \leq \frac{C \pm m\sqrt{(mR)^2 + R^2 - C^2}}{m^2 + 1}$$ (5.3.20)

The condition set 'D' in WHISPER and CME algorithms for the position-domain observation satisfies equations (5.3.17) and (5.3.18) and is described in the TDO algorithm as discussed in (5.3.22). Similarly, for the time-domain observation, if (xi, yi) and (xj, yj) are the position coordinates of the transmitter and receiver probes respectively, then the neighbour distance is approximated by the following equation.

$$P_{criteria} \leq P_t \left[\frac{\lambda}{4\pi\sqrt{(yj - yi)^2 + (xj - xi)^2}}\right]^2$$ (5.3.21)

Where P_t is the power of the probing signal and is constant through the observation for all probes, and λ is the wavelength under consideration. This evaluates the

extent of neighbours to transmitter probes that observe the transmitted AAN. The process can be described in an algorithm as below in (5.3.22):

Steps	Function	Description
BEGIN: T-R Distance Optimisation (xi, yi, xj, yj,$P_{criteria}$,γ)		
		// (i,j) coordinates, Power Criteria and stamp-type **'γ'**
1	i,j ←1	*// initializing variables*
2	While i≤ N	*// all buds are as transmitters*
3	While j≤ N	*// all buds are as receivers*
4	If **γ is time-domain (γ=1)**	*// valid neighbours in time-domain*
5	If (i,j) satisfy condition in(5.3.21) then	*// if (i,j) pair are valid neighbours*
6	Dij← True; Else Dij← False;	*// if yes then true else false*
7	Else	*// If γ is position-domain* **(γ=2)**
8	If (i,j) satisfy condition in (5.3.19) and (5.3.20) then	
9	Dij← True; Else Dij← False;	*// for position domain*
10	j ←j+1	*// next receiving probe*
11	i ←i+1	*// next transmitting probe*
12	**END: T-R Distance Optimisation (D, γ)**	*// return Distance-matrix and stamptype* **'γ'**

(5.3.22)

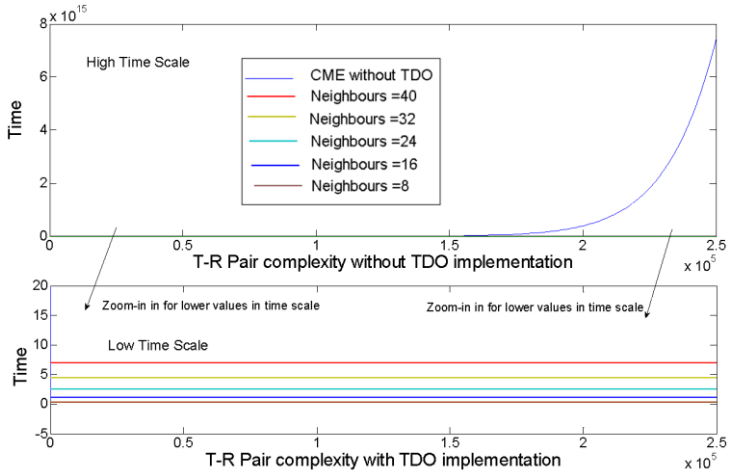

Figure 5-3-14: TDO implementation on CME for controlled sensing

The TDO algorithm limits the receiver probes thereby, reducing the time of observation per probing process. With a large number of probing antennas, TDO can reduce a considerable amount of time by rejecting the non-significant measurements. While performing the position domain measurement, TDO users MCP to perform orientations between T_x and R_x.

Figure 5-3-14 shows how TDO controls the increase in complexity and the performance dampening. The upper graph in figure 5-3-14 shows when the sensing is performed without the TDO, which means that it only depends on the choices of the **T** and **R** sets. The result, in this case, is a steep rise in the time latency with an increase in T-R sets (also mentioned earlier). Conclusively, the graph shoots up exponentially with the increase in complexity, so much, that the time to observe SCIDAS network with 500 sites raises to the order of 10^{15}. The same graph also contains results with the TDO implementation, to show that for a TDO implementation, the time consumption is low enough (high performance) to be barely visible in the upper graph. This is compensated in the lower graph with a time scale of the order of 10^0. As we can see in the lower graph, depending upon the $P_{criteria}$, the TDO would assign a different but very limited set of neighbours to its respective transmitters. This reduces the complexity of the matrix and the latent time in the calculations. The graph shows that with TDO, the SCIDAS can be scaled to any number of buds without contributing any further delays in processing time. As the number of neighbours of a transmitter is limited, the delay in propagation of information from a farther bud is also reduced to very intimate neighbour groups.

Utilisation of the CME-TDO algorithm (Example: the City of Pune, India): Every year, during the popular festival of Lord Ganesha (Ganpati), processions in chunks of groups move across the city for the immersion of an idol of Lord Ganesha at specific destinations. This is a critical cause for network congestion in the areas of accumulations. It is difficult for NSP to estimate the additional sites that can satisfy the situation because of the uncertainty of the exact location of the expected network congestion. CME-TDO algorithm was used to predict the locations of additional sites (see, figure 5-3-15) to cater the huge PTC^2 problem. As there was no APMS, the data obtained from Radio Resource Management (RRM) was considered as equivalent information to that of what may be obtained from APMS and was used to predict the point of accumulations as shown in figures 5-3-15 and 5-3-16. This information was used for a case study that is discussed in Chapter 6.

The CME-TDO algorithm can be used to identify the time and position based variations in the network environment. As most of the entities of the network environment are static and, it is the human intervention that creates most of the itinerance in the environment, the outputs of the CME algorithm can be used to identify the accumulations and movements of these accumulating groups in the AoI.

The advantage of the CME-TDO algorithm is that it can provide a holistic view of the variations in the entire AoI at the same instant and hence, the network optimization, initiated by NIU and executed by other modules of SCIDAS architecture SMU, SRU, and MCP), is more effective and realistic.

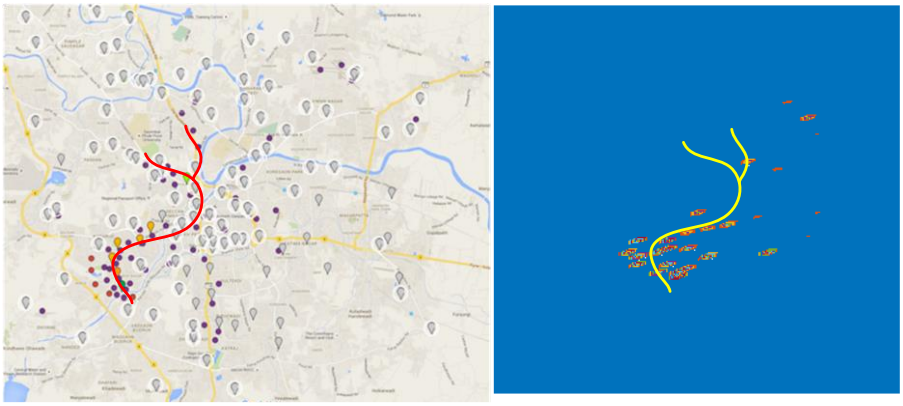

Figure 5-3-15: Prediction of locations of high accumulations in the city of Pune

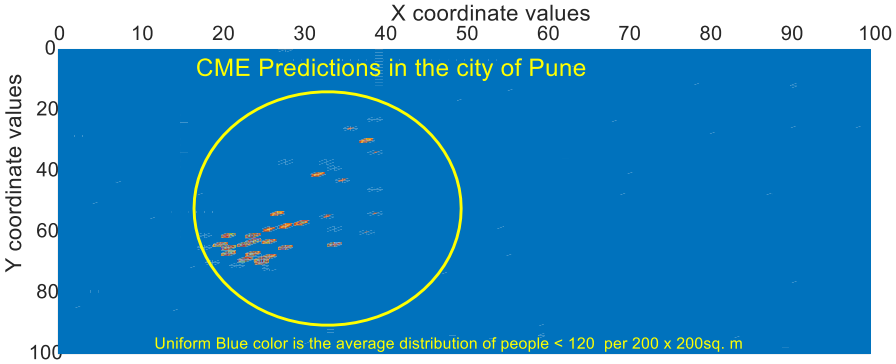

Figure 5-3-16: Locations of accumulations in 10 × 10 sq. km area in the city of Pune

5.3.4. PTC^2 ENVIRONMENT ESTIMATOR (PTC^2 EE)

Both the time and the position based CMEs are assigned to **Π(t)** and **Π(p)** respectively, to give H^{est}. This procedure can be expressed in an algorithm that is defined here as *PTC^2 Environment Estimator (PTC^2 EE)*, as in (5.3.23), given below:

BEGIN: PTC^2 EE (R,T, C_t, C_p, λ_t, λ_p, γ)		
1	$\lambda_t \leftarrow$ **CME (R,T,C_t, (γ=1));**	// *obtain time-dependent Channel Matrix using **CME** as in **(5.3.16)***
2	$\lambda_p \leftarrow$**CME (R,T,C_p, (γ=2));**	//*obtain position-dependent Channel Matrix using **CME** as in **(5.3.16)***
3	$H^{est}(t,p,n) \leftarrow (U\lambda_t)(W\lambda p)$;	// *obtain Place-Time Matrix from equation **(5.3.15)***
4	$\varepsilon_{ij} \leftarrow f(H^{est})$	// **Calculate ε_{ij}** using equation (5.3.35)
END: PTC^2 EE (λ_t, λ_p, ε_{ij})		

(5.3.23)

Both λ_t and λ_p are the accumulation dependent matrices. Hence, the accumulation in a subject location is a function of H^{est}. λ_t represents the subscriber accumulation with time (see, figure 5-3-1), and λ_p represents the subscriber accumulations with position (see, figure 5-3-12). Thus, as discussed in section 3.6 of Chapter 3, equation (5.3.3) thus transforms into an accumulation dependent set of equations as:

$$\Psi(t, p) = H^{est}_{(t,p)}\chi + \xi \tag{5.3.24}$$

Where, $H^{est}(t,p) = A(U\lambda_{t)}(W\lambda_p)$; A is correction factor (5.3.25)

Figure 5-3-1 shows that the wave from a transmitter travels some free space distance before interacting with the user distribution, the absorptions by the ground and other medium entities (human, metals, cement, etc.). Hence, removing the loss due to the free space dispersion will provide an approximate loss from the subject to the receiver. Hence, the coefficients U and W, as mentioned in the equations (5.3.24) and (5.3.25) would accommodate these adjustments as is described below:

$$u_{ij} = \frac{1}{PL(D_{o,ij})} \tag{5.3.26}$$

and

$$w_{ij} = \frac{1}{\left[PL(D_{o,ip})\right]_{ij}} \tag{5.3.27}$$

Estimation of the PTC^2 components: The dynamic path-loss PL_ω, given in equation 3.6.19, between the i^{th} transmitter and the j^{th} receiver can be expressed as:

$$\mathbf{PL_{\omega,ij}} = \overline{\overline{PL}}\left(D_{0ij} + d_{ij}\right)\left(\frac{D_{0ij} + d_{ij}}{D_0}\right)^{N_{AR}(\varepsilon_{ij})} \tag{5.3.28}$$

Where ε_{ij} is the user density within the i-j pair (see, figure 5-3-1 and equation 3.6.19, Chapter 3).

From the above discussions, we have, the net fading in the i-j pair, which can be approximately expressed as

$$\mathbf{PL_{\omega,p,ij}}(t) = \lambda_{t,ij}\lambda_{p(ij)} \tag{5.3.29}$$

As discussed in section 3.5, of Chapter 3, equation (5.3.29) is the coverage needed at any point of interest (or subject) at any time 't' and is the *Place Time Coverage* representation obtained through APMS measurements. The PTC_o scenario in the network can thus be expressed as:

$$\left[\mathrm{PTC_{o,ij}}\right](\mathbf{t},\mathbf{p})_{T\times R} = \left[\mathbf{PL_{\omega,ij}}\right](\mathbf{t},\mathbf{p})_{T\times R} = \left[\lambda_{t,ij}\right]_{T\times R}\left[\lambda_{p}\right]_{T\times R} \tag{5.3.30}$$

Similarly, the *Place Time Capacity* is obtained by equating, (5.3.28) and (5.3.29), which yields:

$$\mathbf{N_{AR}}(\boldsymbol{\varepsilon}_{\mathbf{ij}}(t,p)) = \log_{\left(\frac{D_{0ij}+d_{ij}}{D_0}\right)}\left(\frac{\lambda_{t,ij}\,\lambda_{p(ij)}}{\overline{\overline{PL}}(D_{0ij}+d_{ij})}\right)$$

or

$$\mathbf{N_{AR}}(\boldsymbol{\varepsilon}_{\mathbf{ij}}(t,p)) = \frac{\log\left(\frac{\lambda_{t,ij}\,\lambda_{p(ij)}}{\overline{\overline{PL}}(D_{0ij}+d_{ij})}\right)}{\log\left(\frac{D_{0ij}+d_{ij}}{D_0}\right)} \tag{5.3.31}$$

For the experiment performed as discussed in Chapter 2, the relation of dynamic path-loss exponent with the subscriber density, as mentioned in equation **(2.5.1)**, can be estimated as $(40+78\,\varepsilon_{ij}) \times 3.32$. Hence, for the purpose of the discussion, equation 5.3.31 can be generalised here as:

$$\left[\boldsymbol{\varepsilon}_{\mathbf{ij}}(t,p)\right]_{T\times R} = \frac{\left[\frac{\log\left(\frac{\lambda_{t,ij}\,\lambda_{p(ij)}}{\overline{\overline{PL}}(D_{0ij}+d_{ij})}\right)}{(3.32)\log\left(\frac{D_{0ij}+d_{ij}}{D_0}\right)}\right]-40}{78} \tag{5.3.32}$$

Assuming that each user is entitled to a maximum capacity of '$\boldsymbol{\rho}$', the capacity requirement matrix between T-R (i-j) pair thus can be expressed as:

$$\left[\mathrm{PTC_{ij}}\right](\mathrm{t,p})_{T\times R} = \rho\left[\varepsilon_{\mathrm{ij}}(\mathrm{t,p})\right]_{T\times R} \tag{5.3.33}$$

Knowing the coordinates of the probes, equations (5.3.30) and (5.3.33) can also be expressed in the coordinate system instead of the i-j format. The H^{est} can be very useful in the signal estimation in extremely dynamic conditions. Equation (5.3.24) can be used for the signal estimations in MIMO operations in a varying environment. As shown in figure 5-3-1, and discussed in section 3.6 of Chapter 3, the varying channel matrix equation (5.3.24) can therefore, be used for estimating the signals in MIMO operations, which is given below as:

$$\boldsymbol{y} = \boldsymbol{\mathcal{H}x} + \boldsymbol{n} \tag{5.3.34}$$

Where n is the system noise or the Gaussian additive noise vector with covariance $\mathbf{I}\sigma^2$. With respect to the measure values **y,** the transmit signal can thus be estimated by the zero forcing method [12]:

$$\boldsymbol{x} = (\boldsymbol{\mathcal{H}^T\mathcal{H}})^{-1}\boldsymbol{\mathcal{H}^T y} \tag{5.3.35}$$

Where H is the channel matrix for I set of transmitters and J set of receivers and hence, $\boldsymbol{\mathcal{H}^T} \subset \boldsymbol{H^{est}}$. Each I and J can be either a probe or user with each T-R pair having atleast a single probe.

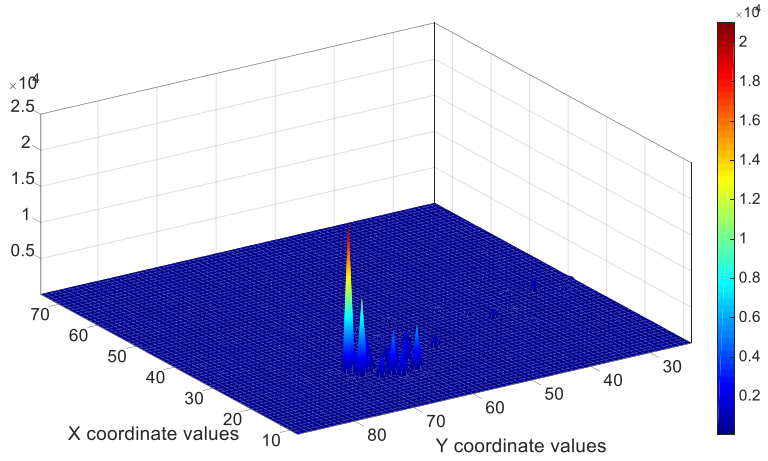

Figure 5-3-17: Estimation of the strength of accumulation at various locations in the City of Pune using PTC²EE algorithm.

Utilisation of PTC² EE algorithm (Example: the City of Pune, India): We have already discussed how the CME-TDO algorithm predicted the wobbles in the network. Locations with higher variations were marked as the high wobbling

locations as shown in figures 5-3-15 and 5-3-16. However, besides the location, it is also required to know the strength at those locations for capacity dimensioning. The PTC^{2}EE algorithm is used to predict the strength of the wobbles in terms of a number of people and the density of their accumulations. Figure 5-3-17 shows the strength of the user accumulation at various locations in the network area (AoI). It is important to note that there are always some users beneath every site and across every position in the network area. This is the "floor user density" and is shown as the blue floor in the graph, which is the people density less than 120 per 200 × 200 sq. meter area.

5.3.5. SILENT PROBING METHOD (SPM)

While WHISLME is an active mode of APMS's probing process, this algorithm silently observes the network by reading the uplink and downlink signals at each bud of the SCIDAS network without any probe signal. However, unlike WHISLME me where the uplink and downlink were the same side of the network, the nature of the transmit signal is complex as it is the actual signal that is transmitted from various users. Therefore, instead of utilising this active observation for the accumulation estimation, the SPM algorithm is used to read the spectrum utilisation at every bud of the network.

Let the system model, in equation (5.3.34), having 'N' SCIDAS sub-buds (sectors, each behaving as separate remote unit) and S users is re-written as :

$$[\boldsymbol{y}]_{\boldsymbol{N}} = \boldsymbol{\mathcal{H}}[\boldsymbol{x}]_{\boldsymbol{S}} + \boldsymbol{n} \tag{5.3.36}$$

Where n is the system noise or Gaussian additive noise vector with covariance $\mathbf{I}\sigma^2$. Also, let $[CG_i]_N$ be the group of 'ik' frequencies (carriers) such that:

$$[\boldsymbol{CG_i}]_{\boldsymbol{N}} = \{\boldsymbol{f_{ik}}\}_{k=1}^{\mathcal{F}_i} \tag{5.3.37}$$

Where $\{\boldsymbol{f_{ik}}\}$ is the number of carriers allocated to the ith sub-bud of the SCIDAS network. If p_{ik} is the transmit power of the ith sub-bud antenna and kth carrier, then the signal-to-noise-plus-interference ratio (SINR) experienced at the Jth receiver due to Ith transmitter antenna for Kth carrier can be described as:

$$\boldsymbol{SINR_{ik,j}} = \frac{\boldsymbol{p_{IK}}\left|\boldsymbol{h_{IJ}}\right|^2}{\sum_{i\neq I}^{N}\sum \boldsymbol{p_{ik}}\left|\boldsymbol{h_{ij}}\right|^2 + \boldsymbol{\sigma^2}} \tag{5.3.38}$$

While performing Silent Probing, the recorded information contains the Carrier Group 'CG', interfering carrier group (ICG) and SINR at each bud for all carriers. The ICGi is the list of interferers that are experienced significantly. The process can be described as below:

	BEGIN SPM(t,μ, L)	
1	i,j←1; t ← t_1	*// indices set to 1 at any time 't_1'*
2	For j ≤ η	*// Measuring the frequency f_j at all probes*
3	For i ≤ N	*// condition for probes*
4	if Power of f_j, p_j ≥ Receive sensitivity and $SINR_{ik,j} > \forall$ then,	
5	K_{ij}←p_j when **μ** = 1 or K_{ij}←1 when **μ** =2;	
6	else K_{ij} ←0;	
7		*// Recording values for every probe*
8	if i= N then END For loop;	*// condition for probes exhaust; i=N*
9	i ←i+1;	*// else next probe*
10	if j = η then END For loop;	*// condition for all carrier measured; j= η*
11	j←j+1;	*// else next carrier*
12	END **SPM(t)**	

(5.3.39)

Where **μ** is the measurement type. And, μ =1 when the signal power level information is needed and μ =2 when the carrier occupancy information needed.The SPM is defined here as the function of time to accommodate the t_{repeat} in equation (5.2.6). When μ =2**,** the matrix $[K_{ij}]$ recorded in this process is the "logical" matrix having only zeros and ones to indicate if the frequency f_j is observed by i^{th} probe above R_x sensitivity level or not. Which means that all signal powers below the R_x sensitivity at a probe 'i' would be ignored. The scalar form of frequencies will transform **Φ** to the bandwidth representation consumed at all buds of SCIDAS.

The carrier group thus, can be described as,

$$\mathbf{\Phi = KF} \tag{5.3.40}$$

Where **Φ** is the carrier set and $[\Phi_i]_{N \times 1}$ is the group of carriers at the i_{th} probe of the m_{th} SRU out of a total of M SRUs. **K** is the matrix of the observed values such that $[k_{ij}]_{N \times \eta}$ represents the power above or below of the received sensitivity at i^{th} probe and the j^{th} frequency. For simplicity, the serving antenna of each sector is referred as a probe and therefore, each SRU can have multiple Probes to form an SCIBUD, which is equivalent to RRH. All discussions will thus be performed at the probe level. **F** is the set of carriers, and $[f_j]_{\eta \times 1}$ is the j_{th} measured at a probe.

5.3.6. PROACTIVE PLACE-TIME PREDICTOR (P_OPP)

Figure 5-3-18 shows a typical SCIDAS deployment with SRU buds deployed on the street poles. This is a good way of saving ample CAPEX (Capital Expenditure) on the new infrastructure. In figure 5-3-18, people (users) accumulate and walk in

groups and eventually may accumulate at some point P. The entire AoI is observed by a series of AANs which are denoted by the blue coloured numbering on the top of alternate street poles, as shown in figure 5-3-18.

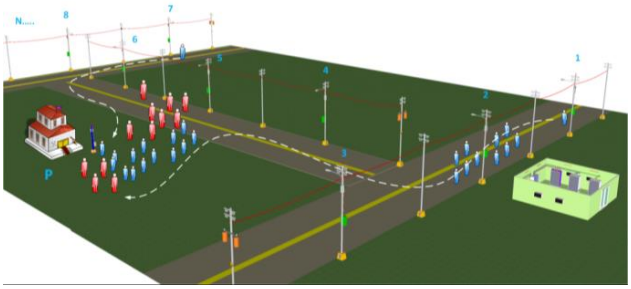

Figure 5-3-18: Place Time Event: Subscriber Movement

For the instantaneous resource allocation, the PTC^2 needs to be followed, and therefore, needs to be constantly observed by the system. The CME-TDO algorithm can be used iteratively to monitor the wobble at various locations, however, to predict future states, the Kalman Filter Process[13] [14] is used here to estimate the sites that need to be densified to fulfill the accumulations and to predict the place time event, as shown in figure 5-3-3. This impinges proactiveness in the system and thus smoothens the flow of accumulation. This algorithm is defined here as Proactive Place-Time Simulator (PoPP) which predicts the future states to closely follow the accumulation movements.

If an accumulation of subscribers is in motion, the state prediction model for the can be expressed as:

$$\mathbb{P}_{\gamma} = \mathbf{A}\,\mathbb{P}_{\gamma-1} + \mathbf{B}\boldsymbol{\alpha} + \boldsymbol{\eta}_{\mathbb{P}} \tag{5.3.41}$$

Where $\mathbb{P}_t$ is the state variable representing the PTC^2 state at any time t. Therefore,

$$\mathbb{P}_{\gamma} = \begin{bmatrix}\text{Position}\\ \text{Velocity}\end{bmatrix} = \begin{bmatrix}\text{P}\\ \text{V}\end{bmatrix} \tag{5.3.42}$$

We know,

$$\text{P(t)} = \text{P(t}-1) + \text{v(t)} + \frac{1}{2}\text{at}^2 \tag{5.3.43}$$

Where P is the position, v is the velocity, and a is the acceleration. In an SCIDAS system, as the variations are observed by the APMS, both velocity and position can be defined as the function of PTC^{2}EE algorithm. Thus, denoting PTC^{2}EE by ₦, we can say from equation (5.3.43) that,

$$\aleph(t) = \aleph(t-1) + \frac{d}{dt}\aleph(t) + \frac{1}{2}\left\{\frac{d^2}{dt^2}\aleph(t)\right\}t^2$$

or, $$\aleph(t) = \aleph(t-1) + \aleph'(t) + \frac{1}{2}\aleph''(t)\,t^2 \quad (5.3.44)$$

Replacing the time domain with the generic domain γ, we have:

$$\aleph(\gamma) = \aleph(\gamma-1) + \aleph'(\gamma) + \frac{1}{2}\aleph''(\gamma)\gamma^2 \quad (5.3.45)$$

Similarly, the velocity component can be expressed as:

$$V(t) = V(t-1) + at \quad (5.3.46)$$

or $$\aleph'(\gamma) = \aleph'(\gamma-1) + \frac{1}{2}\aleph''(\gamma)\,\gamma \quad (5.3.47)$$

Similarly, the sensing prediction can be modeled as:

$$\overline{\chi(t)} = C\mathbb{P}_t + \eta_\chi \quad (5.3.48)$$

Where $\overline{\chi(t)}$ is the predicted measurement of the actual measurement $\chi(t)$.

Hence, the estimate stare can be expressed as:

$$\mathbb{P}_{est} = \mathbb{P}_\gamma + K(t)\left\{\chi(t) - \overline{\chi(t)}\right\} \quad (5.3.49)$$

Solving for A, B and C in equations (5.3.41) and (5.3.48), we have:

$$\boldsymbol{A} = \begin{bmatrix}1 & 1\\ 0 & 1\end{bmatrix}; \boldsymbol{B} = \begin{bmatrix}\gamma^2/2\\ \gamma\end{bmatrix} \; and \; C = [1 \quad 0] \quad (5.3.50)$$

Therefore,

$$\mathbb{P}_\gamma = \begin{bmatrix}1 & 1\\ 0 & 1\end{bmatrix}\mathbb{P}_{\gamma-1} + \begin{bmatrix}\gamma^2/2\\ \gamma\end{bmatrix}\aleph'' + \eta_{\mathbb{P}} \quad (5.3.51)$$

and, $$\bar{\chi}(\gamma) = [1 \quad 0]\mathbb{P}_t + \eta_\chi \quad (5.3.52)$$

The Kalman gain in such a case is given by:

$$K(\gamma) = \bar{\chi}(t)C^{T}\{C\bar{\eta}_{P}C^{T} + \eta_{P}\}^{-1} \quad (5.3.53)$$

and, $\eta_{P} = \{I - K(\gamma)\}\bar{\eta}_{P}$

Where I is the identity matrix.

Solving for above equations will predict the locations under which accumulations will form ahead of time. This creates a proactiveness in the SCIDAS model and accordingly the resource distributions can be planned. We define this algorithm as ***Proactive Place-Time Predictor (PoPP)***. Presently this algorithm follows only one accumulation at a time. As a future work, we can increase complexity to accommodate several accumulations.

5.4. ALGORITHMIC REPRESENTATION OF AMOEBIC PTC^2 RESPONSE MECHANISM (APR)

In Chapter 4, we discussed the Amoebic PTC^2 Response (APR) Mechanism as the collection of five sub-processes namely,

a) Prompt,
b) Ingestion,
c) Digestion & Absorption,
d) Fission and Assimilation, and,
e) Egestion.

The purpose of the APR algorithm is to observe these movements, allocate the suitable amount of additional carriers among the closest server buds, and, iteratively itinerate the process following the movements. Right now, the algorithm is designed to follow a single group, however, can be extrapolated for multiple groups at various locations. The APR algorithms are the composite algorithm that combines all algorithms discussed so far. The procedures involved in this algorithm are given below.

A. APR- Preparatory (APR-Prep): This algorithm sets up the stage for other processes to follow on. The two sub-algorithms (APR1 and APR 2) use CME-TDO and SPM to read the coverage and capacity wobbling in the SCIDAS network. APR1 uses CME-TDO to understand the wobbeling under each bud of the SCIDAS network, and APR 2 performs the carrier aggregation at each bud by reallocating the resources as per the estimated accumulations by APR1. Both algorithms are repeatedly needed to estimate the network dynamics. This is considered as a prerequisite for any intelligent network to understand the dynamics of its network environment.

1	**BEGIN APR-Prep** $x, y, z \leftarrow 1$; // *initializing variables*	
2	**BEGIN APR:1**	// *Estimating variations*
3	Call **CME-TDO**	// Read the accumulation related variations
4	$Z_{TOT} = \sum \varepsilon_{ij}$;	//Calculating total accumulation in the SCIDAS network; see, equation (5.3.32) for ε_{ij}
5	$While\ (i \leq\ N)\ do$	// for all buds that transmitted
6	$While\ (i \leq j \leq\ N)\ do$	// for all buds that received
7	$Z_{i=x_i,y_i,z_i} \leftarrow \frac{1}{6}\sum_{x_j-1}^{x_j+1}\sum_{y_j-1}^{y_j+1} \varepsilon_{ij}$;	// Calculating total accumulation under each bud, considering each i-j pair shares half of accumulation; See, equation (5.3.32) for ε_{ij}
8	$j \leftarrow j + 1$;	// next receiver bud
9	$i \leftarrow i + 1$;	// next transmitter bud
10	$C_{Need,i} \leftarrow Z_i \times\ \Gamma_{max}$	//Capacity need at i[th] bud
11	**END: APR 1**	//Ending Algorithm APR1
12	**BEGIN: APR 2**	//Begin Algorithm APR2
13	$While\ \{OCAP\{CG_j\} \neq C_{need_{x_j,y_j,z_j}} + C_{\Delta j}\}$ do	//perform till number of carriers satisfies the accumulation at j[th] bud.
14	While (j≤ N) do	//when j[th] receiver is under observation
15	$While\ (j \leq i \leq\ N)\ do$	//For all transmitters
16	$While\ (k \leq\ BA)\ do$	// Considering all carriers in a Band
17	$\boldsymbol{SPM(i,j,k)}$;	// call SPM for periodic reading
18	$If\ OCAP\{CG_j\} \leq C_{need_{x_j,y_j,z_j}} + C_{\Delta j}\}$	// until carries are deficient to cater
19	$If\ k < BA$	// condition when all carriers are considered but still deficient
20	$If\ SINR_{ijk} \geq HI_j$	// till a carrier k doesn't spoil SINR
21	$\{CG_j\} \leftarrow f_k$;	// Add to the carrier group of j[th] bud
22	$k \leftarrow k + 1$;	// evaluate for next carrier
23	$Else\ \{CG_j\} \rightarrow f_k$;	// else remove carrier from j[th] group
24	$Else$	
25	$HI_j \leftarrow HI_j - \exists_j$;	// reduced the SINR margin to accommodate more carriers
26	$k \leftarrow k + 1$;	// next carrier
27	$Else\ \{C_j\} \rightarrow f_k$; // when carriers are larger than required, remove from the group	
28	$i \leftarrow i + 1$;	// next transmitter
29	$j \leftarrow j + 1$;	// considering next receiver
30	**END: APR 2; END APR-Prep**	

(5.4.1)

Where,

1	Z_{TOT}	is the total accumulation in the AoI. It is the accumulation of people irrespective of whether they are identified by network service or not. The accumulation is measured by the variations in the received signal strength of the probing signal.
2	$Z_{i=x_i,y_i,z_i}$	is the accumulation at the i^{th} bud or in terms of coordinates, it is the z_i th sector of the SRU bud that is positioned at the x_i th latitude and y_i^{th} longitude (or any reference coordinate system). The accumulation is obtained by summing up the ε_{ij} with respect to each neighbour.The neighbors are represented in coordinate form (x,y pairs) than sequential form. Referring to figure 5-3-12, the neighbours of any bud at (x,y) will be(x-1,y-1), (x-1,y), (x-1,y+1), (x, y-1), (x, y+1), (x+1,y-1), (x+1, y), (x+1,y+1). As the distribution under an SRU bud is considered uniform, each bud, although may have its own unique concentration, therefore, each i-j pair will share the accumulation that eventually is shared by the 3 sectors of SRU. Hence, each Z_i is the concentration under 1 sector, which is 1/6 of the total accumulations around bud 'I'.
3	$C_{Need,i}$ and Γ_{max}	we have assumed that each subscriber can demand Γ_{max} of capacity, and therefore, the total capacity demand created due to Z_i amount of people under bud 'i' is given by $C_{Need,i}$.
4	N	is the number of SRU buds in a SCIWAN (access network under a single SCIN-B or SCIN). The counting 1,2,3 .. N follows the same rule as a usual number system
5	HI	is the health indicator or the tolerance of the system. Here, this parameter only accounts for SINR acceptable to the system; however, in future, many other constraints may be accompanied.
6	$\exists_j$	The least possible value that must be reduced from HI to accommodate more carriers in a system.
7	$OCAP\{CG_j\}$	is a function that relates the capacity that can be offered by a BS with a given set of carrier groups (configured with the BS)

B. APR: The APR algorithm is the combination of above mentioned algorithms in a certain order to carry out accumulation management. The brief form of algorithm is mentioned below:

	Steps Function	Description
	BEGIN: APR(t, **Halt Status,Ω,ρ**) // *Halt status, time and density tolerances*	
1	t←0; P ←P_0; i,j←1; NIU←NIU(0);	// initailise iteration count
2	$While\ \{(t \le T_{max}) and\ (Halt = False)\}\ do$	// Promp observation till any time
3	$Run\ \mathbf{PTC^2EE}\ to\ obtain\ \boldsymbol{H^{est}};\ \boldsymbol{\mathcal{H}} \subset \boldsymbol{H^{est}};$	// *Prerequisite* ***(see, algo 5.3.23)***
4	$[\boldsymbol{Y(t)}]_N = \boldsymbol{\mathcal{H}}[\boldsymbol{X}]_N + \boldsymbol{n};$	// *Monitor network with APMS; see,* ***eq. 5.3.36***
5	$if\left\{\left(\frac{\mathrm{d}}{\mathrm{dt}}[Y(t)]_N \le \boldsymbol{\Omega}\right) \otimes \left(\frac{\mathrm{d}}{\mathrm{dp}}[Y(t)]_N \le \boldsymbol{\rho}\right)\right\}$	// *if change is below tolerance* **Ω** *and* **ρ**
6	$Call\ \boldsymbol{APR-2};$	// ***APR-2*** *updates network*
7	$Else\ if\ \{d/dt(Z_{TOT}) \neq 0\}$	// *see, 5.4.1 for* Z_{TOT}
8	$Call\ \boldsymbol{SPM}$; GOTO 13;	// ***SPM*** *allocates new carriers*
9	$Call$ *APR-Prep*; GOTO 13;	// *Ingestion algorithm*
10	$Wait\ (t_{repeat})$;	// *Breathing period* ***(see, 5.2)***
11	$t \leftarrow t+1$; GOTO 2;	// *Next iteration*
12	Else; GOTO 1;	// End Prompt Mechanism
13	$While\left\{\left(\frac{\mathrm{d}}{\mathrm{dt}}[Y(t)]_N \ge \boldsymbol{\Omega}\right) \oplus \left(\frac{\mathrm{d}}{\mathrm{dp}}[Y(t)]_N \ge \boldsymbol{\rho}\right)\right\}$ do	// *CME-TDO functions*
14	$for\ i \le N$	// Considering N rows
15	$for\ j \le N$	// Considering N columns
16	$if\ \left\{\left(\frac{dY_{ij}}{dt} \neq 0\right) \oplus \left(\frac{dY_{ij}}{dp} \neq 0\right)\right\}$	// Wobbling at (i,j) is not zero; any other tolerance can be assigned
17	$if\ (HI_{ij} \ge SINR_{lowest\_acceptable})$	// *Health at location (i,j)>min(SINR)*
18	$if\ \{CG(ij) \le \varphi(i,j)\}$	// reuse factor
19	$SRU_i(C_o(t)) \leftarrow NIU\{C_{Need,i}(t)\}$	// *NIU allocated carriers to SRU*
20	Else	
21	$\mathrm{CG_{ij}} = \sum_{\mathrm{i-1}}^{\mathrm{i+1}} \sum_{\mathrm{j-1}}^{\mathrm{j+1}} \sum_{\mathrm{k=1}}^{\varphi} \mathrm{CG_{ij}(k)}$;	//Fission and Assimilation; splitting allocated carriers;
22	$SRU_{ij}(C_o(t)) \leftarrow NIU(C_{ij});$	// *NIU allocated carriers to SRU*
23	Goto 5 and $Call\ \boldsymbol{PoPP}$ **;(Parallel)**	//Run the assessment again. inflate new cells; *Digestion & Absorption*
24	Else APR-2 (i,j); Goto 5;	// Reallocate Carriers
25	Else Update NIU; Goto 1;	//Network has no wobble
26	run until $\frac{\mathrm{d}}{\mathrm{dt}}\ \boldsymbol{PoPP} = \mathbf{0}$	//Egestion
27	$j \leftarrow j+1$; $(END\ j\ Loop\ first) i \leftarrow i+1$;	// All locations are covered
	$t \leftarrow t+1$; GOTO 2; **END: APR** // *END of APR*	

(5.4.2)

PERFORMANCE OF THE APR ALGORITHM

5.4.1. ANALYSIS OF THE APR ALGORITHM

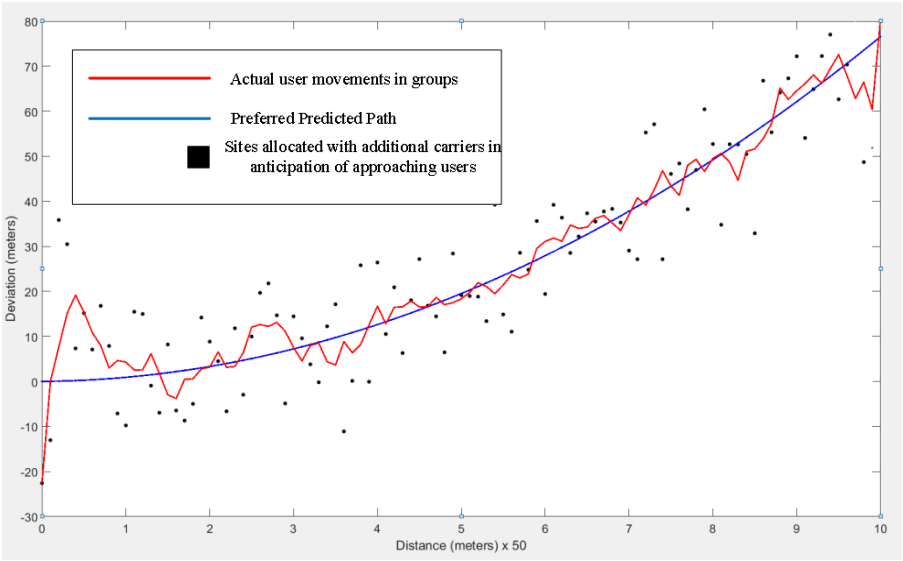

Figure 5-4-1: SCIDAS Following PTC

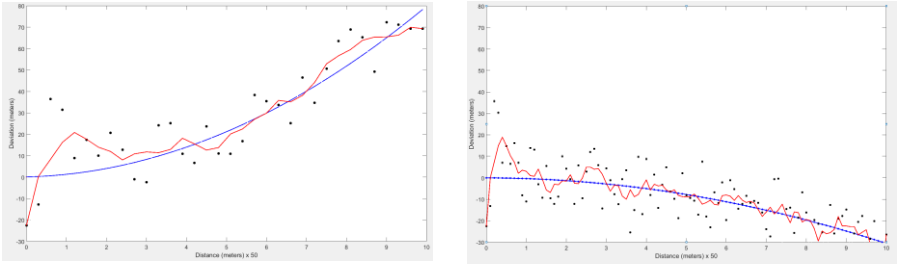

Figure 5-4-1: SCIDAS Following PTC (a) Left: users group approaching North and (b) Right: users group approaching South

Figures 5-4-1 and 5-4-2 show, how SCIDAS would follow the various accumulations from the point of entry until they exit from a SCIN's SCIWAN. This enables SCIDAS to cater for users with limited spectrum to much larger scale than the traditional architectures. By integrating the SRU cells in larger groups, a wider mobility area is offered to a user, thereby, reducing the overheads in handovers, etc.

And, by disintegrating bigger cells into smaller (tradeoff with SINR), a higher spectrum reuse can be offered.

5.5. CONCLUSIONS

We have introduced an architecture in Chapter 4 that can be developed by utilising the incumbent technologies such as DAS, WDM, and Active probing, and innovatively combining them to form a sturdy platform which, eventually, is utilised to support additional modules such as NIU and MCP that can coordinate efficiently to disseminate network resources intelligently and efficiently, especially during the extreme PTC^2 conditions This chapter complements Chapter 4 and takes care of elaborating the sensing and the intelligence of the SCIDAS. The sensing of SCIDAS in performed by the APMS architecture which resides parallely in the SCIDAS as an intelligent sub-architecture. This chapter explains in detail why the choice implementing active probing, how it is accommodated in the SCIDAS architecture and how it works, in terms of mechanisms, to sense the accumulations. We have also proposed a Self Configurability attribute that utilises severals mechanisms to dynamically respond to the ever-changing network environment. These mechanisms are expressed in the proposed algorithms. The mechanisms proposed are the CME, TDO, PTC^2EE and PoPP as the base mechanisms, which are systematically utilised by the primary mechanism that we defined in this chapter as Amoebic PTC^2 Response (APR) to support a dynamic environment. We have classified the process of accepting, managing, splitting and settling of the PTC^2 wobble as an amoebic life-cycle process. Another major contribution of this chapter was purposed to propose an innovative approach to understanding the network dynamics. This is achieved by creating a dynamics channel matrix through systematically stimulating some of the APMS probes and recording the channel response. We showed that by doing so repeatedly, we can estimate the variations between any two Transmitter-Receiver pair. This process is described in the CME algorithm. We have also used Kalman Filter method to follow the moving accumulations and this part of the PoPP algorithm..

REFERENCES

[1] A. Kumar, A. Mihovska, and R. Prasad, “Self Configurable Intelligent Distributed Antenna System for Resource Management in Multilayered Dense-nets,” in *Global Wireless Summit, 2015*, Hyderabad, India, 2015, Presented.

[2] L. Yu, L. Cheng, Y. Qiao, Y. Yuan, and X. Chen, “An efficient active probing approach based on the combination of online and offline strategies,” in *2010 International Conference on Network and Service Management*, 2010, pp. 298–301.

[3] H. Zhou, Y. Yang, X. Qiu, and Z. Gao, “The strategy of probe station selection of active probing in WSNs,” in *Network Operations and Management Symposium (APNOMS), 2014 16th Asia-Pacific*, 2014, pp. 1–4.
[4] J.-P. Linnartz, *Narrowband Land-Mobile Radio Networks*. Boston: Artech House Publishers, 1993.
[5] A. Kumar, A. Mihovska, and R. Prasad, “Spectrum Sensing in Relation to Distributed Antenna System for Coverage Predictions,” *Wirel. Pers. Commun.*, vol. 76, no. 3, doi:10.1007/s11277-014-1724-0 , pp. 549–568, Mar. 2014.
[6] D. Tse and P. Viswanath, *Fundamentals of Wireless Communication*, 1 edition. Cambridge, UK ; New York: Cambridge University Press, 2005.
[7] “Zero-forcing precoding,” *Wikipedia, the free encyclopedia*. 19-Oct-2015.
[8] A. Dickenstein and I. Z. Emiris, Eds., *Solving Polynomial Equations: Foundations, Algorithms, and Applications*, 2005 edition. Berlin ; New York: Springer, 2005.
[9] I. G. Macdonald, *Symmetric Functions and Hall Polynomials*, 2 edition. Oxford; New York: Oxford University Press, 1999.
[10] N. J. Higham, *Functions of Matrices: Theory and Computation*. Philadelphia: Society for Industrial & Applied Mathematics,U.S., 2008.
[11] G. M. Amiraliyev and I. G. Amiraliyeva, “Difference Schemes For The Singularly Perturbed Sobolev Equations,” 2007, pp. 23–40.
[12] M. K. Karakayali, G. J. Foschini, and R. A. Valenzuela, “Network coordination for spectrally efficient communications in cellular systems,” *IEEE Wirel. Commun.*, vol. 13, no. 4, pp. 56–61, Aug. 2006.
[13] M. S. Grewal and A. P. Andrews, *Kalman Filtering: Theory and Practice Using MATLAB*, 3rd Edition edition. Hoboken, N.J: Wiley-Blackwell, 2008.
[14] “computer vision - Intuitive explanation of tracking with Kalman filters - Signal Processing Stack Exchange.” [Online]. Available: http://dsp.stackexchange.com/questions/2066/intuitive-explanation-of-tracking-with-kalman-filters. [Accessed: 10-Jun-2016].

CHAPTER 6. EMPIRICAL ANALYSIS

This chapter presents the empirical realization of the research work discussed so far. In the initial sections of this chapter, we analyse the impact of the Place Time Events (PTEs) on the network dimensioning. Here, the influences of the accumulations, on both the coverage [1] and the capacity [2] of a network dimensioning, are empirically investigated. The solution to these problems, regarding a basic working model, is presented and discussed as an elaboration of our work published in [3].

6.1. INTRODUCTION

As a part of the research work, I was targeting a basic working model of the SCIDAS system. However, in addition to the practical problems and time constraints (see, Chapter1 and Chapter 2), another main constraint was persuading a network service provider to allow performing some tests on a live network. I could manage to get the permission of an Indian service provider; however, the process of finding a suitable time period when the tests could be performed with a minimum loss in the network performance was beyond the research time plan. Meanwhile, during this time, a basic model was developed and an extensive analysis, based on this basic model, was obtained. This chapter gives the empirical analysis of the investigations done so far, as discussed in the previous chapters. As the thesis targets the architectural inefficiency of the present networks to cope with the practical issues, it is important to present an empirical analysis relevant to the practical issues. This chapter presents all the empirical analysis and investigations that were conducted during the research period to endorse the relevance during real-life encounters in relation to network performance.

This chapter is organized as follows. **Section 6.2** describes the experiments performed in the city of Pune and in a suburb of Delhi real-time deployed NSPs. The cost of the solution to cater for the PTC^2 in these places was evaluated and then compared to the SCIDAS deployment hypothesis. **Section 6.3** presents the advantages of having an Active Probing Management System (APMS) by analyzing a model that senses the spectrum with the help of multiple spectrum analysers coordinated and supervised by a common computer. The experiment was performed in a mixed morphology in the Okhla area of Delhi. The results of this research experiment have been published in [3]. **Section 6.4** gives a practical evaluation of the SCIDAS deployment hypothesis in a hotspot area of Delhi, known as Connaught Place. **Section 6.5** concludes the chapter.

6.2. EMPIRICAL ANALYSIS OF PTC^2: SCIDAS APPROACH IN SOLVING THE CASE OF THE CITY OF PUNE

Ganpati Immersion Procession in Pune, India[8].

Ganpati Immersion Procession in Mumbai, India[9].

Figure 6-2-1: Prime elements responsible for PTC and PTCo "Crowd".Huge gathering and collective movements in Pune (Left) and Mumbai (Right) during Ganpati Procession

To analyse the impact of the PTC and PTCo (or jointly PTC^2), some experiments were performed on the live network operational at some places in India. The cities of Pune, Maharashtra, and Panaji, Goa, India were chosen for the PTC and PTCo analysis respectively. To analyse this impact, a live network of service providers in the City of Pune was chosen during the *Ganpati Festival*. In this festival, the people of Maharashtra (a state of India) to which the City of Pune belongs, worship the newly establish idol of Lord Ganesha (Ganpati) at their home or any sacred place for some days, and eventually immerse them in the Ocean (for Mumbai) or a holy river. During the immersion procession, there is a huge crowd gathering at different places that move collectively along a certain defined route until the immersion takes place (see, figure 6-2-1). Similarly, the City of Panaji, Goa, India was chosen during the occasion of Goa Carnival Festival. In this festival, people from various parts of the world gather in Goa for tourist interests and to participate in the carnival. This gives an opportunity of finding groups of crowd itinerating randomly in the crowd. These joint movements induce large PTC^2 impact in the network environment and are discussed in following and final subsections of this section.

Let us discuss the impact of a capacity component of the PTC^2 challenge. The Pune city was chosen due to practical convenience. Similar analysis was also conducted for other cities such as Ajmer, Bangalore, Jaipur, etc., however, only results from Pune city is presented here due to the long range of obtained data that suits the nature of this research.

[8] Source: Times of India : http://timesofindia.indiatimes.com/defaultinterstitial.cms/ Pune

[9] Source: Times of India : http://timesofindia.indiatimes.com/defaultinterstitial.cms/ Mumbai

6.2.1. PTC ANALYSIS IN THE CITY OF PUNE

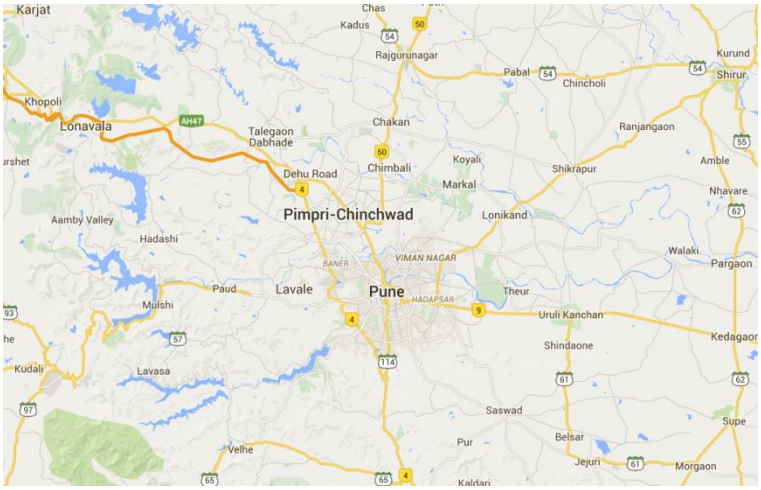

Figure 6-2-2: the city of Pune[10]

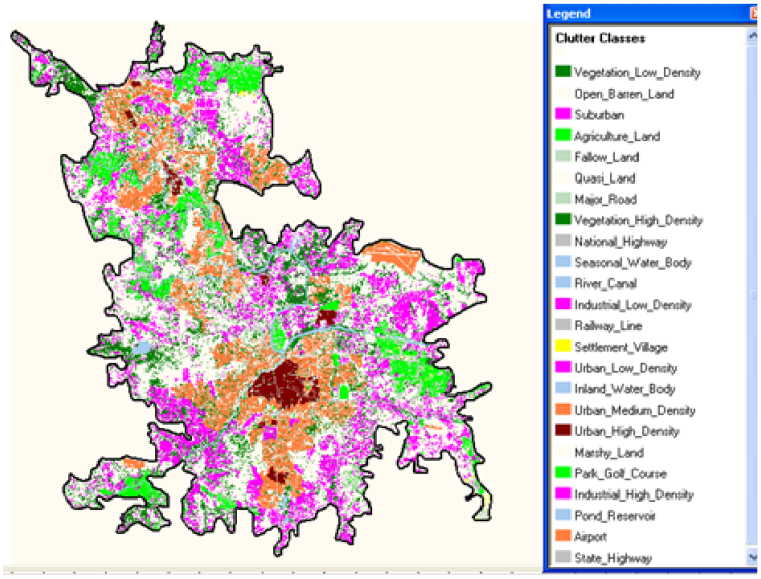

Figure 6-2-3: Clutter distribution of the City of Pune[11]

[10] Source Google® Maps

[11] Clutter details generated by Atoll ® Planning tool

Figure 6-2-2 shows the city of Pune which is chosen to discuss the Place Time Capacity (PTC) impact on a fully operational network. The clutter classification of the city is shown in figure 6-2-3, and Table 6-2-1 shows the values of these categories. It is to be noted that the clutter class NC means "Not Considered" and are the areas that were not part of the network planning and where the service provider is not "keen" to provide any guarantee of the service in these areas. Therefore, the cluttered marked with NC does not contain any network sites, which are expected to be served by the spillages of surrounding sites.

Clutter Type	Surface (km²)	Percentage	Class
Urban_High_Density	10.246	2.14	DU
Urban_Medium_Density	54.618144	11.4	MU
Airport	4.067856	0.85	MU
Urban_Low_Density	56.8146	11.85	SU
Industrial_High_Density	9.518572	1.99	SU
Suburban	7.31268	1.53	SU
Industrial_Low_Density	2.055424	0.43	SU
Quasi_Land	125.984496	26.28	RU
Open_Barren_Land	75.94092	15.84	RU
Agriculture_Land	30.322308	6.33	RU
Fallow_Land	15.300548	3.19	RU
Major_Road	8.30792	1.73	RU
National_Highway	3.008376	0.63	RU
Railway_Line	2.555888	0.53	RU
Park_Golf_Course	1.547588	0.32	RU
State_Highway	0.9407	0.2	RU
Settlement_Village	0.53958	0.11	RU
Vegetation_Low_Density	60.68304	12.66	NC
River_Canal	4.2182	0.88	NC
Seasonal_Water_Body	2.825984	0.59	NC
Vegetation_High_Density	1.243816	0.26	NC
Pond_Reservoir	0.667644	0.14	NC
Inland_Water_Body	0.56882	0.12	NC
Marshy_Land	0.02	0	NC

Table-6-2-1: Clutter classification details

Based on the clutter and capacity characteristics, the network sites for an operator in the city of Pune have been planned and deployed. The network could have been considered an Unostentatious type, if the network site planning remained intact (count and positions) until no additional subscriber base or area is incorporated in the network. However, although the subscriber and the AoI conditions remained constant during the period of the observation, the network showed ostentatious behaviour during the event of the immersion procession of Lord Ganesha in the city.

One such path and the respective serving sites (marked orange in the figures 6-2-4 and 6-2-6) were taken into consideration for observing the deviation in the planned network due to substantial PTC challenge. This path is shown as 'blue' curve from an arbitrary initial point A to the point B, which is a 'Tank' that is constructed for immersing the idol of Lord Ganesha (Site near the Tank is marked green in the figure 6-2-4 and figure 6-2-6). As per experiment, the people's gathering and

movement are observed from point ‘A’ till point ‘B’ where the idols were to be immersed.

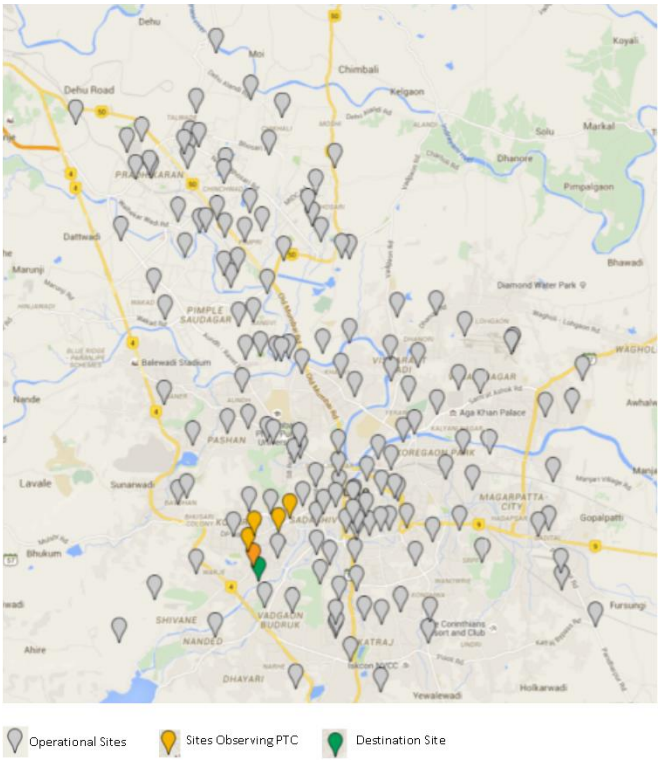

Figure 6-2-4: Operational Sites of a Service Provider in the City of Pune

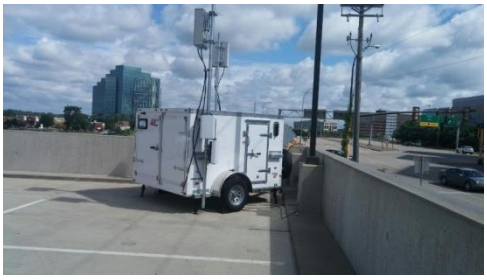

Figure 6-2-5: Cell on wheels [Source: (a) Left: General Dynamics Mission Systems, weblink: https://gdmissionsystems.com/lte/cell-on-wheels/; (b)Right: Advanced Communications and Electronics Systems Co. Ltd., weblink: http://www.aces-co.com/civil_cellonwheels_rd.html]

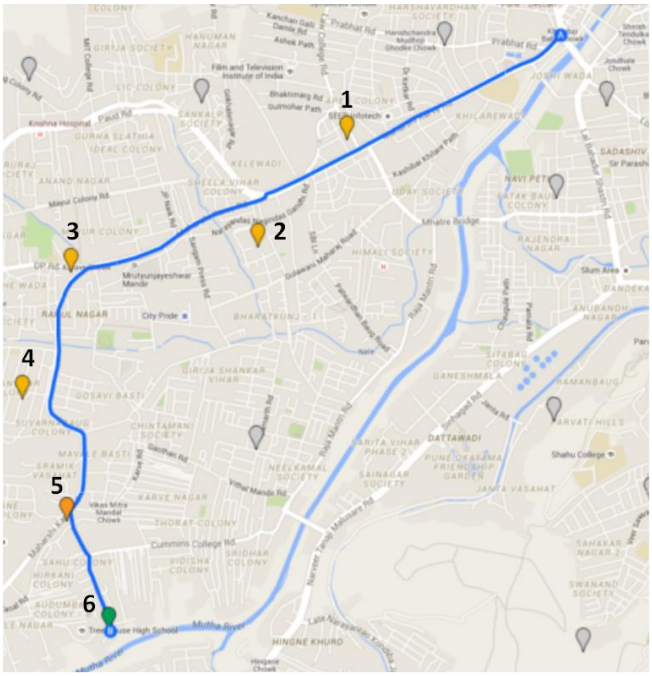

Figure 6-2-6: One of many paths in Pune chosen to observe the procession [Source: google maps]

The parametric values considered for the planning of the network are as follows:

- Maximum traffic per subscriber (T_{sub}): 40mE/ subscriber,
- Erlang Capacity of a BTS (C_{BTS}): 16 E,
- Average loading per sector (C_{load}): 11.2 E,
- Number of sector (BTS) per site (Average): 3.

Where, E is the traffic unit 'Erlangs'.

From these assumptions, we have:

(i) Total Subscriber catered per sector = $S_{PS}= \frac{C_{BTS}}{T_{sub}} = \frac{16000}{40} = 400$,

(ii) Average spare capacity per sector: $C_{avg} = C_{BTS} - C_{load} = 4.8$ E, and,

(iii) Additional subscriber catered per sector: $S_{add}= \frac{C_{avg}}{T_{sub}} = \frac{4800}{40} = 120$.

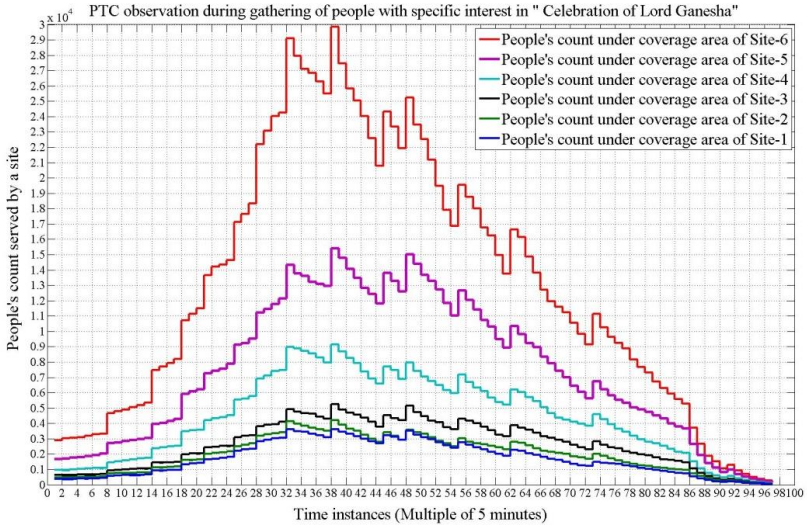

Figure 6-2-7: Statistical data of accumulation of People beneath sites 1-6 during the immersion ceremony in the City of Pune

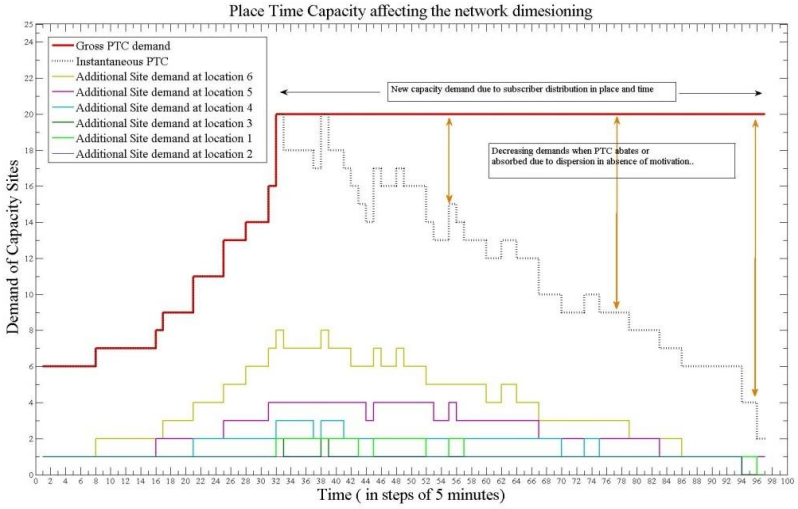

Figure 6-2-8: Variation in Network Dimensioning under the influence of PTC

When a subscriber traverses a cell and makes a call, the additional demand is created in the serving site, and if this additional demand surpasses the serving capacity of a cell, the subscriber experiences a blocking or bottleneck experience that is known as *Cell Congestion*. Hence, the subscribers attempting to make a call beyond C_{BTS} will face the 'call drops' in voice calls or decreasing throughputs for data services. Figure 6-2-7 shows the accumulation of severe PTC at sites 1 to 6 (see, figure 6-2-6). The variations in the network dimensioning, corresponding to these accumulations, is shown in figure 6-2-8.

It can be observed that Site 6 is facing humongous accumulation as it is the destination location and people wish to stay there for a longer duration whereas other groups would be joining at the same time. It is to be noted that the beginning and end of a chunk of the crowd is marked by a start and stop flags as shown in figure 6-2-9. The measurements start at the beginning of a start flag and ends with a stop flag for a chunk to keep congruency in the measurement window as shown in figure 6-2-7 and to exclude the time delay in traversing between two sites.

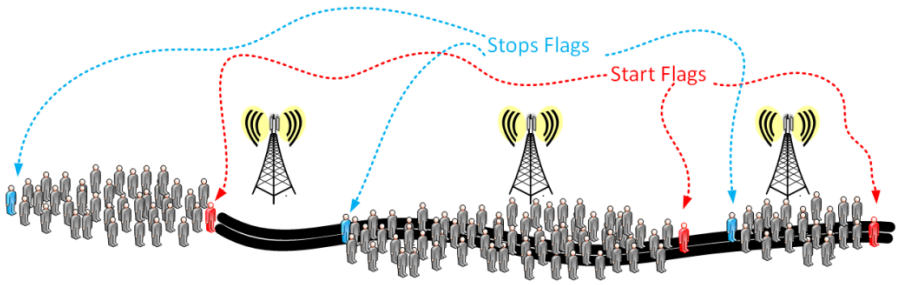

Figure 6-2-9: Flags of measurements

Assuming that only 10 percent of the accumulated subscribers are busy in making calls, the 1/10 of the accumulation was considered responsible for the actual PTC. While examining the network, it was found that some locations were poorly covered due to the blocking of a site service by a building or other significant structures. Then, using the equations **(3.5.37)** and **(3.5.40),** the $\mathbf{N_{add}}$ and $\mathbf{C_{add}}$ were calculated and the sites needed to absorb this additional PTC with respect to existing serving site are given in figure 6-2-8. As per the definition of iPTC discussed in section **3.5**, the instantaneous site demands at individual locations are described with colored and bold curves. The black dotted curve, however, shows the net iPTC which is the total demand of the AoI. It is important to note that the curves in both plots are steps which are due to the cumulative impact of the subscribers in groups as described by equation **(3.5.22)**. Therefore, when a huge group moves from one serving site to another, the demand in the later site shoots up in a very short duration thereby creating a "*staircase effect*". Figure 6-2-10 shows the location and type of the suggested additional sites to cater the PTC burst in the entire city which also shows the PTC sites for the area under examination.

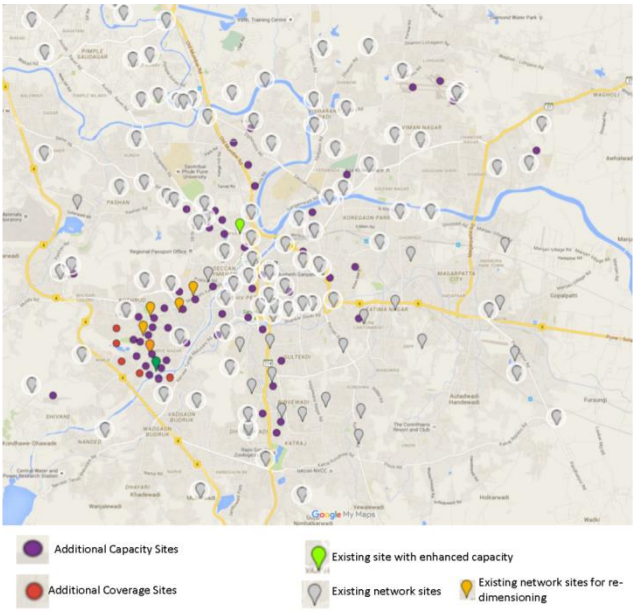

Figure 6-2-10: Network Redimensioning in PTC context

The **CME-TDO** algorithm, as discussed in sections 5.3.2 and 5.3.3, was used to identify the location of the sites. The example mentioned in the section 5.3.3 describes the process of identifying the location of the sites for the current problem. The sites suggested were temporarily deployed by Cell on Wheels (CoW, see figure 6-2-5) that were later converted to permanent sites. The deployment cost of the CoW site is very low as compared to the actual site deployment. However, the long term placement at public places may lead to high rentals and management costs.

It is important to note that although, new sites that are proposed to cater for the additional PTC may solve the problem, there will be no ARPU growth for the service provider. This is because these additional sites are not proposed to cater for new opportunities or subscriber base. Hence, the service provider has to bear the additional CAPital EXpenses (CAPEX) for a new site installation and a recurring OPerational EXpenses (OPEX) to operate these sites (rentals, maintenance, etc.). Therefore, highly dynamic and frequent PTCs may lead to humongous CAPEX and OPEX for the same network. Figure 6-2-11 shows the additional cumulative expense that the service provider may have done for installing and maintaining the additional sites for a period of 10 years. The graph in figure 6-2-11 is calculated on the basis of realistic round figures obtained from the service provider such as:

- ARPU in the AoI: $4.0 per month.

- Cost of installation of a site (Average): $ 80,000 (including equipment's cost etc.).

It can be seen that the impact of the accumulation has plunged 19 additional sites in the network which will remain underutilized for the rest of the time. However, understanding the pressure of losing users, the service provider agreed to spend $1,520,000 as CAPEX amount for the installation of these sites.

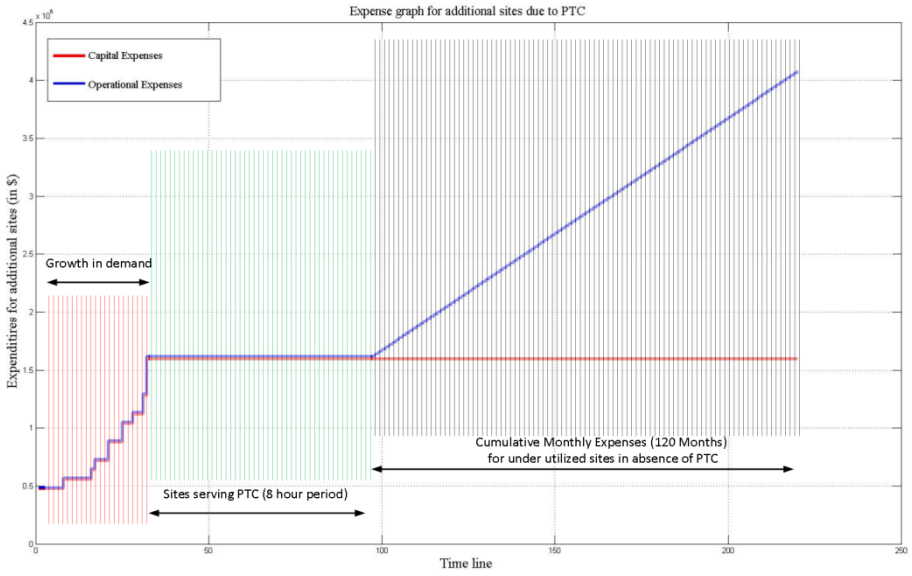

Figure 6-2-11: Expense graph of the PTC affected network

SCIDAS APPROACH IN SOLVING PTC

SCIDAS uses equations **(3.5.28)** and **(3.6.26)** to understand the network environment. For simplicity, equation **(2.5.1)** is used instead of **(3.6.26)** to evaluate coverage predictions. The following considerations were identified for this process:

(i) APMS observations: In Chapter 5 (Section 5.2), the working of APMS is explicitly discussed. APMS can replicate the observations mentioned in the figures 6-2-7 and 6-2-8 and are as below:

a. Maximum accumulation is during 30-40 samples.
b. In sample 34, the total accumulation at all buds was about 62000 people with a maximum of about 30,000 at site 6 and 15000, 8000, 4000, 3000, 2000 at buds 5,4,3,2 and 1 respectively.
c. The total length of the path under consideration is 5.7 km (see figure 6-2-12).

d. The maximum step size of accumulation is 6000 (see, figure 6-2-7, sample 32).

(ii) Network Considerations: Following are the network consideration followed by NSP while dimensioning the network.

a. Maximum traffic per subscriber 40mE,
b. Original network was planned with 4/4/4 TRXs per site, and,
c. Cluster size 4 as there are 48 channels (excluding guards) allocated to the NSP in that service area. Hence, two sites out of 6 reuse the carries.

(iii) SCIDAS considerations: Before applying the **CME** mechanism (see, Chapter 5, section 5.3), SCIDAS has the following considerations:

a. Maximum TRX that an SRU sector can support is 24 (practical design limit identified for RU during the development phase, can be increased in future). Hence, total equipped erlang per SRU, with 2% blocking probability and 10 timeslots reserved for paging, is 168 E [4],
b. The maximum subscriber catered with one SRU is 168 ÷ 40 mE = 4200 subscribers at a time,
c. Each SRU is 60% ustilised in services every time (2520 users are catered everytime, 67.2E spare), and,
d. 50% of the gathering are using the network.

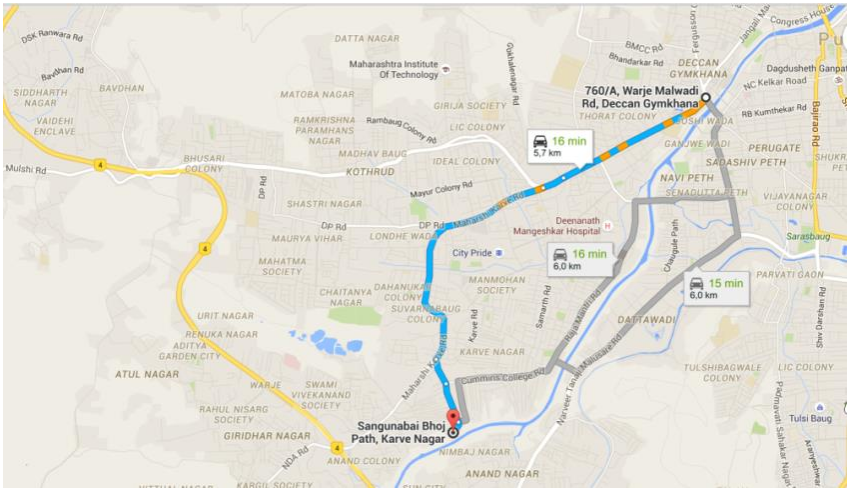

Figure 6-2-12: Path length of the chosen route [Source: google maps]

The SCIDAS approach to this challenge is discussed below:

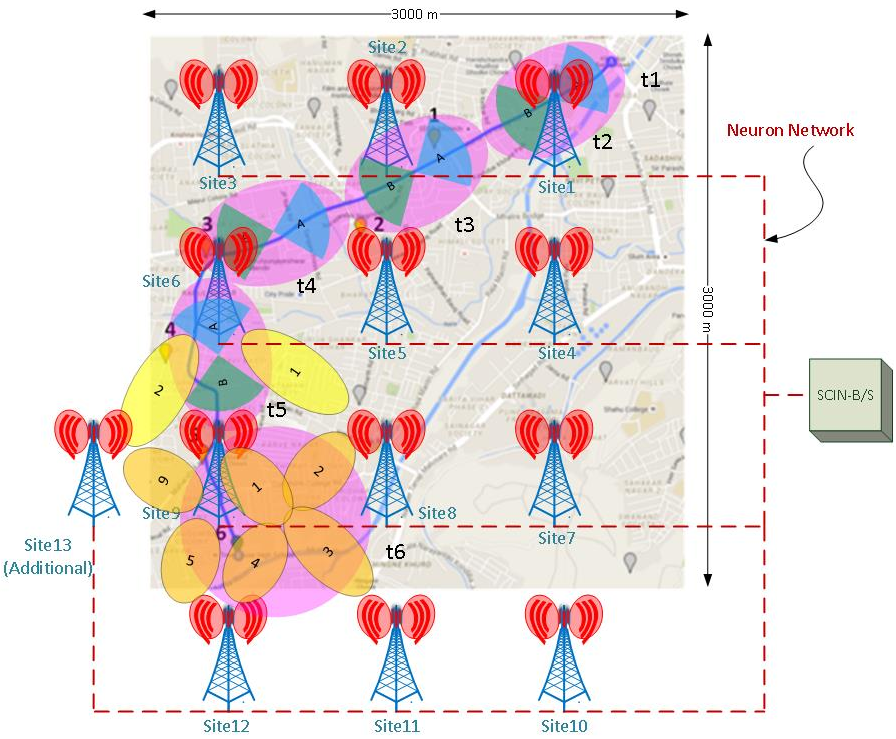

Figure 6-2-13: SCIDAS Deployment hypothesis; SRU-buds distributed across a network

Figure 6-2-13 shows the smearing of the coverage across the area through various SRU-buds. The deployment is independent of the technology and only considers propagational aspects. In this figure, the deployment is uniform for the ease of understanding. It is important to mention here that the number of SRU-buds is higher than the actual number of NSP sites in this area, however, it is less than the additional sites deployed in the network as discussed previously.

From Chapter 3, it is understood that the accumulation wobble can be solved if the PTC^2 is known. First, we consider the PTC part; **equation (3.5.28)** tells that the accumulations can be broken down into two parts, static and dynamic. Figure 6-2-7 reveals that between the sample numbers 26-32, the accumulation at site 6 (site 9 in SCIDAS) has gone up from 24,000 to 30,000 people. Assuming this extra wobble started from site 1, we can say,

- The group of 6,000 people took 30 minutes to travel 5700m or 190m per minute.

- During this time, the region around site 12 is facing an accumulation of 24,000 people.
- Only 50% of the accumulations is using the network.
- Each user can put the maximum demand of 40mE.

Therefore, applying equation (3.5.28) on above, we have:

- The iPTC generated due to movement of 3000 effective users= 120 × 190=22800 Em/s .
- The static PTC (length of imapct) due to 24,000 people = 480E.

Hence, SCIDAS in this situation (a) must hop the resources from site 1 to site 9 with 22800 Em/s and (b) must cater capacity of 480E (12000 × 0.004) throughout the time. As each SRU sector has 67.2 E spare, hence either it can borrow the additional 52.8 Erlangs (equivalent to 9 TRXs) or share the traffic between two neighbours. At present, only 24 TRXs are supported, therefore, the capability to choose neighbours to share the traffic has been implemented. Figure 6-2-13 shows the sharing of subscribers between neighbors and the share is marked as A & B. This sharing hop between the various paired sites is shown in figure 6-2-13 with the speed of 190m/s to match 22800Em/s requirement without disturbing the usual operations (represented by magenta ovals in figure 6-2-13). While SCIDAS is catering the moving subs, the static traffic near site 9 can be shared by extending the coverages of the neighbouring sites using Maneuverable and Controllable Platform (MCP, see, Chapter 4) and, sharing the traffic between 7 sites to compensate 67.2 × 7 = 430.4 Erlangs as shown in figure 6-2-1.

Achievements with SCIDAS Approach -A:

(i) Only 12 sites of SCIDAS could cater the challenge compared to the 25 (19+6) of the conventional approach. The net saving of the equipment, in this case, was 52%.

(ii) Spectrum Utilization Efficiency (SUE) [5]: In the conventional approach, an NSP can only use a portion of the spectrum which is governed by the cluster size and sectors (see, **Appendix 4.1**). Here, it is 4 carriers per sector out of 48 allocated effective carriers that could be planned to maintain cluster size of 4. Hence, the SUE, in this case, will be 4/48 = 1/12 ≈ 8.3%. With the SCIDAS solution, however, by the virtue of DAS, it is possible to use all carriers in each sector. For the present SCIDAS deployment, each sector can support 24 TRXs and therefore, SUE is 24/48 =50%. Hence, the spectrum utilization can be increased from 8.3% to 50% per sector with the SCIDAS deployment.

(iii) Previously, 25 sites were planned to be used to cater the additional accumulation. With 4/4/4/ configuration, these sites could cater 47000

users. However, the maximum effective accumulation during the event was 30,000 users. Hence, the over-planning is approximately 56%.

(iv) 19 additional sites were planned to be deployed to cater the flux. With SCIDAS, no additional sites are needed to be deployed.

This subsection discussed how the PTC has impacted the dimensioning of a capacity driven area. In the next subsection, the Place Time Coverage (PTCo) will be analysed for a coverage driven network.

6.2.2. PTC_O ANALYSIS

The coverage analysis of the challenge mentioned in the previous section refers to the experiment already discussed in Chapter 2, section 2.4 and, here, the extracts of this sub-section are discussed due to its extreme relevance in the present discussion. This experiment was performed in a slightly secluded location where the signal values from the nearby transmitters (point to point) are fairly rare. The frequency band of 1400 MHz was chosen to conduct the measurement as this AoI do not have any terrestrial mobile services in the1400MHz band which could provide decent isolation from interfering signals. Rewriting **equation (3.6.19)** we have:

$$\overline{\overline{\mathrm{PL}}}_{\omega}(\mathrm{D},\mathrm{p},\mathrm{t}) = \overline{\overline{\mathrm{PL}}}(\mathrm{D})\left(\frac{\mathrm{D}}{\mathrm{D}_0}\right)^{\mathrm{N_{AR}(m,p,t)}} \tag{6.2.1}$$

or, in decibels,

$$\mathrm{PL}_{\omega}(\mathrm{D},\mathrm{p},\mathrm{t}) = \mathrm{PL}(\mathrm{D}) + \mathrm{N_{AR}}(\mathrm{m},\mathrm{p},\mathrm{t})\log_{10}\left(\frac{\mathrm{D}}{\mathrm{D}_0}\right) \tag{6.2.2}$$

As, D, D_0, D/ D_0 and, PL(D) are constants, the equation (6.2.2) is comparable to the below equation (equation of a line curve):

$$y = mx + C \tag{6.2.3}$$

Where, $\mathrm{m} = \log_{10}\left(\frac{\mathrm{D}}{\mathrm{D}_0}\right)$ and, $\mathrm{C} = \mathrm{PL(D)}$.

Hence, in the logarithmic scale, the path-loss will experience a linear drop in its value with increase in the material concentration in the environment. To verify this mathematical expression, an experiment was conducted in the city of Panaji, Goa. The idea was to observe the received signal level at some distance while the properties of environmental elements change. The setup consists of a far off land of about 200 × 100 square-meters in dimension, as shown in the figure 6-2-10. As

mentioned earlier, the results and other details are already mentioned in **section 2.4** of **Chapter 2** and rewritten below as**:**

$$y = -76x - 28 \quad (6.2.4)$$

Where, x is the density of people per unit area.

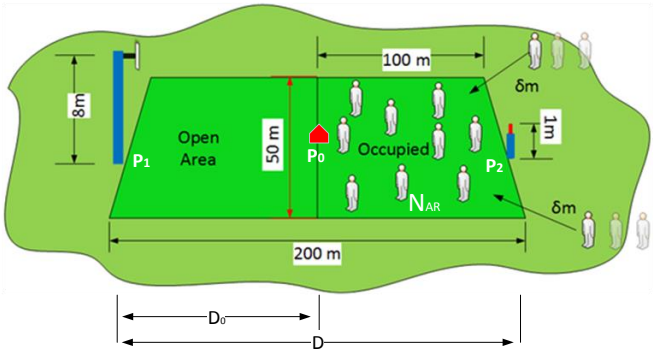

Figure 6-2-14: Experiment Setup

The field measurement details clearly show the fall in signal level on the decibel scale with the density per sq. m of people.

It was found that the 3 Km × 3 Km area could be covered by 12 (13th site is a neighbour) sites with 52 dBm of transmit power (40 dBm EIRP + 12 dBm antenna gain) to achieve an outdoor level of -85 dBm received signal strength and 95% probability. The area where 30,000 people accumulated for the immersion is about 500 × 500 sq.m. From equation (6.2.4), we can say that the density of the accumulation is 30,000 ÷ 250,000 ≈ 0.1 and, therefore, the fall in signal strength due to this accumulation density is -78 ×0.1 ≈ 8 dB. In a conventional approach this can be adjusted with power control, however, in an extreme congestion scenario, it may happen that all the 6 sites of the NSP may have to radiate 48 dBm (63 W) than 40 dBm (10 W). While APMS is monitoring the groups, the rise in power value is chosen more precisely and therefore, only sites 6,8,9,11,12, and 13 have to raise their power.

Achievements with SCIDAS Approach -B:

(i) With a conventional approach, 6 × 3 site sectors may have to compensate the raise in path-loss by raising the power from 10 W to 63 W, and, 19 smaller sites have to radiate at least 10 W. Therefore, for one hour of operation, the extra energy consumed will be 53 × 6 × 3 × 3600(= 3434 KJ) + 10 × 19 × 3 × 3600 (= 2052 KJ) = 5486 KJ. With the SCIDAS

approach, as shown in figure 6-2-13, only 4 site sectors at a time need to radiate higher power that hops along with the group (considering only a group of 6000 people is moving across a network) meaning that power consumed during the event of one hour will be 763.2 KJ and 7 site sectors to cater static PTC shall consume 1335.6 KJ. Hence, power saving with this approach will be 75.6% under normal circumstances.

(ii) It can be seen here that when accumulations happen, the signal level drops, however, SCIDAS can encash that absence of users (when they have left the place of event) as a gain of 8dB. Hence, rarefaction can be utilized by SCIDAS in network sanitization.

6.2.3. ACCOMPLISHMENTS OF SECTION 6.2

The experimental results can be summarized as follows:

(i) The subscribers' accumulations DO impact the network performance. Both the capacity and the propagations are impacted severely. This is in compliance with the theoretical investigations made in **Chapter 3** of this thesis.

(ii) In the absence of any defined technique, tackling such aberrances is the uneconomical, haphazard, bedraggled and calamitous approach. This corresponds to the alternate architectural approach that we proposed in **Chapter 4**.

(iii) The new capacity sites that were deployed that followed (i) identifying those locations affected by PTC, (ii) sharing the problem among various sites, (iii) absorbing excessive PTC by installing additional sites such that the new sites MUST only use the allocated carriers and MUST not deteriorate the SINR below an acceptable limit. Investigating this process deeply, the advantage of *Amoebic PTC*^{2} *Response* (APR) algorithm, is discussed in **Chapter 5** of this thesis is observed.

6.3. SPECTRUM SENSING AND MANAGEMENT OF A LIVE NETWORK BY A BASIC SCIDAS SETUP

The purpose of this experiment was to (i) demonstrate the working of the APMS system by mimicking it with the dedicated measuring devices that are described in details in the Chapter 1 of this thesis, and, (ii) The second measurement is the drive test measurement with drive test tool equipment provided by Agilent®. Drive tests were done to analyse the impact of the SCIDAS implementation on the AoI. A part of the results has been published in [6] [3].

The experiment mentioned in this section is already investigated in our work in [3]. Based on the findings of [3], a new series of research and investigations were carried out. The prime objective of this section is to discuss these new studies and research activities. Therefore, keeping the broad principles intact, and for the sake of clarity, without losing the original design/location of the test bed setup, analysis of results, the extracts of [3] are originally incorporated in quotes.

With a view to verifying the working of the architecture in Chapter 4, the measurement of the test carriers at a 900 MHz band of a service provider operating in the city of Delhi, India was planned. For this, a test DAS network was made, and a micro base station was configured with these test carriers. The test carriers were connected to the test DAS network. For the purpose of measurements, in the DAS network, the measuring facility was placed at each of 4 corners.

"It may be mentioned that for an efficient wireless network, it is important that the Network Management System (NMS) should know the spectrum information at every corner of the network for what it is designed to do in an efficient way [7] [8]. In a heterogeneous traditional cellular network, it is possible as the BTS/Node/Bud itself sends the local information to NMS and when all such information is collectively received from all such BTS/Nodes/Buds, the NMS is able to know the network scenario at any time instant. In a traditional DAS network, this may be a tedious task to achieve. However, if we can make a DAS network that along with its DAS capabilities has the features to extract the information from each of its nodes/buds, then this may prove to be highly preferable infrastructure system for the future networks. This network configuration may provide network information at each of its nodes/buds that may have a serving area of less than 50m radius in the extremely dense area or may be more than 500m in lower suburban areas."[3]. The spectrum sensing campaign was undertaken in the Okhla Region (Delhi, India), which are the medium urban locations of the metropolitan city of Delhi (India).

6.3.1. THE SETUP FOR THE EXPERIMENT

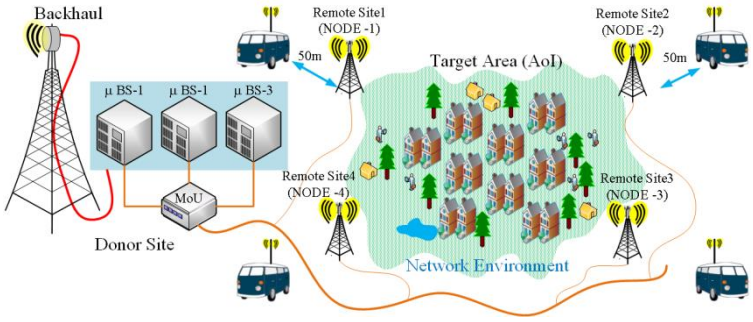

Figure 6-3-1: Graphical Representation of the deployment and the measurement setup

The test-bed setup in Okhla, Delhi was as follows [3]: “

- *An approximately 200m x 200m medium to the dense urban area of Delhi was chosen that was considered as the target area. The cellular service of a cellular service provider in that area was chosen as a test-bed for the network improvisation. Figure-6-3-1 shows the setup that was made for the measurement.*
- *Three micro base stations of service provider ‘S’ in were connected to a Master Optical Unit (MoU) that eventually connected the Remote Optical Units (RoUs) whose antennas were installed at 4 corners of A. The RoUs are places at remote sites in figure 6-3-1*[12] *such that an individual RoU has 3 antennas and RoU unit on temporary ground fixed pole [9].*
- *The micro base stations belong to serving a three-sector site and the site is referred to here as the DONOR SITE. The RF feed cables from the base stations are connected to the MoU of the cascaded DAS network and the carriers that are smeared. These micro BTS (μBS) were connected to the management center through a backhauled network.*
- *Near each of these 4 antennas, a dedicated spectrum scanning system is placed 50m away from each site. All 4 portable computers are synchronised to start and stop the measurements simultaneously through a remote access that can be done by connecting computers to wireless dongles.*
- *The setup emulates the APMS system that was proposed for the SCIDAS architecture, and it would be referred to as* ***Proxy APMS****.*
- *The GSM-900 downlink band was chosen for the spectrum analysis as the target area was primarily served by this band only by various operators.*
- *All distances of the positions were measured using the GPS positioning system.*” [3].

The portable infrastructure, as shown in figure 6-3-2 is used to place the RU equipment and as a temporary but stable system and the same system can be used for omnidirectional antennas (as shown in the figure 6-3-2) and for directional antennas.

6.3.2. MEASUREMENTS, RESULTS, AND, ANALYSIS BEFORE OPTIMISATION

(A) Prerequisites: “

[12] The sectored antenna are connected to the base equipment provided by “**Vihaan Networks Limited** (**VNL**®), Gurgaon (Gurugram), India”

- *The donor cell site already had some carrier groups that were distributed among its three sectors.*
- *As S is an active service provider the donor cell has its neighbouring cell that followed certain frequency reuse plan.*
- *In the target area and its surroundings the service provider had adapted S(4, 4, 3) frequency reuse plan where S means a sector of any cell site and 4, 4, 3 are the numbers of carriers allocated to sectors 1, 2 and 3 respectively.*
- *Except for the donor cell site, none of the other cell sites were disturbed to avoid inferring high costs to the service provider and loss of revenues.*" [3].

Figure 6-3-2: The Portable ODAS Deployment System used for testbed [9][13]

(B) The methodology of the measurement is as follows: "

- *The measurement process had two parts. First, a set of measurements were measured by the dedicated units. The equipment used to perform the measurements is detailed in* ***Appendix 1*** *of this thesis.*
- *The second set of measurements involved the drive tests that were performed in the locality. The drive test equipment was standard Agilent® drive test tool.*
- *The measurements started simultaneously at all 4 locations in sync and with negligible delay. The locations were named as node 1-4 respectively.*
- *The measurements started with the scanning of 935.0 MHz as the centre frequency at all 4 locations.*

[13] Test equipment provided by "**VNL,** India"

- *The maximum level of the received signal of the centre frequency at that time instant was recorded on all 4 computers.*
- *The scanning was then moved to the next step with a step size of 25 KHz at all 4 locations and data of maximum level was recorded on all 4 computers.*
- *The above steps are repeated till the centre frequency reaches to 960.0 MHz.*
- *The collected data were arranged to their time-stamp and made ready for analysis.*" [3].

(C) Analysis of the measured data

The post processing results of the measured data are as follows:

Figure 6-3-3: Measurements at Bud-1 (position 1)

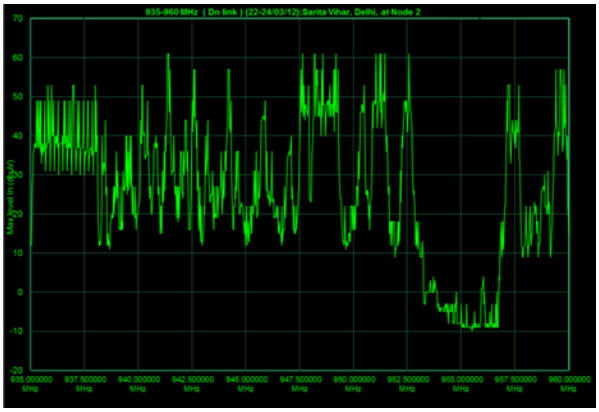

Figure 6-3-4: Measurements at Bud-2 (position 2)

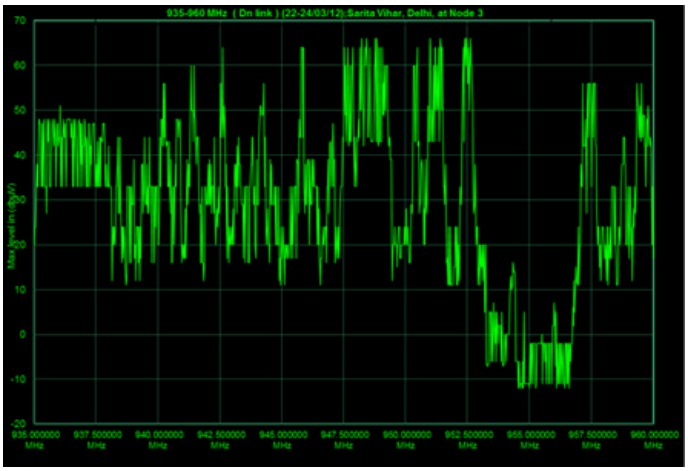

Figure 6-3-5: Measurements at Bud-3 (position 3).

Figure 6-3-6: Measurements at Bud-4 (position 4).

"The outcomes of the measured data are discussed below:

a) As mentioned earlier, figures 6-3-3 to 6-3-6 corresponds to four bud locations respectively.

b) As the first carrier of the GSM900 band is 935.2 MHz with 200 KHz as the bandwidth, the first observation point started with 935.2 MHz.

c) The outcomes of the data analysis were as follows:

(i) The frequencies from 935.2 to 950 MHz were carriers of other service providers, and the peaks belonged to sites installed nearby or collocated with the donor site and are those of other service providers.

(ii) The frequencies from 950.2 to 953.2 MHz had a mix of high peaks, low peaks, and troughs of the received values. It is observed that (a) the high peaks belong to the donor site carriers (b) the low peaks belong to the neighbors of the donor site that are a macro cell in nature, and (c) troughs contain carriers of the neighbours of the donor site that are a micro cell in nature.

(iii) The measurements of the frequencies from 953.2 to 956.8 MHz show very low values implying that the sites belonging to frequencies in this range are fairly isolated from the point of observation.

(iv) *However, it was seen that the frequencies from 954.2 to 954.4 MHz show significant high values, as shown in figures 6-3-5 and 6-3-6, which are the adjacent carriers that illuminate the area around node 3 and 4. On a physical observation, it was found that a six-storey building had been blocking node 1 and 2 from the sources of these carriers.*" [3].

d) "The results are further split into further divisions according to the received level. These divisions are as below:

(i) Received Level < 2 dBμV that is considered as too low to sustain the cellular operations.

(ii) 2 ≤ Received Level < 12 dBμV that is considered as on-road level.

(iii) 12≤ Received Level <22 dBμV that is considered as in-car level.

(iv) *22 dBμV ≤ Received Level that is considered as indoor level.*"[3].

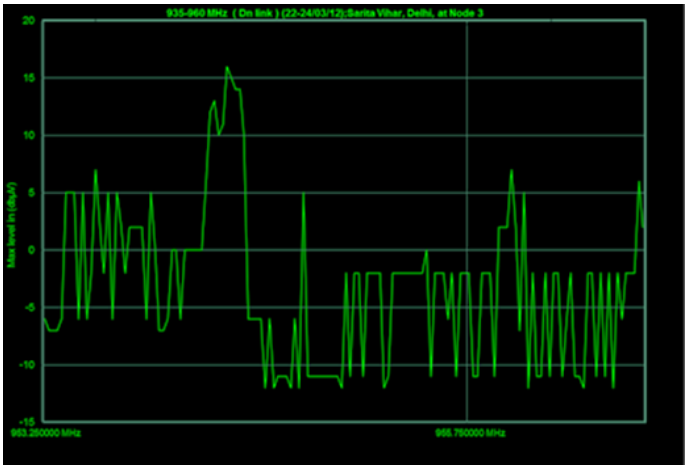

Figure 6-3-7: Obtained readings at Bud 3 for which Bud 1 readings are <7dBm

Expanding the above data for the values for which bud 1 has values less than 7 dBµV, the following plots are obtained for bud 3 and 4 to confirm the observation in sub-section 6-2-1. “

a) It was observed that 950.2 MHz and 950.4 MHz carrier bands have high values of the received level, out of which 950.2 belong to a neighbouring cell site, hence, this needs to be cured. Also, this service provider wants to enhance its capacity by adding some more carriers in system carrier group.

b) *Now, if the current service provider wants to enhance its capacity, it would select a carrier from low values of the received signals, and if it wants to reduce the interference it would remove those carriers from the carrier group that is adjacent to the neighbouring cells. The practical implementation of this example has been shown in the next section*.” [3].

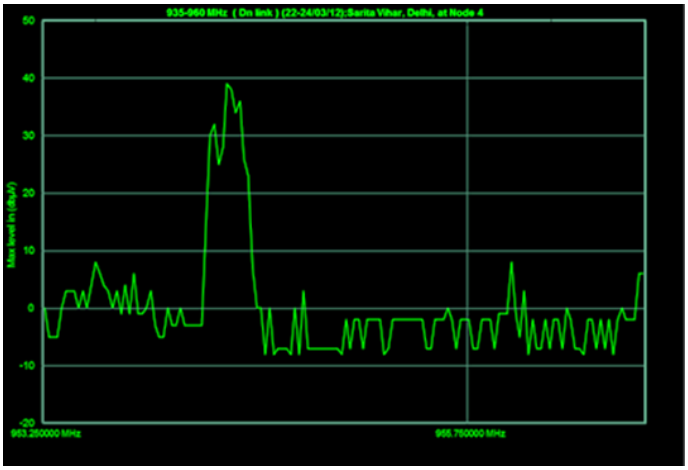

Figure 6-3-8: Obtained readings at Bud 4 for which Bud 1 readings are <7dBm

Figure 6-3-9: Drive test tool set [Source: Agilent® Technologies]

(D) Drive test: During the period when the signals were measured at the spectrum receivers at the four buds, the drive tests were also performed in the area during both, the pre and the post-optimization process. These drive-tests were performed by installing the measurement equipment in a V/UHF MMS van and mounting the receiving antenna on the roof of the vehicle. As the van moved around the area, the received signals from the receiver were recorded in a computer. Figure 6-3-9 shows the example of a drive test tool that was used for these measurements. Figures 6-3-9 and 6-3-10 show the Carrier/Interference ratio (C/I) and the signal strength measurements for pre-optimization, and, figure 6-3-15 is the C/I measurement post optimization.

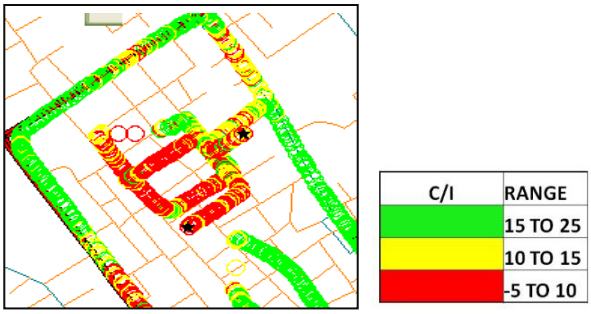

Figure 6-3-10: Carrier to Interference Ratio(C/I) in AoI before optimisation

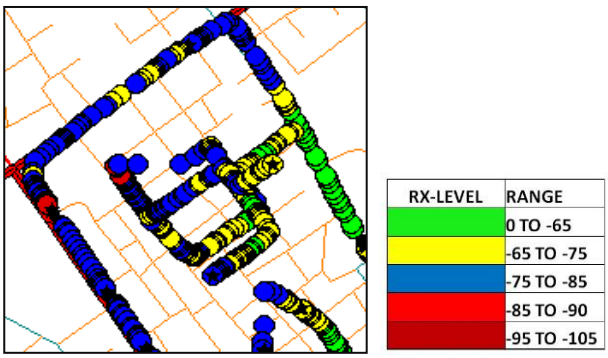

Figure 6-3-11: Signal Power Measurement in AoI

Investigating figures 6-3-10 and 6-3-11, it can be observed that although the signal levels are fairly decent in the AoI (see, figure 6-3-11), the C/I ratio is badly affected. This means that the interferers are having fairly high power levels too. Hence, the measurements obtained from the proxy APMS coincides with the drive test performed in the AoI.

6.3.3. NETWORK SANITIZATION THROUGH ACTIVE PROBING SYSTEM OF THE SCIDAS ARCHITECTURE

As per the SCIDAS architecture, the measurements obtained through APMS will be analysed, and the respective channels will be enabled or disabled as per needs. However, in the absence of an actual Network Intelligence Unit (NIU, see, **Chapter 4**), the replication of this process was performed manually. In spite of this limitation, there was a significant time saving in identifying and correcting the problem.

"*After analysing the data above, some modifications were implemented as follows:*

a) The TRXs of carriers 950.2 and 950.4 were turned off to avoid channel interference.

b) *Instead of that, the spare TRXs in any micro BS were configured with 955.2 and 955.8 as new carriers, in DAS carrier group, to enhance capacity*." [3].

(A) Post optimization measurements by Proxy APMS are as follows in figures 6-3-12 to 6-3-14:

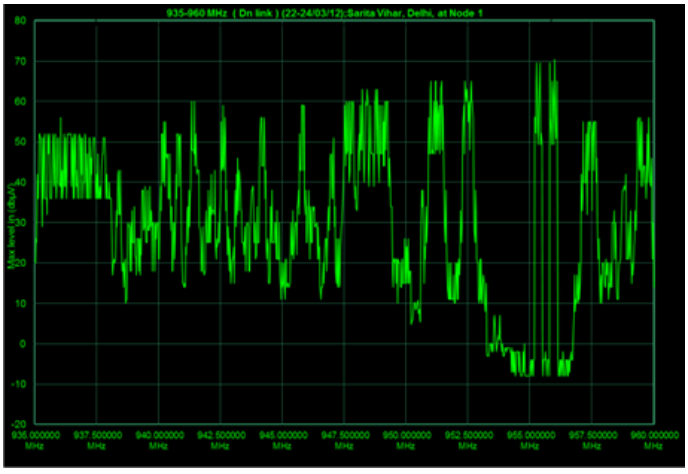

Figure 6-3-12: Post implementation measurement at Bud 1

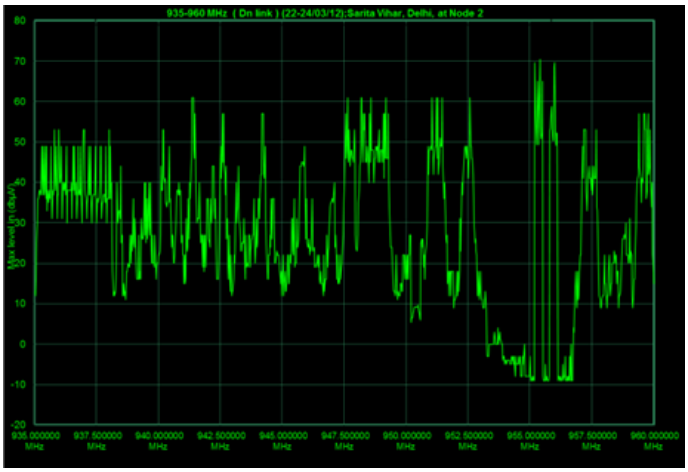

Figure 6-3-13: Post implementation measurement at Bud 2

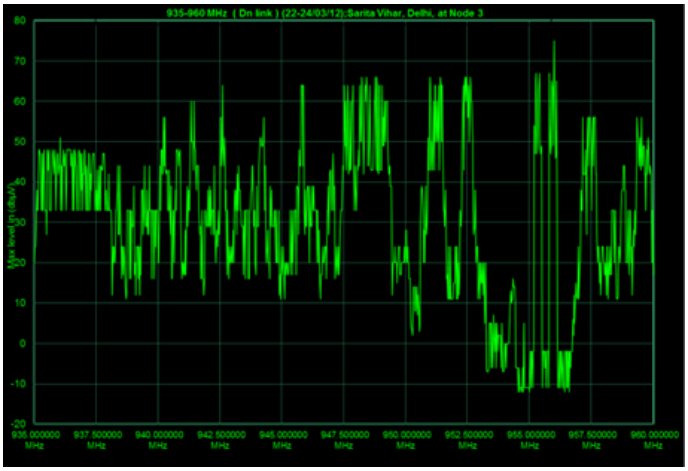

Figure 6-3-14: Post implementation measurement at Bud 3

The post-implementation measurement at the bud 4 is omitted in the present discussion as the post optimisation drive test (discussed sub-section ʻB’) was difficult in the area served by the bud 4 due to an extremely busy road passing through the area.

(B) Post optimization drive test

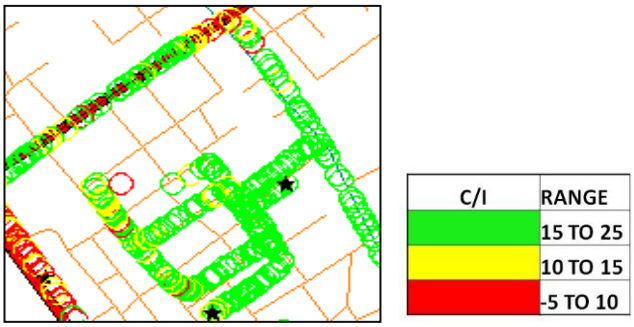

Figure 6-3-15: Carrier to Interference Ratio(C/I) in AoI after optimisation

Figure 6-3-15 shows a significant improvement in C/I ratio. This definitely provides a lot of relief to the users in this area. Figure 6-3-16 shows C/I graphs before and after optimization. It is evident that network is now more sanitized and is reflected by the C/I improvements. The net gain is extremely good; C/I samples is (518-389)/1000 =12.9%. The average Call Success Rate (CSR) is improvised from 54.5 % to 76.02%. The minimum call success rate was also improved from 20% to 32% (see, figure 6-3-17).

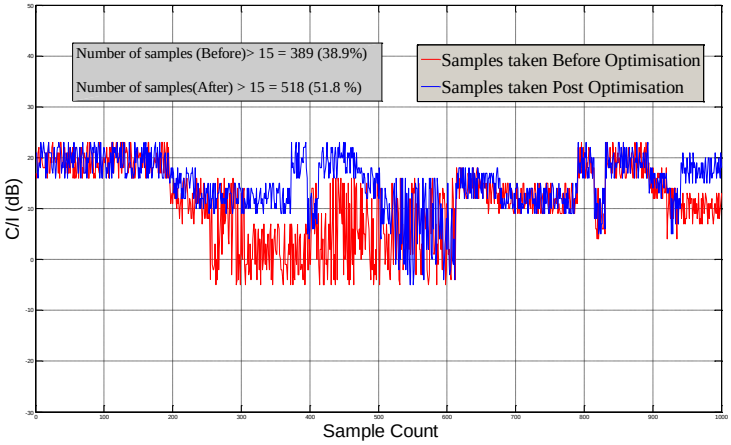

Figure 6-3-16: C/I Improvement with SCIDAS Implementation

Advantages of APMS

Apart from the sensing application, the APMS system can additionally benefit any network system, discussed as below:

1) *Capacity Enhancement*: Usually, the C/I measurements are performed by the user equipment. For this reason, several timeslots are reserved for the

paging of information. In GSM technology, 2-5 timeslots are reserved for paging, etc. [10]. Similar reservations are provided in other technologies also. Assuming that a three sectored site has 4/4/4 TRXs there will be 32 time-slots available (8 × 4) per sector. Reserving 5 for paging and SDCCH etc., we have 27 available time-slots for traffic. From the Erlang B Table in [4] we can see that, with 2% blocking probability, the equipped capacity in such case is 19.3 Erlang. **Appendix 4.2** shows the relevant portion of the Erlang B Table used for the present discussion.

The APMS can reduce the need of excessive paging, and some of the channels can be freed from paging and can be involved for capacity. Assuming, that in the influence of APMS two timeslots are freed for the traffic, again from the Erlang B Table, we have, and with 2% blocking probability the equipped capacity for 29 timeslots is 21.0 Erlangs. This means that there is 8.8% gain in offered Erlang per sector of 4 TRXs. It is important to be mentioned that with maximum subscriber traffic of 40mE, 42 additional subscribers per sector can be served just by introducing APMS System.

2) *Time and Revenue Saving:* The APMS is expected to respond quickly to the system dynamics. Hence, the 12.9% gain in C/I should be done promptly with least delay in response. Assuming that an application needs C/I> 15 everytime while a subscriber is moving in this area and the problem is detected, then, until the time the problem would be corrected, the NSP would lose 12.9% of revenue.

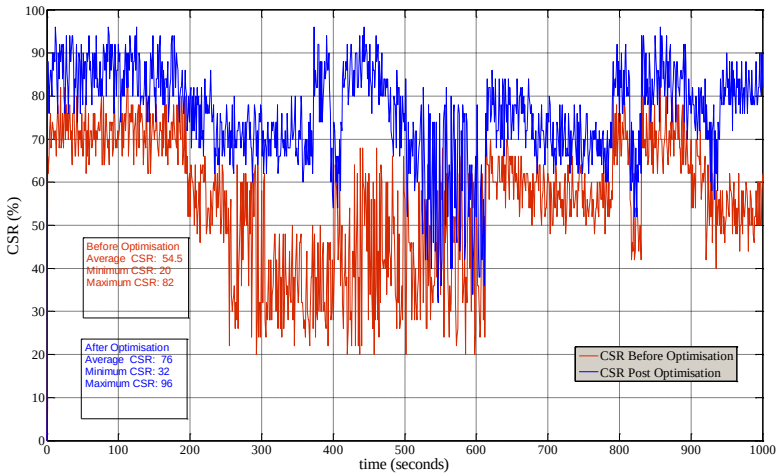

Figure 6-3-17: Call Success Rate analysis in pre and post optimisation

Let us assume that an NSP makes $100 per second from the data usage of the subscribers in that area. Then, while the subscribers are roaming in that area, it is very much probable that during 1 hour of movement, 12.9% of access time is lost. Therefore, the net loss in revenue, in this case will be 100 with a delay of 1 hour will be $ 46,440 and with a delay of 1 day, it can cost $1,114,560.

6.4. SCIDAS COVERAGE DYNAMICS IN A HOTSPOT REGION: A CASE STUDY

In this section, we analyze a case study representative of the SCIDAS dynamics and how it ought to convolve around the varying network environment. For the background scenario we have chosen the Connaught Place (CP) of Delhi as one of the areas whose morphology and demography are of high dense nature (see, figures 6-4-1 and 6-4-2). For the analysis, *Agilent E6482A Wizard Wireless Network Planning and Design Tool*[14] was used to plan and predict the coverage.

Figure 6-4-1: CP subscriber density(left[11]) and building environment(right [12])

The Site Acquisition activity is difficult in this area, and being the political hub of the country, getting permission to construct towers is this area is very difficult. Also, once the government realizes the negative effects of the towers, and starts professing a no-tower policy for urban locations, this area will be the first to get rid of towers. This will make the business case for deploying the SCIDAS.

Three roads are chosen for the initial deployment, namely:

- Inner circle Road,
- Middle circle Road,
- Outer circle Road, and,
- Radial roads.

[14] Reference: http://www.agilent.com/home

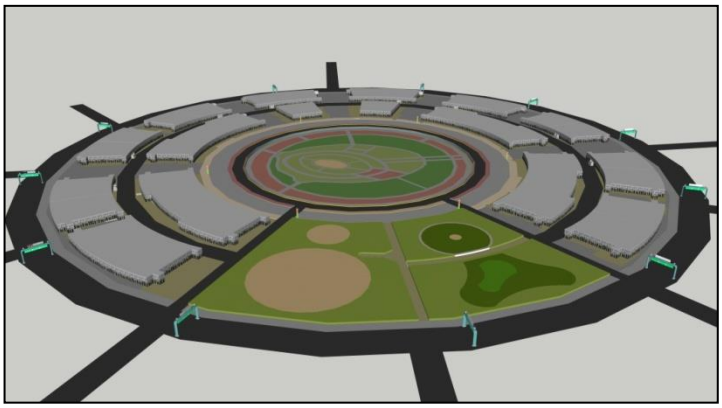

Figure 6-4-2: Overview of the CP area; inner, middle and, outer zones separated by ring roads

Methodology

The network planning is done keeping in mind the following assumptions:

(i) Antenna location: Antenna will be deployed near the lamp posts along the median of the road. On stretches not having lamp posts along the median, the lamp posts along the sides are chosen.
(ii) Antenna: Omni or Directional antenna with 11-15.5dBi gain will be mounted near the lamp post at 6m Height of 7.5m Electric Pole. The antenna will be painted in the same colour as that of the pole.
(iii) SRU: +30dBm SRU is chosen for deployment. This will provide 15 dBm PPC (power per carrier) at 32 carriers.

The following points should be noted here:

- BSs (Operators): The operators who plan to share the infrastructure shall bring in their BSs, and connect the same to the PoI. The specifications of the BS will be as per the equipment they use. However, the maximum RF output power of the BS shall not exceed +10 dBm. The typical power consumption of the BS should be specified at this RF output power.
- SMU (see, Chapter 4): The Smart Master Unit (SMU), which feeds optical power to all remotely located SRUs. SMU takes RF input from the PoI (which is a combined output of all BS sharing this infrastructure) and converts the signal to optical. This optical output should be distributed to the SRUs using a fiber pair (see, **Chapter 4** for details on SMU).
- SRU (see, Chapter 4): The Smart Remote Units (SRUs) are selected based on the composite output power and the maximum carriers that they can support. The power consumption of the SRU to be specified (see, Chapter

4 for details on SRU) based on the number of carriers that are required to be supported, as shown in Tables 6-4-1 to 6-4-3.

- The sole purpose of this design is to provide seamless coverage and capacity across the entire Connaught Place and up to 100m along the radial roads with all operators sharing the same network eventually saving their CAPEX, OPEX and reducing their security and maintenance related issues.

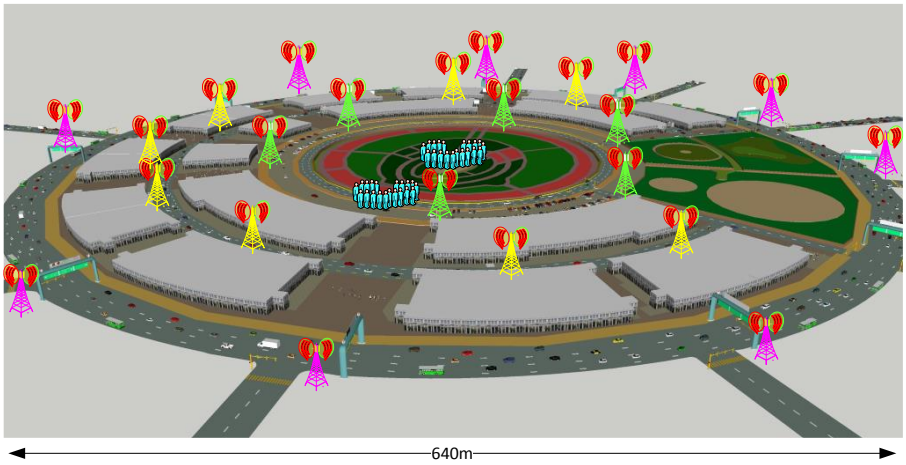

Figure 6-4-3: Planning SCIDAS network; site positions in CP inner, middle and, outer zones

Discussions: The purpose of this work was to demonstrate the working of SCIDAS in a hotspot environment under the PTC influence. A conventional DAS was planned to be utilised above which some automated system had to be laid to control the remote units. Due to practical limitations and security reasons related to a real life time deployment model, only the prediction model has been proposed and evaluated here. The power control and carrier inclusion were automated using scripts that were used by the prediction tool.

The challenge posed on the system is the following (presently GSM technology is investigated, see, Chapter 1 for explanation):

- Stage1: Initially 5000 (at 40 mE per subs traffic) users are in the CP area.
- Stage 2: A group of 5000 more users densely packed in the area of 100m ×100m walks in the groups in the circular roads of CP (see, figure 6-4-3).
- Stage 3: Another group of 5000 users enters the central park see figure 6-4-3).

SCIDAS must respond appropriately based on with the dynamics of the system. Based on the *Amoebic Place Time Response* (APR) algorithm, proposed in Chapter 4, SCIDAS, through APMS must tradeoff between the SINR, the power, and the capacity, the latter being the most desirable parameter. Assuming that there are eight NSPs in the area; the capacity dimensioning under different situations is given in Tables 6-4-1, 6-4-2 and 6-4-3. We have considered that the receiver must receive signal level above -95dBm to maintain C/I of 25 dBm.

Table 6-4-1: Configuration 1 for stage 1

CP - SCIDAS PLANNING

S. No.	No of Carriers	1	2	4	8	16	32	64
		PPC(POWER PER CARRIER)-dBm						
1	SRU27	27	24	21	18	15	12	9
2	SRU30	30	27	24	21	18	15	12
3	SRU33	33	30	27	24	21	18	15
4	SRU40	40	37	34	31	28	25	22

S. No.	Operator Name	No. of TRX	Total no. of TS	TCH Reserved for SDCCH/ GPRS	TCH (Voice)	Equipped Capacity (E)			Subscriber Supported@40mEr		
						100% FR	70% FR 30% HR	60% FR 40% HR	100% FR	70% FR 30% HR	60% FR 40% HR
1	Operator-1	4	32	5	27	19.26	26.34	29.16	482	659	729
2	Operator-2	4	32	5	27	19.26	26.34	29.16	482	659	729
3	Operator-3	4	32	5	27	19.26	26.34	29.16	482	659	729
4	Operator-4	4	32	5	27	19.26	26.34	29.16	482	659	729
5	Operator-5	4	32	5	27	19.26	26.34	29.16	482	659	729
6	Operator-6	4	32	5	27	19.26	26.34	29.16	482	659	729
7	Operator-7	4	32	5	27	19.26	26.34	29.16	482	659	729
8	Operator-8	4	32	5	27	19.26	26.34	29.16	482	659	729
	Total	32				154.1	211	233	5,136	7,024	7,776

Table 6-4-2: Configuration 2 for stage 2

CP - SCIDAS PLANNING

S. No.	No of Carriers	1	2	4	8	16	32	64
		PPC(POWER PER CARRIER)-dBm						
1	SRU27	27	24	21	18	15	12	9
2	SRU30	30	27	24	21	18	15	12
3	SRU33	33	30	27	24	21	18	15
4	SRU40	40	37	34	31	28	25	22

S. No.	Operator Name	No. of TRX	Total no. of TS	TCH Reserved for SDCCH/ GPRS	TCH (Voice)	Equipped Capacity (E)			Subscriber Supported@40mEr		
						100% FR	70% FR 30% HR	60% FR 40% HR	100% FR	70% FR 30% HR	60% FR 40% HR
1	Operator-1	6	48	5	43	21.30	28.70	31.30	533	718	783
2	Operator-2	6	48	5	43	21.30	28.70	31.30	533	718	783
3	Operator-3	6	48	5	43	21.30	28.70	31.30	533	718	783
4	Operator-4	6	48	5	43	21.30	28.70	31.30	533	718	783
5	Operator-5	6	48	5	43	21.30	28.70	31.30	533	718	783
6	Operator-6	6	48	5	43	21.30	28.70	31.30	533	718	783
7	Operator-7	6	48	5	43	21.30	28.70	31.30	533	718	783
8	Operator-8	6	48	5	43	21.30	28.70	31.30	533	718	783
	Total	48				170.4	230	250	5,680	7,653	8,347

Assuming that the users are evenly distributed among the NSPs, for the first stage, APR chooses configuration 1 to accommodate 5000 users. The prediction for this configuration (see, Table 6-4-1) is shown in figure 6-4-5. The power per carrier, in

this case, is 25 dBm with an SRU of 40dBm EIRP. When the influx of the additional 5000 users arrives in the area, configuration 2 (see, Table 6-4-2) was chosen by the APR; as a result, the power per carrier (PPC) configured for the 64 TRXs is bound to be chosen and a loss of 10 dB is imposed in the system. Further, the density of the users incurs additional 4 dBm loss (see, equation 2.5.1). To compensate this, an electrical down-tilt of 2 degrees is added in the system to compensate the loss at the bottom sites. This shrinks the coverage considerably as shown in figure 6-4-6. The drop in signal level spoils (deteriorates) the SINR by 14 dB at the central park area of CP.

Table 6-4-3: Configuration 3 for stage3

CP - SCIDAS PLANNING

S. No.	No of Carriers	1	2	4	8	16	32	64
		PPC(POWER PER CARRIER)-dBm						
1	SRU27	27	24	21	18	15	12	9
2	SRU30	30	27	24	21	18	15	12
3	SRU33	33	30	27	24	21	18	15
4	SRU40	40	37	34	31	28	25	22

S. No.	Operator Name	No. of TRX	Total no. of TS	TCH Reserved for SDCCH/ GPRS	TCH (Voice)	Equipped Capacity (E)			Subscriber Supported@40mEr		
						100% FR	70% FR 30% HR	60% FR 40% HR	100% FR	70% FR 30% HR	60% FR 40% HR
1	Operator-1	8	64	9	55	44.90	52.80	56.40	1123	1,320	1,410
2	Operator-2	8	64	9	55	44.90	52.80	56.40	1123	1,320	1,410
3	Operator-3	8	64	9	55	44.90	52.80	56.40	1123	1,320	1,410
4	Operator-4	8	64	9	55	44.90	52.80	56.40	1123	1,320	1,410
5	Operator-5	8	64	9	55	44.90	52.80	56.40	1123	1,320	1,410
6	Operator-6	8	64	9	55	44.90	52.80	56.40	1123	1,320	1,410
7	Operator-7	8	64	9	55	44.90	52.80	56.40	1123	1,320	1,410
8	Operator-8	8	64	9	55	44.90	52.80	56.40	1123	1,320	1,410
	Total	64				359.2	422	451	11,973	14,080	15,040

In Chapter 4, we discussed that the SCIDAS has the MCP that can manage the antenna azimuths, heights, and orientations both physically and electrically at individual SRU location as per need as per the NIU instructions. Now, here, when another group of 5000 subs accumulates at the central park area, SCIDAS has to play a tradeoff, and, to solve this challenge, when the subscriber concentration is dense, we simulated that the SCIDAS has raised the antenna height (using MCP modules), and the SRUs have increased the power from 30dBm to 40 dBm at each bud individually. The coverage, in this case, was enhanced sufficiently to cater for the central park as shown in figure 6-4-7 (see, legends in figure 6-4-4 to identify the received signal level). To provide the required capacity, 8 TRXs of each NSP were selected (configuration 3). However, this deteriorates the SINR because the signal of one bud would yield interference to the neighbours due to the higher power per bud. In Chapter 5, we discussed how APR algorithm maintains the SINR health at each and every bud by scanning and re-allocating the antenna configuration through MCP, iteratively. In the present case, while producing coverage plot, the APR algorithm plunged several iterations to maintain SINR > 15 dB. The seventh and sixteenth iterations are presented in figures 6-4-8 and 6-4-9 respectively. Figure 6-

4-9 also shows the final prediction incorporating 10,000 additional users and SINR> 15dB.

Legend	Rx Level Range
	> -70 dBm
	> -80dBm
	>-90dbM
	>-100

Figure 6-4-4: Legends showing the colour codes for the respective signal levels

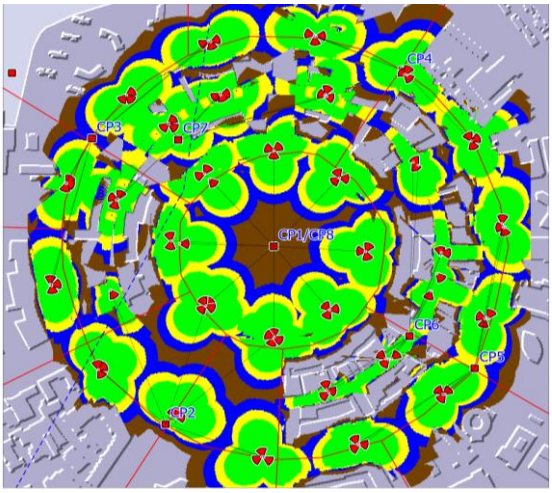

Figure 6-4-5: Coverage of CP with 5000 users (Configuration 1)

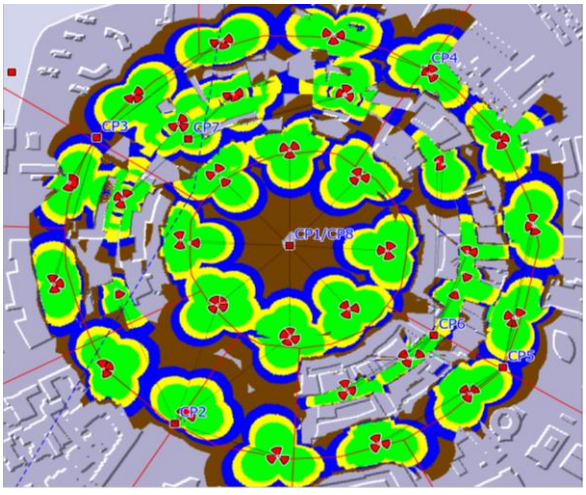

Figure 6-4-6: Coverage after accommodating 5000 additional users (Configuration 2)

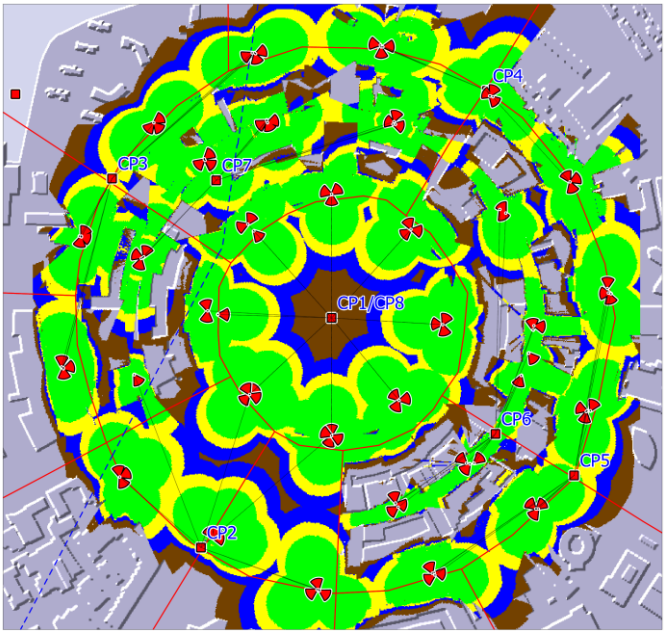

Figure 6-4-7: Coverage prediction with 5000 subs at central park (configuration 3)

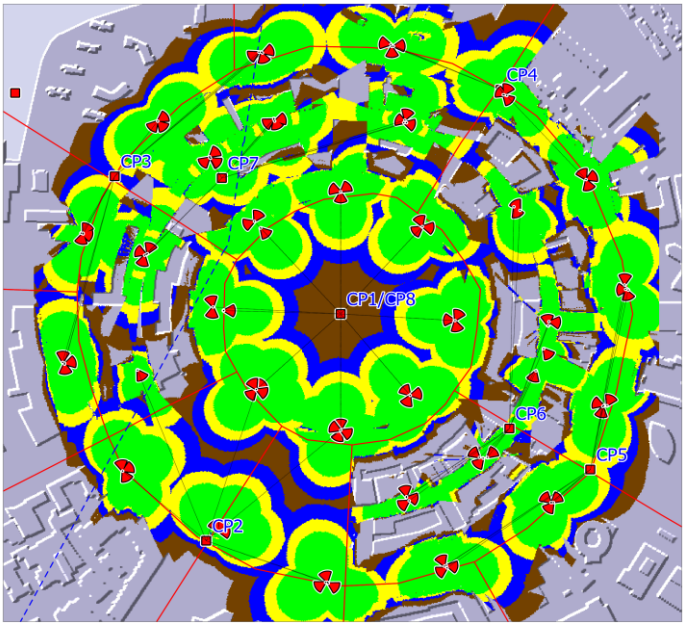

Figure 6-4-8: Coverage prediction after 7 iterations; SINR gain 4dB

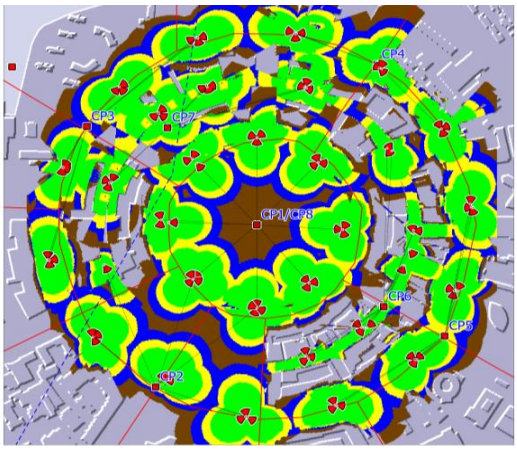

Figure 6-4-9: Coverage prediction after 16 iterations; SINR gain 10 dB

6.5. CONCLUSIONS

This chapter analyzed the concept of PTC^2 within practical and real-life scenarios. We showed how SCIDAS can be incorporated to improve the performance and provide for the required capacity at the point of time and place where this would be required. The empirical analyses discussed here are performed in three areas, city of Pune; Okhla, Delhi; and Connaught Place, Delhi. In the city of Pune, a live network was chosen to estimate the cost of PTC^2 on an NSP and compare with that of having the SCIDAS solution. It was observed that, to cater an accumulation of about 60,000 people, the NSP is planned to deploy 19 additional sites with CAPEX costing around $1,520,000. With the SCIDAS solution, it was observed that to cater the accumulations in that area of Pune; there is no need of additional sites saving 52% on equipment. The spectrum utilization per sector can be increased from 8.3% to 50% during the peak activity time; 56% of over-planning can be saved in this particular investigation. These values can vary from situation to situations. In the experiment performed in the Okhla region, it is investigated that by deploying AMPS, a gain of 12.9% in C/I ratio could be achieved in a short duration of time. The advantage of this promptness is also investigated. Lastly, the experiment in the Connaught Place was performed. The SCIDAS deployment simulation results are presented and discussed here. It was shown that with SCIDAS 17.3% resources could be saved.

REFERENCES

[1] A. Kumar, A. Mihovska, and R. Prasad, “Dynamic Pathloss Model for Future Mobile Communication Networks,” in *18th International Symposium on*

Wireless Personal Multimedia Communications (WPMC) of the Global Wireless Summit-2015, Hyderabad, India, 2015, Presented.

[2] A. Kumar, P. L. Mehta, and R. Prasad, "Place Time Capacity- A novel concept for defining challenges in 5G networks and beyond in India," in *2014 IEEE Global Conference on Wireless Computing and Networking (GCWCN)*, 2014, pp. 278–282.

[3] A. Kumar, A. Mihovska, and R. Prasad, "Spectrum Sensing in Relation to Distributed Antenna System for Coverage Predictions," *Wirel. Pers. Commun.*, vol. 76, no. 3, pp. 549–568, Mar. 2014.

[4] H. Hammuda, "Appendix B: Erlang B Table-Blocked Calls Cleared Model," in *Cellular Mobile Radio Systems*, John Wiley & Sons, Ltd, 2001, pp. 177–185.

[5] J.-P. M. G. Linnartz, "Site diversity in land-mobile cellular telephony network with discontinuous voice transmission," *Eur. Trans. Telecommun.*, vol. 2, no. 5, pp. 471–479, Sep. 1991.

[6] P. S. M. Tripathi, A. Chandra, A. Kumar, and K. Sridhara, "Dynamic spectrum access and cognitive radio," in *2011 2nd International Conference on Wireless Communication, Vehicular Technology, Information Theory and Aerospace Electronic Systems Technology (Wireless VITAE)*, 2011, pp. 1–5.

[7] D. Cabric, A. Tkachenko, and R. W. Brodersen, "Experimental Study of Spectrum Sensing Based on Energy Detection and Network Cooperation," in *Proceedings of the First International Workshop on Technology and Policy for Accessing Spectrum*, New York, NY, USA, 2006.

[8] N. Pratas, N. R. Prasad, A. Rodrigues, and R. Prasad, "Cooperative spectrum sensing: State of the art review," in *2011 2nd International Conference on Wireless Communication, Vehicular Technology, Information Theory and Aerospace Electronic Systems Technology (Wireless VITAE)*, 2011, pp. 1–6.

[9] Headquarters21B, U. V. S. 18 Gurgaon, and H. 122011 India, "Vihaan Networks Ltd." [Online]. Available: http://www.vnl.in/. [Accessed: 06-Apr-2016].

[10] "GSM NPO(NETWORK PLANNING & OPTIMIZATION) by Dinendran(patented)," *Scribd*. [Online]. Available: https://www.scribd.com/doc/23791019/.

[11] "Delhi's bumper-to-bumper traffic for the Diwali rush," *Mail Online*, 09-Nov-2012. [Online]. Available: http://www.dailymail.co.uk/. [Accessed: 07-Apr-2016].

[12] "Image: Connaught Place, New Delhi - Wikipedia, the free encyclopedia." [Online]. Available: https://www.google.com.

CHAPTER 7. CONCLUSIONS AND FUTURE WORK

This chapter presents the conclusions and intended future scope of the research expressed through this thesis.

7.1. CONCLUSIONS

The PhD research targeted solutions to problems to an MWCN that may arise due to unprecedented and random user movements in the network environment. An MWCN gives freedom to it's users to access services while roaming and being anywhere within the network. Roaming, cannot be planned, is unexpected and unpredictable, and this poses an extra burden on the network to account for such situations. Usually, all MWCNs have some extra margins or 'cushions' to cater for the user mobilities, however, the problem begins when such random movements lead to abrupt accumulations at random locations causing deterioration in the offered capacity and poor SINR in the affected area, which we referred to as the 'eccentricity of the network'. Hence, as the eccentricity depends on the time and location of the accumulations, a novel concept of Place and Time-dependent Coverage and Capacity was proposed and analysed to discover the aggregated models/ formulations of these challenges. Initially, it was contemplated to have a primitive working model of a network system that could show some intelligence in handling such issues. The Distributed Antenna System (DAS) was found to be a convenient architecture to mount an intelligence module on top of it. In a quest to find a suitable location of deploying a test-architecture, several on-site field measurements were performed in various locations of various cities across India. These measurements include (i) Spectrum occupancy measurements, (ii) Received signal level measurements, and (iii) Capacity measurements (in terms of call success rate, etc.). All the measurements were performed under the influence of user dynamics and accumulations, i.e., gradual or rapid change in the user density per unit area. Indian cities were chosen for such measurements as (i) Government of India provided the desired facilities (such as measurement vehicle etc.) to conduct these experiments, (ii) Service Provider's nod in using it's live network to perform some tests, (iii) Being a multi-cultured country, Indian cities show lots of dynamics during a course of time with different flavours and patterns which makes it easier to find suitable locations fulfilling needs of the experiment. The measurements campaigns were based on the ITU recommendations in this regard. However, due to some practical limitations and time constraints, the primitive model could not be completely developed in the given time schedule. Nonetheless, the measurements performed during the mentioned course of time hold enormous significance in this research. The measurement analyses contribute to the deeper insight in the behavior

of the network environment with users changing their positions within the network. The measurements also revealed that there was a pattern in the changing of the environmental behavior, which was the motivation for defining these occurrences as phenomena and, envisaging and formulating them.

Chapter 2 of this thesis presented these measurements in line with the recommendations of ITU and, an analysis was performed to identify such patterns. It was found that the user accumulations significantly affect the network dimensioning. The measurements performed in the city of Mumbai during the immersion ceremony of Lord Ganesha revealed that as the crowd would move from one point to another, the spectrum occupancy in the sites where the crowd is, rose rapidly, whereas the point from which the crowd has moved away showed a significant drop in spectrum utilization. This created an imbalance and a wobble of need throughout the path traversed by the crowd that compelled NSP to install temporary solutions such as CoW sites. Further, the measurements performed in Goa conceded that the influx of people between Tx and Rx systems may lead to additional losses and may transform the network environment from rural to dense urban. Similar measurements had already been performed during various occasions and by various researchers, however, finding the patterns between the signal level and concentration of people, shown as the regression line in the measurement plots, is the uniqueness of this research. The measurements presented and discussed were only a few among many similar campaigns, and others had been excluded for lack of space and to allow room for other discussions. Chapter 2 also sets up a platform for further investigations and explorations.

Chapter 3 elaborately discussed that a network must not be dimensioned based only upon land morphology and subscriber count in a service area or AoI and, that the dimensioning must incorporate the dynamics and random accumulations of users. This chapter identified the consequences of the entwining of the place and time phenomena on simple looking events, including the network dimensioning. This tangling of Place and Time with the Network Coverage and Capacity was uniquely defined, for the first time, in this chapter as the Place Time Coverage (PTCo) and Place time Capacity (PTC) or collectively as Place Time Capacity & Coverage (PTC^2). From an NSP's point of view, the PTC^2 is a perpetual challenge that would be faced endlessly in catering for its subscribers. This chapter defined the formulations of PTC^2 so that any network, which is looking for an alternate approach, can evaluate PTC and PTCo and predict the possible eccentricities. The magnitude of these phenomena is the motion of the subscribers either individually or in groups due to any arbitrary triggers, which may impede the proper absorption by the network. Unless and until the place and time repercussions are not incorporated during the capacity and coverage dimensioning of a network, as given by the PTC and PTCo formulations, the present, and future networks would be in ambivalence in handling such situations.

While Chapter 3 defined and formulised the problem of the subscriber accumulations, Chapter 4 attempted to tackle the PTC^2 by proposing an innovative, intelligent and prompt architecture that follows the normative framework of a DAS, which is a well established technique of distributing the resources over an AoI, and utilizing its capabilities to tackle such issues. As to manage the resources, the network must be iterative at every corner of its reach emphasizing the need of approachability of the intelligent module till the last destination (terminal) of the network. Therefore, the system needs to operate in such a way that the resource and intelligence may propagate parallelly in layers. This chapter proposed an innovative architecture to cater for the PTC^2. This architecture was defined as Self Configurable Intelligent Distributed Antenna Systems (SCIDAS) architecture. It hosts many attributes, holistically conceptualized for the first time in this thesis, which enhances its dexterity in accommodating future technologies. Active probing is one of its many features which is especially discussed due to its sheer importance in realizing the network environment in real-time thereby reducing the complexities in predictions and forecasting of network behaviours.

Chapter 5 evaluates the SCIDAS's performance and its ability to sense and manage the PTC^2 challenge. Here, the Active Probing (AcPro) Technique was proposed and evaluated as the sensing sub-architecture of the SCIDAS's intelligent module. The AcPro mechanism was enhanced to an APMS. Two algorithms, which were developed to be executed by APMS to sense the PTC^2 wobbles in the network, were proposed and evaluated. This chapter gave a mathematical and algorthim expression of the PTC^2 management approach. To manage the accumulations, identified by APMS, this chapter proposed and evaluated four primary algorithms that collectively work in coordination to form a holistic algorithm, defined as Amoebic Place-Time Response (APR) that works like amoebic life processes.

Chapter 6 endorsed the research work through (a) empirical analysis of the PTC proposed in Chapter 2, (ii) Presenting the working of the basic SCIDAS prototype though the relevant measurements and, (iii) evaluating the case study of Connaught Place, a suitable location in Delhi, that was chosen for deployment of SCIDAS test-bed which, however, was halted due to practical issues. The case study, however, holds good contributions in terms of the future possibility of SCIDAS deployment.

Overall this thesis concludes its research by conceiving, formulating and measuring a holistic approach aiming to resolve the issues that occur due to subscribers in motion. The holistic approach involves identifying and formulating challenges incurred due to such randomness in user motions and then suggesting a suitable method to counteract these challenges step by step. Successful conceptions and formulations of the challenges and architecture are presented in this thesis that is profoundly acknowledged by various measurement campaigns.

7.2. FUTURE SCOPE

This thesis opens ample opportunities for future research. Chapter 2 stressed on the occupancy measurements in line with the ITU recommendations. The detailed and iterative examinations of such occupancies may provide a decent structure of spectrum utilization which can be used for the evaluation of the scope and outturns of any communication technology (future or incumbent) from both, business and technological point of views.

The proposed SCIDAS architecture opens the research towards investigation of how the Universal Base Stations, Plug & Play Transceivers that can be attached to remote units, QUIKNETS for replacing CoW approaches, being some of them. Another planned research is on how to integrate the future wireless technologies such as Li-Fi and 5G for a smooth transition within the technological generations.

Chapter 5 gives ample scope of developments in algorithms that can work on an SCIDAS-like intelligent architecture. This chapter, for the first time, integrated the network with a separate and independent intelligent module. This sets up an avenue for the amalgamation of Artificial Intelligence and futuristic intelligence such as Quantum Computing to work as an independent module in managing the network resource.

Appendices

Appendix 1

Appendices of this series cover Chapter 1 of the Thesis

The measurement setup, procedures, and system settings belong to our work in [1]. For the sake of clarity and ready reference, the extracts of these descriptions have been referred and incorporated in quotes in this Appendix. The contributions of [1] are also utilised in chapters 3,5, and 6 of this thesis where they have different reference numbers.

Radio Frequency Spectrum Measurements- Systems and Procedures: A Photograph of the V/UHF Mobile Monitoring System deployed for carrying out spectrum occupancy measurements in frequency range 30-300 MHz is shown in figure 1-1.

Figure 1-1: Measurement Vehicles

Figure 1-2 : Receiving Antenna

The receiving antenna system, receiving system, procedure and desired parameters of the measurements including the operation are described in the following sub-sections.

1.1 Receiving Antenna System

"*The short monopole antennas, half-wave dipoles and high-gain antennas for reception of the radio signals are most appropriate for the measurements. For carrying out the measurements, two Omni-directional antenna systems as monitoring antenna covering the frequency bands of interest were used.*" [1]. The antennas are located at a height of 10 m above the ground. The measurements are taken at several adjacent locations (cluster of observation points) using the resultant average value, or by conducting continuously recorded measurements while moving. A typical antenna system deployed for taking measurements is depicted in the following figure 1-2.

1.2 Receiving System

The measuring receiver having inherent stability with respect to gain, frequency, bandwidth and attenuation is deployed for the measurements. Particular attention is drawn to the reference frequency to limit drifting effects on the overall accuracy of field-strength measurements. A spectrum analyser is used as a receiver, when set to zero-span, maximum hold on each frequency and the trace allowed to build up over a number of scans. A number of such measurements taken at regular intervals are then averaged to produce the field-strength reading. The measuring receiver or the spectrum analyser, when computer controlled, has been used to automate measurements and needed subsequently for data storage and analysis. "An RF cable of 15-meter length (total loss of about 3-4 dB) is connected between antenna and receiver as shown in figure 1-3. The detailed diagram of V/U MMS is described in figure 1-4. A typical block diagram of a 2 channel receiving unit installed in V/U MMs is depicted at figure 1-5. Spectrum occupancy measurement efforts for broad spectral ranges always involve a fundamental trade-off between spectral resolution, time resolution, and spectrum coverage. Band ranges are selected to match data collection and analysis needs. High-frequency resolution requires long sweep times resulting in low time resolution. The time resolution of the measurements is in the range of 5-10s, which is not small enough for detailed time-domain characterization of dynamic signals; but, it is suitable for average occupancy measurement."[1]. The sensitivity of the measurement setup is almost in the same range as the sensitivity of the user equipment in the frequency band, in which measurement are performed. It will satisfy that signals being detected for user equipment has sufficient signal to noise ratio (S/N) in the measurement, in order to separate them from the noise floor.

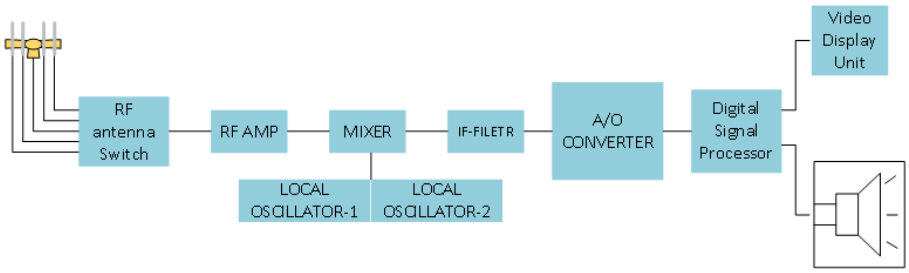

Figure 1-3: Modular diagram of the Receiver System

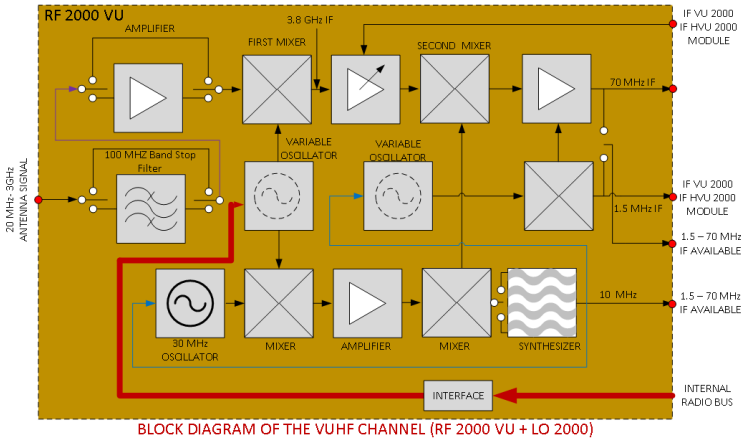

BLOCK DIAGRAM OF THE VUHF CHANNEL (RF 2000 VU + LO 2000)

Figure 1-4 : Very/Ultra High Frequency channel-receiving system

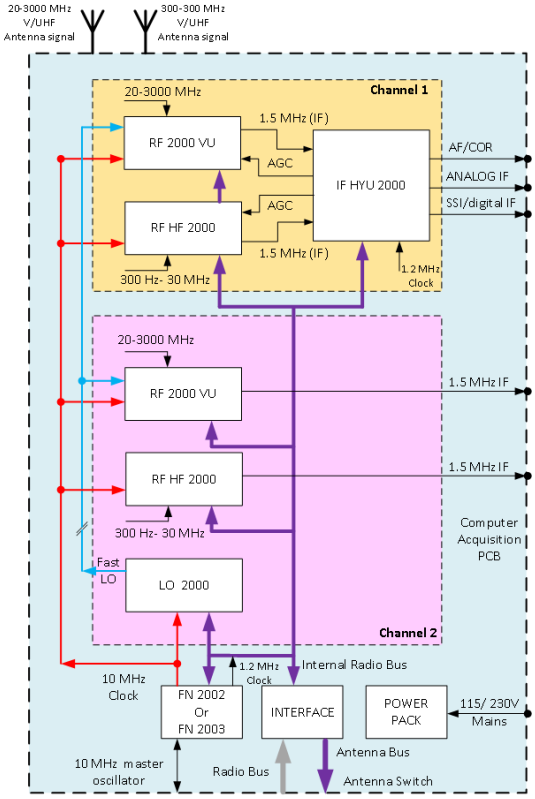

Figure 1-5: A block diagram of a 2-channel receiving unit

1.3 Procedure and desired Parameters for Measurements

Once the complete measuring setup is in position at the location of measurements, the following parameters are tuned before the start of each measurement.

1.3.1 System Settings

The dynamic range is an important parameter of the measuring system that plays two roles i.e. (i) should be sensitive enough to detect the weak signals, and (ii) need to cope with very strong signals from nearby transmitting stations. Adequate care is required for preventing overloading of the receiver during the measurement while determining the suitable RF attenuation and selecting measurement locations. The operating dynamic range of the measuring receiver should be ≥60 dB, and the receiver bandwidth should be wide enough to receive the signal including the essential parts of the modulation spectrum. It is a common practice to calibrate measuring receivers, antennas and antenna cables separately, using nationally or internationally accepted calibration procedures. But for maximum precision, the antenna, feeder, and receiver are calibrated as a single entity. "The following system settings have been made during the measurements: a) noise figure of the receiver at 7 dB, b) Step Size/Detection Filter = 500/300 kHz, c) Start Frequency = 30 MHz, Stop Frequency=3000MHz, and d) Equipment Noise floor with 300 kHz detection is about 0 dBµV" [1]. Further, the following selected factors have been used for calculating different parameters of measurements:

- Peak factor- The peak factor is used to calculate the Mean Square Values (MSV) relative to the modulation rate, frequency deviation, and phase deviation. The Peak factor is kept at 1.414 during entire V/UHF scanning.

- β Ratio- Measuring an emission bandwidth using the beta method consists in measuring the frequency bandwidth such as, below its lower limit frequency and above its upper limit frequency, each mean power transmitted is lower than or equal to a given percentage (β/2) of the total mean power of the transmission. β Ratio is kept at 1 during VHF/UHF scanning.

- Acquisition time (N * nominal duration) – is selected as 273.1 ms for the measurement.

For each sweep of a spectrum region by the receiver, the spectral occupancy (unoccupied/occupied, or 0/100%) at each measured frequency point was estimated by comparing the measured power level to a threshold. From this, the average occupancy in a given frequency range of a sweep was calculated. Repeating this

calculation for every sweep of data resulted in occupancy (%) over the period of measurements by frequency band. The thresholds used to determine occupancy are intended to be set at a fixed offset above the noise floor of the measurement system. Typically the value chosen of 10 dB was set above the noise floor. Due care was taken in choosing the occupancy threshold to avoid system induced inaccuracies in the occupancy calculations. "This system is best suited to carry out measurements close to transmitting set up. This flexibility is characterized by (a) type of vehicle (heavy duty or light), (b) spectrum analyser (s) and related accessories fitted inside the vehicle, and (c) antenna with rotator systems fitted outside vehicle, etc. With this mobile system set up, measurements have been taken in urban, semi-urban and high radio density areas. The mobile monitoring setup automatically uses the data collected relating to licensed or un-licensed information by the monitoring system. The mobile monitoring set up is equipped with a communication receiver, monitoring antennas, GPS, interconnecting cables, batteries and power supplies, etc." [1]. Once the above-mentioned parameters are set, the data displayed in ITU Measurement window are:

- Central frequency of measurements,
- Deviation between central frequency of measurement and frequency specified in the fixed frequency monitoring grid,
- values related to the antenna level measured according to different availability criteria (mean, max, square),
- values related to modulation depth, frequency deviation and phase deviation,
- Calculated bandwidth values using the X dB method on two thresholds,
- Noise measurement (spectral density, power, and noise-to-signal ratio).

1.3.2 Operation- The operation is divided into two sub-bands i.e. 20 to 700 MHz and 700-3000 MHz. The 20/700 MHz selector receives the VHF antenna signals of two sub-ranges (20/160 MHz and 160/700 MHz). There are five "antenna sub-range selectors", which select between the two ranges from control signals. Whereas, the 700/3000 MHz selector receives the UHF antenna signals by selecting the pair of dipole required in this sub-range. The spectrum analysis consists of processing samples of the real time signal to obtain results representing the signal amplitude and phase for each channel

REFERENCE

[1] Kumar, Ambuj; Mihovska, Albena D.; and Prasad, Ramjee, 'Spectrum Sensing in relation to Distributed Antenna System for Coverage Predictions', Wireless Personal Communications, Vol. 76, No. 3, doi:10.1007/s11277-014-1724-0, March 2014, p. 549-568.

Appendix 2

Appendices of this series cover Chapter 2 of the Thesis

Appendix 2.1.

2.1.1 Spectrum Allocations for IMT applications- An Indian Scenario

The radio spectrum assignments, for serving the mobile subscribers, to the service providers differ in a 'Service Area' from country to country because of legacy and other constraints. The availability of radio spectrum also depends on the number of service providers in that 'service area'. To illustrate, in many parts of the world, GSM 900 operates in the frequency band 880-915 MHz paired with 925-960 MHz, whereas in India the band is 890-915 MHz paired with 935-960 MHz. In India, the mobile subscribers are served in a service area by many operators providing 2G (GSM & CDMA) and 3G applications. At present, in India for providing mobile telecommunications services, 800 MHz (CDMA), 900 MHz (GSM), 1800 MHz (GSM) and 2100 MHz (3G) frequency bands are used. In these frequency bands, a total of 130 MHz has been earmarked for such applications. Besides the above, a total of 80 MHz is earmarked for 4G (LTE) applications. In India, an operator has been assigned a maximum of 10+10 MHz in a service area for GSM-based and, 5+5 MHz for CDMA-based applications. In so far as 3G and 4G applications are concerned, 5+5 MHz and 20 MHz (TDD mode) have been assigned respectively to an operator in a service area. A status of allocation and the actual amount of spectrum bandwidths assigned for IMT applications, in India [Source: www.wpc.dot.gov.in],is given in Table 2-1.

Appendix Table 2- 1: Status of spectrum allocation for IMT applications in India

Frequency Band (MHz)	Uplink (UL) Frequency Band (MHz)	Downlink Frequency (DL) Band (MHz)	Amount of Spectrum Stand Assigned to the Service Providers on Pan India Basis
800 (2G CDMA)	824-844	869-889	Entire 20+20 MHz.
900 (2G GSM)	890-915	935-960	Upto 25+25 MHz.
1800 (2G GSM)	1710-1785	1805-1880	Upto 55+55 MHz.
2100 (3 G)	1920-1980	2110-2170	Upto 35+35 MHz
2300 (BWA)	2300-2400	----	40 MHz (TDD mode)

It may be noted that the above-mentioned assignments are far less as compared to other countries worldwide. Hence, in India, there is an acute scarcity of radio spectrum for mobile telecommunication applications. Realizing this, for ensuring adequate availability of spectrum and its allocation in a transparent manner through market-related processes, the National Telecom Policy (2012) of the Government of India has mandated to make available additional 300 MHz spectrum for IMT services by the year 2017 and another 200 MHz by 2020 [7]. In this context, it may be mentioned that, as per the ITU-R Report No. M.2290-0 (01/2014), the estimated future radio spectrum requirements for terrestrial IMT in the year 2020 would be 1960 MHz [8].

2.1.2 Role of International Telecommunications Union in Radio Spectrum Management

The International Telecommunications Union (ITU), besides other functions inter-alia, includes allocation of global radio spectrum and satellite orbits for a variety of radio services. In a nutshell, ITU is the global regulator of the radio spectrum and functions through its Radiocommunications (R) Sector in developing frequency plans for meeting existing and future radio spectrum requirements for all the radio services. It is to mention hat for the sake of clarity and not losing the original definitions and concepts, the extract and quotes, whenever required have been taken from http://www.itu.int/en/ITU-R/. For the purpose of the allocation of frequencies, , ITU has divided the world into three Regions [9] as shown in figure 2-1.

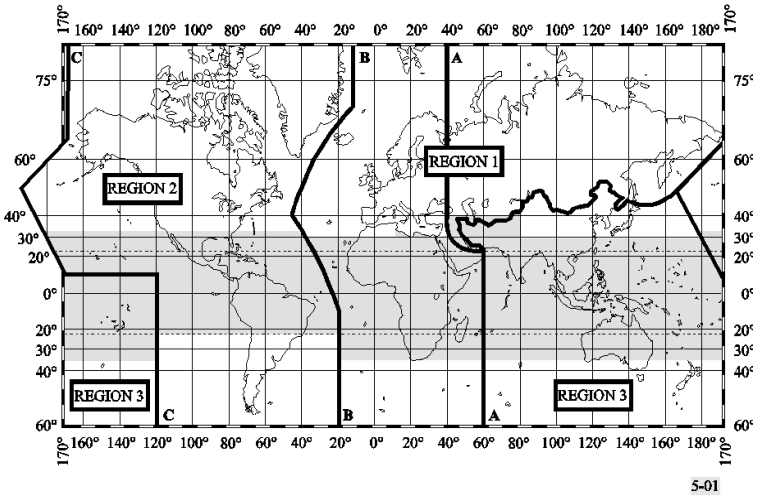

Figure 2- 1: ITU Regions

Region 1 includes the whole Europe, Africa, MiddleEast and northern part of Asia.

Region 2 covers the America.

Region 3 includes the southern part of Asia including India and Ocenia.

2.1.3 Radio Spectrum Bands

It may be mentioned that currently, UHF (300 MHz-3 GHz) and SHF (3-30 GHz), bands are the most suitable for providing commercial mobile (IMT) applications. The deployment and usages of radio spectrum for variety of radio services including for IMT applications depend on the broad principles namely:

- propagation characteristics;
- availability of technology and equipment;
- the suitability of frequency bands for specific applications;
- the Radio frequency spectrum is used efficiently, optimally and economically in conformity with the provisions of national and international laws;
- several frequency bands shall be required in order to meet both the capacity and coverage requirements; and
- high capacity and high-speed data rates are achievable in the presence of contiguous bandwidths in a single band etc.

The allocation of radio frequency spectrum for all the 41 radio services is periodically reviewed by the World Radiocommunication Conferences (WRC), normally held after every 3-4 years. The mobile (MO) service is among the radio services and each frequency band is shared among different services. The Radio Regulations (RR) is periodically revised, complementing the Constitution and the convention of ITU, and incorporating the decisions of WRC. WRC takes input from the various study groups, which perform an executive role, including the planning, scheduling, and drawing a plan for its work at least for a period of four years in advance. Each study group (SG) works through different working parties (WPs), which impart studies including on various questions. A working party prepares draft recommendations and other texts for consideration by the concerned study group including liaison statement for other interconnected study groups. If the study group finds that the urgent time-bound issues cannot be reasonably carried out by a working party, it may constitute a special Task Group (s) and ask for urgent recommendations. The radio regulations as an outcome of WRC are in the form of an international treaty, and all the member administrations are signatory to this. India is also the member administration. RRs are extremely complex with several footnotes and give a detailed picture of the distribution of spectrum for different services in all the three regions. The regional and national frequency plans can be different from the international plan by ensuring that there are no potential international interference situations.

2.1.4 Roadmap of Identification of Various Frequency Bands of IMT Applications

In the mid-1980's work began by ITU for defining the next "generation" of mobile radio standards/mobile networks on a global basis, which led to the allocations of the new globally available frequency bands. The World Administrative Radiocommunications Conference (WARC)-1992 identified 1885-2025 MHz and 2110-2200 MHz making a total of 230 MHz for the terrestrial component of the then 'Future Public Land Mobile Telecommunication Systems" (FPLMTS). At the WRC-2000, all the major existing cellular bands were added, increasing the potential IMT-2000 spectrum availability by approximately three times and also identified the frequency bands namely 806-960 MHz, 1710-1885 MHz and 2500-2690 MHz for the International Mobile Telecommunications (IMT) applications. The earmarking of these frequency bands led to the completion of ITU standards for the third generation of mobile radio technologies and its economically attractive commercial usages of IMT-2000 (3G) in the year 2000.

Further, the new services shall be provided through enhancements of 3G and IMT-Advanced (4G and beyond i.e. 5 G) in the future. The deployment of IMT shall be in accordance with the RRs. Additionally, the frequency bands (i) 450–470 MHz, (ii) 790–960 MHz, (iii) 1710–2025 MHz, (iv) 2110–2200 MHz, (v) 2300-2400 MHz, (vi) 2500-2690 MHz, and (vii) 3400-3600 MHz stand currently allocated for IMT applications.

The demand for another set of additional spectrum for capacity and coverage requirements for IMT applications was considered by WRC-12, which recommended to the ITU Council to include an Agenda item 1.1 in the agenda of WRC-15. Afterwards, a Joint Task Group (JTG) 4-5-6-7 was established for recommending additional spectrum allocations to MO services on a primary basis.

This Joint Task Group had several meetings since July 2012 until July 2014 and according to its Chairman's Report [10] had recommended more than 20 additional frequency bands for IMT applications.

The World Radio Conference (WRC)-2015 held during November 2-27, considered the recommendations of this JTG. After detailed deliberations, WRC-15 identified [Final Acts WRC 15, Geneva (Edition 2016)- http://www.itu.int/pub/R-ACT-WRC.12-2015/en]; among others the frequency bands namely 470-694/698 MHz, 1427-1518 MHz, 1885-2025 MHz, 2110-2200 MHz and 3300-3400 MHz or portions thereof for IMT applications in different Regions.

Incidentally, it may be mentioned that the recently concluded WRC-15 among other issues has also requested ITU-R to study the potential use of additional spectrum above 6 GHz for IMT, and the results of those studies will be considered at the next

WRC-19. The detailed work plan shall be on technical and operational characteristics within the frequency range between 24.25 and 86 GHz for the future development of IMT for 2020 (5 G) and beyond. Additionally, the studies are planned towards sharing and protection criteria in the aforesaid frequency bands for IMT-2020 and beyond.

Appendix 2.2.

2.2.1 A Case Study: Sharing And Compatibility Studies Of Radio Services, In The Frequency Band 470-698 Mhz

It may be mentioned that the frequency bands recommended by JTG and identified by WRC-15 as potential candidate bands for IMT applications (within the scope of MO services) are also shared with a variety of services could be fixed (FX), Mobile (MO), Satellite, Aeronautical, radio navigation and Broadcasting (BC) etc. Therefore, it is a must that detailed studies are required to be carried out for establishing in the band and out band compatibility between IMT and wireless links of other services. These studies are also dependent on local terrain/clutter shielding in an operational area of interest. Such studies would be desirable before deployment of IMT system in a frequency band. It may also be mentioned that shairing and compatibility studies should be appropriately conducted. These studies shall take into account the technical and operational characteristics of IMT systems, with that of the existing frequency bands for IMT and other services/application, including the optimization of these bands targeting to increase spectrum efficiency.

2.2.2 Interference issues and coexistence of Radio Services- Broad Principles

It is well established that while considering and analysing any interference issues, it is required to examine the technical parameters of existing and proposed assignments in the co-frequency and adjacent frequency bands. Broadly, the technical parameters, namely frequency and geographical separations and antenna orientation, which play a dominant role, are required to be evaluated for different scenarios of interference. With a view to studying sharing/co-existence of radio services within the band and out of band scenarios, the simulation models of different parts namely (i) transmitter, (ii) receiver, (iii) antennas, and, (iv) propagation paths need to be developed.

This sub-section highlights various issues needed for the studies and also reports sharing studies in a frequency band using propagation models, which in turn determine the geographical separation distances between different services operating in that frequency band. The geographical separation is normally

dependent on propagation conditions. The free space propagation conditions determine the worst level of separation distance sometimes larger distances. For any assessment of interferences, the propagation loss between a transmitting and receiving locations needs to be determined by using the propagation model (s) using terrain database of that location. Under this scenario, the Recommendations ITU-R P.452 [11] and ITU-R F.758-5 (03/2012) [12] are generally used for calculating the propagation loss, by considering the analytical approach of the propagation conditions.

However, this sub-section only considers interference scenario in terrestrial wireless links operating in a UHF band i.e. 470-698 MHz, which is one of the potential candidate bands for IMT applications. It is to mention that the frequency separation i.e. Guard Band and geographical separation are two key parameters in co-existence scenarios. As per the Recommendation ITU-R F.1191 [13], GB is defined as the frequency separation between the center frequencies of the outermost radio-frequency channels and the edge of the frequency band. GB ensures services/applications with no interference or tolerable/minimum interference. The frequency separation can be defined as [14]:

$$\Delta f = \frac{(2.5 - B_{TX})}{2} + \frac{B_{RX60}}{2} \tag{2.1}$$

Where, B_{TX} is the Emission bandwidth and, B_{RX60} is the 60 dB receiver inter-frequency bandwidth.

Another important parameter that tackles interference issues is the antenna orientation, that impacts reduction in cell size even with lower transmitted power. Several studies reveal that in a particular urban environment, the geographical separation distance decreases considerably for different interference criteria when the antenna angle is appropriately oriented. Further, possible types of interference from IMT system that have been identified impacting Fixed (FX) radio services are:-

(i) Unwanted emissions from IMT in adjacent channels;
(ii) (ii) Adjacent channel interference from unwanted emissions generated by IMT system to Fixed Radio system; and,
(iii) (iii) Co-channel interference between IMT system and Fixed Radio system etc.

It may be worth mentioning that no single frequency range satisfies all the criteria required to deploy IMT systems, particularly in countries with diverse geography and population density. Therefore, in order to meet the capacity and coverage requirements, multiple frequency ranges would be needed. However, in operational

areas, where large contiguous bandwidths are available within a single band, high capacity and high-speed data rates can be achieved.

2.2.3 Sharing Study in 470-698 MHz Band

In this sub-section, a sharing/compatibility study between the proposed IMT system and existing Broadcasting (BC) service in 470-698 MHz is presented. The allocation of various services in the frequency band 470-698 MHz for three Regions is shown in Table 2-2:-

Appendix Table 2- 2: Allocation of Services

Region 1	**Region 2**	**Region 3**
470-790 BROADCASTING	470-512 BROADCASTING, Fixed, Mobile	470-585 FIXED, MOBILE, BROADCASTING
	512-608 BROADCASTING	585-610 FIXED, MOBILE BROADCASTING RADIONAVIGATION
	608-614 RADIO ASTRONOMY Mobile-satellite except Aeronautical, Mobile-Satellite (earth-to-space)	610-890 FIXED, MOBILE, BROADCASTING, RADIONAVIGATION Fixed, Mobile
	614-698 BROADCASTING, Fixed, Mobile,	

As per the above Table, the frequency band 470-698 MHz stands allocated only for Broadcasting (BC) Services in Region 1. In Region 2, 470-512 MHz for BC as a ‘primary service’, 512-608 MHz only for BC service, 608-614 MHz for Astronomy as a ‘primary service’, and 614-698 MHz for BC as a ‘primary service’. As regards, Region 3, 470-890 MHz is allocated for Fixed (FX), Mobile (MO) and BC as ‘primary services’ except for Radionavigation in the band 585-610 MHz. Table 2-3 presents a status of 470-698 MHz band in India. It may be seen from the Table, that as per the current Indian National Frequency Allocation Plan (NFAP) 2011 [15], the broadcasting services in 470-698 MHz share with fixed, mobile, radio navigation, and radio astronomy services. In India, Television (TV) transmitters also operate in this frequency band.

Appendix Table 2- 3: Status of Frequency Band 470-698 MHz

Band	Services	Remarks
470-585 MHz	BROADCASTING, FIXED, MOBILE	The requirement of Fixed and mobile services will be considered in the frequency band 470-520 MHz and 520-585 MHz on a case-by-case basis.
585-698 MHz	FIXED MOBILE BROADCASTING RADIONAVIGATION RADIO ASTRONOMY	The requirement of Digital Broadcasting Services including Mobile TV may be considered in the frequency band 585-698 MHz subject to coordination on a case-by-case basis.

While considering, sharing studies between the proposed IMT applications and the existing Broadcasting Services in 470-698 MHz, an important parameter, the 'no-talk radius' is calculated. This parameter is the distance from the TV transmitter up to which no proposed IMT transmission shall take place. The separation distance is calculated between a proposed IMT transmitting station and TV receive station for a rural environment by calculating propagation loss deploying the modified Hata model as given in the Recommendation ITU-R SM.2028 [16]. For the calculation purposes, it has been assumed that the Indian Broadcaster has digitized their TV operations and is using two channels each of 6 MHz. With a view to allow co-existence of IMT and TV systems, an option could also be to earmark some 20 MHz for TV systems in one corner of the frequency band i.e. 470-698 MHz and also by providing sufficient GB for allowing IMT systems to operate.

Typically, a TV tower radiates power of 10 KW from an antenna height of 100 m and services several TV receivers in that coverage area. The technical parameters namely (i) tower's latitude, longitude; (ii) frequency of operation; and (iii) terrain information of the area surrounded by the TV tower are required to be known. For the purpose of calculation of 'protection separation' with a view to guaranteeing no interference to TV receivers, it may be assumed that the proposed IMT system is a radiating power of 36 dBm from an antenna height of 30 m. With these parameters of BC stations and proposed IMT systems, a 'no talk radius' and 'separation distance' have been arrived at 30 km and 100 km respectively. Hence, for safe protection, a total distance of approximately 130 km shall need to be avoided by the

IMT base stations implying that IMT system providing their service in this zone shall use the channel not used by TV transmitter.

Appendix 2.3.

Classification of Service Areas on the Basis of Mobile Traffic Handling Capacity

2.3.1 The service areas are broadly identified as under:-

a) Dense Urban (DU): DU is the area covered by sites having cells of percentile better than 90 in respect of peak traffic and traffic density. Sites, which don't have a maximum possible configuration, may not be considered.
b) Urban (U): U is the area covered by sites having cells of percentile between 70 and 90 in respect of peak traffic and traffic density. Sites, which don't have a maximum possible configuration, may not be considered.
c) Semi-Urban (SU): SU is the area covered by sites having cells of percentile between 70 and 30 in respect of peak traffic and traffic density.
d) Rural (R): R is the area covered by sites having cells of percentile between 5 and 30 in respect of peak traffic and traffic density.
e) Un-Inhabited Area (UIA): UIA is the rest of area covered by sites, not part of above DU, U, SU and R categories.

According to a definition, an extremely DU area is defined having more than 10, 00000 population and specifically, under this, the scenario includes (i) Business sites (offices of enterprises, businesses, hotels, hospitals, university campuses and similar sites), (ii) Outdoor/indoor public environments (airports, railway stations, harbours, malls, central squares of metropolitan cities and similar sites), and (iii) heavy vehicular environments etc. While urban/semi-urban areas are little/moderately populated and scarcely/sufficiently networked areas, which are mostly environments of "indoor" nature. This scenario includes (i) Small office – small to medium sized branches of offices, classrooms, small hotels, (ii) private residential establishments- houses, flats etc., and (iii) lesser density of vehicular movements. The area(s) that have (1) less scattering behaviour, (2) vacant and clean band, (3) less interference and (4) varying but predictable conditions may serve as initial deployment locations. In other words, areas that have good network conditions can be used as primary deployment locations. In order to summarize the various categories of geographical/service areas along with its typical loss values are characterized in the following Table 2.4

Appendix Table 2.4: Propagation Loss and Service Area Catagory

Category	Typical Loss Values	Area Features
Dense Urban	40 dB The loss is mainly due to thick concrete and metallic structures.	The extensive concentration of building materials like busy airports, high-rise buildings of height >30 meters, walkover bridges, metallic commodities like cars, buses, with a huge population of people. (Manhattan (US), Connaught Place (New Delhi, India)). The area covered by sites having cells of percentile better than 90 in respect of peak traffic and traffic density.
Urban	30 dB The loss is mainly due to building materials and thick concentration of population.	Market Places, offices, cafeterias, residential complex, Railway stations, buildings with height < 30 meters. The urban category also considers decently occupied stadiums and car parking. The area covered by sites having cells of percentile between 70 and 90 in respect of peak traffic and traffic density.
Sub-Urban	20 dB	Residential areas, individual houses, Industry, and Power Plants, etc. The area covered by sites having cells of percentile between 70 and 30 in respect of peak traffic and traffic density.
Rural	15 dB	Farmhouses, Agricultural and Dairy Industries. The area covered by sites having cells of percentile between 5 and 30 in respect of peak traffic and traffic density.
Open with dense low vegetation	10 dB	Countryside, Golf Course, Shooting Range, etc

The propagation area in a wider perspective is categorized in such a manner that each category represents a certain range of propagation loss. The salient challengingissues, encountered while providing an uninterrupted good quality of commercial mobile services, are:

(i) an imbalance distribution of the subscribers;
(ii) accumulation of subscribers in emergency situations like a carnival, sports/cultural events, and man-made/natural disasters;
(iii) demand for additional spectrum bandwidth;
(iv) improper utilization of assigned spectrum during day and night time; and,
(v) poor utilization of spectrum at various locations of a service area.

It is important to mention here that geography of the concerned target area is not homogeneous throughout its span and inevitably varies from point to point. The propagation loss depends on the morphology of the concerned location (foliage, concrete structures, water bodies, etc.). Therefore, the propagation loss in the entire area is not uniform and is liable to vary from point to point.

Appendix 2.4.

2.4.1 Path loss variation due to random accumulation of people - Theoretical Discussion

The outdoor channels that are stationary in time experience multipath dispersions caused by a large number of physical obstacles and can be described using the same simple path loss model. The effect, of movement of people in outdoors, on path loss, has not been studied in much detail. However, in the case of indoors, (channel, a non-stationary and is highly dynamic, due to movement of people), the effect of people movement and equipment on path loss has been studied in detail [25-27]. The gatherings of people, around a low antenna height, over short distances, appreciably vary the received signal level. This is characterized by large path losses and sharper changes in the mean signal level. It may be mentioned that any realistic channel model, besides other parameters, is characterized by the propagation path loss. In the free space, Non-Line of Sight (N-LOS) and Non-Obstructed propagation path, the received signal power Pr (dB), is expressed as:

$$\mathrm{Pr(dBm)} = \mathrm{P_t(dBm)} + \mathrm{G_r(dB)} + \mathrm{G_t(dB)} - 20\log_{10}(4\pi d/\lambda)\ \mathrm{(dB)} \qquad (2.2)$$

Wherein, Pt is the transmitter power, Gr is the receiver antenna gain, Gt is the transmitter antenna gain, d is the separation between transmitter and receiver T-R), and λ is the wavelength of the radio signal. In the presence of obstructions, the received signal will suffer additional attenuation due to movement of people, which can be accounted in the following formula:

$$\mathrm{Pr(dBm)} = \mathrm{P_t(dBm)} + \mathrm{G_r(dB)} + \mathrm{G_t(dB)} - 20\log_{10}\left(\frac{4\pi d}{\lambda}\right)\mathrm{(dB)} - \mathrm{PL} \quad (2.3)$$

Where, PL is path loss due to obstructions i.e. people's accumulation, coming in the way of the propagation path. A simple distance to power relationship, to estimate the path loss of transmitted radio signal, is used. According to this model, when the transmitter and receiver both are located in the same place and seeing each other, the path loss attenuation (dB) is given as:

$$\mathrm{PL} = \mathrm{P_0} + 10\,n\log 10\,x \quad (2.4)$$

Where, 'x' is the separation between transmitter and receiver (T-R), 'n' is the path loss exponent (an important indoor channel parameter), which is equal to a value of '2' in case of free space path loss and its value varies in NLOS obstructed path situations, 'n' may be > 2 and P_0 is the path loss at distance of 100 meters.

The gathering of a large number of people and their movement around the receiving antenna appreciably impacts on signal level that leads to the increase in path loss. Mathematically, it can be modeled with the complex impulse response function 'h (t, x) or H (ω, x)'. The rays leaving from the transmitter and arriving at the receiver location are first determined under LOS condition via specular reflections, penetrations, diffractions and combinations of these phenomena. The additional losses due to the reflection of transmitted ray by human bodies are added to the propagation loss.

The movement of people in the area of the measurement has been assumed to be scattered randomly. In shadowing events, when a group of person comes in the way of a radio signal are assumed to be independent. The propagation loss of a ray subject to multiple shadowing events on the radio signal increases by an additional loss denoted as L_{sh} (dB). In a situation, when 'N' rays are reaching the receiver, there can be 2^N combination of shadowing events. The local average propagation loss of each of event is separately calculated, which is the power sum of the losses of individual shadowed incoming rays at the receiving location. The parameter L_{sh}, the additional shadowing loss depends on a carrier frequency, polarization, individual differences among shadowing persons, the direction of the shadowing person relating to the ray, heights of transmitting and receiving antennas, nearness of shadowing position from the transmitting or receiving location and the number of people shadowing on a radio signal.

APPENDIX 3

Appendices of this series cover Chapter 3 of thesis

Appendix 3.1.

Instances as a matter of chance

The concept of probability is enigmatically attached to almost everything in our life. The growth or cells in our body, the landing of Apollo-11 and Chandrayan on the Moon, Winning a lottery, getting a movie ticket, medicine curing a disease and perhaps the most talked about event, the wave pulse reaching receiver antenna, are the successful outcomes out of many alternate possibilities. There were certainly chances that we were still struggling to reach the moon [1], the first communication device was never built, and Columbus never landed in America [2] [3], etc. As everything is a mere matter of chance, one has to deal with any event cognitively for maximum advantage. As an example, winning a lottery on a specific number is just winning or losing which can be detestable; however, a scheme of "weighted" win may bring a bit of smile on every buyer's face. Similarly, relying on the information received from pulses of the wave from an AM transmitting antenna can be catastrophic than receiving them through multiple OFDM channels from array transmitters [4] [5] [6].

STIMULANT

Whatever the experiment it may be, and whatsoever the outcomes are, there is always a "thing" that participates in the experiment. This thing may be a die, cards, missile, currency, etc. and are responsible for generating outcomes [7]. Such things are defined as *Stimulant* in this document and are considered as self-initiators of the experiment and any other actor (such as us) performing the experiment is ignored in the present discussion.

As this is a fact that, attaining a particular desired outcome out of experiment is a matter of chance, but the obvious incidences are not so obvious. As an example, anything that is tossed up must come down due to the effect of gravity is axiomatized and accepted as universal truth. However, the probability of any object falling due to gravity, howsoever large it is, is always less than one. This enigma is being created due to the definition of probability is given by:

$$P(O) = \frac{\text{Number of desired outcomes}}{\text{Total number of outcomes}} \tag{3.1.1}$$

Here, P(O) is the probability of occurrence of a set of outcomes [8]. The probability of occurrence of all outcomes of any event is unity [9]. This means that the probability of occurrence of a set of outcomes depends on the total possible

outcomes of the event, and therefore, this unity is shared by all possible outcomes of that event. Hence, the total probability is distributed among all the possible outcomes based on their chance of occurrence with maximum possible chance being a unity[9] [10]. Representing the event in terms of all possible outcomes with their respective probabilities is the probability distribution (see, section, subsections of 3.2 for the respective distribution).

As we still don't know if there exists any another possibility than falling due the effect of gravity, this probability is not deterministic [11]. However, since there have been uncountable experiments, in purpose or casual, and not a single shown any other outcome, it is deemed that all "objects" fall down. And not only that they certainly fall down, but also every time and anywhere in the Universe [12] [13]. Such kind of similar incidence/s, whose outcomes are unlikely to change with time and position is cognominated here as an *Unostentatious Event or Unostentatious Incidence / Experiment*.

Unostentatiousness is strictly in relevance to the place and time and not in terms of outcomes. This means that although it is accepted that everything must fall in a gravitational field irrespective of *what time it is* and *at what position event is happening* in the universe, but "where" is still driven by the probability. Nonetheless, for an unostentatious experiment, the contingency of an outcome depends on the way the experiment is performed. While in a game of cards, all cards have the same chance of getting drawn out of the deck in a single deal, the chance of a person visiting a supermarket is higher than visiting a single shop (as the person has more choices in a supermarket). The former is a case where the probability is flat and is an example of the "*Unbiased Unostentatious Event*" whereas the latter is a case of a biased event where the bait converges the probability to bias the occurrence of certain outcomes. As mentioned earlier, the probability of occurrences of these events is independent of position and time.

Appendix 3.2.

Unostentatious Events and Probabilities

The unostentatious event is defined here as:

Any event whose outcomes are the set of consequences of an action that is allowed to perform freely in nature has the capability to incur the same chance of occurrence to any particular outcome irrespective of when and where the action takes place.

This simply means that outcomes of an experiment remain unchanged irrespective of when and where they are performed. The detail discussion of Unostentaniety and, its various forms are discussed in details below:

3.2.1. Discrete Unostentatious Probability Distribution

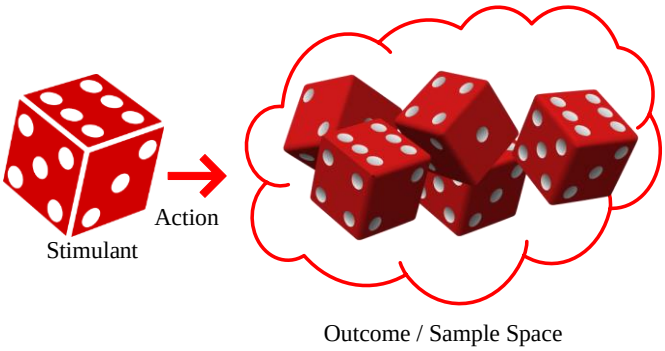

Figure 3-2- 2: A simple stimulant device, a dice, and possible outcomes

Here, we discuss an example from the basic probability study, rolling a dice (see, figure 3-2-1). Let us consider that a dice is rolled. Conventionally, in an absolute random and unbiased situation, it produces six outputs with each having the probability of 1/6 as given in equation (3.1.1) [8] [14]. Hence, it is said that "probability of occurrence of any number (output) in rolling a dice is 1/6", as shown in Table 3-2-1. This is a statistical experiment where the upward face of the dice is regarded as the output/ outcome and the value printed on the face is recorded (or sampled). As there is no such way which can let us know the exact output of a single experiment, this is often regarded as the Random Variable [9].

Appendix Table 3-2- 1: Conventional Probability outputs in an event of tossing a dice[15]

Output Type	Output Value	Probability of Occurrence
Outcome 1	Face 1:1	1/6
Outcome 2	Face 2: 2	1/6
Outcome 3	Face 3: 3	1/6
Outcome 4	Face 4: 4	1/6
Outcome 5	Face 5: 5	1/6
Outcome 6	Face 6: 6	1/6

As the probability of occurrence of any number is equally likely and is independent of its position and time, this is clearly an unostentatious event as discussed before. Nonetheless, this is also a case where the sample space is granulated (quantized) in countable outcomes. This means that whatever times the experiment is performed, the outcomes shall always convolve around the certain specific values. Therefore, this and similar simple examples like tossing a coin, drawing a card from the deck etc. are all invariably discrete events. These kinds of outcomes are discrete in nature and are countable in whole numbers. However, not all outcomes are the result of discrete steps and, therefore, may be continuous in nature.

3.2.2. Continuous Unostentatious Probability Distribution

In discrete probability, the values of outcome are quantifiable and measurable in discrete steps. Such values can be obtained by sampling an experiment at certain intervals. As another example (apart from section 3.2.1), measuring the height and weight of people passing through the main entrance of gym can provide Body Mass Index (BMI) of a person entering and exiting the gym. This can provide the business analytics a probability of a person continue to gym even after achieving the target body weight [16]. This kind of data is discrete in nature as the people visiting a particular gym are limited. However, if the same experiment is carried out in a massive flux environment, such as airports or commercial area, the data points are fairly dense and are quasi-continuous. Higher the samples, more values are obtained between any intervals. In such cases, the outcome values are continuous in nature, and the probability of occurrence is normally obtained in terms of range rather than specific values. These continuous forms of occurrences are termed as distributed probability, and the function that describes this continuous probability is termed as the Probability Distribution/Density Function (PDF) [16].

It is important to mention here that the distributive and discrete nature of an event is highly dependent on the nature of the stimulant. As an example, if the dice that is being rolled is spherical instead of a cube, the outcomes shall be continuous than six discreet values. This will also lower the probability of occurrence of any specific value as ideally, any point on the surface of the spherical dice shall have

the equal chance of being at the top and a total number of such points shall be close to infinity. Therefore, this will need infinite attempts to anticipate any specific outcome. To avoid that, a normal dice is made to be a cube than any other shape so that the probability confines to certain specific and countable orientations of the stimulant (dice) with same possibility of occurrence for each outcome [16] [17].

3.2.3. Unbiased and Biased Unostentatious Probability Distribution

In this research, an experiment is being classified into two categories depending upon its objective namely, unbiased and biased. Rolling a dice, shuffling a deck of cards, doping of an atom in a semiconductor, falling off a rain drop on window pane etc. are some incidences where the possibility of any particular outcome is equally likely. This means that every possible outcome has fair and uniform possibility of occurrence as mentioned in equation (3.1.1). Such kind of experiment is being termed in this here as an unbiased experiment and the probability of outcomes as an unbiased probability. Table 3-1 shows the probability of all possible outcomes of an unbiased experiment, i.e. rolling a dice. In an unbiased event, the stimulant is allowed to operate in an unbounded state. The outcomes of such an experiment are not entangled to any prejudice or conditions. There are many incidences where outcomes are incorporated unconditionally, and the stimulants are allowed to perform in a uniform sample space. However, not all experiments exhibit equally and likely outcomes. Shooting missiles on enemy spots, bowler targeting wicket in the game of cricket, business projections for a fiscal year, etc. are the example where the outcomes tend to converge towards a target value and outcomes of such experiments convolve around specific conditions. Such outcomes have denser probability closer to the target value and rarer otherwise.

The role of the stimulant device is also essential in making the experiment biased or unbiased. For example, if one face of the dice is heavier than others or the corner if defective, the result will not be as even as shown in Table 3-1. Therefore, the sanctity of the stimulant is also essential while evaluating the outcomes. It is deliberate to make this detoured discussion about probability and stimulant. This is to set an Athena for further sections where the play of the "*situational probability*" will be discussed.

3.2.4. BIASED OR NON-UNIFORM DISCRETE UNOSTENTATIOUS PROBABILITY DISTRIBUTION

This is yet another form of unostentatious probability that latently creeps in our activities and severely affects the consequences or outcomes. This is the most common form of probability as it is non-idealistic and therefore does not spare the granular impacts of the natural substances.

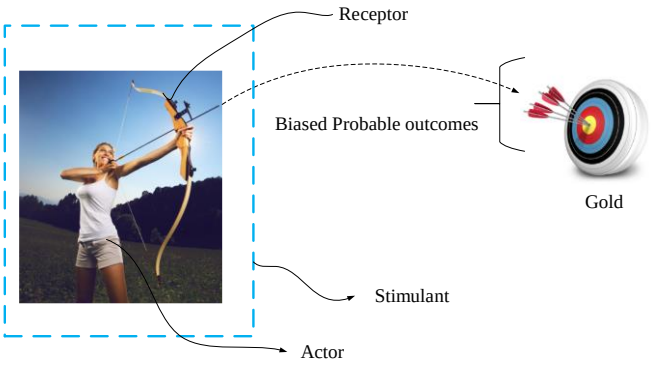

Figure 3-2-3: Archer Aiming at Bull's eye, a biased event[17] [18].

Let us consider the case of an archer (figure 3-2-1) who wants to shoot an arrow at a specific point (bull's eye or Gold). The very fact that the archer makes a deliberate attempt to shoot at a specific point makes the whole situation biased which is unlike the rolling of a fair dice where the outcomes cannot be bent to a specific number. In this case, therefore, the probability of shooting an arrow in a particular direction is not equally and unbiased and, although, the probability of an arrow hitting at a specific point is negligible, however, the possibility of finding arrow around bull's eye area is higher than in any other direction. Such events/ experiments do not have specific output but the range of outputs. If we record the distances of the hits from the "Gold" in millimeters, we get a tabular data (sample) as shown below:

Appendix Table 3-2-2: Sample Archery Data for 1000 hits, [19]

Attempt Count	Distance from Center in Millimeters	Angle in Degrees
1	367.1	92
2	242.4	111.4
3	143.5	212.6
:	:	
k	14.3	271.5
:		
1000	63.2	93.3

Plotting this dataset on the archery target board with axes markings and concentric circles (points), we can see this biased representation of the experiment. From the

plot shown in figure 3-2-3, it can be seen that outcomes are biased and the distribution of “number of occurrences” is more concentrated at the Gold and gradually decreases outwardly. This forms a “Bell Shaped” distribution also known as Gaussian Probability Density Function. A PDF is any function that describes the continuous/ continual probability distribution.

This is just not the case of archery. In fact, any experiment whose outcome is inclined towards a specific value/ condition/ situation is bound to produce a bell-shaped PDF provided that the stimulant device is not bounded in producing certain outcomes. For example in the case of archery, the stretchability and elasticity of the bow string should not be the limit in providing the initial thrust to an arrow.

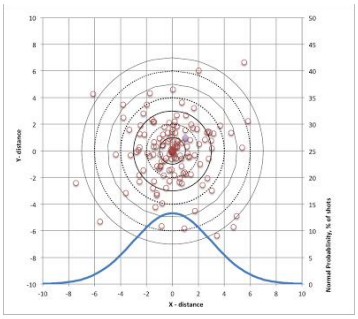

Figure 3-2- 4: Plot showing the attempted hit spots of an Archer who is targeting Gold (0, 0)

3.2.5. Biased Continuous Unostentatious Probability Distribution

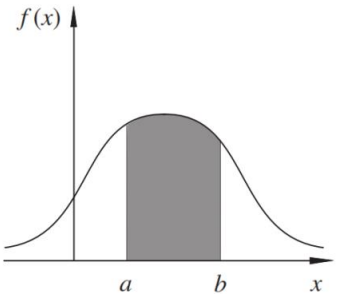

Figure 3-2-5: Normalized Probability Density Function

As the probability of occurrence of all possible outcome is unity and therefore, a PDF represents the normalized values of the true outcomes and said to be normally distributed. Figure 3-2-4 shows a normalized biased probability density function f(x) where ’x’ is an argument variable that describes the possible outcomes. Such function can be described by equation (3.2.1) as below[20] [21]:

$$\int_{-\infty}^{\infty} f(x)dx = 1 \tag{3.2.1}$$

This means that total area under the curve is a unity that corresponds to the fact that the probability of occurrence of all possible outcomes is a unity. Further, the probability that x lies between the boundaries 'a' and 'b' or P (a>x>b) will be the area shown as the shaded region in figure 3-2-4 which is as per equation below [22] [23]:

$$P(a < x < b) = \int_{a}^{b} f(x)dx \tag{3.2.2}$$

Finding the mean of a collection of values is actually identifying the value about which the values weigh even. It is the Origin which is shifted from the original axes origin to some value about which the probability is equally distributed on either side. Usually, the mean of 'n' samples is given by [23]:

$$M = \frac{\text{Total value of n outcomes}}{n} = \frac{\sum_{i=1}^{n} i * k_i}{n} \tag{3.2.3}$$

In the case of discrete probability, the ratio i/n is the probability of occurrence of the sample 'i' and k is the value of the i^{th} sample. Therefore, referring to figure 3-5, the mean of a PDF f(x) can be calculated as:

$$E(X) = \sum xP(x) \tag{3.2.4}$$

This is same as dividing the area under the f(x) curve into small strips of intervals (see, figure 3-2-5) and then multiplying each strip (or range) with the corresponding value of 'x' and then summing all such values. For continuous PDF, equations (3.2.1) and (3.2.4) can be combined to give mean of a distribution given below as:

$$\mu = E(X) = \int_{-\infty}^{+\infty} xf(x)dx \tag{3.2.5}$$

Where 'x' is the domain or the samples of a Random Variable 'X' of a continuous distribution. The Variance of such a distribution measures how far the values are from the mean as below [22] [23]:

$$V(X) = E(X^2) - \mu^2$$

or, $$V(X) = \int_{-\infty}^{+\infty} x^2 f(x)dx - \mu^2$$

or, $$V(X) = \int x^2 f(x)dx - \mu^2 \quad (3.2.6)$$

The variance is also the square of the Standard Deviation (SD) as mentioned below:

$$\sigma^2 = V(x) \quad (3.2.7)$$

A normal of Gaussian PDF of a random variable X is represented by,

$$f_X(x) = \frac{1}{\sqrt{2\pi}\,\sigma} e^{[-\frac{(x-\mu)^2}{2\sigma^2}]} \quad (3.2.8)$$

Where, μ and σ are the Mean and SD as discussed in equations (3.2.5) and (3.2.7).

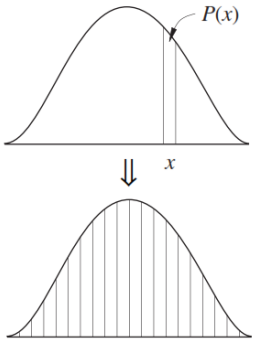

Figure 3-2-6: Mean and Variance of a PDF

REFERENCES

[1] A. Chaikin and T. Hanks, *A Man on the Moon: The Voyages of the Apollo Astronauts*, Reissue edition. New York, N.Y: Penguin Books, 2007.

[2] *Works Issued by the Hakluyt Society*. The Society, 1893.

[3] L. N. McAlister, *Spain and Portugal in the New World: 1492-1700*. University of Minnesota Press, 1984.

[4] N. Blaunstein, *Radio Propagation in Cellular Networks*, 1st ed. Norwood, MA, USA: Artech House, Inc., 1999.

.

[5] S. Kaiser, “On the performance of different detection techniques for OFDM-CDMA in fading channels,” in *IEEE Global Telecommunications Conference, 1995. GLOBECOM ’95*, 1995, vol. 3, pp. 2059–2063 vol.3.
[6] X. Long, F. Zeng, W. Zhang, C. Sun, and L. Guo, “Complementary sequence and its anti-interference performance in multi-carrier CDMA system,” in *Wireless and Optical Communications Conference (WOCC), 2010 19th Annual*, 2010, pp. 1–4.
[7] H. Tijms, *Understanding Probability: Chance Rules in Everyday Life*, 2 edition. Cambridge: Cambridge University Press, 2007.
[8] W. Feller, *An Introduction to Probability Theory and Its Applications, Vol. 1, 3rd Edition*, 3rd edition. New York: Wiley, 1968.
[9] M. H. DeGroot and M. J. Schervish, *Probability and Statistics*, 4 edition. Boston: Pearson, 2011.
[10] A. Field, J. Miles, and Z. Field, *Discovering Statistics Using R*, 1 edition. London ; Thousand Oaks, Calif: SAGE Publications Ltd, 2012.
[11] P. A. L. Ph.D, *Secrets of Antigravity Propulsion: Tesla, UFOs, and Classified Aerospace Technology*. Rochester, Vt: Bear & Company, 2008.
[12] “Relativity, Gravitation and Cosmology,” *Cambridge University Press*. [Online]. Available: http://www.cambridge.org/st/academic/subjects/astronomy/cosmology-and-relativity/relativity-gravitation-and-cosmology?format=PB.
[13] C. W. Misner, K. S. Thorne, and J. A. Wheeler, *Gravitation*. San Francisco: W. H. Freeman, 1973.
[14] “statistics - If I roll two fair dice, the probability that I would get at least one 6 would be.... - Mathematics Stack Exchange.” [Online]. Available: http://math.stackexchange.com/questions/598838/.
[28] \iDie rolling probability: Vide0 Lecture.
[16] O. Knill, *Probability Theory and Stochastic Processes with Applications*, 2009 edition. New Delhi, India: Overseas Press, 2009.
[17] P. Billingsley, *Probability and Measure*, 4 edition. Hoboken, N.J: Wiley, 2012.
[18] T. H. Cormen, C. E. Leiserson, R. L. Rivest, and C. Stein, *Introduction to Algorithms, 3rd Edition*, 3rd edition. Cambridge, Mass: The MIT Press, 2009.
[19] “Archery is Not Normal - Technical Archery.” [Online]. Available: https://sites.google.com/site/technicalarchery/technical-discussions-1/Archery-is-Not-Normal.
[20] Index Fund Advisors, Inc., *IFA.tv - Probability Machine, Galton Board, Randomness and Fair Price Simulator, Quincunx.*.
[21] “The Annals of Statistics on JSTOR.” [Online]. Available: https://www.jstor.org/journal/annalsstatistics.
[22] “Normal distribution,” *Wikipedia, the free encyclopedia*. 10-Mar-2016.
[23] M. Hazewinkel, *Encyclopaedia of Mathematics*. Springer Science & Business Media, 2012.

Appendix 4

Appendices of this series cover Chapter 6 of thesis

Appendix 4.1

Spectrum Utilisation Efficiency

According to the RECOMMENDATION ITU-R SM.1046-1, the spectrum utilization efficiency (SUE), or spectrum efficiency in short, is measured as a ratio of the amount of information transferred over a distance (or communications achieved) to the spectrum utilization factor. The spectrum efficiency allows the maximum amount of service, which can be derived from the given amount of radio spectrum. The spectrum utilization factor, *U*, is defined to be the product of the frequency bandwidth, the geometric (geographic) space, and the time denied to other potential users:

$$\boldsymbol{U = B \cdot S \cdot T} \qquad \textbf{5.1.1}$$

Where,

- *B* : frequency bandwidth
- *S* : geometric space (usually area) and
- *T* : time.

Spectrum utilization efficiency (SUE) is expressed by:

$$SUE = \frac{M}{U} = \frac{M}{B \cdot S \cdot T} \qquad \textbf{5.1.2}$$

where:

M : amount of information transferred over a distance.
From the equation (5.1.1), the spectrum efficiency of a cellular radio system may be defined as:

$$\textbf{SE= Erlangs / (bandwidth} \times \textbf{ area)} \qquad \textbf{5.1.3}$$

Where: erlangs is the total voice traffic carried by the cellular system, bandwidth is the total amount of spectrum used by the system and area is the total service area covered by the system.

Appendix 4.2

Erlang B Table[1]

(Offered Load)	A in Erlangs												
n	P_B (Blocking Probability)												
	0.01%	*0.02%*	*0.03%*	*0.05%*	*0.1%*	*0.2%*	*0.3%*	*0.4%*	*0.5%*	*0.6%*	*0.7%*	*0.8%*	*0.9%*
1	0.0001	0.0002	0.0003	0.0005	0.0010	0.0020	0.0030	0.0040	0.0050	0.0060	0.0070	0.0081	0.0091
2	0.0142	0.0202	0.0248	0.0321	0.0458	0.0653	0.0806	0.0937	0.105	0.116	0.126	0.135	0.1443
3	0.0868	0.110	0.127	0.152	0.194	0.249	0.289	0.321	0.349	0.374	0.397	0.418	0.4374
4	0.235	0.282	0.315	0.362	0.439	0.535	0.602	0.656	0.701	0.741	0.777	0.810	0.8415
5	0.452	0.527	0.577	0.649	0.762	0.900	0.994	1.07	1.13	1.19	1.24	1.28	1.326
6	0.728	0.832	0.900	0.996	1.15	1.33	1.45	1.54	1.62	1.69	1.75	1.81	1.867
7	1.05	1.19	1.27	1.39	1.58	1.80	1.95	2.06	2.16	2.24	2.31	2.38	2.448
8	1.42	1.58	1.69	1.83	2.05	2.31	2.48	2.62	2.73	2.83	2.91	2.99	3.069
9	1.83	2.01	2.13	2.30	2.56	2.85	3.05	3.21	3.33	3.44	3.54	3.63	3.7110
10	2.26	2.47	2.61	2.80	3.09	3.43	3.65	3.82	3.96	4.08	4.19	4.29	4.3811
11	2.72	2.96	3.12	3.33	3.65	4.02	4.27	4.45	4.61	4.74	4.86	4.97	5.07
12	3.21	3.47	3.65	3.88	4.23	4.64	4.90	5.11	5.28	5.43	5.55	5.67	5.78
13	3.71	4.01	4.19	4.45	4.83	5.27	5.56	5.78	5.96	6.12	6.26	6.39	6.50
14	4.24	4.56	4.76	5.03	5.45	5.92	6.23	6.47	6.66	6.83	6.98	7.12	7.24
15	4.78	5.12	5.34	5.63	6.08	6.58	6.91	7.17	7.38	7.56	7.71	7.86	7.99
16	5.34	5.70	5.94	6.25	6.72	7.26	7.61	7.88	8.10	8.29	8.46	8.61	8.75
17	5.91	6.30	6.55	6.88	7.38	7.95	8.32	8.60	8.83	9.03	9.21	9.37	9.52
18	6.50	6.91	7.17	7.52	8.05	8.64	9.03	9.33	9.58	9.79	9.98	10.1	10.3
19	7.09	7.53	7.80	8.17	8.72	9.35	9.76	10.1	10.3	10.6	10.7	10.9	11.1
20	7.70	8.16	8.44	8.83	9.41	10.1	10.5	10.8	11.1	11.3	11.5	11.7	11.9
21	8.32	8.79	9.10	9.50	10.1	10.8	11.2	11.6	11.9	12.1	12.3	12.5	12.7
22	8.95	9.44	9.76	10.2	10.8	11.5	12.0	12.3	12.6	12.9	13.1	13.3	13.5
23	9.58	10.1	10.4	10.9	11.5	12.3	12.7	13.1	13.4	13.7	13.9	14.1	14.3
24	10.2	10.8	11.1	11.6	12.2	13.0	13.5	13.9	14.2	14.5	14.7	14.9	15.1
25	10.9	11.4	11.8	12.3	13.0	13.8	14.3	14.7	15.0	15.3	15.5	15.7	15.9
26	11.5	12.1	12.5	13.0	13.7	14.5	15.1	15.5	15.8	16.1	16.3	16.6	16.8
27	12.2	12.8	13.2	13.7	14.4	15.3	15.8	16.3	16.6	16.9	17.2	17.4	17.6
28	12.9	13.5	13.9	14.4	15.2	16.1	16.6	17.1	17.4	17.7	18.0	18.2	18.4
29	13.6	14.2	14.6	15.1	15.9	16.8	17.4	17.9	18.2	18.5	18.8	19.1	19.3
30	14.2	14.9	15.3	15.9	16.7	17.6	18.2	18.7	19.0	19.4	19.6	19.9	20.1
31	14.9	15.6	16.0	16.6	17.4	18.4	19.0	19.5	19.9	20.2	20.5	20.7	21.0
32	15.6	16.3	16.8	17.3	18.2	19.2	19.8	20.3	20.7	21.0	21.3	21.6	21.8
33	16.3	17.0	17.5	18.1	19.0	20.0	20.6	21.1	21.5	21.9	22.2	22.4	22.7
34	17.0	17.8	18.2	18.8	19.7	20.8	21.4	21.9	22.3	22.7	23.0	23.3	23.5
35	17.8	18.5	19.0	19.6	20.5	21.6	22.2	22.7	23.2	23.5	23.8	24.1	24.4
36	18.5	19.2	19.7	20.3	21.3	22.4	23.1	23.6	24.0	24.4	24.7	25.0	25.3
37	19.2	20.0	20.5	21.1	22.1	23.2	23.9	24.4	24.8	25.2	25.6	25.9	26.1
38	19.9	20.7	21.2	21.9	22.9	24.0	24.7	25.2	25.7	26.1	26.4	26.7	27.0
39	20.6	21.5	22.0	22.6	23.7	24.8	25.5	26.1	26.5	26.9	27.3	27.6	27.9
40	21.4	22.2	22.7	23.4	24.4	25.6	26.3	26.9	27.4	27.8	28.1	28.5	28.7
41	22.1	23.0	23.5	24.2	25.2	26.4	27.2	27.8	28.2	28.6	29.0	29.3	29.6
42	22.8	23.7	24.2	25.0	26.0	27.2	28.0	28.6	29.1	29.5	29.9	30.2	30.5
43	23.6	24.5	25.0	25.7	26.8	28.1	28.8	29.4	29.9	30.4	30.7	31.1	31.4
44	24.3	25.2	25.8	26.5	27.6	28.9	29.7	30.3	30.8	31.2	31.6	31.9	32.3
45	25.1	26.0	26.6	27.3	28.4	29.7	30.5	31.1	31.7	32.1	32.5	32.8	33.1
46	25.8	26.8	27.3	28.1	29.3	30.5	31.4	32.0	32.5	33.0	33.4	33.7	34.0
47	26.6	27.5	28.1	28.9	30.1	31.4	32.2	32.9	33.4	33.8	34.2	34.6	34.9
48	27.3	28.3	28.9	29.7	30.9	32.2	33.1	33.7	34.2	34.7	35.1	35.5	35.8
49	28.1	29.1	29.7	30.5	31.7	33.0	33.9	34.6	35.1	35.6	36.0	36.4	36.7
50	28.9	29.9	30.5	31.3	32.5	33.9	34.8	35.4	36.0	36.5	36.9	37.2	37.6
	0.01%	*0.02%*	*0.03%*	*0.05%*	*0.1%*	*0.2%*	*0.3%*	*0.4%*	*0.5%*	*0.6%*	*0.7%*	*0.8%*	*0.9%*
N							B						

N (or 'n')= number of TS; Presently blocking probability of 2% is considered.

(Offered Load)	A in Erlangs												
n	P_B												
	1.0%	*1.2%*	*1.5%*	*2%*	*3%*	*5%*	*7%*	*10%*	*15%*	*20%*	*30%*	*40%*	*50%*
1	0.0101	0.0121	0.0152	0.0204	0.0309	0.0526	0.753	0.111	0.176	0.250	0.429	0.667	1.00
2	0.153	0.168	0.190	0.223	0.282	0.381	0.470	0.595	0.796	1.00	1.45	2.00	2.73
3	0.455	0.489	0.535	0.602	0.715	0.899	1.06	1.27	1.60	1.93	2.63	3.48	4.59
4	0.869	0.922	0.992	1.09	1.26	1.52	1.75	2.05	2.50	2.95	3.89	5.02	6.50
5	1.36	1.43	1.52	1.66	1.88	2.22	2.50	2.88	3.45	4.01	5.19	6.60	8.44
6	1.91	2.00	2.11	2.28	2.54	2.96	3.30	3.76	4.44	5.11	6.51	8.19	10.4
7	2.50	2.60	2.74	2.94	3.25	3.74	4.14	4.67	5.46	6.23	7.86	9.80	12.4
8	3.13	3.25	3.40	3.63	3.99	4.54	5.00	5.60	6.50	7.37	9.21	11.4	14.3
9	3.78	3.92	4.09	4.34	4.75	5.37	5.88	6.55	7.55	8.52	10.6	13.0	16.3
10	4.46	4.61	4.81	5.08	5.53	6.22	6.78	7.51	8.62	9.68	12.0	14.7	18.3
11	5.16	5.32	5.54	5.84	6.33	7.08	7.69	8.49	9.69	10.9	13.3	16.3	20.3
12	5.88	6.05	6.29	6.61	7.14	7.95	8.61	9.47	10.8	12.0	14.7	18.0	22.2
13	6.61	6.80	7.05	7.40	7.97	8.83	9.54	10.5	11.9	13.2	16.1	19.6	24.2
14	7.35	7.56	7.82	8.20	8.80	9.73	10.5	11.5	13.0	14.4	17.5	21.2	26.2
15	8.11	8.33	8.61	9.01	9.65	10.6	11.4	12.5	14.1	15.6	18.9	22.9	28.2
16	8.88	9.11	9.41	9.83	10.5	11.5	12.4	13.5	15.2	16.8	20.3	24.5	30.2
17	9.65	9.89	10.2	10.7	11.4	12.5	13.4	14.5	16.3	18.0	21.7	26.2	32.2
18	10.4	10.7	11.0	11.5	12.2	13.4	14.3	15.5	17.4	19.2	23.1	27.8	34.2
19	11.2	11.5	11.8	12.3	13.1	14.3	15.3	16.6	18.5	20.4	24.5	29.5	36.2
20	12.0	12.3	12.7	13.2	14.0	15.2	16.3	17.6	19.6	21.6	25.9	31.2	38.2
21	12.8	13.1	13.5	14.0	14.9	16.2	17.3	18.7	20.8	22.8	27.3	32.8	40.2
22	13.7	14.0	14.3	14.9	15.8	17.1	18.2	19.7	21.9	24.1	28.7	34.5	42.1
23	14.5	14.8	15.2	15.8	16.7	18.1	19.2	20.7	23.0	25.3	30.1	36.1	44.1
24	15.3	15.6	16.0	16.6	17.6	19.0	20.2	21.8	24.2	26.5	31.6	37.8	46.1
25	16.1	16.5	16.9	17.5	18.5	20.0	21.2	22.8	25.3	27.7	33.0	39.4	48.1
26	17.0	17.3	17.8	18.4	19.4	20.9	22.2	23.9	26.4	28.9	34.4	41.1	50.1
27	17.8	18.2	18.6	19.3	20.3	21.9	23.2	24.9	27.6	30.2	35.8	42.8	52.1
28	18.6	19.0	19.5	20.2	21.2	22.9	24.2	26.0	28.7	31.4	37.2	44.4	54.1
29	19.5	19.9	20.4	21.0	22.1	23.8	25.2	27.1	29.9	32.6	38.6	46.1	56.1
30	20.3	20.7	21.2	21.9	23.1	24.8	26.2	28.1	31.0	33.8	40.0	47.7	58.1
31	21.2	21.6	22.1	22.8	24.0	25.8	27.2	29.2	32.1	35.1	41.5	49.4	60.1
32	22.0	22.5	23.0	23.7	24.9	26.7	28.2	30.2	33.3	36.3	42.9	51.1	62.1
33	22.9	23.3	23.9	24.6	25.8	27.7	29.3	31.3	34.4	37.5	44.3	52.7	64.1
34	23.8	24.2	24.8	25.5	26.8	28.7	30.3	32.4	35.6	38.8	45.7	54.4	66.1
35	24.6	25.1	25.6	26.4	27.7	29.7	31.3	33.4	36.7	40.0	47.1	56.0	68.1
36	25.5	26.0	26.5	27.3	28.6	30.7	32.3	34.5	37.9	41.2	48.6	57.7	70.1
37	26.4	26.8	27.4	28.3	29.6	31.6	33.3	35.6	39.0	42.4	50.0	59.4	72.1
38	27.3	27.7	28.3	29.2	30.5	32.6	34.4	36.6	40.2	43.7	51.4	61.0	74.1
39	28.1	28.6	29.2	30.1	31.5	33.6	35.4	37.7	41.3	44.9	52.8	62.7	76.1
40	29.0	29.5	30.1	31.0	32.4	34.6	36.4	38.8	42.5	46.1	54.2	64.4	78.1
41	29.9	30.4	31.0	31.9	33.4	35.6	37.4	39.9	43.6	47.4	55.7	66.0	80.1
42	30.8	31.3	31.9	32.8	34.3	36.6	38.4	40.9	44.8	48.6	57.1	67.7	82.1
43	31.7	32.2	32.8	33.8	35.3	37.6	39.5	42.0	45.9	49.9	58.5	69.3	84.1
44	32.5	33.1	33.7	34.7	36.2	38.6	40.5	43.1	47.1	51.1	59.9	71.0	86.1
45	33.4	34.0	34.6	35.6	37.2	39.6	41.5	44.2	48.2	52.3	61.3	72.7	88.1
46	34.3	34.9	35.6	36.5	38.1	40.5	42.6	45.2	49.4	53.6	62.8	74.3	90.1
47	35.2	35.8	36.5	37.5	39.1	41.5	43.6	46.3	50.6	54.8	64.2	76.0	92.1
48	36.1	36.7	37.4	38.4	40.0	42.5	44.6	47.4	51.7	56.0	65.6	77.7	94.1
49	37.0	37.6	38.3	39.3	41.0	43.5	45.7	48.5	52.9	57.3	67.0	79.3	96.1
50	37.9	38.5	39.2	40.3	41.9	44.5	46.7	49.6	54.0	58.5	68.5	81.0	98.1
	1.0%	*1.2%*	*1.5%*	*2%*	*3%*	*5%*	*7%*	*10%*	*15%*	*20%*	*30%*	*40%*	*50%*
N							B						

N (or 'n')= number of TS; Presently blocking probability of 2% is considered.

(Offered Load)	A in Erlangs												
n	P_B												
	1.0%	1.2%	1.5%	2%	3%	5%	7%	10%	15%	20%	30%	40%	50%
50	37.9	38.5	39.2	40.3	41.9	44.5	46.7	49.6	54.0	58.5	68.5	81.0	98.1
51	38.8	39.4	40.1	41.2	42.9	45.5	47.7	50.6	55.2	59.7	69.9	82.7	100.1
52	39.7	40.3	41.0	42.1	43.9	46.5	48.8	51.7	56.3	61.0	71.3	84.3	102.1
53	40.6	41.2	42.0	43.1	44.8	47.5	49.8	52.8	57.5	62.2	72.7	86.0	104.1
54	41.5	42.1	42.9	44.0	45.8	48.5	50.8	53.9	58.7	63.5	74.2	87.6	106.1
55	42.4	43.0	43.8	44.9	46.7	49.5	51.9	55.0	59.8	64.7	75.6	89.3	108.1
56	43.3	43.9	44.7	45.9	47.7	50.5	52.9	56.1	61.0	65.9	77.0	91.0	110.1
57	44.2	44.8	45.7	46.8	48.7	51.5	53.9	57.1	62.1	67.2	78.4	92.6	112.1
58	45.1	45.8	46.6	47.8	49.6	52.6	55.0	58.2	63.3	68.4	79.8	94.3	114.1
59	46.0	46.7	47.5	48.7	50.6	53.6	56.0	59.3	64.5	69.7	81.3	96.0	116.1
60	46.9	47.6	48.4	49.6	51.6	54.6	57.1	60.4	65.6	70.9	82.7	97.6	118.1
61	47.9	48.5	49.4	50.6	52.5	55.6	58.1	61.5	66.8	72.1	84.1	99.3	120.1
62	48.8	49.4	50.3	51.5	53.5	56.6	59.1	62.6	68.0	73.4	85.5	101.0	122.1
63	49.7	50.4	51.2	52.5	54.5	57.6	60.2	63.7	69.1	74.6	87.0	102.6	124.1
64	50.6	51.3	52.2	53.4	55.4	58.6	61.2	64.8	70.3	75.9	88.4	104.3	126.1
65	51.5	52.2	53.1	54.4	56.4	59.6	62.3	65.8	71.4	77.1	89.8	106.0	128.1
66	52.4	53.1	54.0	55.3	57.4	60.6	63.3	66.9	72.6	78.3	91.2	107.6	130.1
67	53.4	54.1	55.0	56.3	58.4	61.6	64.4	68.0	73.8	79.6	92.7	109.3	132.1
68	54.3	55.0	55.9	57.2	59.3	62.6	65.4	69.1	74.9	80.8	94.1	111.0	134.1
69	55.2	55.9	56.9	58.2	60.3	63.7	66.4	70.2	76.1	82.1	95.5	112.6	136.1
70	56.1	56.8	57.8	59.1	61.3	64.7	67.5	71.3	77.3	83.3	96.9	114.3	138.1
71	57.0	57.8	58.7	60.1	62.3	65.7	68.5	72.4	78.4	84.6	98.4	115.9	140.1
72	58.0	58.7	59.7	61.0	63.2	66.7	69.6	73.5	79.6	85.8	99.8	117.6	142.1
73	58.9	59.6	60.6	62.0	64.2	67.7	70.6	74.6	80.8	87.0	101.2	119.3	144.1
74	59.8	60.6	61.6	62.9	65.2	68.7	71.7	75.6	81.9	88.3	102.7	120.9	146.1
75	60.7	61.5	62.5	63.9	66.2	69.7	72.7	76.7	83.1	89.5	104.1	122.6	148.0
76	61.7	62.4	63.4	64.9	67.2	70.8	73.8	77.8	84.2	90.8	105.5	124.3	150.0
77	62.6	63.4	64.4	65.8	68.1	71.8	74.8	78.9	85.4	92.0	106.9	125.9	152.0
78	63.5	64.3	65.3	66.8	69.1	72.8	75.9	80.0	86.6	93.3	108.4	127.6	154.0
79	64.4	65.2	66.3	67.7	70.1	73.8	76.9	81.1	87.7	94.5	109.8	129.3	156.0
80	65.4	66.2	67.2	68.7	71.1	74.8	78.0	82.2	88.9	95.7	111.2	130.9	158.0
81	66.3	67.1	68.2	69.6	72.1	75.8	79.0	83.3	90.1	97.0	112.6	132.6	160.0
82	67.2	68.0	69.1	70.6	73.0	76.9	80.1	84.4	91.2	98.2	114.1	134.3	162.0
83	68.2	69.0	70.1	71.6	74.0	77.9	81.1	85.5	92.4	99.5	115.5	135.9	164.0
84	69.1	69.9	71.0	72.5	75.0	78.9	82.2	86.6	93.6	100.7	116.9	137.6	166.0
85	70.0	70.9	71.9	73.5	76.0	79.9	83.2	87.7	94.7	102.0	118.3	139.3	168.0
86	70.9	71.8	72.9	74.5	77.0	80.9	84.3	88.8	95.9	103.2	119.8	140.9	170.0
87	71.9	72.7	73.8	75.4	78.0	82.0	85.3	89.9	97.1	104.5	121.2	142.6	172.0
88	72.8	73.7	74.8	76.4	78.9	83.0	86.4	91.0	98.2	105.7	122.6	144.3	174.0
89	73.7	74.6	75.7	77.3	79.9	84.0	87.4	92.1	99.4	106.9	124.0	145.9	176.0
90	74.7	75.6	76.7	78.3	80.9	85.0	88.5	93.1	100.6	108.2	125.5	147.6	178.0
91	75.6	76.5	77.6	79.3	81.9	86.0	89.5	94.2	101.7	109.4	126.9	149.3	180.0
92	76.6	77.4	78.6	80.2	82.9	87.1	90.6	95.3	102.9	110.7	128.3	150.9	182.0
93	77.5	78.4	79.6	81.2	83.9	88.1	91.6	96.4	104.1	111.9	129.7	152.6	184.0
94	78.4	79.3	80.5	82.2	84.9	89.1	92.7	97.5	105.3	113.2	131.2	154.3	186.0
95	79.4	80.3	81.5	83.1	85.8	90.1	93.7	98.6	106.4	114.4	132.6	155.9	188.0
96	80.3	81.2	82.4	84.1	86.8	91.1	94.8	99.7	107.6	115.7	134.0	157.6	190.0
97	81.2	82.2	83.4	85.1	87.8	92.2	95.8	100.8	108.8	116.9	135.5	159.3	192.0
98	82.2	83.1	84.3	86.0	88.8	93.2	96.9	101.9	109.9	118.2	136.9	160.9	194.0
99	83.1	84.1	85.3	87.0	89.8	94.2	97.9	103.0	111.1	119.4	138.3	162.6	196.0
100	84.1	85.0	86.2	88.0	90.8	95.2	99.0	104.1	112.3	120.6	139.7	164.3	198.0
N	1.0%	1.2%	1.5%	2%	3%	5%	7% B	10%	15%	20%	30%	40%	50%

N (or ‘n’)= number of TS; Presently blocking probability of 2% is considered.

(Offered Load)	A in Erlangs												
n	P_B												
	1.0%	1.2%	1.5%	2%	3%	5%	7%	10%	15%	20%	30%	40%	50%
100	84.1	85.0	86.2	88.0	90.8	95.2	99.0	104.1	112.3	120.6	139.7	164.3	198.0
102	85.9	86.9	88.1	89.9	92.8	97.3	101.1	106.3	114.6	123.1	142.6	167.6	202.0
104	87.8	88.8	90.1	91.9	94.8	99.3	103.2	108.5	116.9	125.6	145.4	170.9	206.0
106	89.7	90.7	92.0	93.8	96.7	101.4	105.3	110.7	119.3	128.1	148.3	174.2	210.0
108	91.6	92.6	93.9	95.7	98.7	103.4	107.4	112.9	121.6	130.6	151.1	177.6	214.0
110	93.5	94.5	95.8	97.7	100.7	105.5	109.5	115.1	124.0	133.1	154.0	180.9	218.0
112	95.4	96.4	97.7	99.6	102.7	107.5	111.7	117.3	126.3	135.6	156.9	184.2	222.0
114	97.3	98.3	99.7	101.6	104.7	109.6	113.8	119.5	128.6	138.1	159.7	187.6	226.0
116	99.2	100.2	101.6	103.5	106.7	111.7	115.9	121.7	131.0	140.6	162.6	190.9	230.0
118	101.1	102.1	103.5	105.5	108.7	113.7	118.0	123.9	133.3	143.1	165.4	194.2	234.0
120	103.0	104.0	105.4	107.4	110.7	115.8	120.1	126.1	135.7	145.6	168.3	197.6	238.0
122	104.9	105.9	107.4	109.4	112.6	117.8	122.2	128.3	138.0	148.1	171.1	200.9	242.0
124	106.8	107.9	109.3	111.3	114.6	119.9	124.4	130.5	140.3	150.6	174.0	204.2	246.0
126	108.7	109.8	111.2	113.3	116.6	121.9	126.5	132.7	142.7	153.0	176.8	207.6	250.0
128	110.6	111.7	113.2	115.2	118.6	124.0	128.6	134.9	145.0	155.5	179.7	210.9	254.0
130	112.5	113.6	115.1	117.2	120.6	126.1	130.7	137.1	147.4	158.0	182.5	214.2	258.0
132	114.4	115.5	117.0	119.1	122.6	128.1	132.8	139.3	149.7	160.5	185.4	217.6	262.0
134	116.3	117.4	119.0	121.1	124.6	130.2	134.9	141.5	152.0	163.0	188.3	220.9	266.0
136	118.2	119.4	120.9	123.1	126.6	132.3	137.1	143.7	154.4	165.5	191.1	224.2	270.0
138	120.1	121.3	122.8	125.0	128.6	134.3	139.2	145.9	156.7	168.0	194.0	227.6	274.0
140	122.0	123.2	124.8	127.0	130.6	136.4	141.3	148.1	159.1	170.5	196.8	230.9	278.0
142	123.9	125.1	126.7	128.9	132.6	138.4	143.4	150.3	161.4	173.0	199.7	234.2	282.0
144	125.8	127.0	128.6	130.9	134.6	140.5	145.6	152.5	163.8	175.5	202.5	237.6	286.0
146	127.7	129.0	130.6	132.9	136.6	142.6	147.7	154.7	166.1	178.0	205.4	240.9	290.0
148	129.7	130.9	132.5	134.8	138.6	144.6	149.8	156.9	168.5	180.5	208.2	244.2	294.0
150	131.6	132.8	134.5	136.8	140.6	146.7	151.9	159.1	170.8	183.0	211.1	247.6	298.0
152	133.5	134.8	136.4	138.8	142.6	148.8	154.0	161.3	173.1	185.5	214.0	250.9	302.0
154	135.4	136.7	138.4	140.7	144.6	150.8	156.2	163.5	175.5	188.0	216.8	254.2	306.0
156	137.3	138.6	140.3	142.7	146.6	152.9	158.3	165.7	177.8	190.5	219.7	257.6	310.0
158	139.2	140.5	142.3	144.7	148.6	155.0	160.4	167.9	180.2	193.0	222.5	260.9	314.0
160	141.2	142.5	144.2	146.6	150.6	157.0	162.5	170.2	182.5	195.5	225.4	264.2	318.0
162	143.1	144.4	146.1	148.6	152.7	159.1	164.7	172.4	184.9	198.0	228.2	267.6	322.0
164	145.0	146.3	148.1	150.6	154.7	161.2	166.8	174.6	187.2	200.4	231.1	270.9	326.0
166	146.9	148.3	150.0	152.0	156.7	163.3	168.9	176.8	189.6	202.9	233.9	274.2	330.0
168	148.9	150.2	152.0	154.5	158.7	165.3	171.0	179.0	191.9	205.4	236.8	277.6	334.0
170	150.8	152.1	153.9	156.5	160.7	167.4	173.2	181.2	194.2	207.9	239.7	280.9	338.0
172	152.7	154.1	155.9	158.5	162.7	169.5	175.3	183.4	196.6	210.4	242.5	284.2	342.0
174	154.6	156.0	157.8	160.4	164.7	171.5	177.4	185.6	198.9	212.9	245.4	287.6	346.0
176	156.6	158.0	159.8	162.4	166.7	173.6	179.6	187.8	201.3	215.4	248.2	290.9	350.0
178	158.5	159.9	161.8	164.4	168.7	175.7	181.7	190.0	203.6	217.9	251.1	294.2	354.0
180	160.4	161.8	163.7	166.4	170.7	177.8	183.8	192.2	206.0	220.4	253.9	297.5	358.0
182	162.3	163.8	165.7	168.3	172.8	179.8	185.9	194.4	208.3	222.9	256.8	300.9	362.0
184	164.3	165.7	167.6	170.3	174.8	181.9	188.1	196.6	210.7	225.4	259.6	304.2	366.0
186	166.2	167.7	169.6	172.3	176.8	184.0	190.2	198.9	213.0	227.9	262.5	307.5	370.0
188	168.1	169.6	171.5	174.3	178.8	186.1	192.3	201.1	215.4	230.4	265.4	310.9	374.0
190	170.1	171.5	173.5	176.5	180.8	188.1	194.5	203.3	217.7	232.9	268.2	314.2	378.0
192	172.0	173.5	175.4	178.2	182.8	190.2	196.6	205.5	220.1	235.4	271.1	317.5	382.0
194	173.9	175.4	177.4	180.2	184.8	192.3	198.7	207.7	222.4	237.9	273.9	320.9	386.0
196	175.9	177.4	179.4	182.2	186.9	194.4	200.8	209.9	224.8	240.4	276.8	324.2	390.0
198	177.8	179.3	181.3	184.2	188.9	196.4	203.0	212.1	227.1	242.9	279.6	327.5	394.0
200	179.7	181.3	183.3	186.2	190.9	198.5	205.1	214.3	229.4	245.4	282.5	330.9	398.0
	1.0%	1.2%	1.5%	2%	3%	5%	7%	10%	15%	20%	30%	40%	50%
N							B						

N (or 'n')= number of TS; Presently blocking probability of 2% is considered.

(Offered Load)	A in Erlangs												
n	P_B												
	1.0%	1.2%	1.5%	2%	3%	5%	7%	10%	15%	20%	30%	40%	50%
200	179.7	181.3	183.3	186.2	190.9	198.5	205.1	214.3	229.4	245.4	282.5	330.9	398.0
202	181.7	183.2	185.2	188.1	192.9	200.6	207.2	216.5	231.8	247.9	285.4	334.2	402.0
204	183.6	185.2	187.2	190.1	194.9	202.7	209.4	218.7	234.1	250.4	288.2	337.5	406.0
206	185.5	187.1	189.2	192.1	196.9	204.7	211.5	221.0	236.5	252.9	291.1	340.9	410.0
208	187.5	189.1	191.1	194.1	199.0	206.8	213.6	223.2	238.8	255.4	293.9	344.2	414.0
210	189.4	191.0	193.1	196.1	201.0	208.9	215.8	225.4	241.2	257.9	296.8	347.5	418.0
212	191.4	193.0	195.1	198.1	203.0	211.0	217.9	227.6	243.5	260.4	299.6	350.9	422.0
214	193.3	194.9	197.0	200.0	205.0	213.0	220.0	229.8	245.9	262.9	302.5	354.2	426.0
216	195.2	196.9	199.0	202.0	207.0	215.1	222.2	232.0	248.2	265.4	305.3	357.5	430.0
218	197.2	198.8	201.0	204.0	209.1	217.2	224.3	234.2	250.6	267.9	308.2	360.9	434.0
220	199.1	200.8	202.9	206.0	211.1	219.3	226.4	236.4	252.9	270.4	311.1	364.2	438.0
222	201.1	202.7	204.9	208.0	213.1	221.4	228.6	238.6	255.3	272.9	313.9	367.5	442.0
224	203.0	204.7	206.8	210.0	215.1	223.4	230.7	240.9	257.6	275.4	316.8	370.9	446.0
226	204.9	206.6	208.8	212.0	217.1	225.5	232.8	243.1	260.0	277.8	319.6	374.2	450.0
228	206.9	208.6	210.8	213.9	219.2	227.6	235.0	245.3	262.3	280.3	322.5	377.5	454.0
230	208.8	210.5	212.8	215.9	221.2	229.7	237.1	247.5	264.7	282.8	325.3	380.9	458.0
232	210.8	212.5	214.7	217.9	223.2	231.8	239.2	249.7	267.0	285.3	328.2	384.2	462.0
234	212.7	214.4	216.7	219.9	225.2	233.8	241.4	251.9	269.4	287.8	331.1	387.5	466.0
236	214.7	216.4	218.7	221.9	227.2	235.9	243.5	254.1	271.7	290.3	333.9	390.9	470.0
238	216.6	218.3	220.6	223.9	229.3	238.0	245.6	256.3	274.1	292.8	336.8	394.2	474.0
240	218.6	220.3	222.6	225.9	231.3	240.1	247.8	258.6	276.4	295.3	339.6	397.5	478.0
242	220.5	222.3	224.6	227.9	233.3	242.2	249.9	260.8	278.8	297.8	342.5	400.9	482.0
244	222.5	224.2	226.5	229.9	235.3	244.3	252.0	263.0	281.1	300.3	345.3	404.2	486.0
246	224.4	226.2	228.5	231.8	237.4	246.3	254.2	265.2	283.4	302.8	348.2	407.5	490.0
248	226.3	228.1	230.5	233.8	239.4	248.4	256.3	267.4	285.8	305.3	351.0	410.9	494.0
250	228.3	230.1	232.5	235.8	241.4	250.5	258.4	269.6	288.1	307.8	353.9	414.2	498.0
	0.976	*0.982*	*0.988*	*0.998*	*1.014*	*1.042*	*1.070*	*1.108*	*1.176*	*1.250*	*1.428*	*1.666*	*2.000*
300	277.1	279.2	281.9	285.7	292.1	302.6	311.9	325.0	346.9	370.3	425.3	497.5	598.0
	0.982	*0.984*	*0.990*	*1.000*	*1.016*	*1.044*	*1.070*	*1.108*	*1.174*	*1.248*	*1.428*	*1.668*	*2.000*
350	326.2	328.4	331.4	335.7	342.9	354.8	365.4	380.4	405.6	432.7	496.7	580.9	698.0
	0.982	*0.988*	*0.994*	*1.004*	*1.020*	*1.046*	*1.070*	*1.108*	*1.176*	*1.250*	*1.430*	*1.666*	*2.000*
400	375.3	377.8	381.1	385.9	393.9	407.1	418.9	435.8	464.4	495.2	568.2	664.2	798.0
	0.986	*0.990*	*0.996*	*1.004*	*1.018*	*1.046*	*1.072*	*1.110*	*1.176*	*1.250*	*1.428*	*1.666*	*2.000*
450	424.6	427.3	430.9	436.1	444.8	459.4	472.5	491.3	523.2	557.7	639.6	747.5	898.0
	0.988	*0.994*	*0.998*	*1.006*	*1.022*	*1.048*	*1.070*	*1.108*	*1.176*	*1.250*	*1.428*	*1.668*	*2.000*
500	474.0	477.0	480.8	486.4	495.9	511.8	526.0	546.7	582.0	620.2	711.0	830.9	998.0
	0.991	*0.994*	*1.000*	*1.008*	*1.022*	*1.047*	*1.073*	*1.110*	*1.176*	*1.249*	*1.429*	*1.666*	*2.000*
600	573.1	576.4	580.8	587.2	598.1	616.5	633.3	657.7	699.6	745.1	853.9	997.5	1198.
	0.993	*0.997*	*1.002*	*1.010*	*1.024*	*1.049*	*1.073*	*1.110*	*1.176*	*1.250*	*1.428*	*1.665*	*2.00*
700	672.4	676.1	681.0	688.2	700.5	721.4	740.6	768.7	817.2	870.1	996.7	1164.	1398.
	0.994	*0.998*	*1.004*	*1.011*	*1.025*	*1.050*	*1.073*	*1.110*	*1.176*	*1.250*	*1.433*	*1.67*	*2.00*
800	771.8	775.9	781.4	789.3	803.0	826.4	847.9	879.7	934.8	995.1	1140.	1331.	1598.
	0.997	*1.000*	*1.004*	*1.013*	*1.025*	*1.050*	*1.074*	*1.111*	*1.172*	*1.249*	*1.42*	*1.67*	*2.00*
900	871.5	875.9	881.8	890.6	905.5	931.4	955.3	990.8	1052.	1120.	1282.	1498.	1798.
	0.997	*1.001*	*1.006*	*1.013*	*1.025*	*1.046*	*1.077*	*1.112*	*1.18*	*1.25*	*1.43*	*1.66*	*2.00*
1000	971.2	976.0	982.4	991.9	1008.	1036.	1063.	1102.	1170.	1245.	1425.	1664.	1998.
	0.998	*1.000*	*1.006*	*1.011*	*1.03*	*1.05*	*1.07*	*1.11*	*1.18*	*1.25*	*1.43*	*1.67*	*2.00*
1100	1071.	1076.	1083.	1093.	1111.	1141.	1170.	1213.	1288.	1370.	1568.	1831.	2198.
	1.0%	1.2%	1.5%	2%	3%	5%	7%	10%	15%	20%	30%	40%	50%
N							B						

N (or ‘n’)= number of TS; Presently blocking probability of 2% is considered.

REFERENCE

[1] H. Hammuda, “Appendix B: Erlang B Table-Blocked Calls Cleared Model,” in *Cellular Mobile Radio Systems*, John Wiley & Sons, Ltd, 2001, pp. 177–185.

SUMMARY

Coverage and capacity are the decisive parameters of a network performance. The impact of the subscriber, moving, grouping and moving in groups of the above phenomena are defined in a novel way as Place Time Coverage (PTCo) and Place time Capacity (PTC) respectively, and we would refer them collectively as Place Time Coverage & Capacity (PTC2). The dissertation proves through the concept of the PTC2 that the network performance can severely be degraded by the excessive and unrealistic site demands, the network management inefficiency, and the consequence of the accumulation of subscribers substantially and randomly across the area under investigation (defined here as the Area of Interest or AoI).. Both the position and, the time of the position acquired by a subscriber, raises the demand for service at the very location (termed here as PTC wobble), thereby posing an ongoing capacity demand and poor resource utilisation in the present MWCN. This random accumulation, being more intense and rapid in the highly populated metropolitan cities, tend to affect both the signal propagation and the capacity demand at the point of accumulation more severely. This PhD research addresses the PTC2 challenge through a viable solution that is based on injecting intelligence and services in parallel layers through a Distributed Antenna Systems (DAS) network. This approach would enable the remote sites to acquire intelligence and a resource pool at the same time, thereby managing the network dynamics promptly and aptly to absorb the PTC2 wobble. An Active Probing Management System (APMS) is proposed as a supporting architecture, to assist the intelligent system to keep a check on the variations at each and every site by either deploying the additional antenna or by utilising the service antenna. The probing process is an independent layer and does not use paging channels of service technology, thereby, saving extra traffic channels. Further, it is discussed how this architecture can be compatible with multi-technology and dense-net environments. The architecture that is proposed here is termed as Self Configurable Distributed Antenna System (SCIDAS).

ISSN (online): 2246-1248
ISBN (online): 978-87-7112-730-0

AALBORG **UNIVERSITY PRESS**